Condition monitoring of biodegradable oil filled transformer — **Source link**

Kahawaththa Mudiyanselage, Kapila Senarath Bandara

Published on: 03 Jun 2016

Topics: Pressboard, Transformer oil, Insulation system and Mineral oil

Related papers:

- A comparative study of physicochemical, dielectric and thermal properties of pressboard insulation impregnated with natural ester and mineral oil

- Comparative study to understand behaviour of natural ester as transformer insulating liquid

- Influence of moisture content on dielectric properties of pressboard impregnated in mineral insulating oil and natural ester

- Influence of moisture and ageing on dielectric response of ester and mineral oil impregnated pressboard insulation

- Compare the performance of natural ester with synthetic ester as transformer insulating oil

THE UNIVERSITY OF QUEENSLAND

AUSTRALIA

Condition Monitoring of Biodegradable Oil Filled Transformer

Kahawaththa Mudiyanselage Kapila Senarath Bandara

B.Sc., M.Sc.

A Thesis submitted for the degree of Doctor of Philosophy at

The University of Queensland in 2016

School of Information Technology and Electrical Engineering

Abstract

Natural and synthetic ester insulating oils have higher fire points and excellent biodegradable characteristics. Therefore, in order to reduce the adverse environmental impact and to improve the fire safety of transformers, there is an increasing demand for natural and synthetic ester insulating liquids as a transformer insulating oil. However, present understanding on ageing behaviour of ester oil-paper composite insulation system and knowledge on application of existing condition monitoring tools for ester based insulation systems are inadequate. This impedes the cost effective and reliable field applications of ester insulating oils, particularly application of natural esters. To reduce this knowledge gap, series of controlled ageing experiments are performed in this research project to provide a better and comprehensive understanding on ageing behaviour of ester oil-paper insulation systems. Furthermore, applicability of existing chemical and electrical based condition monitoring techniques for ester oil-paper insulation systems is systematically investigated in this research project.

In this thesis, ageing behaviour of dry pressboard insulation in mineral and three different ester insulating oils under simulated transformer operating environment is investigated. Moreover, the ageing behaviour of natural ester-pressboard composite insulation in moisture rich environment is also compared with that of mineral oil-pressboard system. Degree of polymerisation of pressboard samples measured at different ageing interval is used in this research to determine the ageing condition of pressboard. Moreover, applicability of oil related diagnostic parameters such as concentration of dissolved furanic compounds, acidity value, Dielectric Dissipation Factor (DDF), viscosity and colour to assess the degree of degradation of both ester and mineral insulating oils is thoroughly investigated in this research project. The potential of FTIR (Fourier Transform Infrared spectroscopy) techniques for characterising the degree of degradation of paper insulation is also discussed in this thesis. In addition, this thesis concentrates on characterisation of the charge dynamic in insulating oil through modelling of their dielectric responses.

The comparison of gassing behaviour of ester and mineral insulating oils under two different low temperature faults and low energy electric discharge condition is also presented in this thesis. Dissolved Gas Analysis (DGA) results presented in this thesis depicts that faults gases detected in ester and mineral oil samples subjected to a similar fault are akin in type but quantitatively different. The quantity of fault gases produced in two different natural ester oils is also dissimilar. For example, soy-based natural ester produces a large quantity of ethane (C_2H_6) under low temperature overheating condition than sunflower oil based natural ester. Therefore, this research project investigates the applicability of well-established DGA interpretation schemes namely Duval

triangle, IEC gas ratio and IEEE key gas method on ester based insulation systems in order to identify the possible faults based on DGA data.

Investigation of impact of moisture, temperature and ageing on dielectric response of ester impregnated pressboard insulation by Frequency Domain Spectroscopy (FDS) and Polarisation Depolarisation Current (PDC) is a major contribution in this thesis. In order to study that, dielectric responses of well-controlled pressboard insulation samples which are impregnated with four different insulating liquids have been critically investigated. These measurements have been performed with two natural esters, one synthetic ester and one type of mineral oil under varying moisture (0.3%-8.7 %) and different temperature levels (35, 55, 75ºC). In addition, the effect of ageing on dielectric response of natural ester impregnated pressboard insulation has been compared to that of mineral oil impregnated pressboard insulation.

In this thesis, low frequency conductivity based model is proposed to determine the moisture content in transformer solid insulation based on FDS data of unaged pressboard insulation. Furthermore, the effect of ageing and temperature on the proposed model is quantitatively analysed. In order to interpret the FDS data of pressboard insulation in frequency range 10^{-4}-10^{-3} Hz, a hierarchical equivalent circuit is derived based on Dissado-Hill's cluster theory. The equivalent circuit model parameters are then used to explain the influence of diverse oil properties and moisture on microscopic level charge transport and polarisation phenomena in oil impregnated pressboard insulation. Furthermore, this research has used activation energy to characterise the temperature dependent dielectric response of pressboard insulation impregnated in mineral and ester insulating oils. The applicability of commercially available FDS based moisture diagnostic tool on ester based insulation system is also systematically investigated in this research project.

<u>Declaration by Author</u>

This thesis is composed of my original work, and contains no material previously published or written by another person except where due reference has been made in the text. I have clearly stated the contribution by others to jointly-authored works that I have included in my thesis.

I have clearly stated the contribution of others to my thesis as a whole, including statistical assistance, survey design, data analysis, significant technical procedures, professional editorial advice, and any other original research work used or reported in my thesis. The content of my thesis is the result of work I have carried out since the commencement of my research higher degree candidature and does not include a substantial part of work that has been submitted to qualify for the award of any other degree or diploma in any university or other tertiary institution. I have clearly stated which parts of my thesis, if any, have been submitted to qualify for another award.

I acknowledge that an electronic copy of my thesis must be lodged with the University Library and, subject to the policy and procedures of The University of Queensland, the thesis be made available for research and study in accordance with the Copyright Act 1968 unless a period of embargo has been approved by the Dean of the Graduate School.

I acknowledge that copyright of all material contained in my thesis resides with the copyright holder(s) of that material. Where appropriate I have obtained copyright permission from the copyright holder to reproduce material in this thesis.

Publications during candidature

Peer-reviewed Journal Papers:

[1]   **Kapila Bandara,** Chandima Ekanayake, Tapan Saha, Hui Ma "Performance of Natural Ester as a Transformer Oil in Moisture-Rich Environments", J. Energies, Vol.9, Issue 4, DOI: 10.3390/en9040258, 2016

[2]   **Kapila Bandara**, Chandima Ekanayake, Tapan .K. Saha, "Analysis of Frequency Domain Dielectric Response of Pressboard Insulation Impregnated with Different Insulating Liquids", (Accpted 22nd Feb. 2016), IEEE Transactions on Dielectrics and Electrical Insulation., 2016.

[3]   **Kapila Bandara**, Chandima Ekanayake, Tapan .K. Saha, Pratheep Kumar, "Understanding the Ageing Aspects of Natural Ester Based Insulation", (Accpeted 27th August 2015) IEEE Transactions on Dielectrics and Electrical Insulation.

[4]   **Kapila Bandara**, Chandima Ekanayake, Tapan .K. Saha, "Modelling the dielectric response measurements of transformer oil", IEEE Transactions on Dielectrics and Electrical Insulation, Vol. 22, pp. 1283-1291, 2015.

Peer-reviewed Conference Papers:

[1]   **Kapila Bandara**, Chandima Ekanayake, Tapan K. Saha, "Comparative study to understand behaviour of natural ester as transformer insulating liquid", Proceedings of IEEE 10th International Conference on Industrial and Information Systems, pp 117-121, 18-20 Dec. 2015, Peradeniya Sri Lanka.

[2]   **Kapila Bandara**, Chandima Ekanayake, Tapan K. Saha, "Influence of Moisture and Ageing on Dielectric Response of Ester and Mineral Oil Impregnated Pressboard Insulation", Proceedings of IEEE Asia-Pacific Power and Enegy Engineering, pp 1-5, 15-18 Nov. 2015, Brisbane Australia.

[3]   Lakshitha Naranpanawe, **Kapila Bandara**, Tapan K. Saha, Chandima Ekanayake, P. K. Annamalai, "Effect of Pressboard Ageing on Power Transformer Mechanical Vibration Characteristics", Proceedings of IEEE PES Asia-Pacific Power and Energy Engineering Conference , pp 1-5, 15-18 Nov. 2015, Brisbane, Australia.

[4]   **Kapila Bandara**, Chandima Ekanayake, Tapan K. Saha, Hui Ma, "Investigation Of Moisture Influence On Dielectric Response Of Ester Oil Impregnated Pressboard", Proceedings of IEEE Power & Energy Society General Meeting, pp. 1-5, 26-30 July 2015, Denver, Co.

[5]   **Kapila Bandara**, Chandima Ekanayake, Tapan K. Saha, "Compare the Performance of Natural Ester with Synthetic Ester as Transformer Insulating Oil ", Proceedings of IEEE 11th conference on the Properties and Applications of Dielectric Materials, pp. 975-978 ,19-22 July 2015, Sydney, Australia.

[6]   **Kapila. Bandara**, Chandima Ekanayake, and Tapan K. Saha, "Comparative Study For Understanding The Behaviour Of Natural Ester With Mineral Oil As a Transformer Insulating Liquid", Proceedings of IEEE conference on Electrical Insulation and Dielectric Phenomena, pp. 792-795, 19-22 Oct. 2014, Des Moines, IA.

Publications included in this thesis

[1] **Kapila Bandara,** Chandima Ekanayake, Tapan Saha, Hui Ma. "Performance of Natural Ester as a Transformer Oil in Moisture-Rich Environments", J. Energies, Vol.9, Issue 4, DOI: 10.3390/en9040258, 2016.

This paper is incorporated partially in Chapters 4

Contributors	Statement of contribution
Kapila Bandara	Experimental works (75%)
	Result interpretation and discussion (70%)
	Paper writing (70%)
Chandima Ekanayake	Experimental works (15%)
	Result interpretation and discussion (15%)
	Paper writing and review (10%)
Tapan Saha	Experimental works (10%)
	Result interpretation and discussion (15%)
	Paper writing and review (10%)
Hui Ma	Paper writing (10%)

[2] Kapila Bandara, C. Ekanayake, Tapan K. Saha, "Analysis of Frequency Domain Dielectric Response of Pressboard Insulation Impregnated with Different Insulating Liquids", (Accpted 22nd Feb. 2016), IEEE Transactions on Dielectrics and Electrical Insulation.

This paper is incorporated partially in Chapters 6 and 7

Contributors	Statement of contribution
Kapila Bandara	Experimental works (75%)
	Result interpretation and discussion (75%)
	Paper writing (75%)
Chandima Ekanayake	Experimental works (15%)
	Result interpretation and discussion (15%)
	Paper writing and review (15%)
Tapan Saha	Experimental works (10%)
	Result interpretation and discussion (10%)
	Paper writing and review (10%)

[3]   Kapila Bandara, Chandima Ekanayake, Tapan K. Saha, Pratheep Kumar, "Understanding the Ageing Aspects of Natural Ester Based Insulation", (Accpted 27th August 2015), IEEE Transactions on Dielectrics and Electrical Insulation .

This paper is incorporated partially in Chapter 4

Contributors	Statement of contribution
Kapila Bandara	Experimental works (75%)
	Result interpretation and discussion (80%)
	Paper writing (75%)
Chandima Ekanayake	Experimental works (15%)
	Result interpretation and discussion (10%)
	Paper writing and review (10%)
Tapan Saha	Experimental works (5%)
	Result interpretation and discussion (5%)
	Paper writing and review (10%)
Patheep Kumar	Experimental works (5%)
	Result interpretation and discussion (5%)
	Paper writing and review (5%)

[4]   Kapila Bandara, Chandima Ekanayake, Tapan K. Saha, "Modelling the dielectric response measurements of transformer oil", IEEE Transactions on Dielectrics and Electrical Insulation, Vol. 22, pp. 1283-1291, 2015.

This paper is incorporated in Chapter 5

Contributors	Statement of contribution
Kapila Bandara	Experimental works (75%)
	Result interpretation and discussion (75%)
	Paper writing (70%)
Chandima Ekanayake	Experimental works (15%)
	Result interpretation and discussion (15%)
	Paper writing and review (20%)
Tapan Saha	Experimental works (10%)
	Result interpretation and discussion (10%)
	Paper writing and review (10%)

[5]   Kapila Bandara, Chandima Ekanayake, Tapan K. Saha, "Comparative study to understand behaviour of natural ester as transformer insulating liquid", presented in IEEE 10th International Conference on Industrial and Information Systems, pp 117-121, 18-20 Dec. 2015, Peradeniya, Sri Lanka.

This paper is incorporated partially in Chapter 4

Contributors	Statement of contribution
Kapila Bandara	Experimental works (100%)
	Result interpretation and discussion (75%)
	Paper writing (70%)
Chandima Ekanayake	Result interpretation and discussion (15%)
	Paper writing and review (25%)
Tapan Saha	Result interpretation and discussion (5%)
	Paper writing and review (5%)

[6]   Kapila Bandara, Chandima Ekanayake, Tapan K. Saha, "Influence of Moisture and Ageing on Dielectric Response of Ester and Mineral Oil Impregnated Pressboard Insulation", in IEEE Asia-Pacific Power and Enegy Engineering, pp 1-5, 15-18 Nov. 2015, Brisbane Australia.

This paper is incorporated in Chapter 7

Contributors	Statement of contribution
Kapila Bandara	Experimental works (100%)
	Result interpretation and discussion (80%)
	Paper writing (80%)
Chandima Ekanayake	Result interpretation and discussion (10%)
	Paper writing and review (10%)
Tapan Saha	Result interpretation and discussion (10%)
	Paper writing and review (10%)

[7]   Kapila Bandara, Chandima Ekanayake, Tapan K. Saha, Hui Ma, "Investigation of moisture influence on dielectric response of ester oil impregnated pressboard", in IEEE Power & Energy Society General Meeting, pp. 1-5, 26-30 July 2015, Denver, Co.

This paper is incorporated partially in Chapters 6 and 7

Contributors	Statement of contribution
Kapila Bandara	Experimental works (100%)
	Result interpretation and discussion (80%)
	Paper writing (75%)
Chandima Ekanayake	Result interpretation and discussion (10%)
	Paper writing and review (10%)
Tapan Saha	Result interpretation and discussion (5%)
	Paper writing and review (10%)
Hui Ma	Result interpretation and discussion (5%)
	Paper writing and review (5%)

[8]   Kapila Bandara, Chandima Ekanayake, Tapan K. Saha, "Compare the Performance of Natural Ester with Synthetic Ester as Transformer Insulating Oil ", in IEEE 11th conference on the Properties and Applications of Dielectric Materials, pp. 975-978, 19-22 July 2015, Sydney, Australia.

This paper is incorporated partially in Chapter 4

Contributors	Statement of contribution
Kapila Bandara	Experimental works (100%)
	Result interpretation and discussion (80%)
	Paper writing (80%)
Chandima Ekanayake	Result interpretation and discussion (15%)
	Paper writing and review (15%)
Tapan Saha	Result interpretation and discussion (5%)
	Paper writing and review (5%)

[9]   K. Bandara, Chandima Ekanayake, Tapan K. Saha, "Comparative study for understanding the behaviour of natural ester with mineral oil as a transformer insulating liquid", presented in IEEE conference on Electrical Insulation and Dielectric Phenomena, pp. 792-795, 19-22 Oct. 2014, Des Moines, IA.

This paper is incorporated partially in Chapter 5

Contributors	Statement of contribution
Kapila Bandara	Experimental works (100%)
	Result interpretation and discussion (75%)
	Paper writing (75%)
Chandima Ekanayake	Result interpretation and discussion (15%)
	Paper writing and review (15%)
Tapan Saha	Result interpretation and discussion (10%)
	Paper writing and review (10%)

Contributions by others to the thesis

"No contributions by others."

Statement of parts of the thesis submitted to qualify for the award of another degree

"None"

Acknowledgements

Keywords

transformer, condition monitoring, cellulose, mineral oil, natural ester, synthetic ester, ageing, polarisation depolarisation current, frequency domain spectroscopy, cluster theory,

Australian and New Zealand Standard Research Classifications (ANZSRC)

ANZSRC code: 090607, Power and Energy Systems Engineering (excl. Renewable Power), 100%

Fields of Research (FoR) Classification

FoR code: 0906, Electrical and Electronic Engineering, 100%

Table of Contents

List of Figures

List of Tables

Abbreviations

AGU	Anhydroglucose units
DC	Direct Current
DDF	Dielectric Dissipation Factor
DGA	Dissolved Gas Analysis
DH	Dissado and Hill's
DP	Degree of Polymerisation
EP	Electrode Polarisation
EHD	Electro Hydro Dynamic motion
FDS	Frequency Domain Spectroscopy
FTIR	Fourier Transform Infrared Spectroscopy
HMWH	High Molecular Weight Hydrocarbon
I_{pol}	Polarisation current
I_{depol}	Depolarisation current
KFT	Karl Fisher Titration
LFD	Low Frequency Dispersion
q-dc	Quasi–DC conduction
NE	Natural Ester
NEA	Natural Ester A (sunflower oil based insulating oil)
NEB	Natural Ester B (soy oil based insulating oil)
PD	Partial Discharge
PDC	Polarisation Depolarisation Current
RVM	Return Voltage Method
2FAL	2-Furfuraldehyde

2-ACF   2-acetylfuran

5-MEF   5-methyl-2-furfural

2-FOL   2-furfurylalcohol

5-HMF   5-hydroxymethyl-2-furfural

Symbols

k	reaction rate
k_2, k_{10}	constants of 1st order ageing kinetic model
E_a	activation energy corresponding to PB ageing
T	absolute temperature
R	gas constant
θ_h	hotspot temperature
F_{EAQ}	acceleratory ageing factor
P	dielectric polarisation
ε_0	dielectric permittivity of vacuum
ε_r	relative permittivity
ε_∞	high frequency relative permittivity
ω	angular frequency
$\chi(\omega)$	complex susceptibility
$\chi'(\omega)$	real part of complex susceptibility
$\chi''(\omega)$	imaginary part of complex susceptibility
$C(\omega)$	complex capacitance
$C'(\omega)$	real part of complex capacitance
$C''(\omega)$	imaginary part of complex capacitance
$\varepsilon(\omega)$	complex permittivity
$\varepsilon'(\omega)$	real part of complex permittivity
$\varepsilon''(\omega)$	imaginary part of complex permittivity
E	electric filed strength
D	electric displacement vector

$f(t)$	dielectric response function
σ	electrical conductivity
$\chi(\omega)$	complex susceptibility
C_0	geometrical capacitance
τ	time constant corresponds to a relaxation process
K	Boltzmann constant
m	percentage moisture content in pressboard
G	conductance
$Y(\omega)$	complex admittance
η	Viscosity of oil
C_n	universal capacitor
ω_m	angular frequency of loss peak
ω_c	characteristic frequency of q-dc effect

Chapter 1

Introduction

1.1 Overview

Transformers are expensive, indispensable and strategically important pieces of equipment of any electric power system. The insulation system is the most imperative part of a transformer because the lifetime and reliable operation of the transformer are almost solely determined by the condition of its insulation system. There are three main types of transformers namely, oil filled, dry type and gas insulated. However, almost all the load bearing transformers in power delivery systems around the world are oil filled [1]. Electrical grade paper and pressboard are the primary insulation in oil filled transformers. The major composition of paper and pressboard insulation is cellulose which is a homopolymer of D-anhydroglucose units (AGU) bonded together via C1-C4 glycosidic oxygen linkage [2]. Mechanical strength of cellulose insulation materials is often characterised by degree of polymerisation (DP), which is the average number of glucose rings in a polymeric chain.

Mineral oils are still the preferred choice for insulation and cooling purposes in liquid filled transformers due to their low cost, excellent dielectric properties and better compatibility with cellulose materials [3]. A low fire point is a major disadvantage associated with typical mineral insulating oils, which increases the risk of subsequent fire in the case of a transformer failure. Moreover, a high fire risk associated with mineral oil results in increasing the lifetime cost of transformers mainly due to additional works required for fire mitigation. As a consequence, less flammable insulating oils such as high molecular weight hydrocarbons (HMWH) and silicon fluids were introduced in the early 80's as an alternative to the typical mineral oils for improving the fire safety of transformers used in fire sensitive areas and applications. Today, several thousands of transformers filled with silicon and HMWH insulating oils are in service. However, these insulating liquids including typical mineral and less flammable insulating oils create environmental problems mainly due to their poor biodegradable characteristics. New environmental regulations and large costs associated with cleaning up an oil spill from faulty transformers forced utilities to use environmental friendly insulating fluids with high fire safety characteristics. As a result, synthetic based polyol ester with improved biodegradable properties was introduced in 1984. The high cost

associated with synthetic esters compared to other less flammable fluids hampered their wide application and limited their use for traction and mobile transformers and speciality applications. Therefore, in the early 90's interest was evoked among utilities in using edible vegetable oils (natural ester) as an environmental friendly insulating liquid. Natural Esters (NE) are not only readily biodegradable, but they also have excellent fire safety and dielectric properties. Moreover, NEs are far more hygroscopic than mineral oils due to the ester linkages present in their molecular structure, such that moisture solubility of NEs is around 20 times greater than that of mineral oil at room temperature. These properties are desirable factors for the long-term safe operation of transformers. After a preliminary investigation of essential insulation properties of NEs, several types of NE-based insulating oils such as FR3 and BIOTEMP were commercialised by the late 90's and their application for new transformers and retrofilling of existing mineral oil filled units has grown substantially over the last two decades. However, current experience in the use of these liquids is inadequate for cost effective and reliable field applications.

During the course of operation, transformer insulation is subjected to irreversible ageing. The ageing of paper insulation is accomplished by rupturing of covalent and hydrogen bonds within and between cellulose polymer chains under combined influences of heat, moisture and oxygen, which are all present in an operating transformer [4-8]. As a result of a large number laboratory and field investigations, the influence of temperature, moisture and oxygen on ageing of cellulose paper insulation in mineral insulating oil has been well understood. It is generally accepted that the ageing rate of cellulose paper doubles for every increase of 6-8°C in temperature [9] and an increase in moisture content by 0.5 % has a similar influence on the ageing rate. Emsley et al [10] have reported that a decrease in dissolved oxygen content in mineral oil in a transformer from 30,000 ppm to 300 ppm leads to reducing the ageing by a factor of 16. In the last 15 years, several laboratory investigations have been performed to understand the ageing behaviour of typical cellulose insulation materials in ester based insulating oil [11-14]. The main outcome of these studies is that ester oils show a higher resistance to degradation of paper insulation than mineral oil. This advantage of ester oils is mainly caused by their hygroscopic nature. However, the number of studies have been conducted to understand the ageing performance of ester insulating oils are inadequate to improve the confidence of utilities to use ester insulation oil as an alternative to mineral oil. Therefore, one of the main objectives of this thesis is to provide a comprehensive understanding on ageing of cellulose insulation in ester insulating oils.

Oxidation is the main degradation mechanism of both mineral and ester insulating oils. Temperature, the presence of dissolved oxygen and metal catalyst are the most evident factors which govern the rate of oxidative degradation of oil [15-19]. Oxidative degradation rates of

different insulating oils in decreasing order are NE > Mineral oil > Synthetic ester. The basic steps of oxidation reaction in both mineral and ester oils are similar. Ageing by-products and change of physicochemical properties of mineral insulating oils have been well characterised such that the changing of oil properties has been correlated with degradation of their insulation quality and standardised in IEEE Std. C57.152-2013. BS EN 61203-1994 is a similar British standard developed for synthetic ester insulating oils. However, a different chemical composition of NE insulating oils makes their oxidative degradation process more complicated, particularly degradation of intermediate oxidative by products [18]. Moreover, understanding thermo-oxidative degradation of NE insulating oils is still inadequate to produce a complete international standard for correlating the change of their physicochemical properties to degree of deterioration of insulation and cooling characteristics. To reduce this gap, the main work presented in this thesis has been done to measure the properties of two different types of commercially available NE insulating oils and compared their ageing behaviour with conventional mineral oil.

Ageing of the insulation system reduces both the mechanical and dielectric withstand strengths of the transformer. Statistical data related to transformer failures indicates that winding failure due to defects in the insulation system presents the significant percentage of failure statistics [20, 21]. Mechanical strength of conductor paper insulation reduces with ageing and ultimately it becomes brittle which cannot sustain the huge mechanical forces generated by power system faults. As a result turn to turn dielectric failure can occur. Subsequent loosening of clamping pressure causes to reduce the short circuit withstand capability of winding structure leading to a complete transformer failure. Ageing of insulating oil is detrimental to paper insulation in two ways, low molecular acids produced by oil ageing and hotspots produced by depositing of sludge in the cooling ducts accelerate the ageing of paper insulation. Moreover, ageing increases the partial discharge (PD) activities and reduces the breakdown strength of oil. Ultimately, ageing of insulating oil could also lead to a complete insulation failure.

Insulation related transformer failures are often catastrophic and result in significant direct and indirect costs including repair or replacement costs and revenue losses due to unscheduled outages. Therefore, adequate maintenance is required to ensure the good condition of the transformer insulation system. Competitive and liberated energy market forces utilities to change their maintenance strategies from time based to a condition and reliability based where maintenance decisions are no longer driven by the operational time. In such a situation, assessing of a transformer insulation system with reliable methods is a basic requirement of modern power system operation in order to minimise the risk of failures and to avoid forced outages of strategically important units.

Over the past decades, several chemical, physical and electrical based techniques have been well established for determining the condition of mineral-paper insulation systems. Measurements of acidity value, viscosity, colour, interfacial tension, Dielectric Dissipation Factor (DDF) and breakdown voltage are the most common methods that have been used to assess the quality of mineral insulating oil in service. Furfural analysis and Dissolved Gas Analysis (DGA) are also oil related condition monitoring techniques which respectively are utilised to determine degradation of paper insulation and to identify the incipient faults in oil-paper insulation systems of transformers. Measurement of tensile strength, DP value, molecular weight (MW) and moisture determination by Karl-Fischer Titration (KFT) are the typical methods used for analysing the condition of paper insulation. However, practical implementation of these methods to determine the condition of paper insulation is hampered by the difficulty in taking a paper sample from an operating transformer.

Ester insulating liquids possess a completely different chemical structure compared to mineral insulating oil. This leads to a quantitatively different gas generation behaviour for ester insulating oils, but fortunately gas composition is the same for all types of oils. Different types of chemical bonds in ester oils such as C=O, C=C and C-H allylic bonds give this quantitative difference [22]. Both natural and synthetic esters are subjected to hydrolysis degradation and yield acids. Synthetic esters mainly produce short chain acids and they are more reactive and harmful. NEs produce long chain fatty acids which are not as reactive as the acids produced in synthetic esters. The results of several simulated ageing experiments have confirmed that dissolved 2-Furfural aldehyde (2-FAL) concentration found in NEs is several orders of magnitude less than that in mineral oil with paper insulation of a similar degree of ageing [11, 23, 24]. In general, the colour of NE insulating oils changes rapidly due to the higher solubility of decay products in NE because vegetable oil ageing by-products are less carbonaceous [25]. Moreover, ageing by-products of paper insulation could also dissolve greater in ester oils due to their polar nature. Overall one fact is clear, established oil based diagnosis rules for evaluating the condition of mineral insulating oil cannot be directly applied to ester based insulating oils. However, no comprehensive study has addressed this issue yet. Thus, this thesis concentrates on providing a solid framework for assessing the condition of ester based insulation systems in transformers using existing oil based diagnostic techniques such as acidity, viscosity, colour, DDF and DGA.

Moisture is a hazard to an insulation system in several ways: a) acceleration of the ageing of paper insulation, b) lowering the admissible hot spot temperature, c) PD inception becomes significant when the moisture in solid insulation is above 3%, d) reducing the dielectric strength of the insulation system [26, 27]. Therefore, in order to maximise the lifetime and safety of transformers in operation through corrective maintenance actions, it is important to accurately estimate the

moisture content in a transformer insulation system using a reliable technique. Conventionally, moisture in transformer solid insulation is indirectly determined using the so called equilibrium chart method by measuring the moisture content of the oil. This method has been proven to be erroneous because moisture content in insulating oil is highly temperature dependent and moisture equilibrium between oil and paper insulation is hardly achieved.

Dielectric properties of oil-paper insulation systems of transformers change significantly with moisture. Thus, dielectric response measurement techniques have been utilised to determine the moisture and overall condition of transformer insulation systems over decades. Three foremost dielectric response measurement techniques are Return Voltage Method (RVM), Polarisation and Depolarisation Current (PDC) and Frequency Domain Spectroscopy (FDS). There are several limitations in applying the RVM method for insulation diagnostic due to some deficiencies in interpretation of RVM data. For example, estimated moisture content in solid insulation using this technique is often much higher than the actual value, the recommended interpretation scheme is too simplistic and the RVM method does not consider the effect of geometry of the insulation system and oil condition [28]. On the other hand, PDC and FDS are considered as promising techniques for evaluating moisture in transformer solid insulation [27-30]. Moreover, these methods allow users to discriminate the effects of oil condition and moisture content of solid insulation on dielectric response of a transformer insulation system.

In addition to moisture, several other factors influence dielectric response behaviour of a transformer insulation system, such as low molecular acids, oil conductivity and temperature. Thus, the effect of these factors must be taken into account when interpreting the dielectric response data to estimate the moisture content in solid insulation. This issue has been well studied for mineral oil-paper systems over the last two decades but no systematic study has yet been conducted for ester–paper insulation systems. Therefore, implementation of basic guidelines to interpret the dielectric response measurements of aged and new ester–paper insulation systems is an important part of this thesis.

The dielectric spectrum of a material under investigation is characterised by both conduction and polarisation phenomena. Dielectric response of liquid insulation is primarily determined by the conductivity. Generally, polarisation of solid materials is a collection of different relaxation mechanisms such as dipole polarisation, Maxwell-Wagner polarisation and quasi-DC conduction. Overlapping of different polarisation and conduction processes, results in interpretation of raw dielectric response data being difficult. In such situations, in order to discriminate and quantitatively analyse the contribution of conduction and different polarisation phenomena to dielectric response,

several mathematical models namely Debye, Cole-Cole and Havariliak–Negami, Universal law and Dissado and Hill's (DH) cluster model are generally used. However, the majority of models (except DH cluster theory) are suitable only for analytical representation of experimental data. Thus, selection of an appropriate modelling technique to describe physics of charge transport and polarisation phenomena of oil impregnated pressboard insulation is also a main contribution of this thesis. Moreover, this thesis concentrates on characterisation of the charge dynamic in insulating oils through modelling of their dielectric responses.

1.2 Scope of Thesis

The main purpose of this thesis is to develop a comprehensive framework to assess the condition of insulation systems of biodegradable insulating oil (ester oil) filled transformers. In order to do that, the applicability of well-established electrical and chemical based condition monitoring techniques developed for mineral oil-paper insulation systems on ester based transformer insulation is thoroughly investigated. The primary objectives of this thesis are given below.

1. To compare the ageing behaviour of high density pressboard insulation in two commercially available NE based insulating oils and one type of synthetic ester with the ageing of pressboard in a conventional mineral oil.

2. To understand the influence of moisture on the ageing process of pressboard insulation in mineral oil and NEs.

3. To investigate the applicability of existing oil based condition monitoring methods on ester–paper insulation systems and to provide necessary guidelines to improve these methods to comply with ageing characteristics of ester–paper insulation systems.

4. To investigate the applicability of Fourier Transform Infrared (FTIR) spectroscopy method to evaluate the ageing condition of pressboard insulation.

5. To understand the gassing behaviour of ester insulating oils under simulated thermal and electrical fault conditions.

6. To compare the charge transport and polarisation phenomena in NE insulating oil with those of mineral insulating oil through dielectric response modelling.

7. To investigate and compare the impact of moisture and temperature on dielectric response behaviour of mineral oil, NE and synthetic ester impregnated pressboard insulation.

8. To identify the impact of ageing condition on dielectric response behaviour of NE and mineral oil impregnated pressboard insulation.

9. To study the charge transport and polarisation effects in oil impregnated pressboard insulation through appropriate modelling techniques and to compare the impact diverse oil properties on dielectric response using model parameters.

10. To derive a relationship between moisture and dielectric response parameters of pressboard insulation and to identify the effect of temperature and ageing on the established relationship.

11. To investigate the applicability of existing FDS based moisture diagnosing tools on ester-paper insulation systems.

In order to achieve the above defined goals, a series of controlled laboratory experiments were conducted in this research with four types of insulating oils including one type of mineral oil, two types of NEs and a synthetic ester. The objectives (1) to (4) have been accomplished by performing two different accelerated ageing experiments with power transformer proportion of pressboard insulation, insulating oil and copper conductor material. At regular intervals, the measurements mentioned in Figure 1.1 are performed on oil and pressboard samples to analyse their degree of ageing.
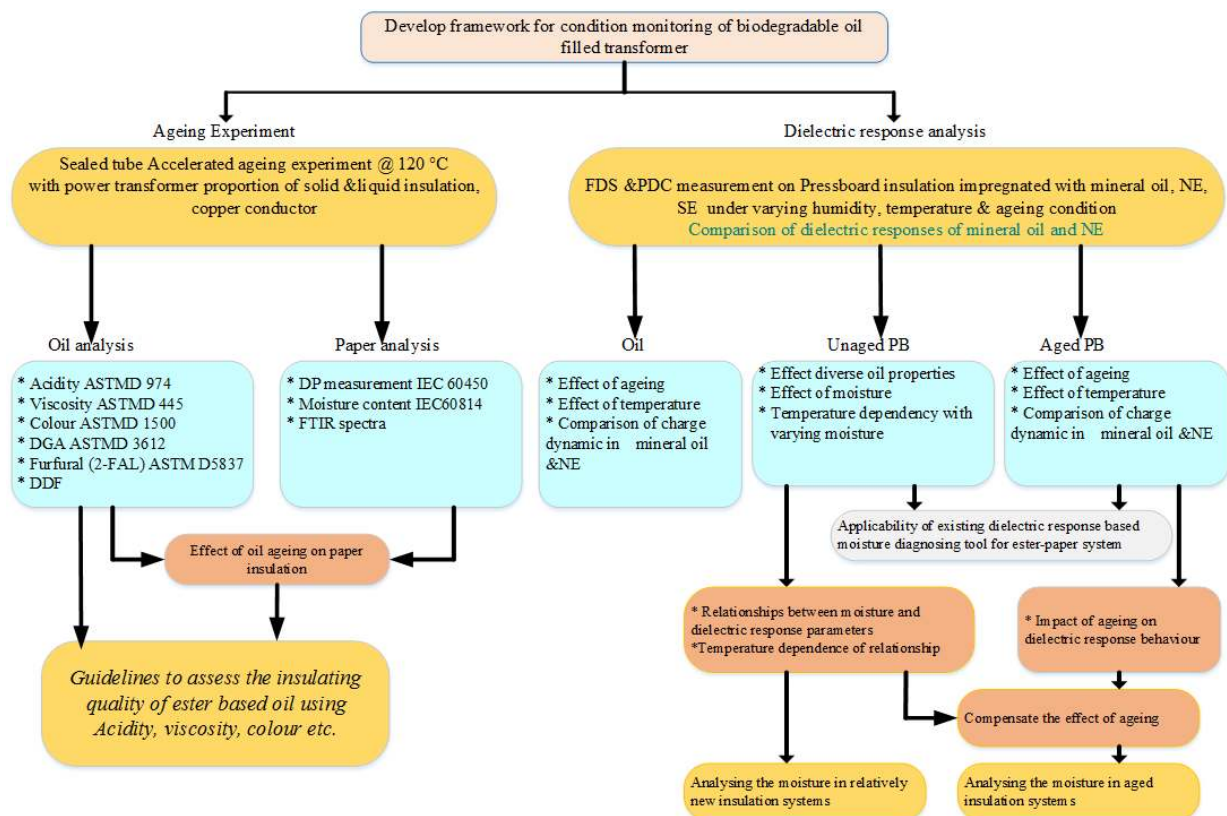
Figure 1.1. Block diagram of research overview

In this research gassing behaviour of mineral and ester oils under two different low temperature faults (120 °C and 150 °C) and low energy electrical discharge condition is investigated to complete

task 5. In order to achieve task 6, FDS and polarisation current responses of mineral oil and one type of NE oil are measured. In addition frequency and time domain dielectric response data of oils is analysed using new equivalent circuit and a mathematical relationship respectively.

The dielectric response results of pressboard insulation presented in this thesis are mainly frequency domain. In this thesis, objectives (7) to (11) have been accomplished by measuring dielectric response on different types of oil impregnated pressboard insulation samples. Measurements are performed over a wide frequency range from 10^{-4} (0.1 mHz) to 10^3 Hz at variable moisture contents (0.3%-8.8%) and temperatures (35, 55 and 75ºC). The effect of ageing condition on dielectric response is investigated only for mineral and NE impregnated pressboard. In order to explain microscopic level charge transport and polarisation phenomena in oil impregnated pressboard insulation, this thesis proposes a new equivalent circuit model based on DH cluster framework theory.

1.3 Thesis Outlines

Chapter 2 provides introductions to chemical composition and degradation mechanisms of insulation materials used in oil filled transformers. Moreover, experimental studies conducted for understanding the ageing behaviour of cellulose insulation in ester base biodegradable insulating oils and thermal degradation of ester oils themselves are reviewed.

Chapter 3 briefly reviews the chemical, physical and electrical based condition monitoring techniques which have been established for assessing the insulation quality of oil-paper systems. From an oil analysis point of view, more attention has been placed on describing the DGA and furfural analysis techniques. Theoretical background and interpretation of both time and frequency domain dielectric response measurements of transformer insulation are deeply discussed in this chapter.

Chapter 4 presents the results of ageing experiments. In this chapter ageing behaviour of pressboard insulation in mineral and ester insulating oils is compared. The ageing rate of pressboard insulation in mineral and NE insulating oils at two different moisture levels is demonstrated. Application of DDF, acidity, viscosity and colour for assessing the degree of ageing of ester insulating oils is discussed in Chapter 4. DGA results presented in this chapter intend to explain the different gassing behaviour of ester insulating oils under intense conditions. At the end of this chapter, applicability of available DGA interpretation tools (Duval Triangle, IEC gas ratio and IEEE key gas methods) on DGA data of ester based insulating oil is investigated.

Chapter 5 mainly analyses the FDS and polarisation current responses of a mineral oil and one type of NE insulating oil. Influence of temperature on dielectric response behaviour of aged and new insulating oil is explained using calculated activation energy. This chapter proposes a new equivalent circuit based on Jonscher's universal capacitor to analyse the low frequency dispersive behaviour in FDS responses of insulating oils. The new exponential model proposed in this chapter to explain polarisation current response of insulating oils allows us to identify the types of mobile ions in the oil and calculate their ionic mobilities.

Chapter 6 reviews the different types of time and frequency domain dielectric response modelling techniques. In this chapter, an equivalent circuit is proposed to discriminate and explain the polarisation and conduction effects of oil impregnated pressboard insulation under sinusoidal excitation of varying frequency. Moreover, application of this model to represent the frequency domain dielectric response data of mineral oil impregnated pressboard insulation is validated. Investigating the suitability of extended Debye and Williams-Watt stretched exponential function to characterise the dielectric response function of oil impregnated pressboard insulation is also a major part of this chapter.

Chapter 7 presents the dielectric response data of mineral oil and ester oils impregnated pressboard insulation samples under varying moisture, temperature and ageing conditions. A new mathematical model is presented in this chapter to correlate the low frequency conductivity and moisture content of pressboard insulation. This chapter uses the proposed hierarchical equivalent circuit in Chapter 6, based on DH cluster theory to explain charge transport and polarisation effects in oil impregnated pressboard. The selected equivalent circuit parameters are then used to determine the influences of moisture and diverse oil properties on dielectric response behaviour of pressboard insulation. In this chapter, temperature dependence of FDS of different types of oil impregnated pressboard insulation is analysed using calculated activation energy required for constructing so-called master curve.

Chapter 8 summarises the major findings and work presented in this thesis. Moreover, suggestions for future research are given at the end.

Chapter 2

Insulation in Power Transformers

2.1 Introduction

The insulation system is the most imperative part of a transformer and the lifetime of the transformer is almost solely determined by the condition of its insulation system. According to the materials used in an insulation system, transformers can be mainly categorised into three groups namely; oil filled, dry type and gas insulated transformers. However, insulation systems of almost all the load bearing transformers around the world are composed of cellulose paper based materials and insulating oil. Mineral oil, which is carefully refined from crude oil has been widely and economically used as an insulating liquid in power transformers for several decades. In order to improve the fire safety and reduce the environmental impacts, there is growing interest in using vegetable oil-based insulating liquids (NE) and synthetic esters in transformers as a potential substitute for mineral oil. Insulation breakdown in a transformer is a major issue, which can lead to a costly catastrophic failure. Thus, continuous assessment of a transformers insulation system has become a vital aspect of the modern power system. However, it is only possible with a better understanding of the behaviour of both liquids and solid insulation in typical transformer operating environments. In order to that, this chapter aims to discuss physical and chemical properties of cellulose based insulation materials and insulating liquids including their ageing mechanisms. A literature review on cellulose insulation material ageing in both mineral and ester based insulating liquids is also presented at the end of this chapter.

2.2 Development of Transformer Insulations

In the early days, materials which were plenty in nature and could be easily processed were used as electrical insulation [31]. However, after the invention of the electrical transformer in 1892, the field of insulation underwent dramatic changes because it was required to have materials which could withstand high electric and thermal stresses. In early transformers, cellulose and non-cellulose materials including low grade pressboard, cotton, silk, jute and asbestos in air were used as insulation [32]. Moreover, "boiled-in-oil" pressboard made up of cotton rags and paper clippings

was widely used in transformers before 1920 [32]. Bakelised papers started to be used in transformers from about 1915 and were continued until 1960. By early 1930, Kraft paper insulation (cellulose) with a combination of mineral oil became the predominant dielectric in transformers and they are still widely used. There have been several advancements in the cellulose paper insulation manufacturing process to improve their thermal stability and insulation properties for satisfying the high thermal and electrical stresses in modern transformers. The introduction of thermally upgraded paper in late 1950 was one of the major improvements in cellulose insulation technology because it led to a significant increase in the lifetime of transformers [33, 34]. Nowadays paper insulation produced from mixes of different cellulose based materials (Kraft and cotton) and blends of cellulose and synthetic materials is also used in transformer insulation applications.

2.3 Cellulose insulation

2.3.1 Overview of cellulosic insulation

Cellulose insulation is still the preferred choice for solid insulation in transformers from distribution level to large scale power transformers (10 kVA to 1500 MVA). However, it is not the best but it is economical and manufactured from a renewable source, which is plentifully available from soft wood. Cellulose insulation materials show excellent dielectric and mechanical properties in combination with insulating oil [35, 36]. Moreover, they have no melting or softening point and their mechanical strength does not significantly reduce at relatively low temperatures. These are the key features of cellulose insulation materials, which still make them irreplaceable.

According to [37], several tonnes of cellulose materials are used in a substation unit, mainly in the form of paper and pressboard. Cellulose paper is commonly used to insulate the conductor winding because its tensile strength is sufficient to enable cellulose paper to wind in a cylindrical form around the conductors at high speed [38]. Pressboard is more desirable for providing insulation at angles and corners where electric field stress is high. In particular, pressboard is largely used for the main insulation between LV and HV windings as barriers and spacers. Calendared board is a type of pressboard insulation generally used to produce washers and tubes of the insulation system. There is a special type of pressboard called pre-compressed board. It is ideal for strong support blocks and spacers which provide the desired mechanical strength to the insulation system. Both electrical grade paper and pressboard are generally made of unbleached Kraft wood, cotton, or a mixture of Kraft wood and cotton pulp. Detailed technical specifications of all types of papers and pressboards used in transformers for electrical insulating purposes as well as for structural purposes are specified in ASTM Std. D 4063, IEC Std. 60641-3-1 and IEC Std. 60641-3-2 [39, 40].

2.3.2 Chemistry of Cellulose

Cellulose is a natural homopolymer of D-anhydroglucose units (AGU) bonded together via C1-C4 glycosidic oxygen linkage as shown in Figure 2.1(a) [2]. Cellulose is often characterised by the degree of polymerisation (DP), which is the average number of glucose rings in a polymeric chain. Intramolecular hydrogen bonding between adjacent glucose units imparts linearity in cellulose polymeric chains. Intermolecular hydrogen bonding further forms hierarchically arranged highly crystalline microfibrils in the matrix of lignin and hemicellulose, which ultimately develops into a fibre [2, 5]. Physically, cellulose is a semi-crystalline material in nature, which has domains of high microcrystallinity and amorphous regions as shown in Figure 2.1(c). The crystalline domains are formed by arranging cellulose chains into a monoclinic lattice structure. Regions where cellulose molecules meander between crystalline domains are called amorphous domains.
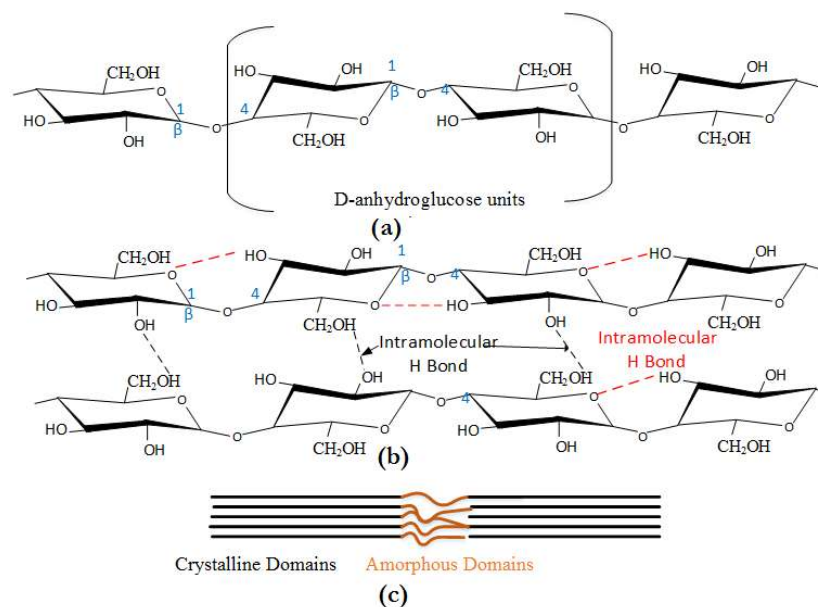
Figure 2.1. Chemical and physical structure of cellulose

2.3.3 Adsorption of moisture in cellulose insulation

Hygroscopic nature is a feature of all cellulose insulation materials due to their porosity and hydroxyl side groups in molecular structure because water molecules easily form hydrogen bonds with hydroxyl groups in cellulose molecules [41]. Water absorption by cellulose material primarily takes place in an amorphous region and in the pores of the cell walls. Thus, when the paper/pressboard insulation is exposed to a humid environment, it absorbs moisture and reaches an equilibrium state, where water pressure in the gaseous phase is equal to that of the adsorbed phase (cellulose paper/pressboard). The process of water absorption is almost solely determined by the temperature and relative humidity of the environment [26]. At a room temperature of 23ºC, cellulose paper can retain about 5 to 8% of moisture where the relative humidity of the atmosphere

is about 50%[41]. Change of percentage moisture content in a cellulose paper under varying temperature and relative humidity is shown in Figure 2.2 (a). An increase of moisture content in insulation paper leads to a decline in its dielectric and mechanical properties [26, 42]. Thus, it is recommended to keep cellulose insulation in a transformer in as much of a dry state as possible. The factory drying process reduces the moisture content in paper/pressboard insulation in new transformers to about 0.5% [26, 41].
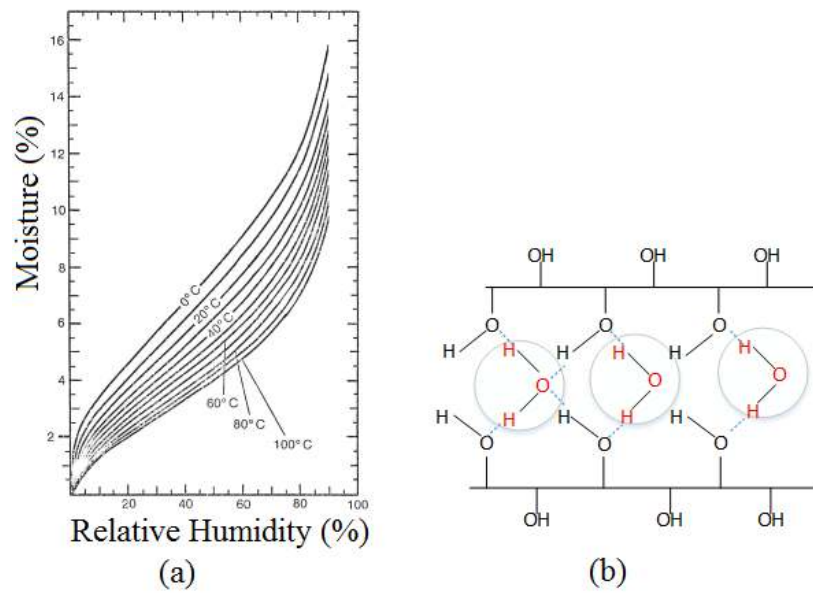
Figure 2.2. (a) Moisture adsorption curve of cellulose paper [26],(b) Schematic representation of bonding water molecules to OH groups of cellulose [41]

2.3.4 Oil impregnation

It is quite possible to have air spaces between and inside the fibres of cellulose paper; pressboard and thick laminated pressboard blocks used in the transformers insulation system. Though air spaces between fibres are individually tiny, they still occupy a considerable amount of volume in the solid insulation material which contributes to absorbing more water. Moreover, the presence of air pockets in the solid insulation causes partial discharges under AC field stress. During the course of oil impregnation, air spaces in the solid insulation are filled with oil and the absorption of water and partial discharges due to electric field concentration in air pockets are thus avoided.

Impregnation of a thin layer of paper insulation is quite easy, but impregnation of solid insulation blocks with larger thicknesses is extremely difficult. During the impregnation of oil, it is very important to ensure that no cavities are left inside the cellulose insulation to avoid dangerous electrical discharges [43]. Dynamics of oil flow into a cavity (capillary) can be expressed with Poiseuille's law (eq (2.1)). As explained by eqns (2.1) and (2.2), it is clear that the process of oil

flow into a capillary is mainly governed by three factors namely oil viscosity, capillary radius and air pressure inside the capillary. It means the reduction of air pressure inside the capillaries (P_I) is important for an efficient impregnation process. Therefore, the oil impregnation process is generally performed under very high vacuum condition [43-45].

$$\frac{dv}{dt} = \frac{\pi}{8\eta} \frac{r^4}{L} \left(P_0 - P_I \right) \tag{2.1}$$

Where V is the volume of oil inside the capillary, r is average equivalent capillary radius, L is the depth of impregnation increasing with time and η is the viscosity of oil.

$$P_0 = P_E + P_s \tag{2.2}$$

Where, P_E is the external pressure and P_S is the pressure created by the capillary action of oil.

Substitute $V = \pi r^2 L$ into eq(2.1)

$$L = \frac{1}{2} r \left(\sqrt{\frac{P_E + P_S - P_I}{\eta}} \right) \sqrt{t} \tag{2.3}$$

According to the eq (2.3), the time taken for complete impregnation is principally decided by the viscosity of the oil. Viscosity of ester oil is higher than that of conventional mineral oil. Therefore, efficient impregnation of cellulose insulation materials with ester oils is doubtful to some extent. This may be part of the reason for a slow down on their application in large transformers [43]. In general, the viscosity of insulating oils decreases with temperature. Therefore, impregnation of transformer solid insulation with ester oils should be performed at a higher temperature to have a similar degree of impregnation with mineral oil at a lower temperature.

2.3.5 Kraft paper and pressboard

Electrical grade Kraft paper and pressboards are produced through an unbleached Kraft pulping process of wood pulp derived from coniferous, or softwood trees, such as spruce and hemlock [37, 46, 47]. Unbleached wood pulp is desirable in manufacturing Kraft paper/pressboard because residual bleaching agents make insulation paper more conductive [17]. In general, the wood pulp should be a mixture of a high percentage of softwood and a low percentage of hardwood to provide mechanical strength and smoothness to paper insulation. Usually, softwood is coarser and has lengthy fibres compared to hardwood. Both soft and hard woods are mainly composed of cellulose, lignin and hemicellulose (Pentos). Softwood typically contains 40-55% cellulose, 15-35% of lignin and 25-40% of hemicellulose [5]. Lignin is a brownish complex polymer of aromatic alcohols which cements bundles of cellulose fibre together as shown in Figure 2.3. Hemicellulose is a

complex group of water-soluble polysaccharides (polymer of glucose) with a lower degree of polymerisation of about 200. Overall, wood pulp has a microscopic fibrous structure as shown in Figure 2.3.
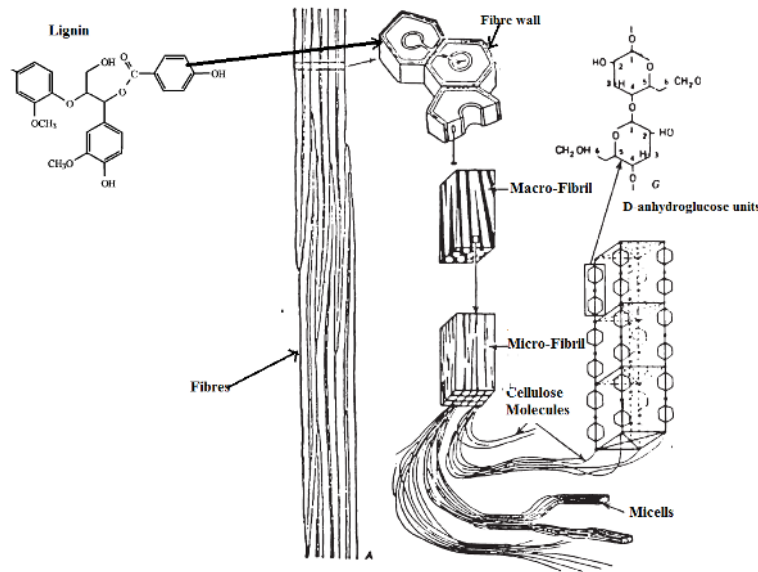
Figure 2.3. Micro structure of wood fibres [37, 48]

During the process of manufacturing Kraft paper and pressboard insulation, raw wood pulp is subjected to a series of chemical and physical processes such as Kraft pulping, refining and roll-forming [17, 37, 46]. This complete process results in increasing cellulose content in Kraft paper to about 90% and decreases both lignin and hemicellulose content to about 3-7% [49, 50]. This is necessary to provide enough mechanical strength and thermal stability to Kraft paper and pressboard.

Mechanical strength of Kraft paper/pressboard insulation is almost solely determined by the degree of polymerisation (DP) of cellulose molecules in paper/pressboard insulation. The average DP value of natural cellulose molecules in wood pulp is around 20,000. Chain scission during Kraft and drying processes causes to reduce the average DP value of paper insulation to about 1200.

2.3.6 Cotton Paper

Cotton fibres are an alternative source which is used to produce electrical grade insulation paper/pressboard with high tensile, tear and burst strength and good dielectric properties [17, 46]. Cotton fibres used in insulation paper manufacturing mainly come from new cotton rags and the first-grade cotton linters remaining on the cotton seed after removing the staple fibres. Staple fibres are taken for cloth manufacturing [51]. Cotton fibres comprise a higher concentration of cellulose than wood fibres. [52]. Cellulose content in cotton fibres pulp is in the range 62%-98%. It makes a

condition to pulping use 0-alkaline way to reduce cleavage of cellulose and helps to increase the thermal ageing property of cotton based papers [52]. Cotton fibres are typically longer than wood fibres. Moreover, cotton fibres are smoother than wood fibres and it results in weak intrinsic bond strength (inter and intra hydrogen bond). Thus, in order to increase the mechanical strength of the cotton paper, it requires more work in crushing and refining stages to increase the side groups in the cotton fibre and enhance intrinsic bond strength. Paper insulation is also produced from a mixture of unbleached Kraft wood pulp and cotton pulp. Mixing of Kraft wood pulp with cotton improves the dielectric and mechanical strength of paper insulation [17, 53]. Moreover, Kraft-cotton composite paper shows a better oil absorption capability. There is a great importance of a high oil abortion property in the use of Kraft-cotton composite paper to insulate some parts of a transformer winding, where oil impregnation is extremely difficult even under high vacuum conditions.

2.3.7 Special types of cellulose paper

Crepe paper, high extensible paper, thermally upgraded paper and diamond dotted press paper are four different types of cellulose insulation which have been specifically manufactured to meet certain requirements in insulating transformers. Crepe paper is produced from normal Kraft paper, such that a drum of Kraft paper is unrolled and passed through an aqueous bath containing a creping compound, it is then collected by a second drum rotating at a slower speed than the first drum [37]. Crepe paper is an extensible material which has approximately 20 % of elongation in machine direction. When insulating some parts of the transformer such as connection leads to an on-load tap changer and electrostatic control rings, the elongation property of crepe paper is very important because it allows the shaping of the paper to form bends and irregular shapes [17]. The chief disadvantage of crepe paper is that it shows a tendency to lose its elasticity property over time.

CLUPAK paper is the ideal alternative to crepe paper. It is highly extensible paper insulation with good burst, stretch and cross machine tear properties. The process of manufacturing CLUPAK paper is almost the same as normal Kraft paper. The difference is the last step called roll-forming has been modified to add an elasticity property to CLUPAK paper, such that rolling is performed in conjunction with moisture and heat.

In the process of manufacturing thermally upgraded paper, nitrous compounds such as urea, melamine, dicyandiamide and polyacrylamide (upgrading agents) are added in the pulping stage to protect cellulose from oxidation [54]. Upgrading agents chemically modify the cellulose molecules such that some of the less stable hydroxyl groups in the cellulose structure are being replaced with more stable CH_2CH_2CN groups as shown in Figure 2.4 (cyanoethylation) [46, 54].
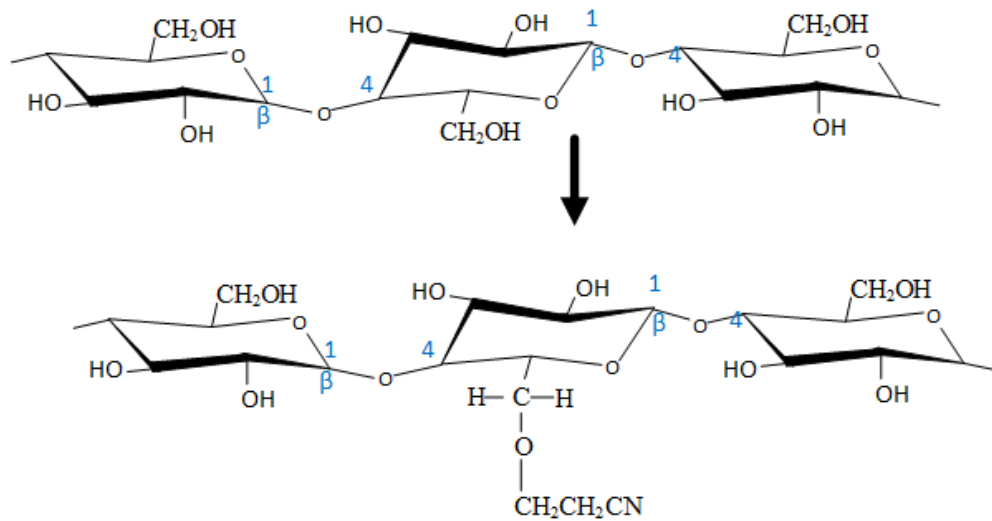
Figure 2.4. Process of cyanoethylation [54]

2.4 Degradation of Cellulose Insulation

2.4.1 Overview of Cellulose ageing

Ageing of cellulose insulation is an irreversible rupturing of covalent and hydrogen bonds within and between cellulose polymer chains under combined influences of heat, moisture and oxygen, which are all present in operating transformers [4-8]. The major consequence of ageing is that paper insulation converts into a brittle material, which has almost lost its mechanical strength [55]. It may lead to irreversible internal damage to the insulation system or catastrophic failure particularly in a situation where winding insulation experiences huge mechanical stresses due to short circuit faults in the power system [9]. In addition, the broken paper particles disperse in oil and they can align with local electric fields and create short circuit paths leading to catastrophic failure [36].Therefore, a good understanding of the processes involved in ageing of paper insulation is important to trigger early warnings of insulation failure, through interpretation of cumulative ageing by-products dissolved in oil, which are easily accessible. Degradation of cellulose insulation is a combination of pyrolysis, oxidation and hydrolysis reactions, which are predominantly governed by temperature, reactive oxygen species and moisture respectively.

2.4.2 Pyrolysis degradation of cellulose paper

Heating of cellulose beyond 130ºC tends to break the glycosidic bonds and open the glucose rings [6]. Such chemical degradation of cellulose, only due to intense heat in the absence of an oxidising agent and moisture is known as pyrolysis. Pyrolysis of cellulose mainly yields solid carbon

containing products (char), water, carbon oxide (CO_2 and CO) carbonyl compounds, hydroperoxide and volatile tar including epoxy-bridged molecules namely 1,6-anhydro β-D-glucopyranose (levoglucosan) [5, 6, 38, 50, 56].

Further, pyrolysis of levoglucosan produces a different class of substances including carboxyl acids (Pyruvic acid, laevulinic acids and acetic acid), aldehyde, alcohol (acetone and methanol), heterocyclic compounds also known as furanic compounds (2-furaldehyde-2FAL and 5-hydroxymethyl-furfural-5HMF) and a lesser amount of aromatic and aliphatic hydrocarbons [5, 26, 57]. Formation of levoglucosan proceeds via homolysis reaction followed by elimination of a water molecule (dehydration of ^1C and ^2C atoms) and internal rearrangement to a more stable ^1C to ^6C oxygen bridge structure as shown in Figure 2.5 [50, 58, 59]. Elimination of two further molecules of water and one formaldehyde from a levoglucosan molecule and rearrangement of internal bonds yield 2-FAL which is the most stable furanic compound.
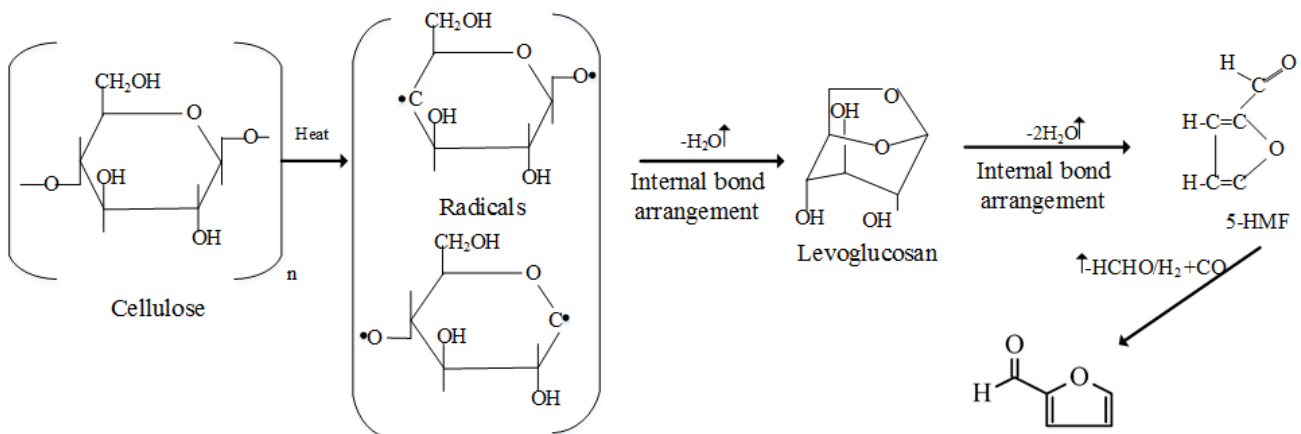
Figure 2.5. One probable cellulose pyrolysis mechanism via levoglucosan to 2-FAL [5, 59]

In general, the average hottest-spot temperature is 110 ℃ and 95 ℃ for transformer insulation systems rated at 55 ℃ and 65 ℃ of average winding temperature rise. However, the local hot spot temperature could be greater than 130 ℃ under an overloading condition or due to a problem with the cooling system. In such conditions paper insulation around the hot-spot is subjected to pyrolytic degradation. Moreover, pyrolysis could be the main mechanism for degradation of paper insulation in a new sealed type transformer with relatively dry paper insulation.

2.4.3 Hydrolysis degradation of cellulose paper

Moisture and low molecular acids are the two factors which largely influence the hydrolytic degradation of cellulose insulation paper/pressboard. Hydrolysis of cellulose is a catalysed reaction, which is almost exclusively controlled by the total concentration of H^+ ions from dissociation of low molecular acids in water [60-62]. The whole process is a dissociable acids catalysed reaction

and water plays a role as a reactant without participating in the reaction rate controlling steps [62]. Thus, the presence of dissociable acids causes hydrolytic degradation of cellulose paper even with low moisture concentration. However, water causes to dissociate acids and in this way it has a profound influence on hydrolysis reaction. Hydrolytic degradation of cellulose yields water and low molecular carboxyl acids namely formic acetic and laevulinic. Therefore, it is an auto-catalytically accelerated reaction [61, 63].
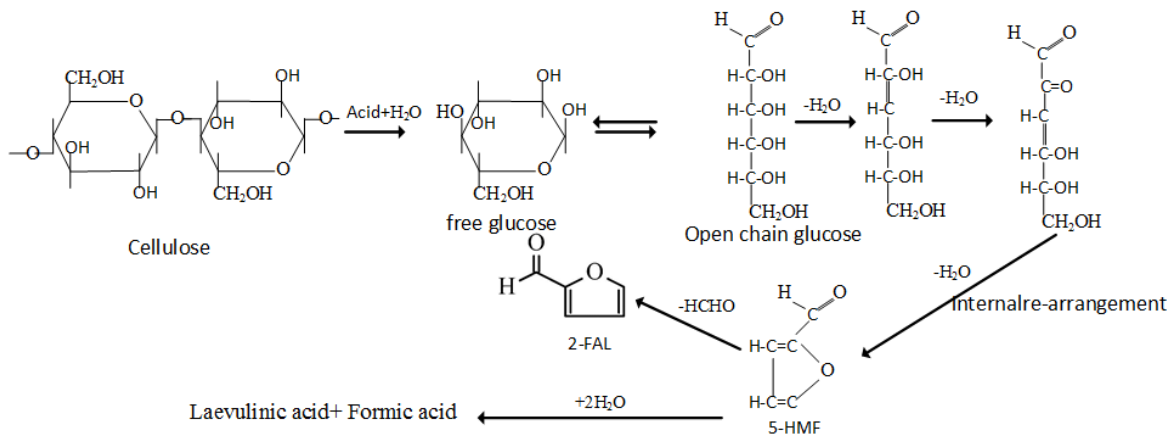
Figure 2.6. One probable hydrolytic degradation mechanism of cellulose via enol path to form 2-FAL and carboxyl acids [6, 64]

In the first step of hydrolysis reaction, the combined influence of water and acid cleaves the glycosidic bond yielding free glucose molecules [6, 64]. This chain scission reaction consumes one molecule of water. Unstable free glucose molecules are subjected to further hydrolysis and it takes place via formation of an epoxide or an enol followed by series of chain opening, dehydration and an internal bond-arrangement to form 5-hydroxymethyl-2-furaldehyde (5-HMF) [56, 65]. Hydrolytic degradation of one monosaccharide unit (glucose) to a 5HMF releases three water molecules. Thus, net production of water molecules per reaction is two. 5-HMF is not a stable compound and it decomposes into different types of furanic compounds including 2-FAL, 2-acetyfuran (2-ACF), 2-furoic acid, 2-furfuryl alcohol (2-FOL) 5-methyl-2-furfural (5-MEF) [6]. The reaction between 5-HMF and water yields laevulinic and formic acids [64]. High temperature causes to dissociate formic acid into carbon monoxide and water. Moreover, laevulinic acid tends to polymerise and produces dark brown polymer known as caramel followed by formation of sludge. Figure 2.6 shows the basic steps of hydrolytic degradation of cellulose via enol path.

For an in-service transformer, moisture in its paper insulation can increase to about 2% after 10-15 years of operation because moisture is a by-product of cellulose ageing. Moreover, a leaking seal may also cause to increase the moisture in the insulation system. In such conditions hydrolytic

degradation of cellulose can occur at normal transformer operating condition becoming the dominant ageing mechanism of paper/pressboard insulation.

2.4.4 Oxidative degradation of cellulose paper

Primary and secondary hydroxyl groups in a pyranose ring of cellulose molecules are highly oxidation susceptible sites. Thus, in general these hydroxyl groups involved in initiating oxidative degradation of cellulose yield carbonyl (aldehyde) and carboxyl (acidic) compounds as primary by-products [6, 66]. This causes to weaken the glycosidic bond and makes an acidic condition, which induces chain scission via hydrolysis. Thus, the whole process is a mixture of oxidative and hydrolysis reactions [63].
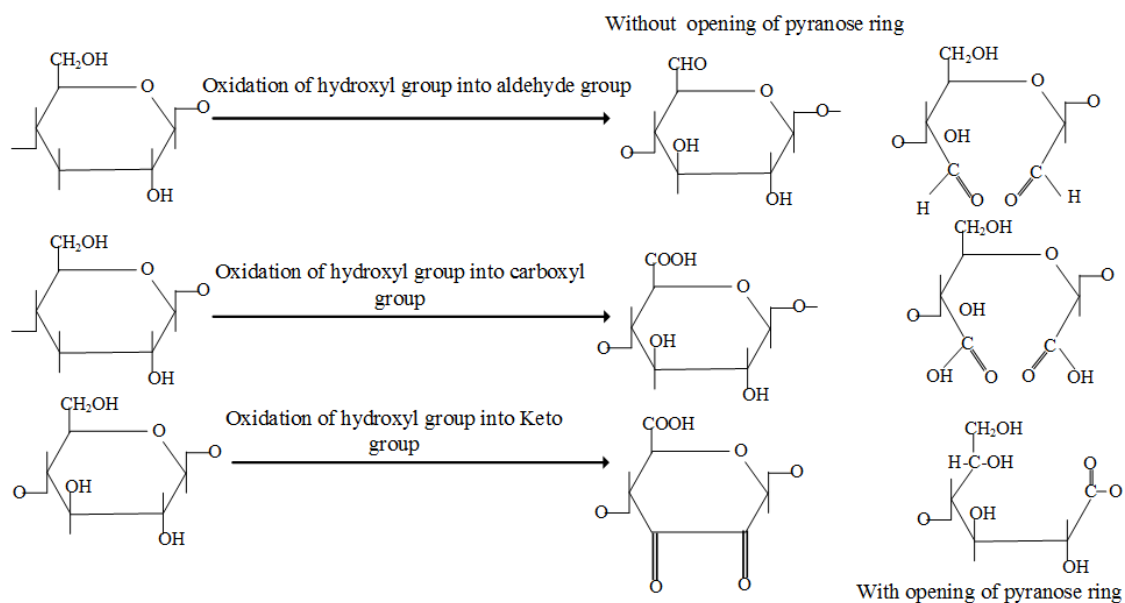
Figure 2.7. Probable mechanism of oxidation of hydroxyl groups in cellulose molecules

Figure 2.7 shows the probable oxidative mechanism of cellulose. Oxidation of secondary hydroxyl groups in cellulose molecules perhaps causes to open the pyranose ring of cellulose, but it doesn't always. Overall, oxidation of cellulose is a slow combustion reaction and mainly produces water and carbon dioxide [62]. Lundgaard et al [62], have specifically reported that oxidative degradation of cellulose and hemi-cellulose in insulation paper forms furanic compounds (5-HMF, 2-FAL, 2ACF, 2-FOL) and carboxyl acids including formic and laevulinic acids.

Oxidation reaction in cellulose paper is autocatalytically accelerated by reactive oxygen species like hydroxyl radical (OH $^\bullet$) from decomposition of hydrogen peroxide (H_2O_2) [62, 63]. In the transformer operating environment H_2O_2 is produced by reaction between oxygen and water in the presence of transition metal cations such as Cu^+/Cu^{2+} or Fe^{2+}/Fe^{3+}. In the case of a free breathing transformer, the oil is in direct contact with air and it causes to increase the dissolved oxygen

content in oil to about the range of 2000-3000 ppm. In such a condition, oxidative degradation of cellulose materials in typical transformer operating condition could be more pronounced than hydrolytic and pyrolytic degradation.

2.4.5 Kinetic model for cellulose paper degradation

A kinetic model of degradation of cellulose paper insulation which demonstrates the decrease of average DP over ageing time is useful in estimating the lifetime of a transformer insulation system. Emsley and Stevens [5] have found that most of the published ageing data on cellulose paper materials is shown to be in good agreement with the pseudo-zero rate kinetic model developed by the Ekenstam in 1936 for linear polymer degradation. As shown in eq (2.4) the rate of reaction k of pseudo-zero model is constant throughout the ageing process and it is assumed to be proportional to the number of unbroken polymer chain bonds available in the system Moreover, reaction rate depends on the availability of reactants such as moisture, acids and oxygen.

$$\frac{1}{DP_t} - \frac{1}{DP_0} = kt \qquad (2.4)$$

Where DP_0 and DP_t represent the average degree of polymerisation at the initial (t=0) and at any time t respectively. However, Emsley et al [49] have reported that pseudo-zero law eventually breaks down when DP of cellulose paper insulation reaches a value of 200. Thus, it has been suggested that the use of a first order kinetic model with two coefficients (k_2 and k_{10}) as shown in eq (2.5) is more appropriate than pseudo-zero model with one coefficient under such a condition.

$$\frac{1}{DP_t} - \frac{1}{DP_0} = \frac{k_{10}}{k_2}\left(1 - e^{-k_2 t}\right) \qquad (2.5)$$

Emsley has characterised the temperature dependence of reaction rate using so-called Arrhenius relationship as shown in eq (2.6).

$$k = A \times e^{\left(\frac{-E_a}{RT}\right)} \qquad (2.6)$$

Where E_a is the activation energy of reaction in Jmol[-1], T is temperature in kelvin, R is the gas constant (8.314 Jmol[-1]K[-1]) and A is a pre-exponential factor in h[-1]. From their investigations, Lundgaard et al [62] and Emsley [5] have claimed that activation energy for a degradation reaction of Kraft paper is about 114 kJmol[-1] and 111 kJmol[-1] respectively and it does not depend on the condition of the reaction environment. This has been recently confirmed by the activation energy value of 106 kJmol[-1] obtained in an ageing study performed with grade 3 press paper in different

moisture and oxygen conditions [53]. Factor (*A*) shows great dependence on the availability of reactants such as moisture, low molecular acids in paper and dissolved oxygen in oil. An increase of these reactants results in magnifying pre- exponential factor (*A*) by several orders of magnitude leading to a higher reaction rate. Combining eqns (2.4) and (2.6), the expected lifetime of the paper insulation at a given temperature can be calculated using eq (2.7).

$$expected\ life\ (year) = \frac{\frac{1}{DP_{end}} - \frac{1}{DP_{start}}}{A \times 24 \times 365} \times e^{\frac{E_a}{RT}} \tag{2.7}$$

Assuming that temperature is the only cause of degradation of paper insulation, IEEE loading guide also proposes a relationship in the form of eq (2.8) to evaluate the lifetime of transformer insulation [67].

$$PerunitLife = 9.8 \times 10^{-18} \times e^{\left(\frac{15000}{\theta_h + 273}\right)} \tag{2.8}$$

Where θ_h is the hotspot temperature and the time taken for falling DP of paper insulation to 200 at 110 °C (150 000 hrs) is assumed to be 1 per unit. A new parameter called acceleratory factor F_{AA} is introduced in the IEEE loading guide to quantify the degradation of paper insulation under varying temperature conditions. F_{AA} can be calculated using eq (2.9) and it is equal to 1 at the reference temperature 110 °C. Acceleratory factor is then used to calculate the equivalent ageing factor (F_{EQA}) as given in eq (2.10).

$$F_{AA} = e^{\left(\frac{15000}{383} - \frac{15000}{\theta_h + 273}\right)} \tag{2.9}$$

$$F_{EQA} = \frac{\sum_{n=1}^{N} F_{AA,n} \Delta t_n}{\sum_{n=1}^{N} \Delta t_n} \tag{2.10}$$

Per unit life loss of paper insulation can then be determined by dividing the multiplication of F_{EQA} and time (*t*) by normal insulation life (150 000 hrs).

$$per\ unit\ life\ loss = \frac{F_{EqA} \times t}{Normal\ lifetime} \tag{2.11}$$

Table 2.1 Pre-exponential factor and activation energy of pseudo-zero kinetic model from literature

	Test Condition	Pre-exponential factor A (h^{-1})	Activation energy (kJmol^{-1})
Lundgaard [62]	Dry Kraft paper	2.0±0.5E+08	111
	Dry Kraft paper with acidic oil	2.4±0.7E+08	111
	Kraft paper with 1% water	6.2±2.9+08	111
Lelekakis [53]	Low oxygen with 0.5% water	1.28E+08 ±7E06	106
	High oxygen with 1.6% water	4.44E+09 ±5E08	106
	Low oxygen with 2.7%water	3.00E+09 ±6E08	106

Compared to the Emsley model (eq (2.7)), the major drawback of the IEEE lifetime estimation criteria is that it has not taken into account the effect of reactance in the system such as oxygen, water and acids [46]. It causes to overestimate the expected lifetime of paper insulation in a transformer with IEEE loading guide criteria. Figure 2.8 compares the calculated lifetime curves of paper insulation using parameters obtained in [53, 62] and eq (2.7) with IEEE lifetime curve. Here DP_{start} and DP_{end} are taken as 1000 and 200 respectively.
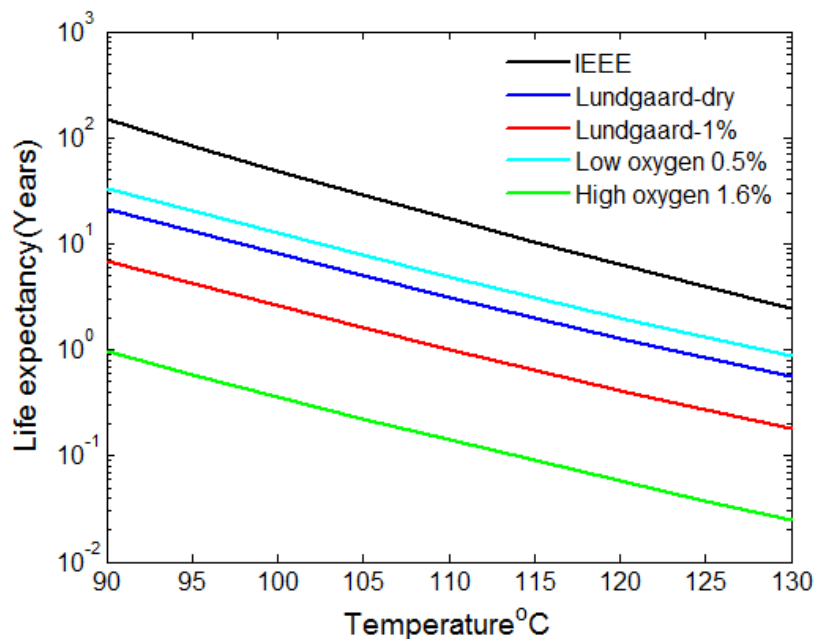
Figure 2.8. Comparison of life expectancy curve of paper insulation from different literature [53, 62, 67]

2.5 Insulating Liquids in Transformers

2.5.1 Overview of insulating liquids

Petroleum based oil (mineral), silicon oil, synthetic ester and NE based oils are currently being used as insulating liquids in oil filled transformers. The amount of oil used in a transformer depends on the power and voltage rating. Typically, a pole-mounted unit rated at 25 kVA may contain about 100 litres of oil, whilst a large power transformer in a substation rated at a few hundreds of MVA may contain about 40 000 to 100 000 litres of oil [1, 37]. Insulating oil in a transformer plays dual roles as an electrical insulant and a heat transfer fluid. When the oil is functioning as a heat transfer fluid, it absorbs heat from the core and windings and then transmits to the external cooler surfaces of the transformer which are artificially or naturally cooled.

Mineral oil is still being commonly and economically used in almost all power transformers around the world due to its wide availability, good insulation properties, low cost and its compatibility with cellulose insulation materials [1, 68-70]. IEC Std. 61100 classifies typical mineral insulating oil as O class flammable fluid with a fire point of 180 ℃ [71]. Low fire point of mineral oil increases the risk of explosion of mineral oil filled transformers. A fire originating from mineral oil filled transformers causes potential damage to human life and other nearby infrastructure. Thus, additional works such as implementing a fire wall, fire safety, deluge systems and fluid containment are required when a mineral oil filled transformer is installed [14]. Therefore, it is expected that they be filled with an insulating liquid with a high fire point, when installed at critical places such as underground tunnel, ships and high density populated areas.

Silicon based insulating oil is a K class, less flammable synthetic fluid which can be used for such an application. However, use of both mineral and silicon oils in transformers can have significant negative environmental impacts such that they contaminate soil and natural waterways in the case of an accidental spill, due to their poor biodegradable properties [14, 72].

From safety and environmental points of view, mineral or silicon oils are no longer the best insulating liquids for transformers. In such situations there is a rapidly growing interest for the use of ester-based insulating liquids in power transformers [69]. Natural and synthetic esters are the currently used ester-based insulating liquids in the transformer industry. Both esters are readily biodegradable, less toxic and less flammable K class fluids. In Germany, NEs are considered as nonhazardous to water and an ultimately biodegradable substance according to aquatic biodegradation tests [11]. According to section 450.23 of U.S. National Electrical Code, NEs are defined as less flammable fluids [11]. The chief disadvantage of NEs is their high oxidation

susceptibility and therefore it is recommended only to use NEs in sealed type transformers. NEs are widely used in distribution level transformers [23, 71] and there is a growing trend to use NEs in high voltage and high power transformers [73-75]. FR3 and BIOTEMP are two commercially available NE based insulating liquids. Synthetic esters (MIDEL 7131) are generally used in both traction and distribution level transformers and less common in power transformers due to their high cost.

Table 2.2 Typical physicochemical properties of different insulating liquids [76]

Properties	Units	Test method	Typical Mineral oil	Typical BIOTEMP	Typical FR3	MIDEL 7131 synthetic ester
Fire Point	°C	ASTM D 92	180	360	362	322
Flash Point	°C	ASTM D 92	160	325	326	275
Specific Gravity	g/ml	ASTM D 1298 @20°C	0.88	0.914	<0.92	0.97
Kinematic Viscosity	cSt	ASTM D 445 @ 40°C	12	42	34	29
Relative Permittivity			2.2	3.2	3.2	3.2
Oxidation Stability	% per mass	Sludge after 72 h	<0.1	0.01	solid	non
Neutralization number (Acidity)	mg KOH/g	ASTM D 974	-	0.03	0.02	<0.015
		IEC 61099 9.11	-	<0.03	-	<0.03
Biodegrada-bility	%	CEC L-33-A-93	-	99	>99	30
		EEC Standard 79/831	83	-	-	-

Insulating liquids are produced by different manufacturers. However, all must meet certain specifications to use as an insulant and heat transfer fluid in transformers. Generally, all types of insulating liquids primarily should have high electrical strength, good thermal conductivity, low viscosity, high fire point, low pour point, excellent chemical stability and the ability to absorb gases that may evolve in certain intense conditions [17]. Moreover, better compatibility with cellulose insulation materials is of the utmost importance. IEC Std. 60296 and ASTM Std. D 3487 cover the technical specifications for mineral insulating oils used in power and distribution electrical apparatus including transformers and breakers. The technical specifications and methods of handling NE based insulating liquids used in similar type of apparatus are detailed in ASTM Std. D 6871-03 (2008) and IEEE Std. C57.147 (2008). New synthetic esters are produced in accordance

with IEC Std. 61099. Table 2.2 compares the typical properties of four different types of commercially available insulating liquids.

2.5.2 Mineral insulating oil

2.5.2.1 Chemistry and overview

Crude oil is subjected to a special refining process to produce mineral insulating oil, such that characteristics of the resulting oil comply with certain specifications which are compulsory to be used as an insulating liquid in high voltage apparatus like transformers and breakers. In the first stage of the refining process, crude oil is distilled at atmospheric pressure and then the residue is further distilled under vacuum [17]. Raw oil (distillate of vacuum distillation) is then subjected to a series of physical and chemical treatments to selectively remove unnecessary contaminants including sulphur, oxygen, nitrogen, olefines-alkenes, n-paraffin and polar organic substances [1, 17]. The presence of these contaminants in insulating oil causes a chemical instability.
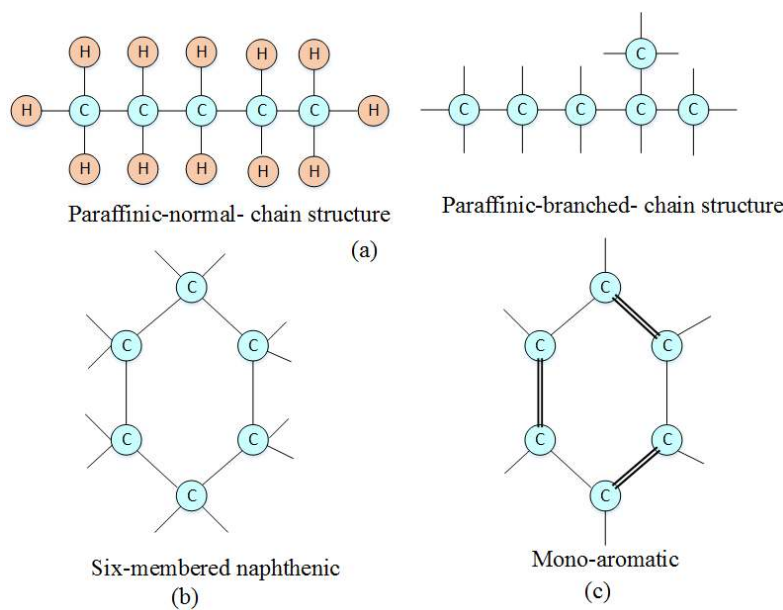
Figure 2.9. Molecular structure of three main groups of hydrocarbon molecules in mineral insulating oil (a) Paraffinic, (b) Naphthenic, (c) Aromatic

Refined mineral oil is a complex mixture of hydrocarbon molecules which mainly fall into three major groups namely paraffinic, (cyclo-paraffinic) naphthenic and aromatic [1, 17, 77]. As shown in Figure 2.9 (a) paraffinic molecules have a linear or branched structure. Naphthenic molecules have a ring structure with five, six or seven carbon atoms. However, six-membered ring configuration shown in Figure 2.9 (b) is the most common in naphthenic molecules. Aromatic molecules also possess a ring structure of cyclized six carbon atoms. The major difference between aromatic and naphthenic molecules is that there are alternative single (C-C) and double bonds

(C=C) in the aromatic ring as seen in Figure 2.9 (c). There are two main classes of aromatic molecules namely mono-aromatic and poly-aromatic whose structure includes single and two or more aromatic rings respectively. Though, aromatic molecules have unsaturated carbon double bonds, mono-and di-aromatic molecules show surprising good chemical stability. On the other hand, by-products of oxidation of some aromatic compounds accelerate the further oxidation of oil. Thus, during the refining process, aromatic content in mineral insulating oil is reduced to about (5-10%) to achieve optimal oxidation stability [17, 77].

2.5.2.2 **Ageing of mineral insulating oil**

Oxidation is the main degradation mechanism of hydrocarbon oil. Temperature, the presence of dissolved oxygen and catalyst metal are the most evident factors which govern the rate of oxidative degradation of mineral oil [15-17]. It has been reported in the literature that the rate of oxidation reaction exponentially increases with temperature (the reaction rate doubles for every 8-9 °C rise in temperature) [17, 77].
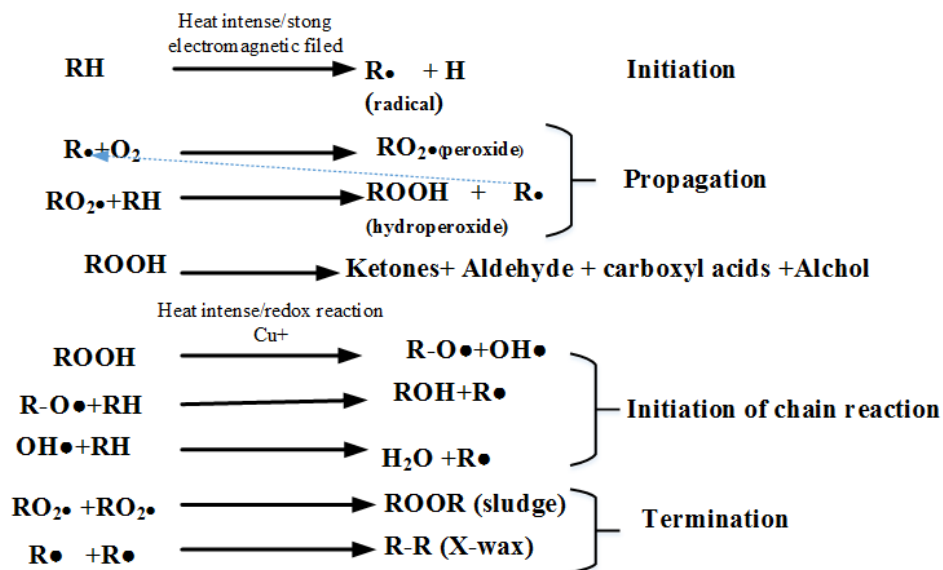
Figure 2.10. Major step of mineral oil oxidation [16, 77]

The breakdown of healthy hydrocarbon molecules into two free radicals due to intense heat and strong electromagnetic field produces a conducive environment to create an oxidation reaction in oil. These radicals react with oxygen and produce highly reactive peroxide molecules. Reaction between peroxide and a hydrocarbon molecule forms a hydroperoxide and a radical. Intense heat causes hydroperoxide molecules to dissociate into alkoxy and hydroxyl radicals leading to a chain reaction as shown in Figure 2.10. Copper which is readily available in a transformer promotes redox reaction in oil and dissociates hydroperoxide in a way similar to heat. Unstable hydroperoxide can also be decomposed into ketone and water. The oxidation of ketones forms aldehydes and carboxyl

acids [78, 79]. These by-products make oil more conductive and result in negative impacts on dielectric withstand characteristics.

An increase of radical population in the oil causes the enhancement of random reaction between radicals leading to a formation of large insoluble colloidal substances (sludge and X-wax) having a molecular weight in-between 500 and 600 [16]. This results in the colour of the oil turning darker and decreases the heat transfer capability due to an increase in viscosity. Reaction between large colloidal substances and metal also produces metallic soaps, lacquers, aldehydes, alcohols, ketones and organic acids [16, 77]. These reactive chemical intermediates are largely absorbed by the transformer winding leading to a deposit of heavy tarry acidic sludge on winding insulation. It causes hotspots to form and increase the rate of ageing of cellulose paper insulation. The overall degradation process of oil is irreversible and impairs its heat transfer and dielectric properties. Thus, oxidation inhibitors are added to delay the oxidative degradation of oil. 2,6 di-tertiary-butyl phenol, 2,6 di-tertiary-butyl para-cresol, or metal deactivators such as benzotriazole and its derivatives are some of the oxidative inhibitors included in mineral insulating oil, which does not have natural inhibitors [71, 80].

2.5.3 Natural ester insulating oils

2.5.3.1 Chemistry and overview

NE based insulating oils are commonly produced from soy, sunflower and rapeseeds mainly due to availability, low cost and having characteristics allowing them to be used as a heat transfer fluid and insulant in transformers [71]. Raw vegetable oils contain a myriad of unnecessary compounds including, gums, wax, metal particles, volatile compounds and free fatty acids. These substances show adverse impacts on appearance and performance of oil. Therefore, raw oil is subjected to a series of chemical and physical treatments namely, degumming, refining, bleaching and deodorization to selectively remove unwanted substances and improve the quality standard (appearance, chemical stability) of oil [81, 82].

In the case of insulating oil manufacturing, a special bleaching technique is applied to ensure low electrical conductivity of the resulting oil, a desired property for insulating oil. Finally processed oil is degassed and dehumidified to extract dissolve oxygen and moisture respectively. According to IEEE Guide for acceptance and maintenance of NE fluids in transformers, NEs are compatible and miscible in all proportions with conventional mineral insulating oil, but it causes the lowering of the flash and fire point of the resulting oil [83]. Concentration of mineral oil in excess of 7 % causes the reduction of fire point of NE to below 300 ℃.

NE molecules are called triglycerides whose molecular structure has three fatty acid molecules chemically linked to a glycerol molecule as shown in Figure 2.11 [84]. Constituents of all types of NE are almost the same. On the other hand, as listed in Table 2.3 fatty acid composition of vegetable oils extracted from different sources are dissimilar to some extent.
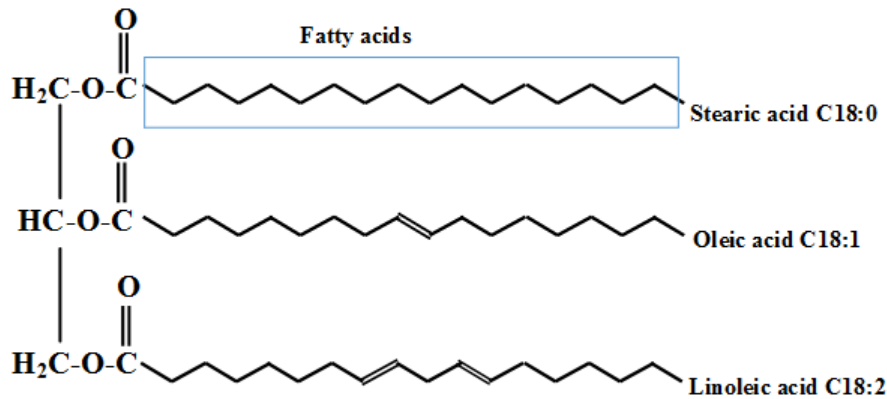
Figure 2.11. Molecular structure of Natural ester [84]

In general, saturated, mono-unsaturated and polyunsaturated fatty acids with two or more carbon double bonds are available in NEs. The number of carbon atoms in saturated and mono-unsaturated fatty acids (oleic) are typically in the range between 8 to 22 and 10 to 22 respectively [79, 81]. Di and tri-unsaturated fatty acids namely linoleic and linolenic mostly have 18 carbon atoms. Physicochemical properties of NEs such as viscosity, pour point and oxidation stability are solely determined by their fatty acids composition. Saturated fatty acid is a chemically stable compound. However, an increase of saturated fatty acid content in the oil causes an increase in the viscosity and to freeze oil to solid below room temperature. On the other hand, increases of polyunsaturated fatty acids composition in oil results in lowering both pour point and viscosity. However, polyunsaturated fatty acids are highly susceptible to oxidation. The relative oxidation susceptibility of saturated: mono: di: tri: unsaturated C-18 (18 carbon atoms) fatty acids is roughly 1:10:100:200 [81]. Therefore, an increase in unsaturated fatty acids composition significantly reduces the chemical stability of oil.

Low pour point, low viscosity and high oxidation stability are desirable properties of insulating liquid in transformers. Therefore, high oleic (HO) vegetable oils are chosen in manufacturing insulating oil to ensure low pour point, low viscosity and desirable oxidation stability of the resulting oil. BIOTEMP insulating liquid is produced from high-oleic sunflower oil, which contains 5 % of saturated stearic acid (C:18:0), 86 % of mono-unsaturated oleic acids (C18:1), 6 % of linoleic acid (C:18:2) and 0.1 % of linolenic (C18:3) [76]. Due to ester groups in their molecules

structure, NE based insulating oils are more hygroscopic than typical mineral oil and their moisture solubility is about 1000 ppm at 25 ºC. Moreover, they possess higher kinematic viscosity than mineral oil as listed in Table 2.2. NE insulating oils are generally more oxidation susceptible than conventional mineral oil. Therefore, in addition to 2,6-di-tert-butyl-para-cresol, complex phenols and amines are also included as the oxidation inhibitors in NE based insulating oils [85]. Though, oxidation inhibitors can provide enough oxidation stability, NE based insulating oils are recommended to only be used in sealed type transformers.

Table 2.3 Fatty acids composition of different vegetable oil [76, 81, 84]

Type of oil	Palmitic C16:0 +Stearic acid C18:0 (%)	Oleic acid C18:1(%)	Linoleic C18:2(%)	Linolenic C18:3(%)
HO sunflower	5	86	6	0.1
HO Soy	3-5	75-85	2-5	2-5
HO rapeseed	4-6	75-85	6-10	3
Typical sunflower	10	19	65	-
Typical soy	15	24	54	7

2.5.3.2 Degradation of NE insulating oils

Oxidation is the major degradation mechanism of NEs and it is also a radical chain reaction similar to the mineral oil oxidation. Metals such as tin, iron and copper act as effective catalysts in oxidation of NE whereas lead shows very little impact. Since the strength of a hydrogen-carbon bond next to carbon-carbon double bond sites in fatty acid groups is weak, free radicals are easily formed in NEs by eliminating a hydrogen atom from the methylene group next to a double bond [18, 84]. It has been reported in the literature [18] that vegetable oils containing polyunsaturated fatty acids auto oxidise even at room temperature but mono-unsaturated fatty acids (oleic acids) oxidise only at high temperature. Thus, it is clear that the degree of unsaturation is the major factor which determines the oxidation stability of NEs.

As shown in Figure 2.12, reaction among free radical, oxygen and oil molecules results in formation of triglyceride hydroperoxides and another radical propagating oxidative reaction [18, 79]. Triglyceride hydroperoxides break down to form more radicals leading to a chain reaction in a way similar to mineral oil oxidation. A myriad of non-volatile and volatile compounds including smaller oxygen containing by-products such as alcohols, aldehydes (octanal and nonanal with some heptanal), ketones (2, 4-heptadienal) and high molecular acids are also produced by decomposition of triglyceride hydroperoxides [18, 68, 71]. At the last stage of oxidation, secondary non-volatile substances of oxidation are subjected to cyclisation and polymerisation processes leading to a

formation of high molecular weight compounds including gel and lacquer [18]. Concurrently the viscosity of NEs measurably increases and it degrades the cooling capability of oil.
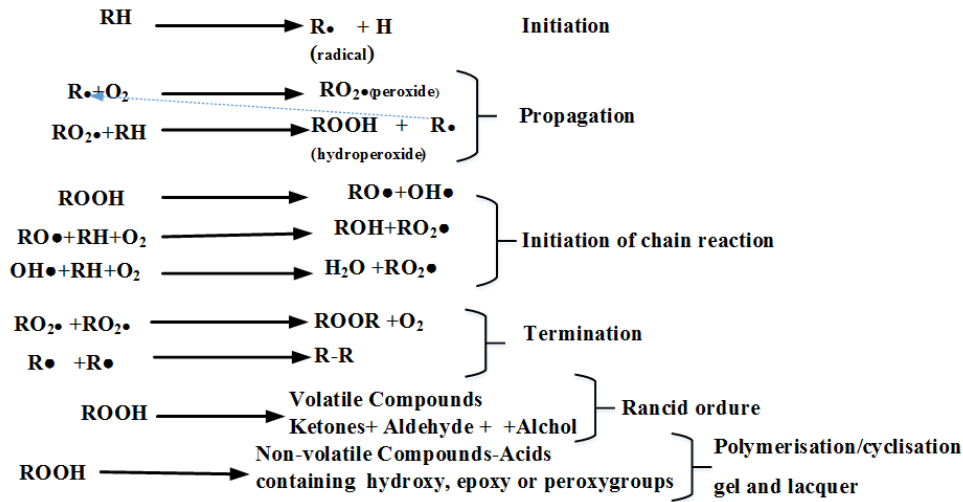
Figure 2.12. Major steps of NE self-oxidation (R denotes hydrocarbon unit) [18, 68]

In the case of NEs, hydrolysis is another degradation reaction, which concurrently occurs with oxidation. This is an autocatalytic reaction because free fatty acid molecules themselves accelerate the hydrolysis reaction [84]. There are three major steps in the hydrolysis reaction in NEs, which are also reversible as shown in Figure 2.13 [86]. In general hydrolytic degradation largely increases the acidity of NEs over time.
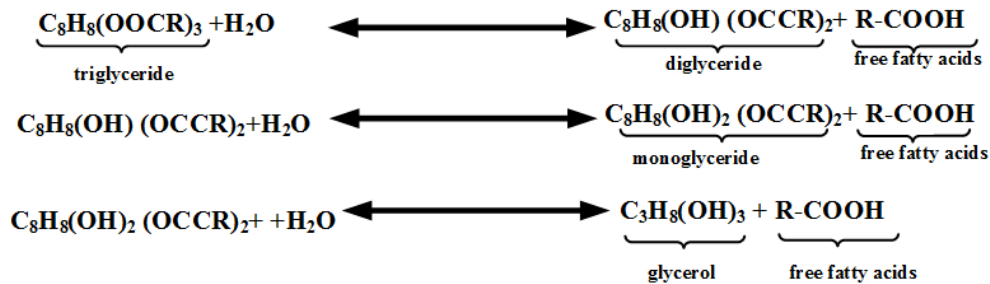
Figure 2.13. Major steps of NE hydrolysis degradation

2.5.4 Synthetic ester insulating liquids

2.5.4.1 Chemistry and over view of synthetic ester oil

Chemical reaction between polyol (molecules with more than one alcohol group) and synthetic or natural carboxyl acids yields synthetic esters whose molecular structure have multiple saturated fatty acid groups (mostly 2, 3 and 4) connected to the polyol backbone. There are seven main types of synthetic esters namely diester, phthalate, trimellitate, pyromellitate, dimer acid ester, polyols, and polyoleates [87]. Pentaerythritol ester is an example of a commercially available synthetic ester

insulating oil which is produced from a branched mono-acid containing 5 to 18 carbon atoms and alcohol pentaerythritol [71, 87]. The molecular structure of Pentaerythritol synthetic ester which has four fatty acid groups connected to a central polyol backbone is shown in Figure 2.14. Since synthetic ester insulating oil molecules only contains saturated fatty acids, it possesses excellent oxidation stability compared to both mineral and natural ester. Detailed technical specifications of new synthetic ester insulating oil are available in IEC 61099 [88] and an in-service maintenance guide that is published as in IEC 61203 [89].
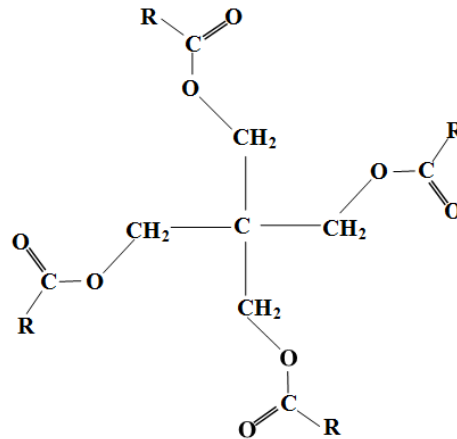
Figure 2.14. Synthetic ester insulating liquid molecules with 4 fatty acids groups

2.5.4.2 **Ageing of synthetic ester insulating oils**

Synthetic ester insulating oils slowly oxidise at high temperature which is accompanied by production of gases (CO, CO_2 and H_2). Thermo-oxidative degradation of synthetic ester oil is also a free radical chain mechanism.
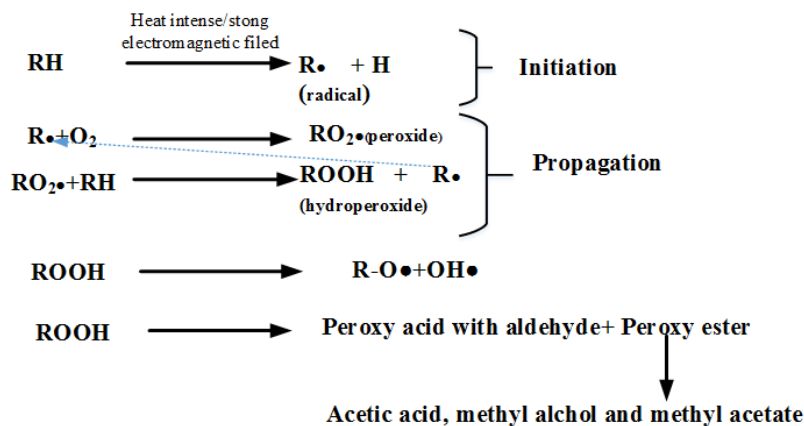
Figure 2.15. Major steps of SE oxidative degradation

At the initial step, α-acylhydroperoxide is formed in a way similar to the oxidation of hydrocarbon [90]. This intermediate by-product then decomposes via two routes, one the usual degradation into

free radicals via O-O bond splitting and the other route involving hydroperoxide decomposition into both peroxy acids (together with an aldehyde) and so-called peroxy ester [90]. The liquid phase oxidation of these peroxy esters yields low molecular carboxyl acid (acetic), methyl alcohol and methyl acetate. Figure 2.15 illustrates the major steps of synthetic ester oxidative degradation. As explained in [90], it is assumed that α-acylhydroperoxide is produced in synthetic ester in a way similar to the production of hydroperoxide in hydrocarbon oils.

Synthetic esters are also subjected to hydrolysis degradation at high temperature. The acids generated via hydrolysis of synthetic esters are shorter chain acids. These acids are more aggressive than those from NEs and are more corrosive at elevated temperature.

2.6 Review the Experimental Studies on Ageing of Oil-paper Insulation in Transformers

2.6.1 Mineral oil-paper insulation

During the last several decades ageing behaviour of typical mineral oil-paper insulation has been extensively studied [4-7, 10, 53, 55, 60-62, 65, 91-93]. Collectively these studies have mainly investigated the exclusive and combined effects of heat, moisture and oxygen on degradation of cellulose paper insulation in mineral oil. Shroff et al [47] have quoted that in an ideal situation where air and water are excluded from the oil-paper system, typical wood pulp paper has a lifetime of 38 years at 90ºC. On the other hand, presence of some air and 2% water reduces the lifetime to about 2 years. They have also reported that an increase of temperature by 10ºC reduces the lifetime of wood pulp paper by a factor of 3.

Lundgaard et al [62] have claimed that both moisture and oxygen accelerate the ageing of cellulose materials in mineral oil. However, the effect of water on cellulose ageing is paramount such that 4 % increase of moisture in paper insulation reduces expected lifetime by a factor of 40 whereas saturation of oil with oxygen only reduces it to one-half. Lundgaard et al [61] have underlined that low molecular weight carboxyl acids are mostly absorbed by paper material and this behaviour enhances the acids catalysed hydrolytic degradation of cellulose insulation material in mineral oil. Since water enhances dissociation of acids, in combination they show significant synergetic effect on ageing of paper insulation.

Emsley et al [7] have reported that heat and water accelerate the ageing of paper insulation in mineral oil and they are about equally effective individually and show a significant productive effect in combination. Moreover, oxygen is also synergetic with heat but this synergism is less pronounced than of that with water. This study suggests that interaction between water and oxygen

causes a shielding effect, which reduces the interaction between water and cellulose and eventually results in reduction of paper ageing rate with low water and low temperature conditions.

Emsley and Stevens [5, 36] have stated that the degradation kinetic of paper insulation in mineral oil can be represented with a pseudo-zero order kinetic model and most of the published data on cellulose ageing is in good agreement with this model. They have related the reaction rate of pseudo-zero order kinetic model to temperature via so-called Arrhenius relationship which is mainly characterised by a factor called activation energy. This analysis yields an activation energy 111 kJmol^{-1} for the degradation of cellulose materials in mineral oil and it remains constant under different reaction conditions. This value has been confirmed by Lundgaard [62] and Lelekakis et al have obtained a similar value of 106 kJmol^{-1} with upper and lower confidence levels of 124 kJmol^{-1} and 87 kJmol^{-1} respectively.

2.6.2 Ester-paper insulation

Wilhelm et al [68] have performed an ageing experiment to evaluate the influence of moisture, oxygen, heat and the presence of cellulose insulation material on the deterioration of NE based insulating liquids. They have used two types of commercially available insulating liquids namely FR3 and BIOTEMP. In their study, the ageing extent of insulating oils is characterised by measuring kinematic viscosity, acidity and DDF over ageing. This study underlines that the viscosity of NEs measurably increases over ageing in an oxygen rich environment due to the oxidative degradation. On the other hand, hydrolytic degradation of NEs in the presence of moisture shows no influence on the viscosity of oil but acidity of oil markedly increases over ageing. The results of this study also confirm that an increase of temperature intensifies both oxidative and hydrolytic degradation of NE insulating liquids.

Hosier et al [69] have investigated the potential of five different food grade vegetable oils to use as insulating liquid in high voltage equipment through an accelerated ageing experiment. The ageing extent of oil is characterised by measuring viscosity and DDF over the ageing time. The major difference between vegetable oils used in this study is the degree of unsaturation of their fatty acids composition. Their ageing experiment has been performed in an open air environment in both the presence and absence of copper as a catalyst. The major finding of their study is that olive oil which contains a high percentage of mono-unsaturated fatty acid shows excellent resistance to ageing (comparable to FR3). On the other hand, oils with high poly-unsaturated fatty acids are more prone to oxidative degradation. They suggest that vegetable oils high in mono-unsaturated fat are suitable for electrical insulating purposes after carefully processed to offer low dielectric loss.

Tenbohlen et al [84] have performed an accelerated ageing experiment using three types of NEs, one synthetic ester and one traditional mineral oil in both sealed and open environments with and without transformer materials. The main objective of this study is to compare the ageing behaviour of NEs with respect to synthetic ester and mineral oil. Moreover, ageing of cellulose paper in NEs is also compared with that of in synthetic ester and mineral oil. This study has realised that hydrolytic degradation of both natural and synthetic esters causes to increase the acidity of those oils over thermal ageing. The results of this experiment underline the necessity of preventing direct contact of NE oils with air because viscosity of NEs aged under an air supply shows an extreme increase due to severe oxidation. This study has also confirmed that NEs offer better performance concerning ageing of cellulose paper insulation than both mineral oil and synthetic ester oils.

Fofana et al [16] have performed an open beaker ageing experiment to compare the oxidation stability of commercially available naphthenic based mineral oil, NE and synthetic ester insulating oils. In this paper, DDF, dissolved decay by-products and turbidity of oil are measured to determine the degree of oxidation over ageing. This study has revealed that after 1800h of ageing, the dissolved decay by-products and turbidity of mineral oil are many times greater than those of NE. It confirms the ability of NE to dissolve more sludge. On the other hand, oxidation of NEs forms a lower amount of sludge than mineral oil.

J.C Duart et al [94] have compared the lifetime of Kraft paper insulation in typical mineral oil and (BIOTEMP) NE insulating oil through an accelerated ageing experiment performed under a nitrogen sealed environment. They have considered the 50% retained tensile strength as the end of life criteria. Their ageing test cells contain Kraft paper, high density pressboard, low density pressboard, insulating oil (mineral or NE) and a typical power transformer proportion of core steel and copper. In their study, dry insulation with 0.4% moisture and wet insulation with 0.9% of moisture have been separately aged to compare the impact of moisture. This study has calculated the temperature at which end of life is reached in 65,000 hrs for normal dry Kraft insulation in BIOTEMP is 114 ℃ whereas that of Kraft insulation in mineral oil is 98 ℃. On the other hand, that of wet insulation in BIOTEMP is 100℃, confirming that an increase of moisture accelerates the ageing of paper insulation in NE in a way similar to mineral oil-paper insulation systems investigated in several studies [53, 62].

Coulibaly et al [95] have performed an accelerated ageing experiment at 130℃ in sealed vessels to compare the ageing behaviour of cellulose insulation materials in three different insulating liquids including one type of mineral oil and NE and a synthetic ester. This study has been performed in both oxygen rich and low oxygen environments. In addition to insulating oil and paper, copper has

been included into the ageing vessels to remain consistent with the condition of a real transformer. The results of this study indicate that both paper and pressboard insulation in natural and synthetic ester oils age at a slower rate than those in mineral oil in both oxygen rich and low oxygen environments. They have hypothesised that this protective effect of both esters on cellulose is due to their hygroscopic nature. On the other hand, this study has underlined the limitation in use of furanic compounds for diagnostic purposes of ester filled transformers, since the measured (2-FAL) concentration in both types of esters is much lower than that of in mineral oil over ageing.

Lijun et al [96, 97] have compared the ageing behaviour of typical Kraft paper insulation in commercially available NE insulating oil (BIOTEMP) with that of conventional naphthenic based mineral oil through an accelerated ageing experiment performed at three different temperatures. Their study confirms that NEs slow down the ageing of Kraft paper leading to a longer life expectancy. They have hypothesised that this advantage of NE over mineral oil is due to two reasons. NEs are far more hygroscopic than mineral oil. Thus, NEs attract more water from paper insulation than mineral oil and it causes a slowing down of the hydrolytic degradation of paper insulation immersed in NE. Moreover, they assume that hydrolysis of NEs yields free fatty acids and they are chemically bonded to cellulose molecules via trans-esterification. These esterified fatty acids arrange in parallel with the cellulose chain to form a water barrier and further weaken the hydrolysis degradation of cellulose. The calculated activation energy (E_a) values in this study for degradation of paper in mineral oil and NE are (86.94 ± 18.05) kJmol^{-1} and (151.24 ± 8.28) kJmol^{-1} respectively. These values are in good agreement with the activation values reported in [55].

Liao et al [24] have performed a sealed tube accelerated ageing experiment to understand the ageing behaviour of typical Kraft insulation paper and thermally upgraded paper in a commercially available NE (BIOTEMP) and conventional mineral insulating oils. This study has identified that both Kraft and thermally upgraded paper show better thermal stability in NE than in mineral oil. Results of this study show that levelling off DP (LODP) of both types of paper insulation aged in NE is about 100 to 400 higher than that of paper insulation aged in mineral oil. It results in increasing the life expectancy of NE filled transformers. These scholars have hypothesised that this protective behaviour of NE ester on paper is mainly due to the hydrophilic nature of NE, the tendency for hydrolytic degradation of NEs themselves and trans-esterification of long chain fatty acids onto the C_6-hydroxyls groups of cellulose molecules. They assume that these effects restrain the hydrolytic degradation of paper insulation. One interesting phenomenon that can be seen in their result is that 2-FAL concentration in NE is much lower than that of in mineral oil in similar ageing condition.

In the last two decades, there have been several studies performed to understand the ageing behaviour of electrical grade cellulose material in NEs [11-14] and to investigate the thermal stability of NE insulating oils themselves [33, 98]. The major finding of their studies is that NEs show resistance to thermal ageing of cellulose insulation materials and it confirms the longer life expectancy and high overloading capability of NE filled transformers. One notable fact is that acidity of NEs abruptly increases during thermal ageing due to hydrolysis of NEs themselves. These studies have also identified that viscosity of NEs greatly increases due to thermal ageing in an oxygenate environment and this behaviour significantly decreases the heat transfer ability of oil.

This literature review has revealed that a number of comprehensive studies conducted for understanding the ageing behaviour of cellulose insulation in different types of ester oils at once is limited. Moreover, ageing behaviour of moderately wet cellulose insulation in ester oils has not yet been investigated through a systematic study. This research proposes that studying the ageing behaviour of moderately wet cellulose insulation in NE liquids is very important. This is because of an increasing trend in retrofilling of mineral oil filled transformers with NE based insulating oils, the solid insulation of such units (which have been operated over 15-20 years) could possess moisture content of about 2%.

2.7 Summary

Cellulose and mineral oil are still the preferred choice for transformer insulation because they are economical and plentiful in nature. However, mineral oils possess fire and environmental hazards due to their low fire point and poor biodegradable characteristics respectively. Thus, there is growing interest to use ester oils as a substitute for mineral oil due to their superior biodegradable properties and high fire point. Cellulose material and oil insulation in transformers degrade under combined influences of intense heat, moisture and oxygen which are available in the operating environment of transformers. Therefore, the degree of ageing of both paper and oil insulation of transformers is needed to be investigated through reliable methods. The next chapter will mainly discuss the existing well-established methods for diagnosing oil-paper insulation systems of transformers.

Ageing characteristics and changing of physicochemical properties of cellulose-mineral oil composite insulation have been extensively studied during the last several decades. On the other hand, there are limited numbers of systematic experimental and field studies that have been performed to comprehensively investigate the long-term behaviour of cellulose-ester composite insulation in a transformer operating environment. Thus, the present understanding on ageing behaviour of cellulose-ester composite insulation systems is inadequate. This limits the cost

effective and reliable field applications of ester insulating oil. Therefore, further investigation is necessary to understand the ageing behaviour of cellulose material in ester oils under different environmental conditions and to realise a change of physicochemical properties of ester oils over ageing. The experimental works presented in Chapter 4 of this thesis are mainly intended to address this issue.

Chapter 3

Condition Monitoring of Transformer Insulation

3.1 Introduction

Transformers are indispensable and strategically important pieces of equipment in any power system. Their availability and reliability are necessary to run a power system economically and efficiently. It has already been mentioned in the previous chapter that during the course of operation, the transformer insulation system is subjected to an irreversible ageing. Ageing of the insulation system causes a reduction in the ability of the winding structure to withstand high compressive and axial forces generated in a fault condition of the power network. Statistical data of transformer failures indicates that winding failures due to defects in the insulation system present the significant percentage of failures [20]. Transformer failure can be catastrophic and result in significant direct and indirect costs including repair or replacement costs and revenue losses due to unscheduled outages. Therefore, adequate maintenance is required to ensure the condition of transformer insulation system is good. A competitive and liberated energy market forces utilities to change their maintenance strategies from time-based to condition and realiability based where maintenance decisions are no longer driven by operational time [99]. In such a situation, assessing the condition of transformer insulation with reliable non-invasive diagnostic tools is a basic requirement to take the right maintenance actions at the right time and avoid costly inadvertent outages. This chapter presents the background of existing transformer insulation condition monitoring techniques which mainly fall into two types, namely chemical and electrical.

3.2 Overview of Electrical Based Techniques

Breakdown voltage (BDV), partial discharge (PD) measurements, dielectric absorption ratio (DAR), polarisation index (PI) and power frequency loss factor (DDF) are the typical electrical based traditional diagnostic tools which have been used to assess the quality of oil-paper insulation in transformers individually and collectively. The destructive nature and lack of information provided by some of these techniques impede their current wide application in condition monitoring

[100]. On the other hand, development of signal processing methods has enabled noise reduction and classification of PD sources. Thus, there is a growing trend to adapt PD-based diagnostic techniques in conjunction with modern signal processing tools to identify incipient faults in transformer insulation systems.

With the advancement in fast computers and digital technology in the early 1990's, dielectric polarisation based diagnostic tools namely polarisation and depolarisation current (PDC), recovery voltage measurement (RVM) and frequency domain spectroscopy (FDS) were introduced [101]. These techniques are collectively known as dielectric response measurements. Dielectric response measurements have proven their applicability in condition monitoring of transformer insulation and are now widely used.

3.3 Conventional Dielectric Tests

3.3.1 Power frequency breakdown voltage measurements

BDV at power frequency is the most commonly used parameter to assess the quality of insulating oils. It primarily measures the ability of the oil to withstand electrical stresses. Breakdown voltage indicates the presence of contaminants such as water, cellulosic fibre, dirt and conductive particles in the liquid insulation. The presence of a significant concentration of contaminants results in a lower BDV. IEC Std. 60156 and ASTM Std. D1816-4 prescribe the standard test procedure for analysing breakdown voltage of insulating liquids having a petroleum origin. ASTM D1816 and IEC 60156 specify different types of electrodes, electrode gaps, voltage ramp rates, stir times between tests and sample sizes. Since ester based insulating oils possess a higher viscosity than typical mineral oil, IEEE Std. C57.147-2008 recommends longer rest time (about 15 minutes at room temperature) than the standard values provided in IEC and ASTM standards before analysing the BDV to allow air bubbles to escape [83].
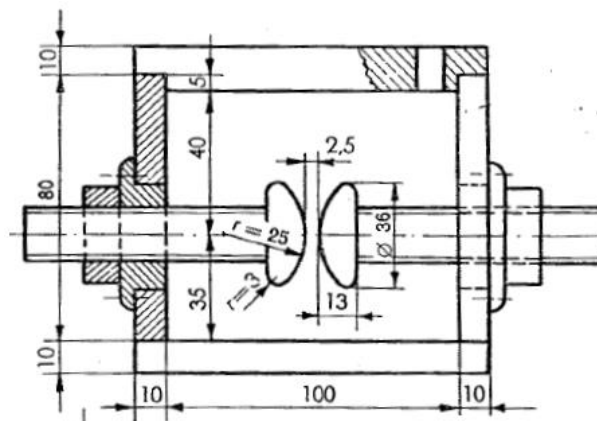
Figure 3.1. Example test cell and electrode arrangement in IEC 60156 [102]

Figure 3.1 shows a commonly used test cell and electrode arrangement suggested in IEC 60156 which is used in this research to measure the BDV of insulating oils.

3.3.2 Overview of IR, DAR and PI measurements

IR is a basic dielectric parameter which can be used to assess the insulation system of a transformer. In this method, a DC step voltage is applied across the insulation being investigated and the charging current is measured over 1 minute. IR is then calculated using eq (3.1). This test is typically performed periodically and a substantial reduction of IR over time indicates the necessity of further investigation for the cause.

$$IR = insulation\ resistance\ at\ 1\ min = \frac{Applied\ Voltage}{Current\ at\ 1\ min} \tag{3.1}$$

DAR and PI are extensions of IR measurement and these dielectric parameters are calculated by using IR values at 30 seconds, one minute and 10 minutes as given in eqns (3.2) and (3.3). Under a DC step voltage, the current flowing through an object of insulation consists of three components namely, charging current, absorption current and conduction current. Absorption current represents the polarisation current due to molecular charge shifting in the insulation and it is assumed to decay to zero over time. Thereby, both DAR and PI should possess values greater than 1. In general, insulation in good condition has DAR and PI values greater than 1.6 and 2 respectively. Table 3.1 provides the necessary guidelines to assess a transformer insulation system using PI [103]. Generally, the value for PI of insulating oils is equal to 1 and it leads to a low PI for new transformer insulation in spite of its good condition. Therefore, it is recommended not to use the PI method to assess the condition of the oil-paper composite insulation in a new transformer [100, 103].

Table 3.1. Guidelines for evaluating transformer insulation using PI values based on IEEE Std. C57.152-2013 [103]

Polarisation index	Condition
Less than 1	Dangerous
1-1.1	poor
1.1 1.25	questionable
1.25 to 2.	fair
Above 2.0	good

$$DAR = \frac{1 \, min \; insulation \; resistance \left(megohm \right) reading}{30 \, sec \; insulation \; resistance \left(megohm \right) reading} \tag{3.2}$$

$$PI = \frac{10 \, min \; insulation \; resistance \left(megohm \right) reading}{1 \, min \; insulation \; resistance \left(megohm \right) reading} \tag{3.3}$$

3.3.3 Dielectric Dissipation Factor measurement at mains frequency

DDF is a dimensionless parameter measured at power frequency which has been known as an effective method to assess the overall condition of transformer insulation over decades [100, 103, 104]. DDF of a transformer mainly characterises the moisture and degree of contamination of its insulation system. In the case of obtaining DDF, an AC voltage of power frequency is applied across the transformer insulation system. The test voltage used in field measurements is typically in the range 100 V to 10 kV. However, most field measurements are performed at rated voltage or at a maximum of 10 kV [104]. When an AC voltage is applied across an insulator, there is a current flowing through it. This current mainly has two components namely, capacitive and resistive current. Basically, DDF also known as tanδ is the ratio of resistive current to capacitive current. The resistive current of an insulation system in good condition is much lower than the capacitive current. Thereby, the source voltage is nearly 90 degrees lagging the source current which means DDF is very small. Any deterioration of the insulation causes an increase in the resistive current and gives rise to DDF.
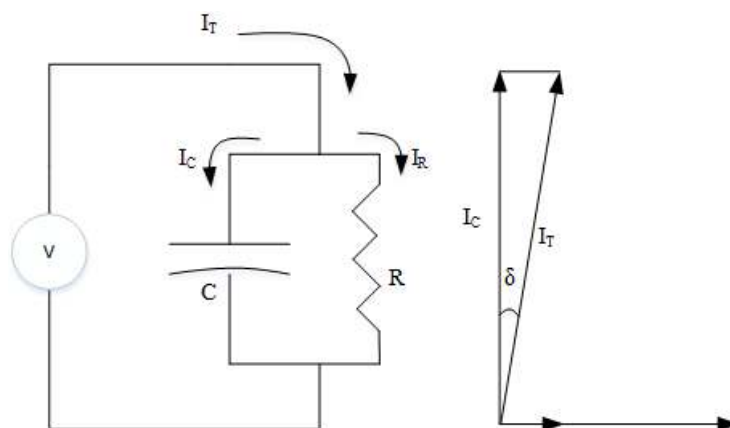
Figure 3.2. Simple vector diagram for dissipation factor measurement [104]

When assessing the conditions of transformer insulation with this method, the measured DDF is usually compared with the previous and factory test results. Thus, this method provides the greatest benefit when performed periodically [103]. DDF largely depends on temperature, therefore care

must be taken to consider measurement temperature to draw an accurate conclusion based on DDF measurement results. Table 3.2 provides necessary guidelines based on IEEE Std**.** C57.152-2013 and IEEE Std. 62-1995 to evaluate the condition of transformer insulation using this technique. It can be seen in Table 3.2 that limiting values for DDF have been defined for the range of transformers based on voltage rating. This is because DDF is a dimensionless parameter which is not affected by the geometrical parameters of the insulation system of transformers.

Table 3.2. Recommended diagnostic characteristics based on DDF [103, 104]

Insulating oil	Voltage rating	Limit of DDF @ 20 ºC (%)	
		New transformer	Service-aged transformer
Mineral oil	≤ 230 kV	< 0.5	1
	≥ 230 kV	< 0.4	0.5<DF<1 acceptable
			DF>1 should be investigated
NE	all	1	1

Since this is a single frequency measurement, it only allows for limited assessment of the insulation condition of a transformer. Moreover, DDF does not have enough information to resolve individual effects of oil and solid insulation. In the case of old transformers, DDF at power frequency predominantly characterises the condition of the oil insulation. These deficiencies of the single frequency DDF measurement may lead to an erroneous interpretation of the condition of transformer solid insulation. Figure 3.3 shows an example of the drawback of power frequency DDF method where DDF at 50 Hz of moderately and heavily aged transformers solely characterises the condition of the oil.
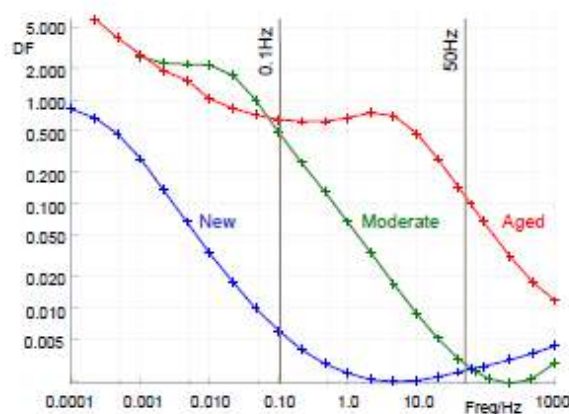
Figure 3.3. DDF of three transformers with different ageing condition [100]

DDF is also used to evaluate the change of quality of insulating oils due to contamination and deterioration in service or as a result of handling. ASTM Std. D 924 and IEC Std. 60247 prescribe the standard procedure to obtain DDF of insulating oils in the commercial frequency range of 45-65 Hz and 40-62 Hz respectively. As per IEEE Std. C57.147-2008, the maximum acceptable DDF of new NE based insulating liquids is 0.002 at 25 ℃ with the test method specified in ASTM D 924. That of new synthetic ester insulating liquids at 90 ℃ is 0.03 [105]. As per IEEE Std. C57.152-2013, limiting value for DDF of both serviced aged mineral oil and NE insulating liquids is 0.005 at 25 ℃. On the other hand, IEEE Std. C57.147-2008 suggests a provisional acceptable limiting value of 0.03 for service aged NE insulating oils at 25 ℃. According to British Std. EN 61203 that of service aged synthetic ester insulating oils is 0.01 at room temperature.

The results of several studies point out that DDF of NE insulating oils increases far beyond the limiting value specified in IEEE Std. C57.152-2013 even aged under oxygen free environment [98, 106, 107]. Thus one can claim that the provisional limiting value provided in IEEE Std. C57.147-2008 is more appropriate for quality assurance of service aged NE insulating liquids.

3.4 Dielectric Response Measurements

3.4.1 Dielectric polarisation and basic principles

Both liquid and solid insulation materials can be categorised into two groups, namely polar and non-polar [108]. Polar materials contain permanent electrical dipoles which can be molecular dipoles due to the chemical interaction between dissimilar atoms in the molecular structure or localised bipolar space charges [109]. In non-polar materials there are no permanent electrical dipoles and balancing of positive and negatives charges exists at an atomic level. Overall, insulation materials are electrically neutral though they have a microscopic level of localised bound or space charges [109, 110].

Soon after an insulation material is subjected to an external electric field, bound and space charges show relative microscopic movement in the direction of the electric field which leads to non-zero microscopic dipole moments. This is simply called dielectric polarisation. Generally, three main polarisation mechanisms can be observed in insulation materials, namely deformation (electron or atomic), ionic and dipolar polarisation. Moreover, some of the insulation materials possess different types of polarisation mechanisms such as interfacial polarisation (space charge polarisation) and hopping charge carrier polarisation [109, 111-116].

Deformation polarisation: This arises due to the elastic displacement of electron clouds relative to the nuclei of an atom or sets of atoms (molecule). This is a fast temperature independent mechanism which is effective when the frequency of applied electric field is in the optical range [117].

Ionic polarisation: This occurs when the positive and negative ions in a lattice structure of a material are displaced by an electric field in such a way that positive ions displace in the direction of the electric field while negative ions shift in the opposite direction. This phenomenon is effective in infra-red frequencies and shows a weak temperature dependence [108].

Dipolar Polarisation: This occurs in materials containing molecules with permanent dipoles. These dipoles are randomly distributed as shown in Figure 3.4 (a) due to the action of thermal energy and give zero net polarisations as long as no external field is applied. When an electric field is applied across a polar material, dipoles tend to align themselves with the electric field as shown in Figure 3.4 (b) and gain electrical polarisation. This is also quite a fast phenomenon which is effective when the frequency of applied field in the range MHz to GHz. This mechanism is strongly counteracted by the thermal motions of molecules and thereby, dipolar polarisation is considered as a highly temperature dependent mechanism.
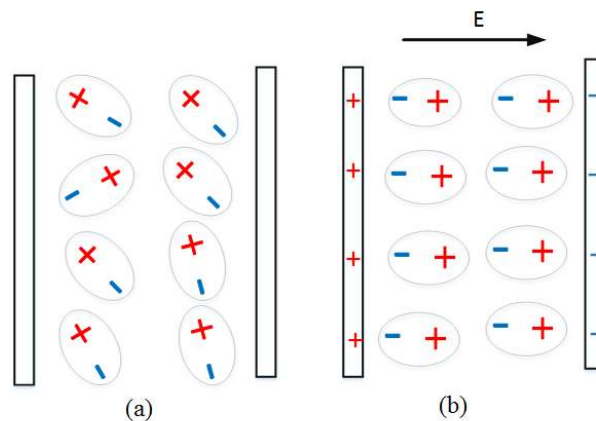
Figure 3.4. Orientation (dipole) polarisation (a) without Field, (b) Polarised under an external filed

Interfacial polarisation: This type of polarisation can typically be found in composite materials such as oil impregnated cellulose where materials in contact have different electrical conductivities. When an electric field is applied across such a material, movable positive and negative charges become deposited on the interface of different materials and act as some kind of electric dipoles[109]. This phenomenon is quite a slow process which is effective in the power frequency range or below.

Hopping charge carrier polarisation: This is a different class of polarisation mechanism that can mostly be found in solid materials which are heterogeneous on a microscopic scale in nature such as

rock, ceramic, humid cellulose, humid sand, porous structures and most of the biological systems [115, 118]. As shown in Figure 3.5, hopping charge carriers spend most of the time in localised sites x_1 or x_2, if they are subjected to small thermal vibrations [110]. However, occasionally they make a jump over the potential barrier **W**. This phenomenon is somewhat similar to an induced dipole and creates polarisation. The probability of transition between two preferred sites (x_1 and x_2) is predominantly determined by the distance between the sites and the height of the potential barrier. An application of an electric field over the material increases the probability of charge hopping transition from site x_1 to x_2 ($R_{12} > R_{21}$) or vice versa. Therefore, under an electric field, when the hopping charge carriers are not traversing the entire physical dimension of the sample, this phenomenon gives rise to polarisation. This is quite a slow process and effective at sufficiently low frequencies.
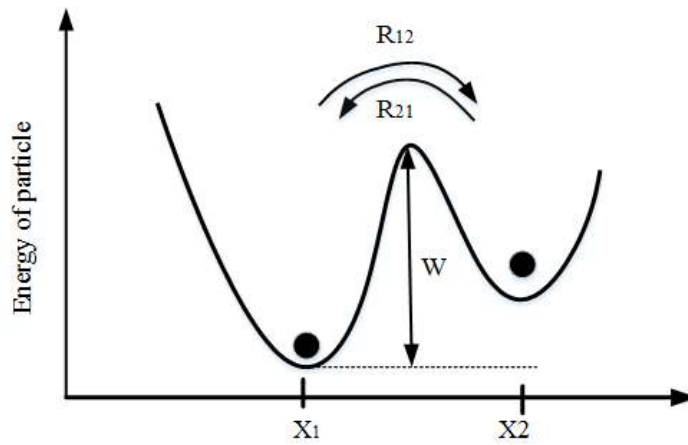
Figure 3.5. A double potential well for representing hopping charge carrier polarisation [117]

3.4.2 Theory of dielectric polarisation

Polarisation **P** is a vector which represents the dipole moment per unit volume of matter and it can be expressed as [108]:

$$P = \frac{\langle M \rangle}{V} \quad (Cm^{-2}) \tag{3.4}$$

Where, *M* is the macroscopic dipole moment of the whole sample volume *V* and bracket ⟨⟩ represents the ensemble average. It is generally accepted that the dielectric polarisation of most insulation materials linearly changes with an applied electric field. Assuming that the insulation materials considered here are isotropic and uniform, the general relationship between the electric field *E* and polarisation can be presented as:

$$P = \varepsilon_0 \chi_e E \tag{3.5}$$

Where, ε_0 is the dielectric permittivity of vacuum (8.854×10^{-12} Fm^{-1}) and χ_e denotes the dimensionless electric susceptibility of the material under consideration. According to the first Maxwell equation, electric displacement vector and polarisation can be related as in eq (3.6).

$$D = \varepsilon_0 E + P \tag{3.6}$$

Then using eqns (3.5) and (3.6) electric displacement vector can be rearranged as:

$$D = \varepsilon_0 \left(1 + \chi_e\right) E = \varepsilon_0 \varepsilon_r E \tag{3.7}$$

The relative permittivity (dielectric constant) of the material under consideration in the linear region is denoted by $\varepsilon_r = 1 + \chi_e$ which does not depend on the magnitude of the applied field. On the other hand, relative permittivity of a material depends on the microscopic morphology and chemical composition of the material. Furthermore, other external factors including frequency of applied electric field and sample temperature significantly influence the relative permittivity of the material under consideration.

As explained in section 3.4.1, it is clear that when an insulation material is exposed to an electric field, some of the polarisation processes develop within a very short time while others take quite a long time. Therefore, polarisation of insulation materials under an external electric field always possesses time dependence behaviour and it reaches an equilibrium condition over a period of time. Time dependence polarisation $P(t)$ of insulation material due to any arbitrary time varying electric field $E(t)$ can be written as in eq 3.8 [109, 117, 119]. $P(t)$ has two major components namely rapid and slow polarisation. The slow polarisation part is the convolution integral of the applied electric field and dielectric response function $f(t)$ of the insulation material being investigated. $f(t)$ is always a monotonically decreasing function.

$$P(t) = \underbrace{\varepsilon_0(\varepsilon_\infty - 1)E(t)}_{\text{Rapid polarisation}} + \underbrace{\varepsilon_0 \int_{-\infty}^{t} f(t-\tau)E(\tau)d\tau}_{\text{Slow polarisation}} \; (\text{ for } t < 0, f(t) = 0) \tag{3.8}$$

ε_∞ denotes the relative permittivity of the material at high frequency, which is referred to as fast polarisation process appearing in the material. Using eqns (3.7) and (3.8) the time varying displacement current density $J_D(t)$ can then be presented as eq (3.9).

$$J_D(t) = \varepsilon_0 \frac{\partial E(t)}{\partial t} + \frac{\partial P(t)}{\partial t} \tag{3.9}$$

In addition to the bound and space charges, insulation materials contain free movable charges. Thus, under an electric field of *E(t)* the current density *J(t)* through an insulation material with volume conductivity of σ can be mathematically represented as eq (3.10) where it is a summation of conduction and displacement currents.

$$J(t) = \underbrace{\sigma E(t)}_{Conduction\ current} + \underbrace{\varepsilon_0 \left\{ \varepsilon_\infty \delta(t) + f(t) \right\} E(t)}_{Displacement\ current} \tag{3.10}$$

Once an insulation material is subjected to a sinusoidal time varying electric field $E(\omega)=E_m e^{j\omega t}$, polarisation at any arbitrary frequency can be mathematically calculated by taking a Fourier transform of eq (3.8). Thereby, frequency domain dielectric polarisation *P(ω)* of an insulation material can then be written as [110]:

$$P(\omega) = \varepsilon_0 \left\{ (\varepsilon_\infty - 1) + \underbrace{\left(\chi'(\omega) - j\chi''(\omega) \right)}_{\chi(\omega)} \right\} E(\omega) \tag{3.11}$$

Where *χ(ω)* is the frequency dependence complex susceptibility of the material under investigation which is equivalent to the Fourier transform of the dielectric response function *f(t)*.

Then, total current density *J(ω)* in frequency domain can be expressed as:

$$J(\omega) = j\omega\varepsilon_0 \left\{ \varepsilon_\infty + \chi'(\omega) - j\left(\frac{\sigma}{\varepsilon_0 \omega} + \chi''(\omega) \right) \right\} E(\omega) \tag{3.12}$$

When the dielectric response function obeys causality, which means no reaction before action, real and imaginary susceptibility can be interrelated by so-called Krammers-Kronig (K-K) transformation as in eqns (3.13) and (3.14).

$$\chi'(\omega) = \frac{2}{\pi} \lim_{a \to \infty} \int_0^a \frac{x\chi''(x)}{x^2 - \omega^2} dx \tag{3.13}$$

$$\chi''(\omega) = -\frac{2\omega}{\pi} \lim_{a \to \infty} \int_0^a \frac{\chi'(x)}{x^2 - \omega^2} dx \tag{3.14}$$

3.4.3 Dielectric response in time and frequency domain

3.4.3.1 Overview

PDC and RVM are the time domain dielectric responses which characterise the dielectric properties of the materials with respect to electrical conduction and slow polarisation processes under DC field

stress. FDS presents the response of the material to sinusoidal excitation of varying frequency. A notable fact is that dielectric response of a wide range of solid materials including oil impregnated cellulose [116, 120-125], poly-oxymethylene, and porous glass [126] are principally governed by the absorbed moisture. Therefore, dielectric response measurements in time and frequency domains have been significantly increased in use during the past two decades to estimate the moisture content in cellulose based insulation of transformers.

3.4.3.2 PDC response measurement

Figure 3.6 (a) shows the principle circuit used for PDC measurement. Here, a step voltage of U_0 is applied to the fully discharged insulation object at $t = 0$ s and the current through the circuit is measured with an electrometer connected in series with the source voltage and the insulation object over a time period of t_c s. Using eq (3.10) and assuming that the geometric capacitance of the test object is C_0, the resultant polarisation current ($I_{pol}(t)$) can be expressed as eq (3.15) [119, 127].
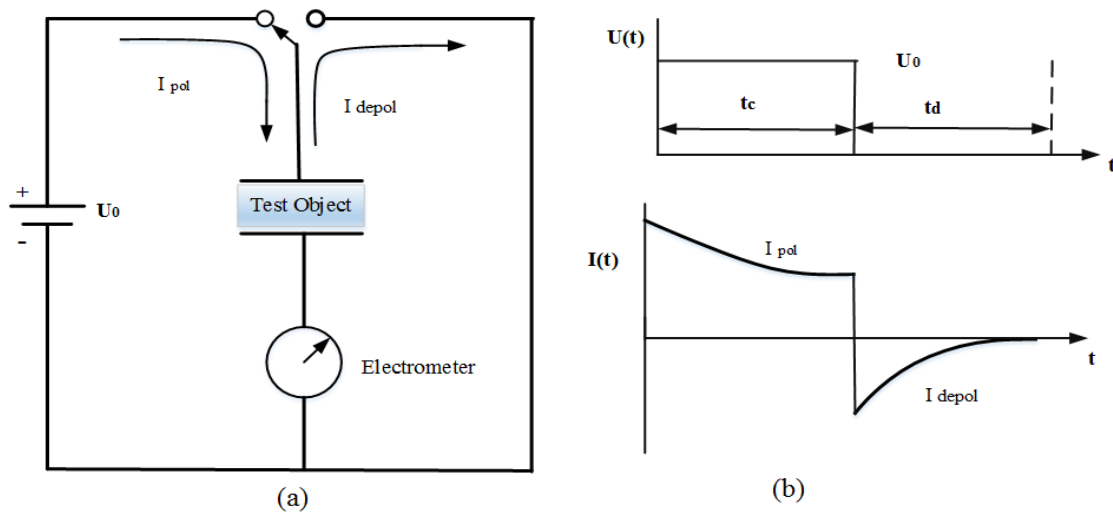
Figure 3.6. (a) Principle circuit of PDC measurement, (b) General shape of polarisation and depolarisation current [119]

$$I_{pol}(t) = \left\{ \overbrace{\frac{\sigma}{\varepsilon_0}}^{conductive} + \overbrace{\varepsilon_\infty \delta(t) + f(t)}^{Displacement} \right\} C_0 U_0 \quad for\ 0 \le t \le t_c \qquad (3.15)$$

Impulse function $\delta(t)$, represents the current spike in $I_{pol}(t)$ at t=0 due to the charging of geometric capacitance of the test objects. It can be seen from eq (3.15) that $I_{pol}(t)$ characterises the material being investigated with respect to its volume conductivity, dielectric response function and high frequency permittivity. If t_c is sufficiently large enough, the effect of polarisation disappears from the measured polarisation current response and thereby, it is equal to the conduction current.

At the time equal to t_c, applied voltage is removed and terminals of the test object are short-circuited via an electrometer. This condition is similar to an application of $-U_0$ voltage across the test object at $t=t_c$. Using the principle of superposition, the resultant depolarisation current flowing through the circuit in the reverse direction (I_{depol}) due to the relaxation of polarised species can be explained as eq (3.16).

$$I_{depol}(t) = -\{\varepsilon_\infty \delta(t-t_c) + f(t-t_c) - f(t)\} C_0 U_0 \quad for\ t_c \leq t \leq \infty \tag{3.16}$$

As shown in eq (3.16), depolarisation current is not affected by the conductivity and thereby, dielectric response function can be presented as eq (3.17) when the condition $f(t) >> f(t+t_c)$ for $t >0$ is satisfied. Moreover, assuming that the material is macroscopically homogeneous, DC conductivity can be calculated using eq (3.18).

$$f(t) \approx \frac{-I_{depol}(t)}{C_0 U_0} \tag{3.17}$$

$$\sigma = \frac{\varepsilon_0}{C_0 U_0} \{I_{pol}(t) + I_{depol(t)}\} \quad for\ t > t \tag{3.18}$$

However, $f(t)$ of most of the solid materials decreases slowly with time leading to a longer measurement time to satisfy the condition $f(t) >> f(t+t_c)$ for $t >0$ [117].

3.4.3.3 RVM

In this method, step voltage of U_0 is applied across the fully discharged test object over a time period of t_c s. Then step voltage is removed and the test object is short circuited for a time period of t_d s. To perform RV measurement, the discharging process is interrupted after t_d s and a high impedance voltmeter is connected across the terminals of the test object.
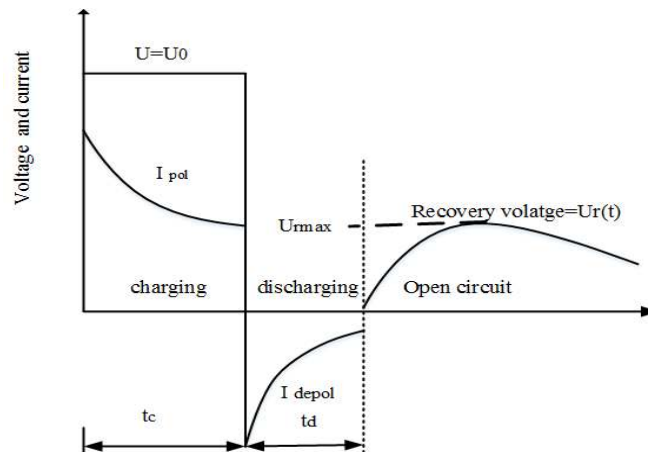
Figure 3.7. Current and voltage responses during a RVM

During the short circuited time period (t_d), activated polarisation processes with different time constants are relaxed to different levels. Thereby, soon after the voltmeter is connected, charge redistribution occurs in the system and it gives rise to a voltage across the terminal of the test object as shown in Figure 3.7.

The recovery voltage $U_r(t)$ build up across the electrodes of the test object possesses the following relationship.

$$\sigma U_r(t) + \varepsilon_0 \frac{dU_r(t)}{dt} + \varepsilon_0 U_0 \{f(t) - f(t - t_c)\} + \varepsilon_0 \frac{d}{dt} \int_{t_c + t_d}^{t} f(t - \tau) U_r(\tau) d\tau = 0 \in \text{ for } t_c + t_d < t < \infty \quad (3.19)$$

$$U_r(t = t_c + t_d) = 0 \quad (3.20)$$

$U_r(t)$ can be analytically derived from eq (3.19), if the DC conductivity (σ), high frequency-permittivity (ε_∞) and dielectric response function $f(t)$ of the insulation material are known [117].

3.4.3.4 **Frequency Domain Spectroscopy (FDS)**

In this technique, a sinusoidal voltage of varying frequency $U(\omega)$ is applied across the insulation object and the current response is measured in terms of magnitude and phase angle. Then the frequency dependence complex capacitance $C(\omega)$ of the test object can be derived using eq (3.21).

$$I(\omega) = j\omega \underbrace{(C'(\omega) - jC''(\omega))}_{\text{Complex\_Capacitance}} U(\omega) \quad (3.21)$$

If the geometric capacitance (C_0) of the test object is known, frequency dependence complex permittivity can be explained as:

$$I(\omega) = j\omega \left(\underbrace{\varepsilon_\infty + \chi'(\omega)}_{\varepsilon'(\omega)} - j \underbrace{\left(\overbrace{\frac{\sigma}{\varepsilon_0 \omega}}^{\text{Conduction loss}} + \overbrace{\chi''(\omega)}^{\text{Dielectricloss}} \right)}_{\varepsilon''(\omega)} \right) C_0 U(\omega) \quad (3.22)$$

Where, $\varepsilon'(\omega)$ is the real part of permittivity which has two components; $\chi'(\omega)$ and ε_∞. $\chi'(\omega)$ represents the contribution of polarisation to the capacitive current. $\varepsilon''(\omega)$ is the imaginary part of permittivity which associates with energy loss of the insulation material. Energy loss has two components, resistive loss due to the conduction effect and dielectric loss due to the inertia of bound and space charges when they are displaced by an electric field. The frequency dependence complex capacitance or permittivity is generally known as FDS.

It can be seen in eq (3.22) that the contribution of conduction effect to the imaginary permittivity $\varepsilon''(\omega)$ is inversely proportional to the frequency. Thereby, it becomes more dominant at low frequencies. However, most of the solid insulation materials possess low frequency dispersion (LFD) phenomenon which means the contribution from dielectric loss to imaginary permittivity at low frequencies is significant. In such a situation, K-K transformation or dielectric response modelling techniques can be used to distinguish the effects of conduction and polarisation.

In the case of a transformer, measured frequency domain dielectric response is largely influenced by the geometry of its insulation system. When the geometrical information of the insulation system of a transformer is not readily available, DDF(ω) is frequently used to represent dielectric response of the transformer as it is the ratio of $\varepsilon''(\omega)$ to $\varepsilon'(\omega)$.

$$\text{DDF}(\omega) = \tan(\delta) = \frac{\varepsilon''(\omega)}{\varepsilon'(\omega)} \qquad (3.23)$$

3.5 Application of PDC and FDS Measurements for Condition Monitoring of Transformers

3.5.1 PDC measurements

Use of PDC response measurement for condition monitoring of power transformer insulation has been widely discussed in the literature [128-133]. The general shape and magnitude of PDC response of a transformer at different time ranges are distinctly characterised by the conditions of solid and liquid insulation in such a way that PDC response in the initial time range (t<100 s) reflects the condition of oil whereas long-time (t>1000 s) polarisation and depolarisation currents are mainly influenced by the condition of paper insulation [119, 132, 134, 135]. Exponential time decaying current in-between them is preliminary characterised by the interfacial polarisation phenomenon arising at the interface of oil–paper insulation. The interfacial polarisation effect is largely influenced by the geometry of the insulation system.

Generally, an increase of oil conductivity results in higher initial polarisation and depolarisation currents. On the other hand, long-time polarisation and depolarisation currents increase due to an increase of paper insulation conductivity. The conductivity of both oil and paper insulation markedly changes with ageing and moisture. Thus, it provides information about the quality of oil and paper insulation with respect to moisture content and ageing. However, to calculate the oil and paper conductivities from a measured PDC response; exact design details are required along with composition of the transformer insulation system. Exact design data is not readily available from

the utilities. In such a situation, considering the relative volume proportion of oil and paper insulation in a transformer insulation system is adequate for conductivity analysis [119, 136]. Assuming that the relative amount of paper insulation in the composite insulation system of a transformer is *X*, Saha et al [119] propose the following eqns to calculate conductivity of oil and paper insulation distinctly.

$$\varepsilon_e = \frac{\varepsilon_{paper}\varepsilon_{oil}}{\varepsilon_{paper}(1-X)+\varepsilon_{oil}X} \tag{3.24}$$

Where, ε_e, ε_{oil}, and ε_{paper} represent the effective permittivity of the composite system and permittivity of oil and paper insulation respectively. The conductivities of oil and paper can then be calculated using eqns (3.25) and (3.26) respectively.

$$\sigma_{oil} = \frac{\varepsilon_0\varepsilon_{paper}}{\varepsilon_e C_0 U_0} I_{pol}(+0) \tag{3.25}$$

$$\sigma_{paper} = \frac{\varepsilon_0 X}{C_0 U_0} I_{dc} \tag{3.26}$$

Where, $I_{pol}(+0)$ represents the initial polarisation current just after the first transient and I_{dc} denotes the long-time DC current which is the difference between polarisation and depolarisation current.
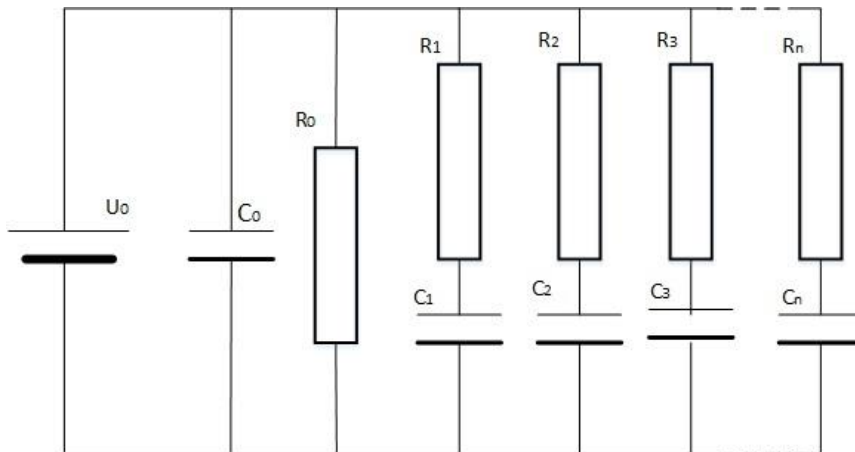
Figure 3.8. R-C equivalent circuit model for linear dielectric

A well known R-C equivalent circuit shown in Figure 3.8 which is used for modelling the PDC response of linear dielectric materials has been adopted in most of the PDC interpretation schemes developed for transformers [129, 130, 132, 134, 135]. In this case, dielectric polarisation behaviour of a transformer insulation system is characterised using a series of Debye relaxation processes with different time constants. They are represented by parallel branches each containing a series connection of resistor and capacitor as shown in Figure 3.8 [132]. R_0 and C_0 of the equivalent

circuit characterise the conductive current and geometric capacitance of the insulation system. Accordingly, depolarisation current corresponding with the R-C equivalent circuit can be explained with eq (3.27).

$$I_{depol}(t) = \sum_{1}^{n} A_i . e^{(t/\tau_i)} \quad where \; \tau_i = R_i C_i \tag{3.27}$$

Where, τ_i and A_i are the time constant and pre-exponential factor corresponding to ith R-C branch of the equivalent circuit respectively.

T. Leibfried et al [135] presented PDC responses of oil and paper insulation with distinct R-C equivalent circuits. Then an equivalent hierarchical circuit has been derived considering the R-C models of oil and paper insulation and the geometry of the insulation system to represent the complete transformer insulation. In this way, they propose to calculate PDC response of a transformer using the R-C equivalent circuit parameters of oil and paper insulation with known properties and then compare with the measured response to interpret the condition of the insulation system.

Der Houhanessian et al [130, 137] consider the insulation system of a transformer as a multilayer structure of oil and paper insulation. They propose series connection of R-C equivalent circuit elements (for oil and paper insulation) to model the PDC behaviour of transformer insulation. Their interpretation scheme to evaluate the condition of an insulation system based on model parameters is almost similar to that of Leibfried.

Application of the above modelling techniques to analyse the condition of transformer insulation is hampered by a lack of information about the design, geometry and arrangement of insulation within the transformer. Saha et al [132, 134] consider the insulation system of a transformer as a "black box" and use a single level R-C equivalent circuit to represent PDC response of the whole system. They interpret the physical behaviour of the model parameters in such a way that R_i-C_i values corresponding to the smaller time constant branches reflect the condition of oil and magnitudes of R_i-C_i elements of the larger time constant branches provide information about the condition of paper insulation. Moreover, when the quality of insulating liquid is good, R values of the smaller time constant branches tend to increase while capacitance values tend to decrease leading to lower initial polarisation and depolarisation currents. On the other hand, decrease in R values and increase in C values of the smaller time constant branches reflect the bad quality of the insulating oil. A similar interpretation has been proposed to analyse the quality of paper insulation using R_i-C_i parameters of large time constant branches. The main advantage of this method over other R-C

equivalent circuit based PDC analysis methods is that this technique enables interpretation of the condition of both oil and paper insulation distinctly without prior knowledge about their relative arrangements.

3.5.2 FDS measurements

FDS of a transformer insulation system contains information about polarisation and conduction effects associated with both oil and paper insulation materials. Therefore, adequate understanding of frequency domain dielectric response behaviour of individual materials is required to analyse FDS results of transformer insulation systems. In general, all types of insulating oils show solely conductive behaviour and thereby, FDS of an insulating liquid can be characterised using its DC conductivity (σ_{oil}) and dielectric constant (ε_{oil}) as in eq (3.28). DC conductivity of new mineral and ester insulating oils at 20 ℃ is typically in the range 0.05-1 pS/m and 5-20 pS/m respectively [27]. Ageing may cause to increase the conductivity of oil to a large value (1000 pS/m).

$$\varepsilon(\omega) = \varepsilon_{oil} - j\frac{\sigma_{oil}}{\omega\varepsilon_0} \tag{3.28}$$

Several scholars have reported that moisture, temperature and ageing largely influence the frequency domain dielectric response of oil impregnated cellulose paper insulation by intensifying both conduction and polarisation phenomena [27, 123, 124, 127, 138-140]. Thereby, an increase of temperature and moisture causes to shift the dielectric response towards a higher frequency. The frequency shift due to a temperature change can be characterised by an equation of Arrhenius type (eq (3.29). Activation energy E_a indicates the degree of temperature dependence of dielectric response and is calculated in eV [141].

$$\omega_T = \omega_{ref}\, e^{\left(\frac{-E_a}{K}\left(\frac{1}{T}-\frac{1}{T_{ref}}\right)\right)} \tag{3.29}$$

Where, ω_T and ω_{ref} are the frequencies, which have same magnitude in their dielectric responses at temperatures T and T_{ref}, respectively. K represents Boltzmann constant (8.6173324(78)×10^{-5} eV).

Chandima et al [138] have found that activation energy of oil impregnated paper insulation varies in the range 0.8-1.1 eV with a tendency to increase with moisture. Koch et al [27] suggest activation energy of 0.9 eV to characterise temperature dependence of cellulose material whereas that for mineral oil is 0.4 eV. According to [142], activation energy of oil impregnated paper is typically in the range 0.9-1 eV and that of mineral oil in between 0.4 eV and 0.5 eV. Linhjell et al [124] have

reported that activation energy value of impregnated and non-impregnated cellulose paper insulation is typically in the range 1-1.05 eV and 0.9-1.03 eV respectively.

Linhjell et al [124] have also observed that the minimum $\varepsilon''(\omega)$ of FDS of oil impregnated paper insulation is sensitive to moisture content in such a way that an increase of moisture gives exponential rise to the minimum of $\varepsilon''(\omega)$ as in eq (3.30).

$$\varepsilon''_{min} = A_1 e^{B_1 m} \tag{3.30}$$

Here A_1 and B_1 are constants which take the values 0.014 and 0.24 for paper and 0.013 and 0.22 for pressboard. m is the percentage moisture content.

Saha et al [143] suggest that the increase of moisture gives rise to both real and imaginary permittivity and this behaviour is sensitive to measured frequency and temperature. They propose two empirical formulas as in eqns (3.31) and (3.32) to correlate the real and imaginary permittivity at any arbitrary frequency f and temperature T to the moisture content m.

$$m = \left(f^{0.0011T+0.233} \times \left(\frac{\varepsilon'}{\varepsilon_0} - 3 \right) \times 10^{0.6499-0.0081T} \right)^{\frac{1}{-0.8511\log(f)+1.7780}} \tag{3.31}$$

$$m = \left(f^{0.0032T+0.2265} \times \left(\frac{\varepsilon''}{\varepsilon_0} \right) \times 10^{1.2571-0.0177T} \right)^{\frac{1}{-0.2797\log(f)+2.13}} \tag{3.32}$$
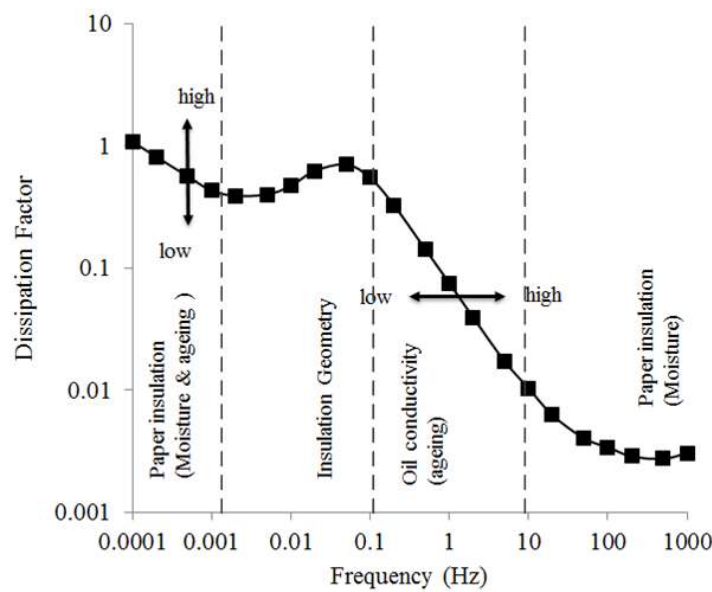
Figure 3.9. Typical dielectric response of oil-paper insulated transformer [27]

Figure 3.9 elucidates the general interpretation for dielectric response of the oil–paper insulation system of a transformer. As seen in Figure 3.9, dielectric response of the paper insulation dominates in the frequency range 10^1-10^3 Hz. In the mid frequency range (10^{-1}-10^1 Hz) dissipation factor increases with slope of -1 /decade toward the low frequency and this region can be attributed to the conductive effect of oil. It is followed by the peak originated by the interfacial polarisation phenomenon due to accumulation of space charges at the oil-paper interface. With further decreasing frequency, the response of the composite system follows the dielectric properties of paper insulation and dielectric response in this frequency region is largely influenced by the moisture and ageing by-products in the paper insulation [27, 100].

In [27, 127, 139, 141], a moisture determination technique has been proposed which is based on a comparison of measured FDS of a transformer over a wide range of frequency to a mathematically modelled dielectric response. This method has been proven to be effective in determining moisture in the paper insulation of transformers. Accuracy of this method is based on the accuracy of the pool of data which is used for mathematical modelling. The database mainly contains dielectric response data of oil impregnated paper insulation taken at different moisture, temperature and ageing conditions. For mathematical modelling, the cylindrical insulation structure between low and high voltage windings of a transformer is represented by so-called X-Y model as shown in Figure 3.10 (b). *X* is the ratio of the sum of thickness of all barriers in the duct, lumped together and divided by the duct width [144]. *Y* is the ratio of the total width of all spacers to the length of periphery of the oil duct. Typically, the value of *X* is in the range 20-50 % and *Y* possesses a value in the range 15-25 %. In order to estimate the moisture content in the solid insulation, this method combines the dielectric response data in the pool using the X-Y model to give the best fit with the measured response at a given temperature. Most of the commercialised FDS based moisture diagnostic tools such as MDOS use this method.
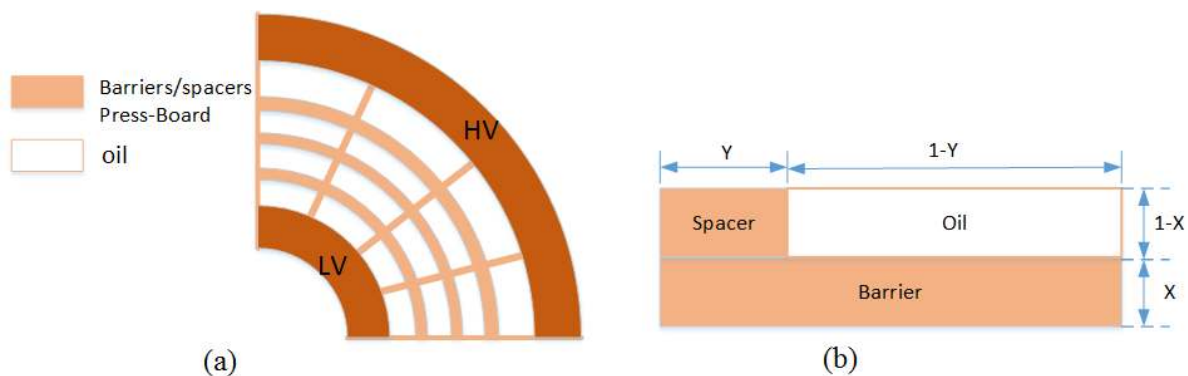
Figure 3.10. (a) Representation of typical transformer insulation, (b) Equivalent X-Y model

However, a very limited number of studies have investigated the FDS behaviour of ester impregnated paper insulation [97, 145] and the present understanding of the impact of moisture, ageing and temperature on FDS behaviour of ester-paper insulation system is inadequate. Thus, one cannot claim that well established FDS data interpretation schemes developed for mineral oil based insulation systems are applicable for ester based transformer insulation systems.

3.6 Chemical Based Techniques

3.6.1 Overview of chemical based condition monitoring techniques

Over several decades, several chemical based diagnostic techniques have been used to assess the condition of oil and paper insulation in transformers. Most of the established chemical methods have been developed for insulating oil because the insulating oil in a transformer contains a significant amount of diagnostic information and it can be easy to take an oil sample even from an operating transformer. Measurement of viscosity, acidity and determination of moisture content of oil with KFT method are the most frequently utilised chemical based techniques to determine the degree of degradation of insulating oils. In addition, interfacial tension (IFT) and colour of oil can also be used to assess the quality condition of insulating oils. Dissolved gas (DGA) and furfural analysis are also widely used oil associated chemical techniques to identify the incipient faults and characterise the ageing of solid insulation respectively.

Measurement of average DP, tensile strength and moisture content of paper insulation with KFT are widely used techniques in laboratory investigations for characterising the properties of paper insulation. Further, use of FTIR spectroscopy, molecular weight measurement by gel permeation chromatography (GPC) and thermo-gravimetry analysis of cellulose paper insulation has also been quoted in some of the literature [63, 146, 147]. However, practical use of these paper-based techniques is hampered by the dificulty in taking paper samples from an operating transformer.

This section will only provide a brief overview of commonly used chemical diagnostic techniques in the field and their interpretation schemes.

3.6.2 Moisture analysis using KFT and equilibrium chart techniques

KFT is a well-established analytical method which has been developed for assessing the moisture content in a range of liquid and solid materials. IEC Std. 60814 provides a detailed procedure to estimate the moisture content in both insulating oil and oil impregnated solid insulation using KFT technique. The principle behind it is based on the reaction between iodine (I_2) and sulfur dioxide (SO_2) in the presence of water [127, 148]. In the mixed solution, iodine is first produced by an

electrolysis reaction followed by a reaction between iodine and water. The amount of electricity (coulomb) required for the electrolysis reaction is in proportion to the amount of iodine required for reacting with the water. According to the stoichiometry of the reaction, one mole of iodine reacts with one mole of water and thereby, when 1 mg of water exists in the system, 10.72 C of electricity is required to complete the reaction. This principle is used in KFT method to determine the water content in oil and oil impregnated paper insulations.

Though the moisture content of paper insulation can be directly measured using KFT technique, the application of this method in the field is impeded by the difficulty in taking a paper sample from an operating transformer. Moreover, difficulty in extracting strongly bonded water from the cellulose paper is another problem in the use of KFT method on paper insulation. Therefore, it has been a common practice to determine the moisture content in oil using KFT method and then estimate the moisture in solid insulation using so-called equilibrium charts [149]. The equilibrium charts are created by combining the moisture isotherm of cellulose paper and oil assuming that relative moisture saturation of oil and impregnated paper is equal under the equilibrium condition. Over the years, several equilibrium charts have been established for mineral oil-paper systems to correlate the moisture content in oil and paper insulation under equilibrium condition [150, 151]. Since the esters have higher moisture solubility than typical mineral oil, one cannot use the equilibrium chart developed for a mineral oil-paper system for an ester-paper systems. Thus, Zhaotao et al [152] have obtained new equilibrium charts for NE-based insulation systems in transformers. Koch et al [42] have developed sets of equilibrium charts for both natural and synthetic ester-paper insulation systems. Figure 3.11(a) and (b) show two different equilibrium charts reported in the literature for mineral oil-paper and NE-paper systems respectively.
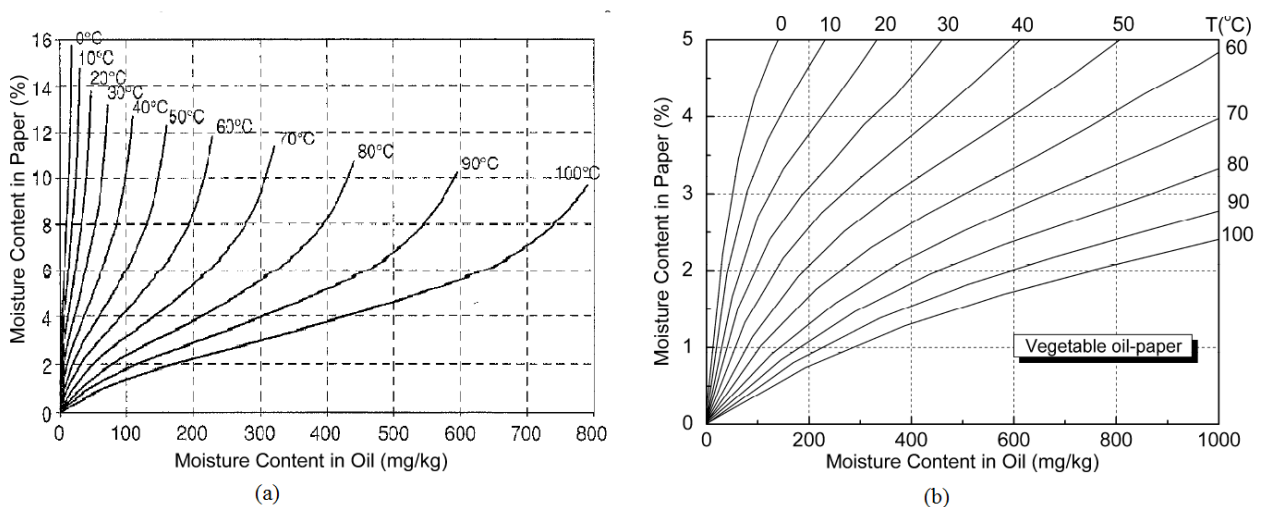
Figure 3.11. Equilibrium chart (a) Mineral oil-paper (MIT curve) [150], (b) NE- paper [152]

Operating transformers experience dynamic temperature variations. Therefore, moisture equilibrium condition in such transformers is hardly achieved. On top of that it is hard to eliminate the moisture ingress to oil samples during sampling and transportation to the laboratory. These factors largely influence the equilibrium chart method leading to a high uncertainty in estimated results.

3.6.3 Formation of dissolved gases in transformers and method of analysis

Intense heat generated due to abnormal conditions in oil filled transformer such as arcing, overheating of insulation, pump failure and overloading, decomposes oil and paper insulation into low molecular combustibles H_2 (Hydrogen), CH_4 (methane), C_2H_2 (acetylene), C_2H_4 (methylene), C_2H_6 (ethane), CO (carbon monoxide) and incombustible CO_2 (carbon dioxide) gases in varying quantities [153, 154]. It has been reported in the literature that gas formation patterns of mineral and ester based insulating liquids (natural and synthetic) are almost similar but there are some quantitative differences in the ratios of gases formed [155-158].
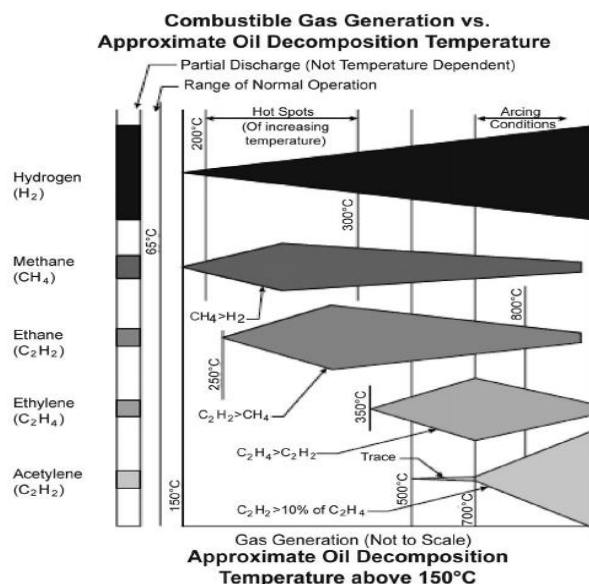
Figure 3.12. Gas generation chart for typical mineral insulating oil [159, 160]

The type and composition of gas formation depends on the degree of localised temperature rise or energy contained in a fault because the energy needed for scission of molecular bonds and their recombination into different types of gases is not similar. Figure 3.12 demonstrates the relative composition of gases evolving in typical mineral insulating oil at different temperatures above 150 ℃. The dissolved gases evolved due to the decomposition of oil-paper insulation are partly dissolved in oil. Therefore, determining the concentration or specific proportion of such gases dissolved in oil provides an early indication of developing faults in transformers. Moreover, this method enables status checks on new and repaired units and convenient scheduling of maintenance.

Table 3.3 gives details of common dissolved gases found in transformer oil and their relation to typical fault types in transformers.

Table 3.3. Fault indicator gases in mineral oil [157]

Fault gas	Key indicator	Secondary indicator
H_2 (Hydrogen)	Corona Partial discharge	Arcing overheating
CH_4(Methane)		Corona arcing and overheating of oil
C_2H_6(Ethane)		
C_2H_4(Ethylene)	Overheated oil	Corona arcing
C_2H_2(Acetylene)	Arching	Severely overheated oil
CO(Carbon monoxide)	Overheated cellulose	Arcing in cellulose
CO_2(Carbon dioxide)		Overheated cellulose, arcing in cellulose
O_2(oxygen)		Indicator system leak
N_2(Nitrogen)		Indicator system leak

A detailed procedure for analysing the dissolved gases in mineral insulating oils is prescribed in IEC Std. 60567 and ASTM Std. D 3612-2. In order to extract the gases dissolved in oil, all the methods described in IEC 60567 ((Toepler, Partial Degassing, Stripping, Head Space) and ASTM D3612-2 (Vacuum Extraction, Stripping and Head Space) can be utilised and extracted gases can be analysed using gas chromatography techniques. Cigre working group D32 suggests to increase the equilibrium time necessary for gas extraction to about 10-15 minutes or higher when the dissolved gases in a non-mineral oil sample (natural and synthetic esters) with high viscosity are analysed [156].

3.6.4 Interpretation of DGA results

IEC Std. 60599 (2007) and IEEE Std. C57.104 (2008) provide general guidelines for interpreting the DGA results of mineral oil impregnated electric equipment in service. According to IEEE Std. C57.104, equipment variables such as type, location, and temperature of the fault etc. and variables associated with the sampling and measuring procedures have to be considered when interpreting the significances of DGA data. IEC gas ratio, IEEE key gas, Duval's triangle and Rogers's ratio are the key methods which have been used for decades to identify the possible faults occurring in operating transformers based on DGA results.

IEC gas ratio method identifies six broad classes of faults in oil filled transformers using the pattern of hydrocarbon gases dissolved in oil as given in Table 3.4. In addition, IEC 60599 suggests to use CO_2/CO and O_2/N_2 ratios for identifying paper involvement in a fault and detecting abnormal oxidation of oil respectively.

In the IEEE key gas method, the principle type of gas and relative proportions of other combustible gases are considered to identify four different types of basic faults, namely overheating of oil, overheating of cellulose, partial discharge and arcing. The principle gases corresponding to those faults are ethylene, carbon monoxide, hydrogen and acetylene respectively.

Table 3.4. DGA interpretation table IEC 60 599 [161]

Case	Characteristic fault	$\frac{C_2H_4}{C_2H_4}$	$\frac{CH_4}{H_2}$	$\frac{C_2H_4}{C_2H_6}$
PD	Partial Discharge (Note 3 and 4)	NS	<0.1	<0.2
D1	Discharge low energy	>1	0.1-0.5	>1
D2	Discharge high energy	0.6-2.5	0.1-1	>2
T1	Thermal fault(t<300 ℃)	NS	>1 but (NS)	<1
T2	Thermal fault (300 ℃ <t<700 ℃)	<0.1	>1	1-4
T3	Thermal fault (>700 ℃)	<0.2	>1	>4

NOTE 1 In some countries the ratio C_2H_2/C_2H_6 is used rather than ratio CH_4/H_2
NOTE 2 The above ratios are significants and should be calculated only if at least one of gas concentration and rate of gas increase above the typical value (IEC 60599- clause 9)
NOTE 3 CH4/H2 <0.2 for partial discharge in instrument transformer
 NS -Non-significant whatever the value

Roger and Doernenberg are two different ratio methods reported in [154] and both methods collectively utilise five different gas ratios as shown in Figure 3.13. In the Doernenberg method, ratios R1, R2, R3 and R4 are compared to limiting values enabling suggested fault diagnosis [149]. Rogers technique considers only three gas ratios (R1, R2 and R5). Flow charts for interpreting DGA data using Doernenburg and Rogers methods are given in [154]

$$R1=\frac{CH_4}{H_2} \quad R2=\frac{C_2H_2}{C_2H_4} \quad R3=\frac{C_2H_2}{CH_4} \quad R4=\frac{C_2H_6}{C_2H_2} \quad R5=\frac{C_2H_4}{C_2H_6}$$

Figure 3.13. The gas ratios used in Doernenburg and Rogers methods

The Duval triangle is a graphical method where coordinates of corresponding DGA results are represented in an equilateral triangle as shown in Figure 3.14 (a-d). Eqns (3.33) to (3.35) demonstrate the method of calculating triangle coordinates. Duval triangle 1 shown in Figure 3.15 (a) which has been defined for a transformer filled with mineral oil allows detection of seven basic types of possible faults in a service unit namely; PD, D1; D2; T1, T2, T3 and DT(mixtures of electrical and thermal faults) [162]. Due to the different gas generation behaviour of different types of mineral oils in the market, the low temperature faults are mistakenly identified as PD or T2 by Duval triangle 1. Therefore, Duval triangles 4 and 5 have been developed to remove these uncertainties. In Duval triangles 4 and 5, C_2H_2 has been replaced with C_2H_6. Considering the different gassing behaviour of commercially available non-mineral insulating liquids (silicon oil,

natural and synthetic esters), Duval triangle 3 has been developed. For constructing Duval triangle 3, some of the boundary zones of triangle 1 are modified as given in Table 3 of [162] to comply with the gassing behaviour of corresponding alternative insulating liquids.
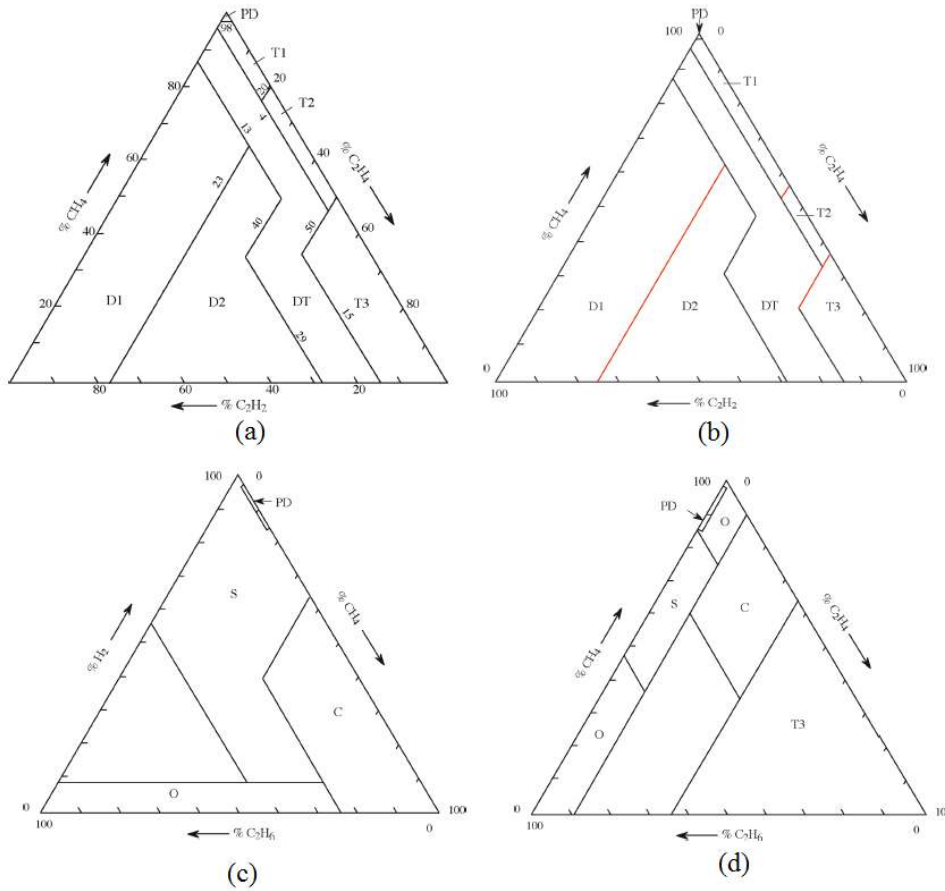
Figure 3.14. Duval triangle (a) Triangle 1, (b) Triangle 3 for FR3, (c) Triangle 4, (d) Triangle 5

$$\%C_2H_2 = \frac{100x}{(x+y+z\_)} \tag{3.33}$$

$$\%C_2H_4 = \frac{100y}{(x+y+z\_)} \tag{3.34}$$

$$\%CH_4 = \frac{100z}{(x+y+z\_)} \tag{3.35}$$

The mentioned conventional DGA interpretation schemes have been updated recently. A. Akbari et al [163] have proposed an artificial neural network and agent based software diagnosis tools to automate the interpretation of DGA data and reduce the risk of mistaken diagnosis. Duval pentagon is a recently developed graphical DGA interpretation technique which is based on use of five main hydrocarbon gases [164]. Each summit of the pentagon corresponds to one gas. In this technique relative percentages of each hydrocarbon gases are plotted on the axis between pentagon centre

(0%) and pentagon vertex (100%). The Duval pentogon1 allows to identify six basic electrical and thermal faults (PD, D1; D2; T1, T2, and T3). Duval pentagon 2 enables discrimination of three basic electrical faults ((PD, D1; D2) and four advance thermal faults (T3-H -thermal fault oil only, C–Carbonisation of paper, O-overheating (<250 ℃) and S-stray gassing of oil). Umar Farooque et al [165] have proposed artificial neural network based implementation for Duval pentagon.

3.6.5 Furan analysis

It was mentioned in Chapter 2 that thermal degradation of cellulose paper insulation used in electrical equipment yields a class of heterocyclic compounds including 2-furfural aldehyde (2-FAL), 2-acetylfuran (2-ACF), 2-furoic acid, 5-methyl-2-furfural (5-MEF), 2-furfurylalcohol (2-FOL) and 5-hydroxymethyl-2-furfural (5-HMF) [9, 10, 166, 167]. Figure 3.15 shows the chemical structures of the six furanic compounds. These compounds are partly dissolved in oil medium and can be determined using either of the methods described in IEC Std. 61198 or ASTM Std. D 5837 which are based on High-Performance Liquid Chromatography (HPLC) aided with a liquid or solid extraction procedure. These methods allow detecting even trace quantities of furanic compounds dissolved in oil in the ppb (parts per billion) range.
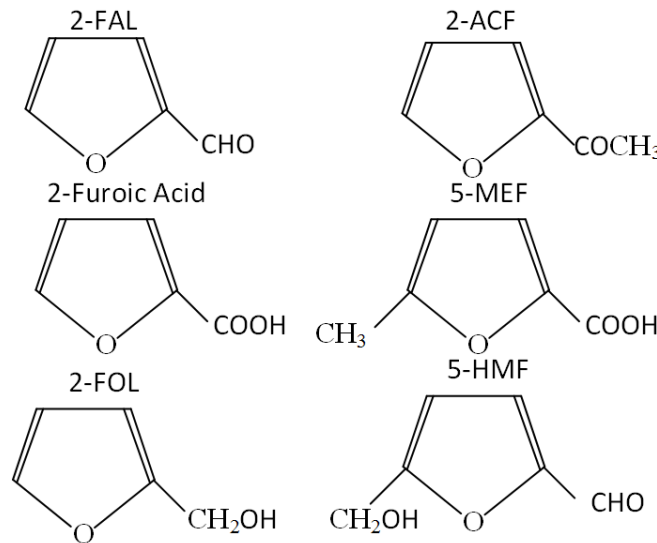
Figure 3.15. Chemical structures of furanic compounds [9]

It has been reported in the literature [6, 168] that all five furanic compounds except 2–FOL are quite stable below 100 ℃ in the absence of oxygen. Moreover, 2-FAL, 2-ACF and 5-MEF show relatively good stability when the temperature is above 100 ℃ and below 160 ℃. Emsley et al [7] have also made almost the same conclusion such that apart from 2-FOL all other furanic compounds are relatively stable at temperatures up to 140 ℃. Hence, furanic compounds dissolved in insulating oil are solely related to degradation of paper insulation and most of them are relatively

stable in the transformer operating environment, analysis of these compounds has been successfully applied as a non-invasive technique to characterise the condition of solid insulation of transformers in service [9]. 2-FAL is the main derivative of paper degradation which presents in the highest amount in oil and thereby, 2-FAL is the most commonly measured furanic compound for diagnostic purposes [26, 168, 169].

Several scholars have reported the presence of dissolved 2-FAL in oil when cellulose paper insulation is aged in typical mineral insulating oil [10, 47, 56, 93, 167, 170]. Emsley et al [10] suggested that formation of 2-FAL due to ageing of cellulose paper insulation is more effective in the presence of water and oxygen. Moreover, the main production of 2-FAL occurs when the DP value of cellulose insulation falls below 400. They have also observed that cotton paper produces less 2-FAL than Kraft paper. It has been reported in recent literature that 2-FAL production from cellulose paper insulation immersed in natural and synthetic ester is noticeably lower than that from cellulose insulation immersed in typical mineral oil [11, 24, 95]. However, there are not enough laboratory investigations or field measurements to confirm this behaviour.

Shroff et al [47] have reported the existence of a linear relationship between DP value of cellulose paper insulation and 2-FAL concentration dissolved in mineral oil in logarithm scale. Pablo [56, 171] has proposed a different set of empirical formulas to correlate dissolved 2-FAL concentration in mineral oil and DP value of paper insulation based on results of his accelerated ageing experiments. Table 3.5 presents some of the referred empirical formulas presented in literature for correlating DP and 2-FAL concentration in oil. As seen in Table 3.5, one can clearly notice that there is no universal generalised relationship existing between DP and 2-FAL concentration dissolved in oil. Moreover, the established relationships in literature are valid only under the particular condition where the corresponding relationship has been derived.

Table 3.5. Established relationship for correlating 2-FAL concentration in oil and DP of paper

Reference	Ageing Conditions	Proposed 2-FAL(ppm)-DP correlation
De Pablo [56]	25/1 (paper/oil) (based on cellulose chain scission theory)	$2FAL = \dfrac{7100}{DP} - 8.88$
De Pablo [56]	As above 20 % of cellulose age faster	$2FAL = \dfrac{4301}{DP} - 5.38$
De Pablo [171]	100/1, 2 % moisture in paper, aged in open air at -120°C	$\log(2FAL) = 3.41 - 0.00264$
Karcler [167]	10/1, 3.85 moisture in paper, aged at 85 °C in absence of air in non-inhibited oil	$\ln(2FAL) = 8.75 - 0.013DP$
Chendong [172]	24/1 Dried paper aged at 140 and 148 °C	$\log(2FAL) = 1.51 - 0.0035DP$

Over the last two decades, massive numbers of survey studies have been conducted to investigate the typical concentration of furanic compounds in operating transformers. The study conducted by S.D Myers laboratory in North America contains test results of 12341 mineral oil samples taken from different transformers around the world which represent a vast array of climates, operating regimes, transformer manufacturers and types of mineral oils. Statistics of this study present that 2-FAL concentration in 96.3 % of the transformer population is below 1 ppm (mg/kg) and 98.3 % of the transformer population contains insulating liquid with 2-FAL concentration of less than 2.5 ppm. Based on a statistical survey of more than 5000 transformers, Pablo et al [171] have reported that 2-FAL concentration in more than 90 % of the European transformer population is in the range 1-5 ppm. This is considerably higher than the ones obtained by Myers. A study conducted by Japanese researchers has pointed out that 2-FAL concentrations of all the transformers considered in their study (98) are below 0.31 ppm [173]. Based on the above information, one can clearly conclude that threshold values for 2-FAL suggested in some literature are not valid in a real situation for diagnostic purposes [174]. Moreover, the 2-FAL concentration dissolved in oil is influenced by several factors including the type and ageing condition of insulating oil, type of paper insulation, temperature, moisture content in oil and paper insulation and the presence of oxygen in the system, etc. Therefore, Cigre working group D1.01 (TF13) has underlined that it is difficult to use any mathematical relationship or absolute value based on dissolved 2-FAL concentration in oil for assessing the condition of solid insulation in an operating transformer [9]. On the other hand, the use of rate of change of 2-FAL is more appropriate for diagnostic purposes [9].

3.6.6 Neutralisation number (Acidity value) and colour

In the case of mineral insulating oil, an increase in the neutralisation number mainly reflects the degree of deterioration of oil under oxidising conditions. Short chain acids produced by degradation of mineral oil are detrimental to an insulation system and create some problems by oxidising metallic parts. However, a rise in the neutralisation number of synthetic and natural ester insulating oils does not merely represent oxidising conditions because hydrolytic degradation of esters also yields acids. Since degradation of cellulose insulation releases water, hydrolysis reaction in ester oil in a transformer could become pronounced with time. Synthetic esters mainly produce short chain acids and these acids accelerate the ageing process of paper insulation and create corrosion on copper conductors. However, hydrolysis reaction in NEs produces long chain fatty acids and they are not harmful to the insulation system or other components in transformers.

Since chemical activity of acids generated in different insulating oils is not similar, different limiting values for the neutralisation number have been proposed for in service mineral, synthetic

and natural ester insulating oils. As per British Std. EN 61203, synthetic ester insulating oil with satisfactory conditions for further use in electrical equipment with a voltage rating of 35 kV or lower should be less than 2 mgKOH/g [105]. Acceptable maximum neutralisation numbers for in service mineral and NE oils of < 69 kV voltage class are 0.2 mgKOH/g [175] and 0.3 mgKOH/g [103] respectively.

Acidity value measurement results of several laboratory studies point out that the neutralisation number of NE insulating oils can increase far beyond a specified limiting value even after aged in a sealed environment with minimum oxygen [68, 79, 95, 176]. In addition, results of some studies have confirmed better ageing performance of cellulose material in NE with a higher acidity level than that of in a typical mineral oil [24, 95]. Therefore, one can claim that a proposed limiting neutralisation value for service aged NE oils is arguable.

The colour of oil is a primary parameter which reflects the degree of degradation and possible contamination of oil during use. A numeral value based on international colour standards (ASTM D1500) is generally used in expressing colour changes. As per IEEE Std. C57.152-2013, new mineral oil has a clear appearance with a colour number in the range 0-0.5 and severely aged dark brown colour mineral oil has a colour number of greater than 7 [103]. Mineral oil of marginal condition has a bright yellow colour and its colour number is in the range 2.5-4.0. Synthetic ester with a clear appearance without being excessively dark in colour is considered as an insulant with acceptable condition for further use [105]. In the case of NE, colour changes have not yet been standardised for quality assurance. IEEE Std. C57.147-2008 has provided a provisional limiting value (1.5) for colour number of service aged NE insulating oils

3.7 Summary

Widely used electrical and chemical based techniques and their interpretation schemes for assessing the overall conditions of oil and paper insulation in transformers are briefly reviewed in this chapter. It has been identified that complete international standards have not yet been tailored for assessing the quality of NE-paper insulation systems based on oil related chemical diagnostic methods including acidity value, DDF, viscosity, furfural content, colour and DGA. Moreover, experimental results presented in the literature show contradictions with the set limit values in IEEE standards for DDF and acidity of serviced aged NE oils. Therefore, application of these chemical based methods for assessing the condition of NE-paper composites insulation is needed to be investigated. The systematic laboratory study conducted in our research to address this issue is presented in the next chapter.

FDS and PDC methods have mainly been utilised to estimate the moisture in the solid insulation of transformers. However, application of these two methods on ester filled transformers has not yet been considered. Ester insulating oils have higher conductivity and moisture solubility than typical mineral oil. Moreover, conductivity of ester oils increases largely over thermal ageing compared to mineral oil. This research claims that these factors could have a significant influence on time and frequency domain dielectric responses of ester filled transformers. However, no systematic study has considered this issue yet. Therefore, it is required to understand the influence of different physical properties of new and aged ester insulating oils on dielectric response behaviour of cellulose paper based materials through a systematic laboratory study. The work presented in Chapters 5 and 7 is intended to address this issue.

Chapter 4

Understanding the Ageing Behaviour of Ester-paper Insulation Systems

4.1 General

Ageing behaviour of mineral oil-paper composite insulation has been extensively studied over 100 years. Moreover, condition monitoring of mineral oil filled transformers has been well characterised by the copious laboratory and field studies conducted during the past several decades. It is a well-known fact that there is little experience in the use of ester based insulating oils in power transformers. Hence, the applicability of existing oil related condition monitoring techniques for ester filled transformers is yet to be validated. Furthermore, international standards for analysing the degree of insulation quality of service aged NE insulating oils have not yet been completely tailored. A limited number of methodical researches have addressed these issues in the last two decades. In order to reduce this knowledge gap, an improved understanding on ageing behaviour of ester–paper composite insulation in typical transformer operating conditions is required. Therefore, the work presented in this chapter mainly focuses on studying the ageing behaviour of ester-paper insulation systems through a series of laboratory experiments.

An accelerated sealed tube ageing experiment conducted in a controlled environment is the most widely used laboratory method for studying the ageing behaviour of insulation materials. Moisture largely influences the ageing of oil immersed cellulose insulation in transformers and it is an uncontrollable parameter because moisture is a by-product of cellulose ageing. Therefore, in this research project, the influence of moisture on the ageing behaviour of cellulose pressboard insulation immersed in three different types of biodegradable oils has been extensively studied through an accelerated sealed tube ageing experiment conducted at 120 ℃. A decrease in the degree of polymerisation is used as a primary parameter to characterise the ageing degree of pressboard. Appropriateness of FTIR technique for understanding the structural changes of pressboard insulation over thermal ageing is also discussed in this chapter. Moreover, the furanic compounds dissolved in ester and mineral oils are analysed in order to identify their relationships with ageing

conditions of pressboard insulation. The applicability of a number of chemical and physical parameters, including acidity value, DDF, viscosity and colour for assessing the quality of aged ester insulating oils is also discussed in this chapter. Moreover, comparisons are made based on the limiting values provided in related IEEE and British standards and properties of mineral oil under similar ageing conditions. Interpretation of DGA data of ester insulating oils for identifying faults is also a major part of this chapter. This chapter is primarily based on three publications by the PhD candidate [177-180].

4.2 Material Used for Experiment

This study used high-density electrical grade pressboard insulation with textured surfaces comprising of 100 % sulphate wood pulp. The density and thickness of the pressboard were 1.2 gcm^{-3} and 1.5 mm respectively. Four different types of insulating oils including one type of uninhibited mineral oil (Shell Diala), two types of commercially available NE-based insulating oils and a synthetic ester (SE) were utilised for experimental investigations. Here onwards, two types of NEs are identified as NEA and NEB. NEA has been produced from high oleic sunflower oil which contains 5 % of saturated stearic acid (C:18:0), 86 % of mono-unsaturated oleic acids (C18:1), 6 % linoleic acid (C:18:2) and 0.1 % of linolenic (C18:3). NEB used in this study is made of soybean oil, which contains about 24 % of oleic acids and 54 % of linoleic acids. The synthetic ester insulating oil used for this research is pentaerythritol ester. The main properties of all four types of degassed oils are listed in Table 4.1. In order to degas and dry the oil, a sealed steel container with 3 l of oil was connected to a vacuum pump. Then temperature of oil and air pressure inside the container were maintained at 70ºC and < 1 kPa over 12 hrs respectively.

Table 4.1. Properties of degassed oil

Properties	Shell Diala	NEA	NEB	SE
Acidity (mg KOH/g)	0	0.03	0.02	0.01
Viscosity mm^2/s @ 40 ºC	10	37	14	30
Moisture (ppm)	1	35	10	38
Colour	Pale yellow	Bright yellow	Light green	Pale yellow

4.3 Experimental Setup

Two different types of thermal ageing experiments were performed in this study: (1) with dry pressboard insulation, (2) with moderately wet pressboard insulation. This was intended to understand the impact of moisture on the ageing behaviour of cellulose insulation in different

insulating oils. Dry pressboard insulation samples were rectangular shaped strips (150x15x1.5 mm). The wet samples were disc shaped of 100 mm diameter. In both cases, oil impregnated dry pressboard samples were first prepared using the following method.

Initially, pressboard samples were inserted into a steel container. The container was hermetically sealed and it was placed in a temperature controlled oven. Then a high rotary oil vacuum pump was connected to the container and pressboard samples were dried under a very high vacuum level (<1 kPa) at 65 ℃ for 24 hrs. The temperature was then increased to 95 ℃ and the drying process was continued for another 24 hrs. The temperature was then reduced to 40 ℃ and degassed oil was infused into the container while kept under a vacuum condition. The oil filled container with dry pressboard was kept in the oven for 7 days at 60 ℃ to achieve optimal impregnation. Figure 4.1 illustrates the procedure that was followed for oil impregnating under vacuum. Here, the container with dry pressboard (B) was connected to the vacuum pump whilst positive N_2 pressure was applied on oil through the top valve of the container (A). Due to the positive pressure gradient, oil flows from container A to container B. Using this method dried pressboard insulation samples impregnated with Shell Diala mineral oil, NEA, NEB and synthetic ester were prepared separately.
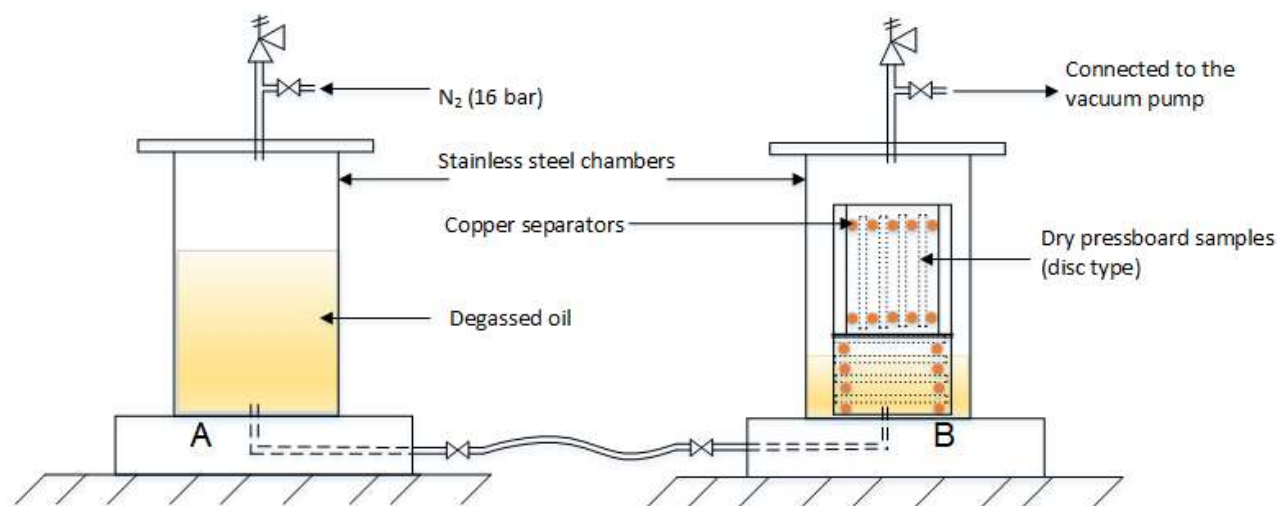
Figure 4.1. Schematic of oil impregnation process under vacuum condition

In order to prepare wet samples with about 2 % of initial moisture content, firstly dried disc shaped pressboard samples were prepared using the above mentioned method with Shell Diala mineral oil, NEA and NEB. Oil impregnated dry pressboard samples were then inserted into three different sealed containers where relative humidity inside the containers was controlled at 11% using a saturated salt solution prepared with LiCl (Lithium Chloride).

In each of the containers, 20 specimens were arranged in a horizontal and a vertical stack. Pressboard specimens were separated by small copper bars to allow moisture diffusion through both surfaces. This moisture conditioning process was performed over 28 days at 50 ºC to absorb about 2 % moisture. The relative humidity and temperature inside the container were closely monitored with a Vaisala MMT 162 moisture sensor during the whole moisture conditioning process. Figure 4.2 shows the humidity controlled container with Vaisal sensor which was used in this research.
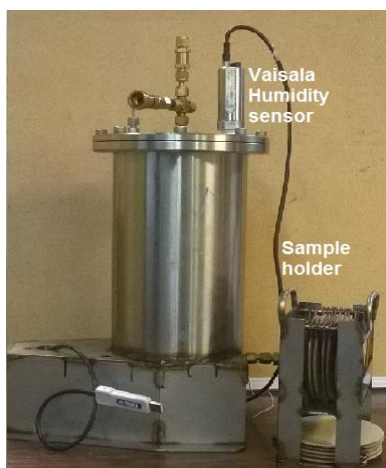
Figure 4.2. (a) Humidity controlled container and sample holder for arranging disc type sample as a vertical and horizontal stack

In order to prepare a saturated salt solution, the methodology described in ASTM E-102-02 was utilised. A measured quantity of LiCl (40 g) was placed in a plastic container with a depth of about 5cm. Then demineralised water was added in about 2 ml increments and stirred well. Addition of water was stopped when the salt solution became pulp slurry, which contained undissolved salt and free water as shown in Figure 4.3.

Figure 4.3. LiCl saturated salt solution

Moisture contents of unaged both dry and wet pressboard samples were measured using the classic KFT method and results have been listed in Table 4.2. Wet pressboard samples impregnated with synthetic ester were not utilised in this research. In addition, the degree of polymerisation (DP) of all types of oil impregnated unaged pressboard samples was measured. Since a similar drying process was applied for all cases, the average value of measured DP was considered as the initial DP of all samples. The calculated average initial DP value was 1284.

Table 4.2.Initial percentage moisture content in oil impregnated pressboard

Type of pressboard	Type of oil used for impregnation			
	Mineral	NEA	NEB	SE
Dry	0.5	0.7	0.4	0.6
Wet	2.2	2.4	2.0	-

The ageing of oil impregnated dry pressboard was performed in specially designed glass tubes. Firstly 16 g of dry pressboard, 175 ml of degassed oil and 16g of copper conductors were placed into the glass tubes. AP 101 high vacuum grease was applied to the ground glass joints of the test tube to ensure a fully sealed environment. Then air in the tube headspace was pumped out until the pressure decreased to a level between 10-20 kPa. The headspace was then filled with dry nitrogen. This process comprised three major steps as shown in Figure 4.4. Four sets of ageing test tubes which contained oil, dry pressboard and copper were prepared using this method from each type of oil.
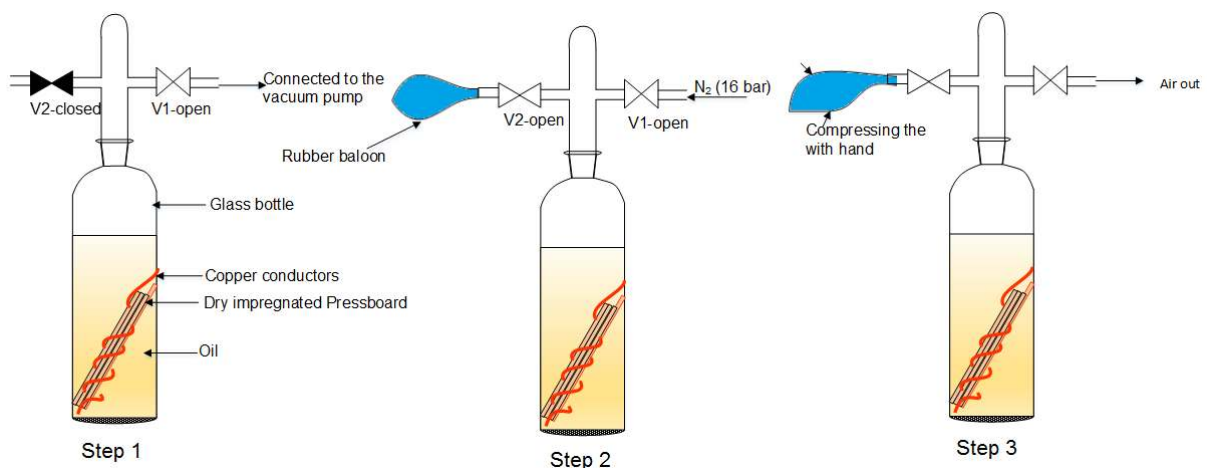
Figure 4.4. Basic steps used in the laboratory to prepare sample for thermal ageing

Finally, for accelerated ageing, the glass tubes were then placed in an aluminium heater block as shown in Figure 4.5 (a). The temperature of the heater block was adjusted to 120ºC. Temperature

hysteresis of the heater block was ±2 ℃. A FLUKE 51-II thermometer with ±0.1 ℃ of accuracy was utilised to monitor the temperature of the heater block over the thermal ageing period. A thermal image of an ageing tube was also taken as an additional measurement. Ageing was stopped at regular intervals for obtaining oil and paper samples for analysing. Before sampling, ageing tubes were kept at room temperature for 7 days allowing equilibrium of ageing by-products between pressboard and oil to be reached.

The ageing experiment of wet pressboard insulation was performed in steel containers. The moisture conditioned pressboard samples (20 specimens were arranged in a horizontal and a vertical stack), degassed oil and copper bars were inserted into three different stainless steel containers, in such a way that the mass ratio between oil, pressboard and copper was maintained at 10:1:1. All the containers were hermetically sealed and headspaces of the containers were filled with dry nitrogen. Then containers were placed inside an oven for ageing. The ageing process was carried out at 120 ℃. Positions of the steel containers were interchanged at regular intervals. Thus, one could assume that the heating effect on all the ageing containers was nearly the same. The ageing process was stopped at regular intervals (28, 35, 48, 62, 73 and 84 days) and the containers were kept at room temperature for 7 days before obtaining oil and pressboard samples. It is worthwhile to mention that the ageing containers had to be opened for taking pressboard samples. Thereby, it was required to fill the headspaces of the ageing containers with dry nitrogen before resumed ageing.
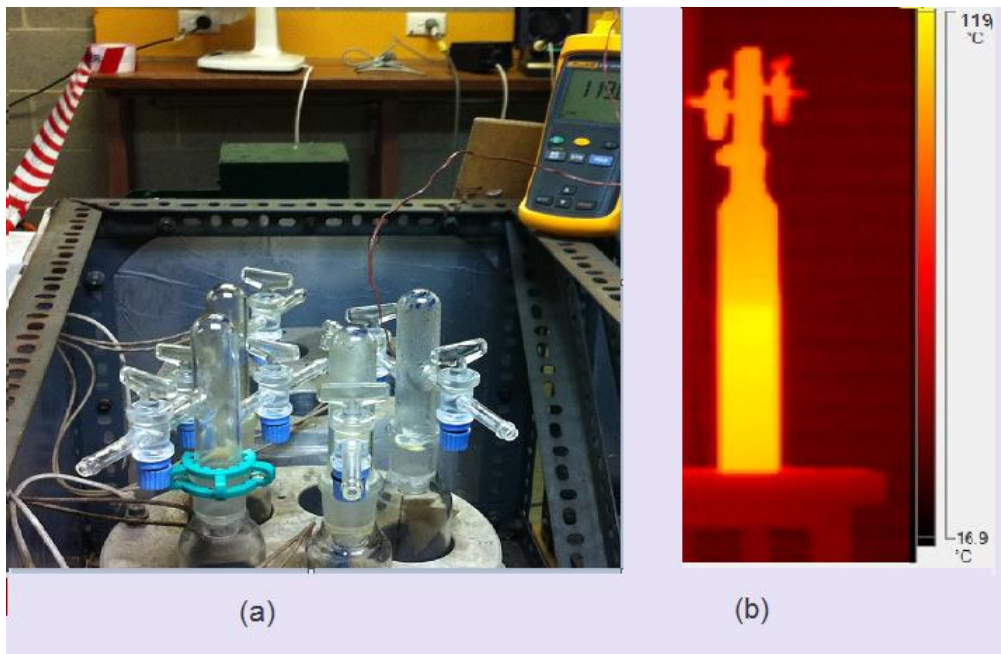
Figure 4.5. (a) Ageing of dry pressboard in an aluminium heater block, (b) Thermal image of a glass tube during ageing process

4.4 Analysing the Ageing of Pressboard Insulation

In this study, the test method given in IEC Std. 60450–2004 is used to measure the average viscometric degree of polymerisation of new and aged pressboard insulation. In this method after the pressboard has been cleaned, it is stripped off to provide enough sample size for the DP analysis. Then, the analysis is performed for two different pressboard samples from the same batch and the average is reported. Figure 4.6 (a) to (c) respectively compares the degradation of both dry and wet pressboard insulation thermally aged in mineral oil, NEA and NEB. A decrease in average DP values of dry pressboard insulation aged in synthetic ester is presented in Figure 4.6 (d).
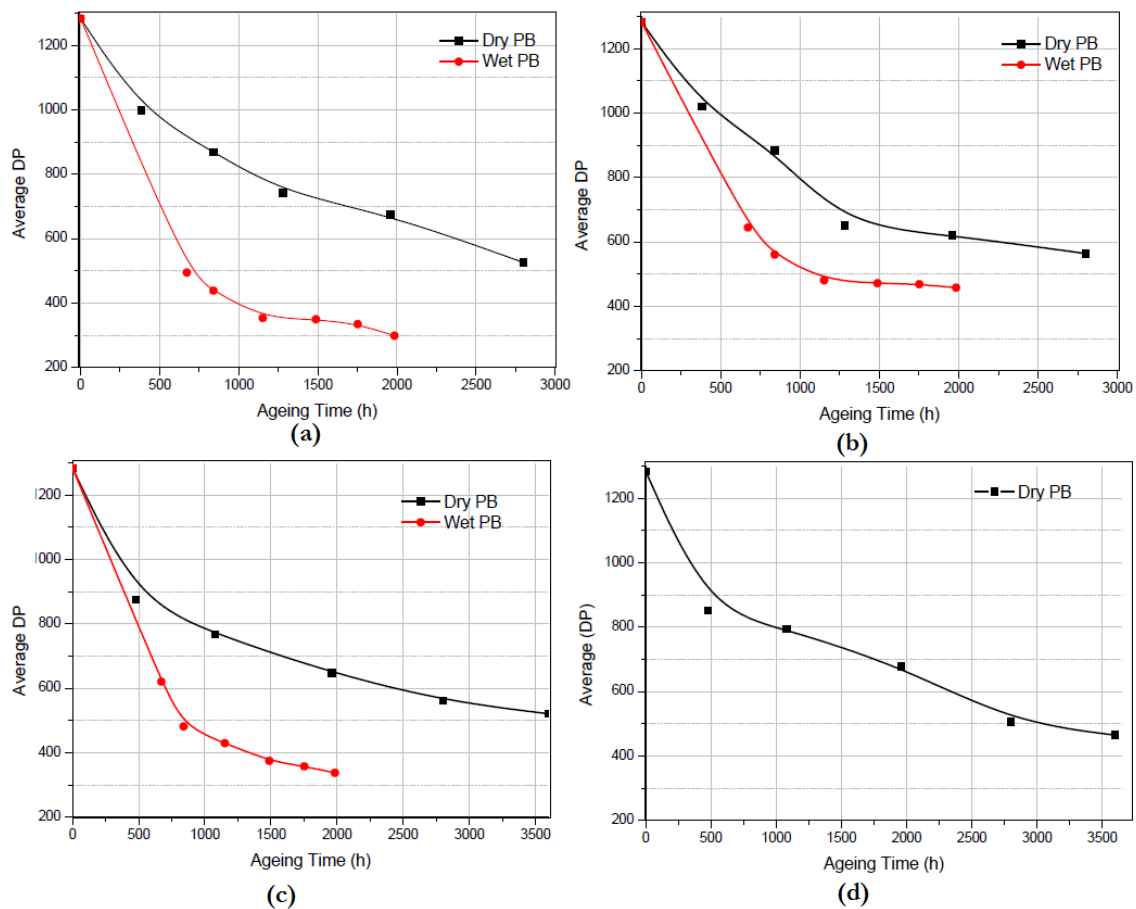
Figure 4.6. Decrease of average DP value of pressboard insulation (PB) over thermal ageing (a) in mineral oil, (b) in NEA, (c) in NEB, (d) in SE

One notable fact that can be seen in Figure 4.6 is the measured average DP of pressboard insulation decreased rapidly at the beginning and then it declined at a relatively lower rate regardless of the types of oil used in the ageing system. This is due to the typical structural features of cellulose. There are long chain cellulose polymers in new pressboard insulation [91] which may contain weak links in the middle [5]. This naturally occurs in every 500 glucose monomers. These weak links are sliced easily by thermal stresses and it would account for fast initial drops in DP [5]. Further, amorphous regions of cellulose degrade more rapidly than the crystalline regions, which would also

support the rapid initial ageing [8]. This may be because the majority of water and acid produced during ageing sit in the amorphous regions [115] due to their greater permeability. On the other hand, greater existence of crystalline regions does not allow water and acids to penetrate [62].

It can be seen in Figure 4.6 (a) and (d) that dry pressboard insulation in mineral and synthetic ester insulating oil possesses similar ageing trends. This conclusion is made because the average DP values of pressboard aged in mineral oil and synthetic ester are 521 and 510 respectively after 2800 hrs of ageing. Moreover, reduction of DP of pressboard aged in corresponding oils during the period of 1960 hrs to 2800 hrs is 153 and 163. This ageing behaviour of pressboard insulation in synthetic ester complies with the results in [84]. On the other hand, the ageing behaviour of dry pressboard insulation displayed different trends in NE insulating oils compared to that of in mineral oil in such a way that DP decrease for pressboard insulation aged in NEA and NEB during 1960 hrs to 2800 hrs is 67 and 82 respectively. It indicates that cellulose insulation ages at a comparatively lower rate in NE insulating oils when it reaches midlife.

If one analyses the degradation behaviour of wet pressboard, it can be clearly seen that DP of wet pressboard decreases rapidly compared to dry pressboard. In this research, ageing experiments with both dry and wet pressboard have been performed under a minimum oxygen supply (under a nitrogen cushion). Thereby, one could attribute the fast ageing rate of wet pressboard insulation to a pronounced hydrolytic degradation reaction in oil-paper system in a moisture rich environment. The notable fact is that the reduction in DP of wet pressboard insulation in NEA and NEB is substantially lower than that of mineral oil throughout the ageing. This behaviour is more significant in the initial period of ageing. Moreover, degradation of wet pressboard in NEA is negligibly small during the last 832 hrs and its DP is 100 to 150 higher than the DP of pressboard aged in mineral oil over the whole ageing period. This behaviour is comparable to the ageing experimental results presented in [11, 24]. As it is proposed in [24], one could assume that pressboard insulation aged in NEA has reached a levelling off degree of polymerisation (LODP). However, this is a misleading interpretation because LODP of cellulose paper insulation occurs when the DP value reaches about 200 due to the slower ageing rate of crystalline domains.

Emsley et al [5] have reported that kinetic degradation of oil impregnated paper insulation in, vacuum, air and oxygen in the temperature range 100 to 200 °C can be characterised using Ekenstam pseudo-zero model as given in eq (2.4). It means that the number of chain scissions ($1/DP_t - 1/DP_0$) increases linearly with ageing time. Emsley [5], Lundgaard [62] and Lelekakis [53] have claimed that this linear relationship continues until the DP of paper insulation falls to about 200. Consequently, reaction rate (k) is the gradient of the plot of the number of chain scissions

versus ageing time. The reaction rate of oil immersed paper insulation is mainly controlled by three factors, namely temperature, moisture content and dissolved oxygen in oil. In this research, temperature has been maintained at a constant level throughout the experiment and the influence of oxygen on pressboard ageing is not significant. Thus, any change of reaction rate can be ascribed to a variation of moisture in the pressboard insulation.
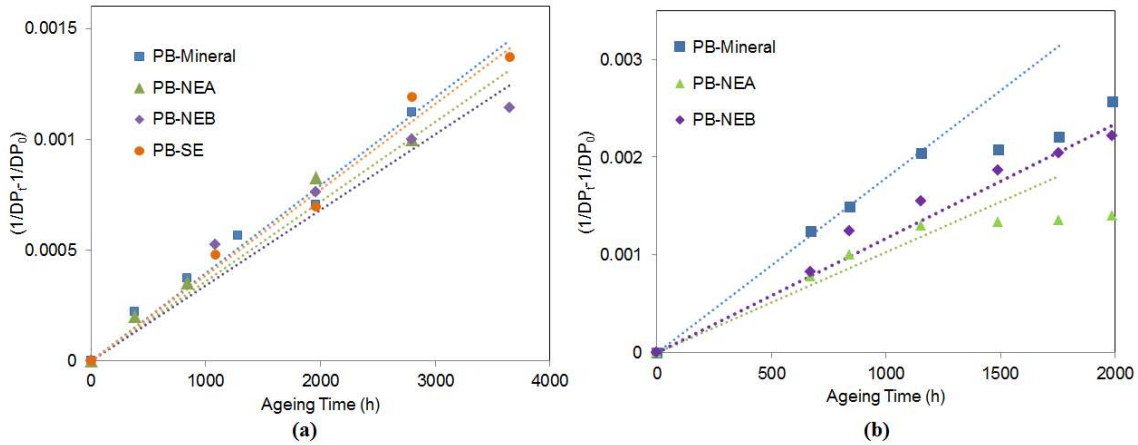
Figure 4.7. $1/DP_t - 1/DP_0$ vs. ageing time (a) Dry PB, (b) Wet PB

Figure 4.7 (a) and (b) present plots of the number of chain scissions versus ageing time for dry and wet pressboard insulation respectively. It can clearly be seen that ($1/DP_t - 1/DP_0$) of dry pressboard insulation aged in all types of oils changes linearly. It means, the reaction rate is constant over the whole ageing process. Moreover, degradation of wet pressboard in NEB also possesses an approximately constant reaction rate.
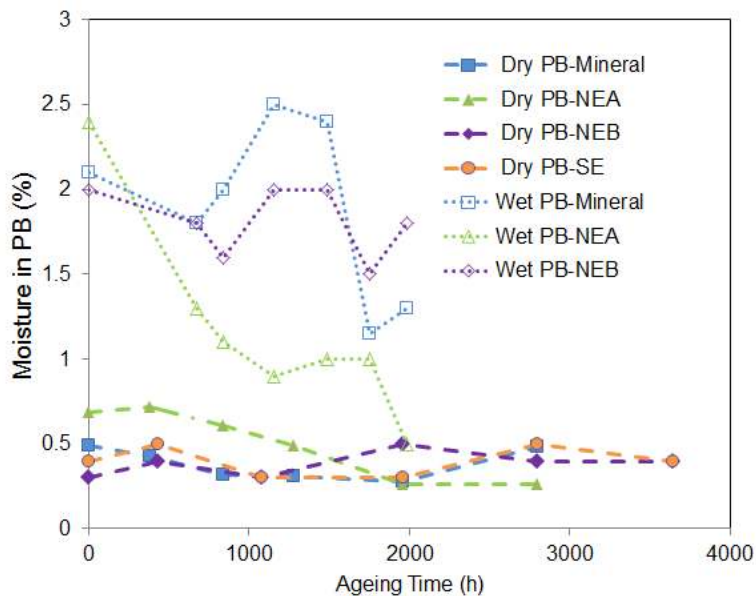
Figure 4.8. Measured moisture content in PB insulation over thermal ageing with KFT

It can be seen in Figure 4.8 that moisture content of all types of dry pressboards remains nearly constant at around 0.5 % and that of wet pressboard aged in NEB persists in the range 1.5-2.1 % giving them nearly constant reaction rates. On the other hand, the reaction rate corresponding to the degradation of wet pressboard insulation in mineral oil and NEA reduces abruptly after 1152 hrs. This behaviour can mainly be attributed to the reduction of their moisture contents. As suggested in [62], this research considers the reaction rate of the wet pressboard insulation aged in mineral oil and NEA in the first 1152 hrs as the corresponding reaction rate for their initial moisture contents. The calculated k values for all the cases considered in this study are listed in Table 4.3. In the case of dry pressboard, the pressboard samples aged in mineral oil have a slightly higher reaction rate than that of pressboard aged in both natural and synthetic esters. The reaction rates corresponding to ageing of wet pressboard insulation samples in mineral oil, NEA and NEB are 4.5, 2.8 and 3.4 times greater than that of dry pressboard in corresponding oils respectively. The involvement of heat and oxygen in the ageing of both dry and wet insulation samples is similar. Therefore, one could clearly presume that high initial moisture content in wet samples is responsible for their high reaction rates.

Table 4.3. Calculated reaction rate and A factor

Moisture condition	Parameter	Oil types			
		Mineral	**NEA**	**NEB**	**SE**
Dry	$k\ (h^{-1})$	3.96×10^{-7}	3.6×10^{-7}	3.43×10^{-7}	3.85×10^{-7}
	$A\ (h^{-1})$	2.25×10^{8}	2.0×10^{8}	1.95×10^{8}	2.18×10^{8}
Wet	$k\ (h^{-1})$	17.88×10^{-7}	10.34×10^{-7}	11.64×10^{-7}	NA
	$A\ (h^{-1})$	10.14×10^{9}	6×10^{8}	6.62×10^{8}	NA

Emsley et al[5] have shown that temperature dependence of paper insulation ageing rate (k) follows the Arrhenius relationship given in eq (2.6) which is governed by the factor called activation energy (E_a). It has been reported in [5, 53, 62] that E_a for ageing of cellulose insulation in insulating oil is independent of the reaction conditions such as moisture level and oxygen and it possesses a value of 111 kJmol^{-1}. Assuming that reaction rates of dry and wet pressboard insulations considered in this study also have the same activation energy, corresponding A factors have been calculated and listed in Table 4.3.

The life expectancy of pressboard insulation in all four types of oils in the temperature range 80ºC-140 ºC have been calculated using eq (2.7). It is assumed that DP_{start} and DP_{end} are equal to 1284 and 200 respectively. The life expectancy curve obtained for wet pressboard insulation in mineral

oil is comparable with that of pressboard insulation aged under a minimum oxygen condition and 2% of moisture [53]. It validates the accuracy of our experimental results and calculations.
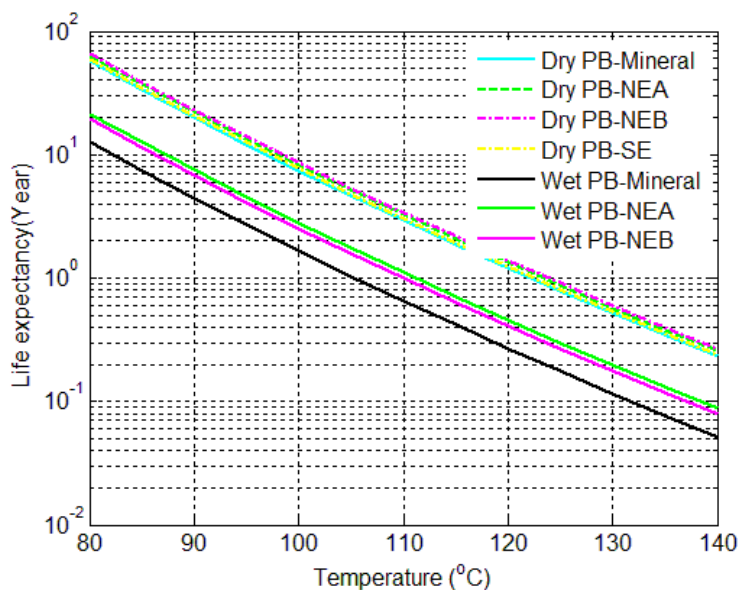
Figure 4.9. Comparison of life expectancy of PB insulation

It can be seen in Figure 4.9 that pressboard insulation has a longer life expectancy in NEA and NEB than that of in mineral oil. This advantage is more substantial in the case of wet pressboard. Overall one could make a generalised statement such that NE insulating oils delay the thermal ageing of cellulose insulation materials and it confirms the longer life expectancy and high overloading capability of NE filled transformers. Most of the studies claim that this advantage of NE insulating liquids is mainly due to their high moisture solubility [11, 97].

At a high temperature NEs attract more water from paper insulation than mineral oils and it causes to slow down the hydrolytic degradation of cellulose insulation. Moreover, hydrolysis reaction in NEs consumes free water, causing a shielding effect which reduces the interaction between water and pressboard [24]. This could also be a reason for decreasing hydrolytic degradation of cellulose insulation in NE insulating liquids. Hydrolysis of NEs produces long chain fatty acids. These fatty acids are chemically bonded onto the C6-hydroxyls group of cellulose molecules which make them more thermally stable [97]. This could also be a reason for the better thermal stability of cellulose material in NE insulating oils.

However, it can clearly be seen in Figure 4.9 that life expectancy of dry pressboard insulation in NE insulating oils is not very significant as reported in [14, 95, 97, 181]. This is due to a problem of the ageing experimental setup used in this research for dry pressboard insulation. During the ageing process, the bottom part of the glass tube which contained oil and pressboard was inside the heater

block whilst the long tube shape lid was completely exposed to the ambient surroundings. This leads to a high temperature gradient between the top of the oil and top of the lid as shown in Figure 4.5 (b).
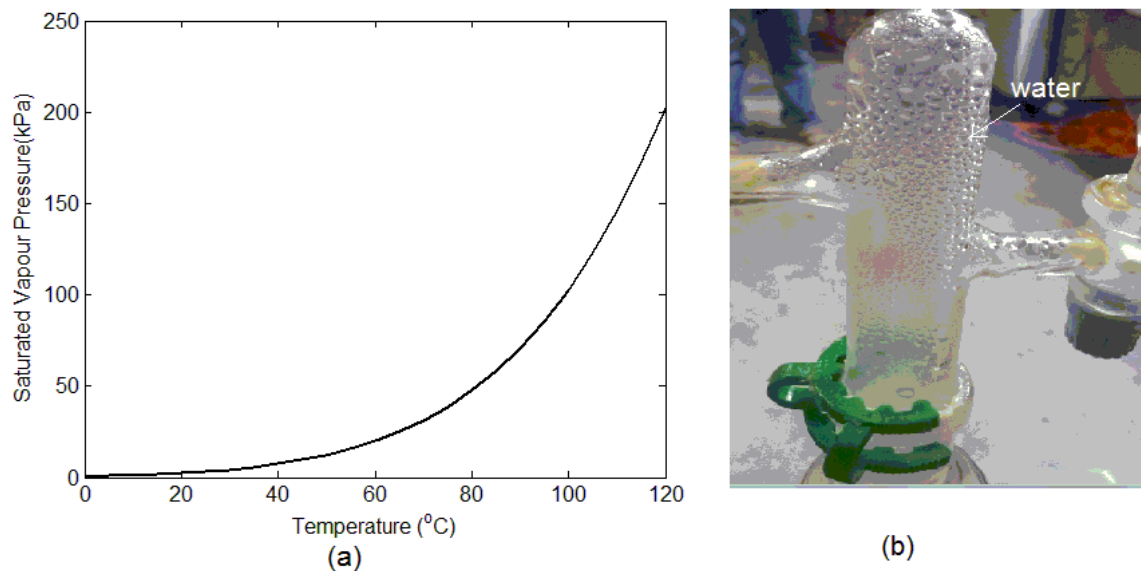
Figure 4.10. (a) Saturated vapour pressure vs. temperature [182], (b) Water sit on the wall of the tube shape cap

At high temperature moisture solubility in oil is high and thereby moisture migrates from paper to oil then to the gas space [125] because the headspace has been filled with dry nitrogen. The top region of the gas space has a low temperature resulting in a lower saturated vapour pressure as given in Figure 4.10 (a). This behaviour causes to produce liquid water on the wall of the lid (cold trap) of the glass tube as shown in Figure 4.10 (b). Then liquid water travels downward along the glass wall due to gravity and it becomes vapour near the top of the oil due to the high top oil temperature. This cycle continues for the whole ageing process minimising the moisture content in the oil-paper system and reducing the involvement of moisture in ageing of pressboard insulation. Subsequently, this mechanism masks the advantage of high moisture solubility of ester insulating oils giving a nearly similar reaction rate for pressboard insulation in both mineral and ester insulating oils.

4.5 Analysing the Furanic Compounds

It has already been mentioned in Chapter 3 that furanic compounds detectable in oil are solely related to degradation of paper insulation. Thus, this research has analysed the five main types of furanic compounds dissolved in oil namely 2-FAL, 2-ACF, 5-MEF, 2-FOL and 5-HMF in order to identify their relationships with ageing conditions of pressboard insulation. The concentrations of these furanic compounds in oil have been identified and quantified by using a high-performance

liquid chromatography technique according to ASTM Std. D5837-99. Figure 4.11 (a)-(e) presents the concentration of furanic compounds detected in oils which are aged with dry pressboard insulation whilst Figure 4.11 (f)-(j) displays the concentration of those compounds measured in oils aged with wet pressboard.
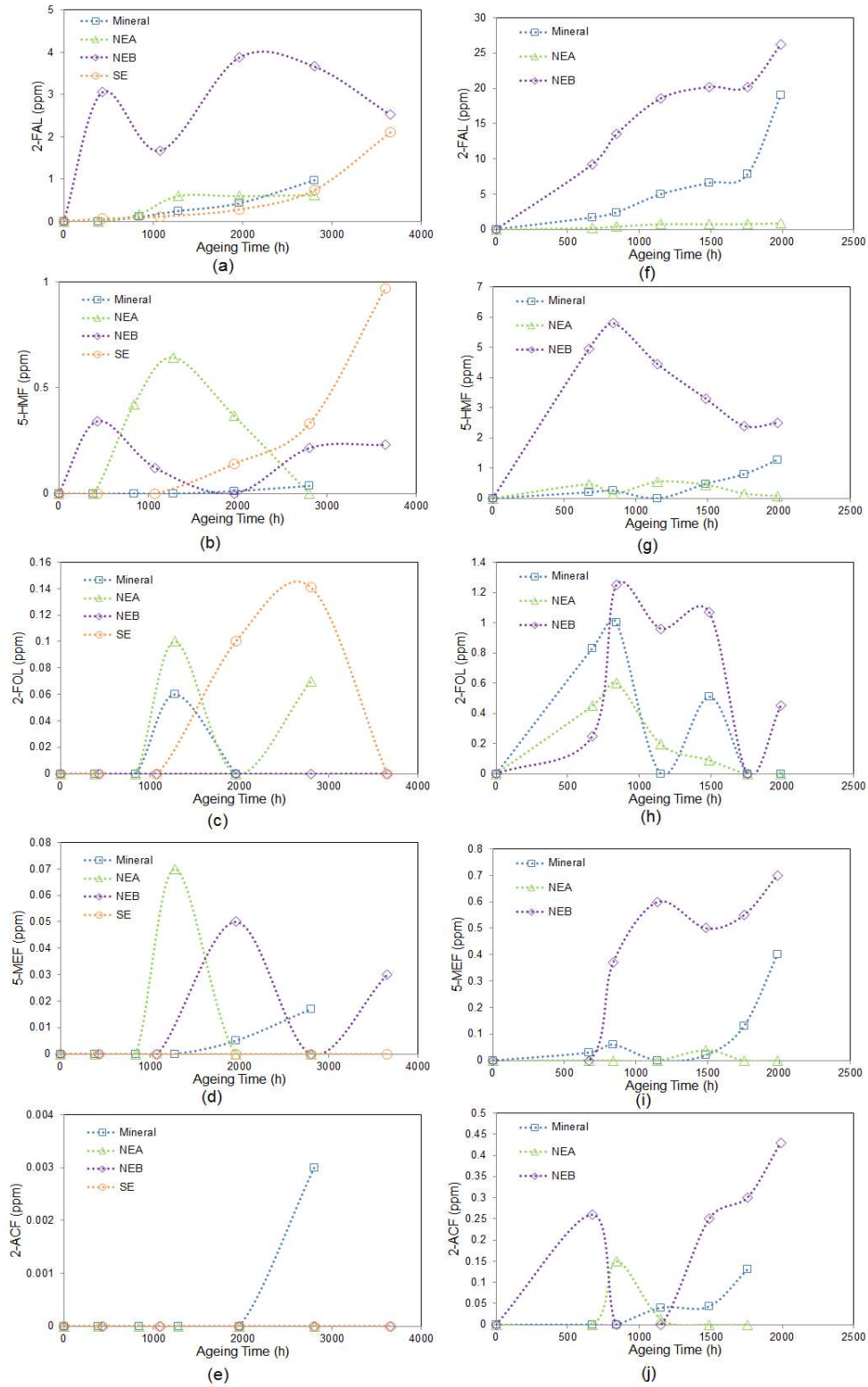
Figure 4.11. Dissolved furanic compounds in oils (a)-(e) with dry PB, (f)–(j) with wet PB

In both cases where oil was aged with dry and wet pressboard, the highest amount of furanic compound detected in all types of oils is 2-FAL. 5-HMF and 2-FOL are the second and third highest furanic compounds respectively detected in all types of oil in most of the cases. 5-MEF and 2-ACF have been measured in lesser quantity in most of the cases. This is mainly due to the fact that production of these furanic compounds due to degradation of pressboard insulation in decreasing order is 2-FAL> 5-HMF> 2-FOL [8]. Moreover, 2-FAL is a more stable compound at 120 ºC than 5-HMF and 2-FOL. This could be another possible reason for detecting the highest concentration of 2-FAL in all cases. These results show good consistency with most of the experimental data in literature where 2-FAL has been detected as the highest furanic compound in oil [7, 10]. Overall, measured concentrations of all furanic compounds in oils which were aged with wet pressboard are greater at indicating a faster ageing rate of wet pressboard insulation than dry pressboard.

At around 120˚C, the most likely ageing mechanisms of cellulose are hydrolysis and oxidation [63]. This experiment has been conducted under a minimum oxygen environment and thereby, one could assume that hydrolysis is the main degradation mechanism of pressboard in this study. The high concentration of 5-HMF detected in oil aged with wet pressboard confirmed this hypothesis because hydrolysis degradation of cellulose mainly proceeds through the formation of 5-HMF [9, 50]. 5-HMF mainly retains in paper (pressboard in this case) as it is a high polar substance. This could be a possible cause to have a big difference between 2-FAL and 5-HMF concentrations detected in oil even under a pronounced hydrolytic degradation condition.

The notable fact that can be seen in Figure 4.11 (a) and (f) is that 2-FAL concentration in NEB is the highest for both cases with dry and wet pressboard followed by that in mineral oil at similar ageing condition. Moreover, Figure 4.11 (f) shows that 2-FAL concentration in both NEB and mineral oil increases rapidly during the last 232 hrs. This is possibly due to the fact that the DP of pressboard in those samples has fallen below 400 [10]. It can be seen in Figures 4.11 (a) and (f) that measured 2-FAL concentration in NEA is relatively low compared to that in mineral oil and NEB after a similar ageing time. This behaviour is more significant for the case of oil aged with wet pressboard. These results show good consistency with experimental data in [23,24] where 2-FAL has been generally detected in very low concentration in aged BIOTEMP oil. In both cases, the DP value of pressboard aged in NEA has not dropped below 400, this could be a possible reason for detecting a low concentration of 2-FAL in aged NEA. In an oil-paper system, 2-FAL can be subjected to thermal and hydrolytic decomposition and this mechanism is more pronounced in an

acidic environment [23]. Thus, one can also assume that a significant increase in acidity of NEA oil over thermal ageing partly accounts for detecting a low concentration of 2-FAL in aged NEA oil.

In order to predict the DP value of paper insulation, log-linear relationships between dissolved 2-FAL concentration in oil and DP value of paper insulation has been widely used [56, 171]. Figure 4.12 shows that ln (2-FAL) and the DP value of pressboard insulation aged in mineral oil, NEB and SE can be represented using linear relationships with good accuracy. On the other hand, it is difficult to establish a linear relationship between ln(2-FAL) and DP for NEA–pressboard system with reasonable accuracy. However, eqns (4.1) to (4.4) are best fitting curves obtained using 2-FAL and DP data corresponding to mineral oil, NEA, NEB and SE oils respectively. The relationship corresponds to mineral oil-pressboard system gives DP values of 488, 384 and 343 for 2-FAL concentration of 2, 5 and 7 ppm respectively. If one uses relationship obtained by Pablo [56], it gives DP of 551, 376 and 310 for a similar concentration of 2-FAL confirming the consistency of our results in this DP region for mineral oil-paper systems. On the other hand, established relationships show dependence on oil type. It means that the existing 2-FAL based interpretation schemes developed for a mineral oil-paper insulation system based on absolute values and rate of change may not be directly used for ester based insulation systems.
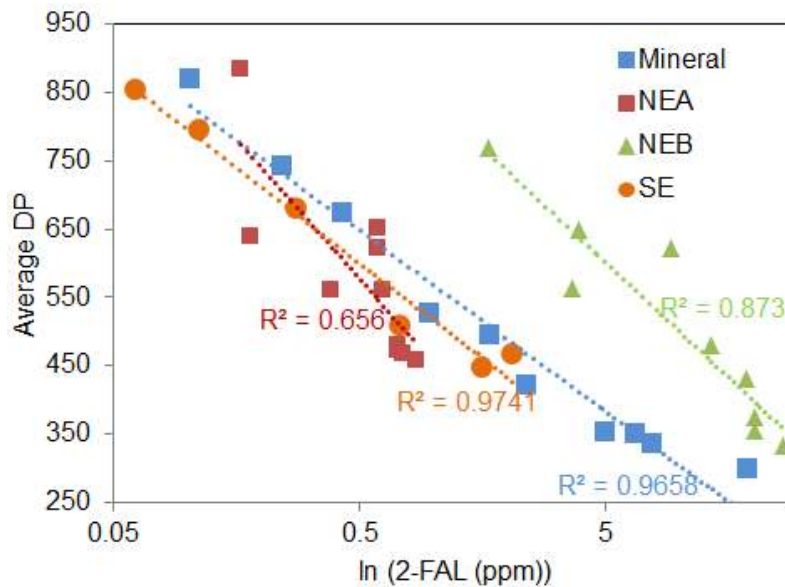
Figure 4.12. Relationship between DP and 2-FAL concentration of oil

$$DP = -114 \times \ln(2\text{-}FAL) + 567 \tag{4.1}$$

$$DP = -177 \times \ln(2\text{-}FAL) + 457 \tag{4.2}$$

$$DP = -146 \times \ln(2\text{-}FAL) + 845 \tag{4.3}$$

$$DP = -121 \times \ln(2 - FAL) + 516 \tag{4.4}$$

4.6 Characterising the Structural Changes in Pressboard Insulation Using FTIR Method

In this method, the vibrational spectrum of a particular type of molecule is distinctively analysed. FTIR spectrum is a unique physical property of a relevant molecular structure. Therefore, FTIR spectra can be used as a fingerprint for material identification. When a material is exposed to an IR radiation, molecular bonds selectively absorb energy from particular wave bands and oscillate. The energy required for oscillation depends on the bond type, molecule size, spatial position of molecular bonds and type of vibration. In this method, absorbance frequencies of functional groups (e.g. OH, CH_2) are used as a key to unlock the black box of molecular structure. In addition, corresponding frequencies provide qualitative as well as quantitative information; because an absorbance energy peak assigned to a particular functional group increases proportionally with the number of times that functional group appears within the molecules.

This research has analysed the FTIR spectra of pressboard insulation samples in spectral band 4000-400 cm^{-1} using Thermo Scientific^{TM} FTIR spectrometer. Attenuated Total Reflectance (ATR) mode has been utilised to acquire the FTIR spectra. In this technique, the penetration depth of light into the sample is about 0.5-3 µm. Therefore, this method primarily characterises the surface properties of each sample under investigation. Small samples required for FTIR measurement are prepared from bigger pressboard specimens taken from the ageing vessel. Reproducibility of results has been confirmed by taking two consecutive FTIR measurements on each sample.

4.6.1 Esterification of fatty acids with cellulose

Hydrolysis of triglyceride molecules produces long-chain fatty acids. In general, carboxyl acid molecules (fatty acids in this case) can be esterified to C-6 hydroxyl group in cellulose [96, 183]. This phenomenon has been verified with X-ray photoelectron spectroscopy and FTIR techniques in [24, 96]. Furthermore, using molecular modelling techniques, it has been verified that the esterified fatty acid molecules are distributed in parallel to the cellulose surface due to the multi-hydroxyl construction of cellulose.

In this research, esterification of fatty acids with cellulose has been characterised by analysing the FTIR spectra of dry pressboard samples aged in mineral oil and NEA at different ageing statuses. The FTIR spectra on the textured surface (outer surface) of pressboard samples is utilised in the analysis. As shown in Figure 4.13 (b), the intensity of the peak at 1740cm^{-1} of FTIR spectra of

pressboard aged in NEA which can be assigned for ester group has increased upon ageing. On the other hand, it can be seen in Figure 4.13 (a) that there is no significant change of ester peak of FTIR spectra of pressboard aged in mineral oil. Thus, this observation confirms the chemical bonding of long chain fatty acids to cellulose polymer in pressboard insulation aged in NEA through the process called trans-esterification.
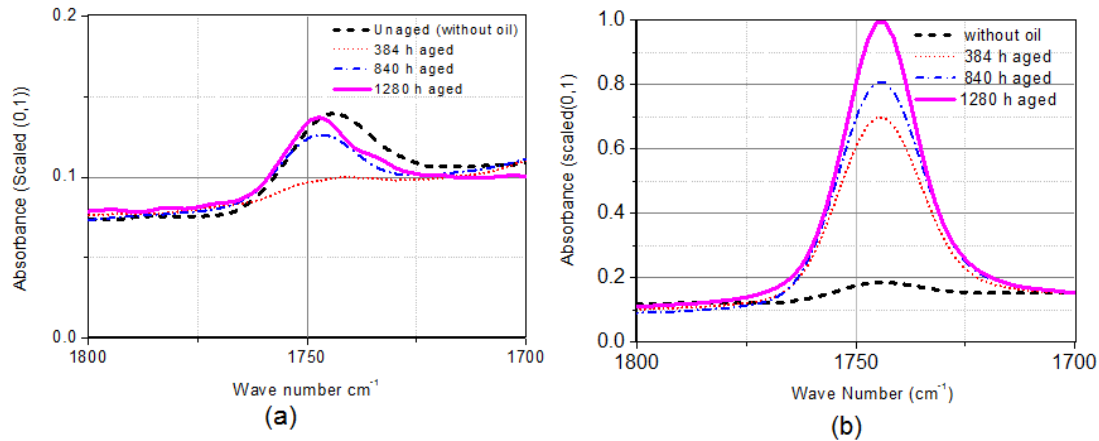
Figure 4.13. Development of ester peak due to esterification of pressboard insulation (a) PB aged in mineral oil, (b) PB aged in NEA

4.6.2 Analysing the cellulose ageing

In order to characterise the ageing condition of pressboard with FTIR technique, FTIR spectra on the smooth inner surface of the outer layer of wet pressboard insulation has been analysed at three different ageing states. Effects of oil and moisture on measurement results have been minimised by cleaning surface oil with acetone soaked paper towel and then keeping cleaned samples at a constant relative humidity of 23% over 14 days. Figure 4.14 (a) to (b), (c) to (d) and (e) to (f) respectively compare the variation of FTIR spectra of mineral oil, NEA and NEB impregnated pressboard insulation over thermal ageing.

In general, a broad peak with the maximum located close to 3340 cm^{-1} can be assigned to stretching vibrations of hydroxyl groups [184]. It is a typical characteristic of cellulose [185]. It can be seen in Figure 4.14 (a), (c) and (e) that the intensities of absorbance peaks located close to 3325 cm^{-1} and 3275 cm^{-1} have decreased with ageing. This indicates the reduction of inter and intramolecular hydrogen bonding on the pressboard due to faster degradation or other chemical changes. Further, it can be attributed to the reduction of molecular weight (DP). The absorbance peaks corresponding to hydroxyl groups of strongly and loosely bonded water molecules in cellulose are generally appeared at 3200 cm^{-1} and 3600 cm^{-1} in the FTIR spectra of cellulose [186]. Thereby, one clearly confirm

that reduction of peaks at 3325 cm^{-1} and 3275 cm^{-1} is mainly caused by the reduction of inter and intra molecular hydrogen bonds on pressboard surface.

One notable fact is that reduction of the spectral band corresponding to the hydroxyl group is more pronounced in pressboard aged in NEB. It could be due to the reduction of more hydrogen bonds over ageing. This may result in lower mechanical strength of pressboard aged in NEB compared to that of pressboard aged in mineral oil despite its higher DP value. However, for a conclusive interpretation, further investigations will be required to understand the reduction of mechanical strength of pressboard insulation due to loss of more hydrogen bonds during thermal ageing.
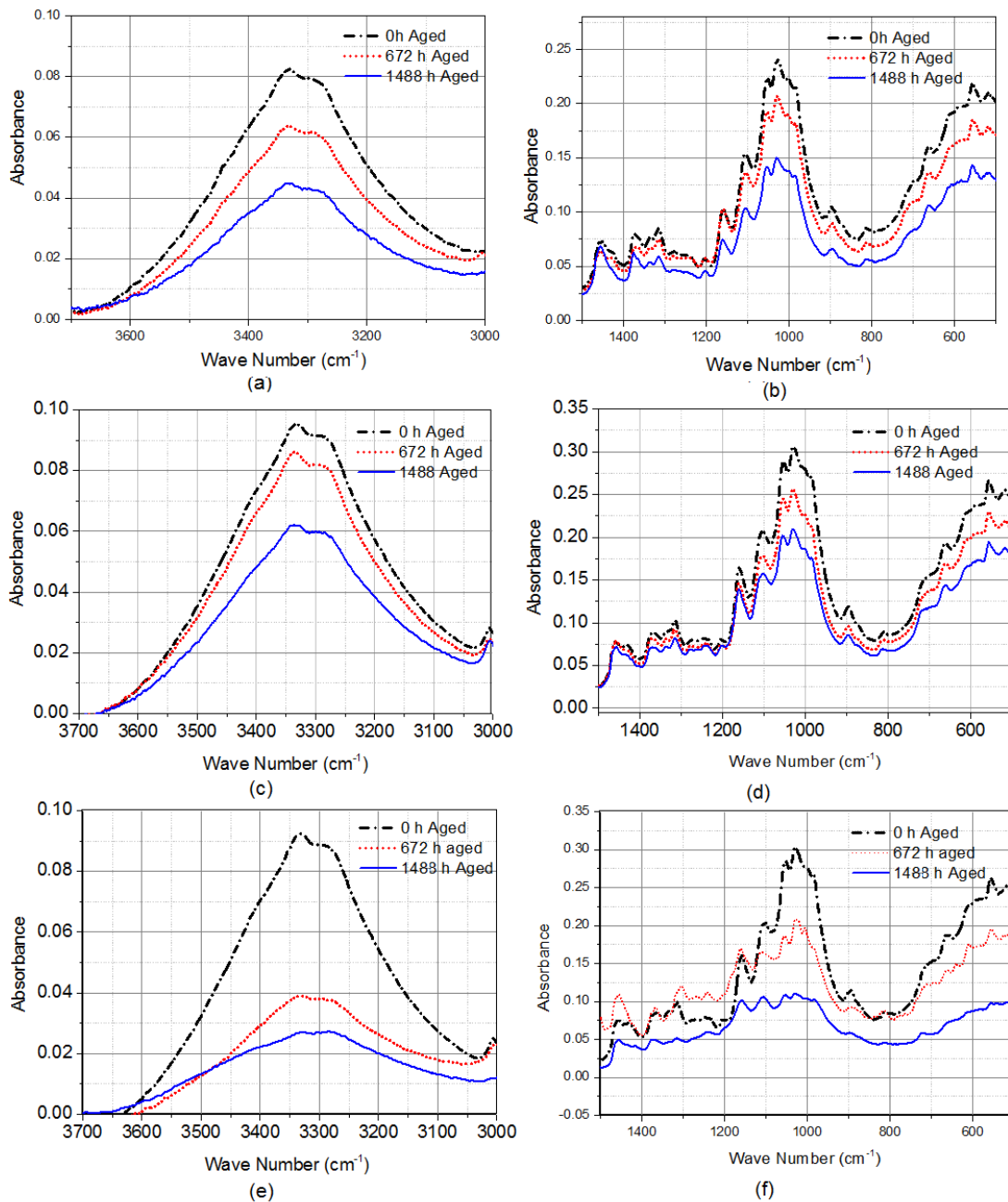
Figure 4.14. FTIR spectra of aged wet PB in (a)-(b) Mineral oil, (c)-(d) NEA, (e)-(f) NEB

It can be seen in Figure 4.14 (b), (d) and (f) that the absorbance spectra of pressboard insulation in the spectral band 1500 cm^{-1} to 500 cm^{-1} shows a decreasing trend over thermal ageing regardless of the types of impregnated liquids. This spectral band primarily represents the vibration of molecular bonds in a cellulose polymer chain as given in Table 4.4. Therefore, reduction of absorbance intensity peaks in this spectral band can be assigned to the reduction of particular bonds in cellulose polymer due to a decrease in the DP of pressboard insulation over ageing. This changing pattern of FTIR spectra of pressboard insulation with reduction of DP provides an indication of novel ways of monitoring solid insulation in an oil filled transformer using a FTIR sensor. However, Figure 4.14 clearly shows that FTIR spectra of pressboard insulation are significantly influenced by the type of impregnated oil. Thus, this issue needs to be investigated as a priority.

Table 4.4. Wave bands assigned for different bonds in cellulose polymer [185, 187]

Wave number (cm^{-1})	Functional group
1215	C–O–C stretching (Aryl-alkyl ether linkage)
1170	C–O–C stretching vibration (Pyranose ring)
1115	C-C and C-O stretching Pyranose ring stretch
1050, 1060	C-O valence vibration (C-OH groups)
700-400	C-C stretching

Dominant ageing mechanisms of pressboard highly depend on the working temperature. Around 120 ºC, the most likely ageing mechanisms of cellulose are hydrolysis and oxidation [63]. These degradation processes produce several carbonyl and carboxyl compounds. Peaks corresponding to these by-products appear in the wave band 1500-1800 cm^{-1} of FTIR spectra of pressboard.
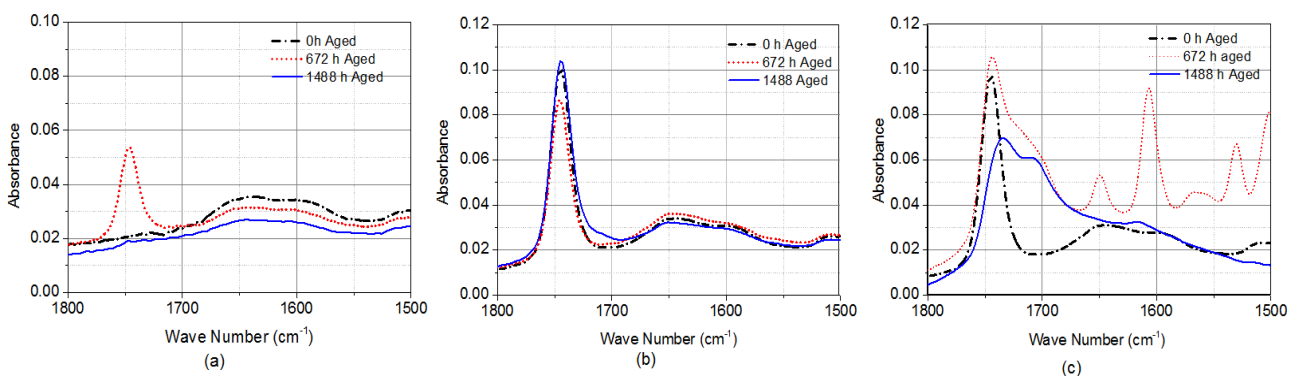
Figure 4.15. FTIR spectra in carbonyl region upon ageing for (a) PB aged in mineral oil, (b) PB aged in NEA, (c) PB aged in NEB

Figure 4.15 (a) shows that a new absorbance peak appears at 1745 cm^{-1} in FTIR spectrum of 672hrs aged mineral oil impregnated pressboard indicating a presence of carboxyl compounds. This peak has diminished after 1488 hrs of ageing because these intermediates are thermally unstable. In the case of pressboard aged in NEA, the spectral band corresponding to carbonyl and carboxyl ageing by-products remains unchanged. On the other hand, there are several new peaks appearing in FTIR spectrum of pressboard aged for 672 hrs in NEB. It can be seen in Figure 4.15 (c) that the ester peak of 672 hrs aged pressboard sample (1740 cm^{-1}) becomes broader due to formation of carboxyl compounds. In addition, new peaks at 1650 cm^{-1} and 1610 cm^{-1} can be assigned to enolic and ketones compounds [63]. These two peaks have disappeared in FTIR spectrum of 1488 hrs aged NEB impregnated pressboard. It indicates that carbonyl intermediate ageing by-products of NEB-pressboard composite system are thermally unstable and they could further decompose into volatile substances. Overall, one could conclude that ageing mechanisms of pressboard insulation in mineral oil, NEA and NEB are somewhat different and it causes to produce different intermediate ageing by-products.

4.7 Variation of Acidity Level of Oil over Thermal Ageing

This research investigates the applicability of a neutralisation number (acidity) for determining the quality of aged ester insulating liquids considering mineral oil as the benchmark. The method prescribed in ASTM Std. D 974 has been utilised to determine the acidity level of new and aged oil samples. Figure 4.16 (a) and (b) show the change of acidity of oil samples aged with dry and wet pressboard respectively.

The acidity of mineral oil aged with dry pressboard insulation remains at 0.01 over the whole ageing process while that of mineral oil aged with wet pressboard increases to 0.14 after 1984 hrs of ageing. However, in both cases the acidity of mineral oil has not reached the limiting value given in [103] indicating their appropriateness for further use. The notable fact that can be seen in Figure 4.16 is the acidity of ester insulating oils is several orders of magnitude higher than that of mineral oil under similar ageing condition. Moreover, acidity values of ester oils show clear rapid increasing trends with ageing time. This behaviour is of paramount significance for NE oils aged with wet pressboard such that acidity values of aged NEA and NEB oils samples at 1984 hrs are 20 times and 4.5 times respectively greater than the limiting value (0.3 mgKOH/g) specified for service aged NE insulating oil with satisfactory conditions for further use in electrical equipment. Figure 4.16 (a) shows that acidity of synthetic ester oil aged with dry pressboard has also largely increased at the last stage of ageing but has stayed under the limit specified in [105] (2 mgKOH/g) indicating good quality even after ageing over 3650 hrs at 120 ºC.
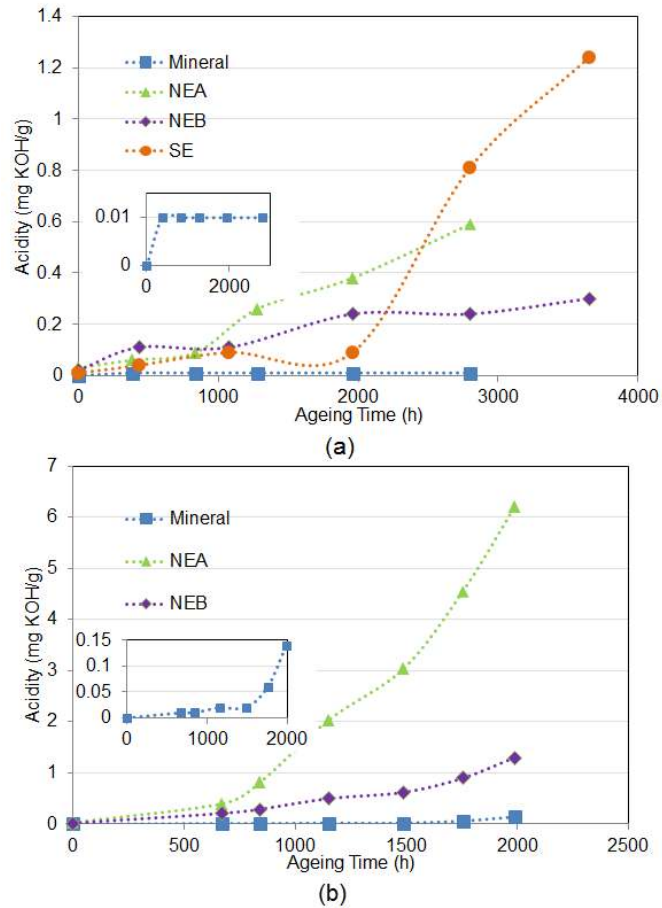
Figure 4.16. Change of acidity of oil over ageing (a) oil aged with dry PB, (b) oil aged with wet PB

It is generally accepted that oxidation of insulating oil and degradation of cellulose insulation in transformers results in increasing the acidity level of oil [176]. However, oil samples considered in this study have been aged under minimum oxygen supply (headspaces of ageing chamber were filled with dry nitrogen). Therefore, a severe oxidation of oil cannot be expected. In the case of ester, hydrolysis is another degradation process, which produces free fatty acids as a by-product [84]. Moisture solubility of all types of oils exponentially increases with temperature causing migration of moisture from pressboard to oil at high temperature. This behaviour enhances the hydrolysis reaction in ester oils. Thus, one can clearly state that the acidity level of both natural and synthetic ester oils increases mainly due to their hydrolytic degradation. This is confirmed by the dramatic increase in acidity of NEA and NEB oils which have been aged with wet pressboard.

In general, an increase of acidity in oil enhances paper degradation via acid catalyst hydrolysis. However, acids which cannot provide H^+ ion through dissociation do not support degradation of cellulose via hydrolysis [61]. NEs mainly yield high molecular acids, which are not as readily dissociated as low molecular acid produced by the ageing of mineral and synthetic ester oils. Moreover, low molecular acids are readily absorbed by cellulose. On the other hand, high molecular

acids are not absorbed by cellulose and they are mainly persisting in the oil phase [47]. These are the main facts which are responsible for the observed slower ageing rate of pressboard insulation in NE insulating oil even after the acidity level increased to a very high value. In the case of synthetic ester oils, short chain high reactive acids are mainly produced by hydrolytic degradation. This would partly account for having a faster ageing rate of dry pressboard insulation in synthetic ester in spite of its higher moisture solubility compared to both mineral and NE insulating oils.

Table 4.5. Specified limiting value for acidity of serviced age insulating oils

Type of oil	Limiting acidity value (mg KOH/g)
Mineral (IEEE Std. C57.152-2013)	0.2 (for < 69 kV voltage class)
	0.15 (for 69 kV<230 kV voltage class)
Natural ester (IEEE Std C57.147-2008)	0.3 (for < 69 kV voltage class)
	0.3 (for 69 kV<230 kV voltage class)
Synthetic ester (BS EN 61203 (1994),	2.0 (for <35 kV voltage class)

The acidity value measurement results of several laboratory studies including results shown in Figure 4.16 show that acidity of NE insulating oil can increase far beyond specified limiting values even after being aged in a sealed environment with minimum oxygen [68, 79, 95, 176]. In addition, results obtained in this study and data given in [24, 95] confirm the better ageing performance of cellulose insulation material in NE with such a high acidity level compared to that of typical mineral insulating oil. Moreover, this research hypothesis that acids produced in NEs does not cause extra corrosion in copper conductors and core steel. This is because of the fact that copper conductors and a steel sample holder used in this study have not shown any sign of corrosion even after 1984 hrs of ageing with NE oil. It means the proposed limiting acidity value of NE given in Table 4.5 is too low. Moreover, this research proposes to measure the low molecular acids content in addition to measuring the total acidity value for diagnostic purposes of in-service aged NE oil.

4.8 Variation of (DDF) of Oil over Ageing

Dielectric dissipation factor is a widely utilised electrical method to determine the degree of deterioration of insulating oil in service. An increase in DDF is mainly caused by contamination of ionic or polar particles and excessive water. This research has analysed the variation in DDF of ester insulating oils after thermal ageing considering mineral oil as the benchmark. All the measurements have been conducted in a standard three electrodes test cell at 50 Vrms using commercially available equipment, an IDA 200. It is worth mentioning at the beginning that none

of the oil samples considered in this study were saturated with water. Thereby, one could interpret that there is no influence of moisture on measured DDF of oil and instead find the ageing by-products of oil-pressboard composite material to be mainly responsible for changing of DDF with ageing [188].

The DDF results presented in Figure 4.17 correspond to oil temperature of 55ºC. It clearly appears that there is a rapid rise in DDF of all types of oils aged with dry pressboard in the early stage of ageing. This research assumes that dissociation of peroxy radicals generated in the early stage of oil oxidation is responsible for the initial rise of DDF of oils aged with dry pressboard. This is because of the fact that some amount of oxygen could have dissolved in oil during sample preparation (diffusion coefficient of oxygen in fluid hydrocarbon at 25 ºC is about 1.8-2.6 cm^2s^{-1} [189]). Thus, it can be expected to have only limited oxidation in the oil until dissolved oxygen is consumed.

Figure 4.17. Variation of DDF of different oils due to thermal ageing (a) Oil aged with dry PB, (b) Oil aged with wet PB

It clearly appears in Figure 4.17 (a) that DDF of mineral and NE oils aged with dry pressboard remains nearly constant in the last stage of ageing indicating that there is no severe degradation in mineral and NE oils after initial oxidation. This is confirmed by a very small colour change of

mineral and NE oils after 2800 hrs of ageing with dry pressboard (Figure 4.18). In the case of synthetic ester, there is a rapid increase in DDF in the last stage of ageing. This is mainly caused by an increase of low molecular acid in synthetic ester due to hydrolytic degradation. It can be seen in Figure 4.17 (a) that DDF at the final stage of ageing is highest of synthetic ester and lowest of mineral oil, while NEs show intermediate behaviour. These results show good agreement with the data provided in [95] confirming the accuracy of our experimental results. Figure 4.17 (a) shows that except for synthetic ester oil aged for 3650 hrs with dry pressboard, all the oil samples can be categorised as good oil based on limiting values of DDF suggested in corresponding IEEE and BS standards.

It clearly appears in Figure 4.17 (b) that there is a continuous increasing trend in DDF of both mineral and NE oils aged with wet pressboard insulation. If one compares Figure 4.17 (a) and (b), it can be clearly identified that DDF of mineral and NE oils aged more than 1488 hrs with wet pressboard is greater than that of corresponding oil aged with dry pressboard over 1960 hrs. This effect is of paramount significance for NEs such that DDF values of NEA and NEB at 1984 hrs of ageing with wet pressboard are almost 19 and 14 times respectively greater than that of corresponding oils aged with dry pressboard over 1960 hrs. However, the equivalent magnification factor of mineral oil is about 3.8. It is generally accepted that DDF of oil increases due to the presence of dissociable impurities such as soot, dust and aging by-products (acids, peroxide) [95]. It means ageing of NE oils with cellulose and metal substances in a moisture rich environment produces more conductive dissociable substances leading to higher DDF. On the other hand, one can assume that conductive ageing by-products of paper insulation dissolve easily in NEs due to their polar nature [16] and this behaviour results in a large increase in DDF of NEs. Figure 4.17 (b) shows that except 1984 hrs aged NEA and NENB oil samples, IEEE Std. C57.152-2013 and IEEE Std. C57.147-2008 respectively characterise all the mineral oil and NE oil samples aged with wet pressboard are in good condition for further use. If one uses IEEE Std.C57.152, all NE oil samples aged more than 1152 hrs with wet pressboard are categorised as not being in good condition for further use. Moreover, NE oil samples aged over 1152 hrs can be rated as oil with marginal condition.

Overall, the results shown in Figure 4.17 indicate that DDF values of ester insulating oils are higher than mineral oil at any ageing condition. The difference in DDF of aged mineral and esters oils is of more paramount significance and somewhat similar behaviour has been observed in several studies reported in literature [16, 84, 98]. Thus, this research concludes that the limiting DDF value suggested in IEEE Std. C57.152-2013 for service aged NE insulating oil is too low because it has

proposed a value of 0.5% at 25 ℃ for both service aged mineral and NE insulating oils. On the other hand, limiting the DDF value suggested in IEEE Std. C57.147-2008 is more appropriate for quality control of NE insulating oils.

4.9 Change of Oil Colour and Viscosity over Thermal Ageing

As explained in Chapter 3, the colour of oil is a visual parameter which reflects the degree of degradation and possible contamination of oil during use. A numeric value based on international colour standards (ASTM D1500) is generally used in expressing the colour changes of oil. It clearly appears in Figure 4.18 that new mineral oil and synthetic esters have a clear appearance with a colour number in the range of 0-0.5 while that of new NEA and NEB oil is about 1.

Figure 4.18. Change of oil colour over thermal ageing

It can be seen in Figure 4.18 that there is very little change in colour of both NE and mineral oil aged with dry pressboard over 2800 hrs. Based on colour change, one could conclude that thermal stability of NE insulating oils is comparable to mineral oil under minimal oxygen and moisture environment. In the case of synthetic ester, the colour change after 2800 hrs of ageing is

insignificant indicating excellent thermal stability of synthetic ester insulating oil compared to both mineral and NE oils.

Figure 4.18 shows that a dramatic change in colour of mineral oil, NEA and NEB has occurred after 1984 hrs of ageing with wet pressboard insulation. Moreover, Figure 4.19 (a) indicates the colour number of both mineral and NE oils is increasing with ageing time. This behaviour is more significant for NEA such that its colour has turned to black after 1752 hrs of ageing. Further, colour scale of NEA has reached 8 which is the maximum value according to ASTM D 1500. After 1984 hrs of ageing, the colour of mineral oil has become amber and its colour number has a value of 3. NEB possesses intermediate behaviour by changing its colour to dark brown and possessing a colour number of 5-6 after 1984 hrs.

In the case of mineral oil, initial oxidation produces free radicals and changes the oil colour into amber and further oxidation evolves soluble by-products which darkens the colour of aged oil [16]. However, in this study ageing has been conducted under a nitrogen environment and thereby severe oxidation cannot be expected. This hypothesis is confirmed by the fact that kinematic viscosity of both types of oil remains constant over ageing as shown in Figure 4.19 (b). In a severe oxidation condition, the intermediate oxidative by-products are polymerised yielding high molecular weight substances leading to a rise of viscosity. Thus, this research concludes that colour change in NE insulating oils aged with wet pressboard is mainly due to the migration of more paper ageing by-products to acidic oil, particularly carbonised compounds and not due to deterioration of oil. Moreover, one can clearly claim that hydrolytic degradation of ester insulating oils does not have an influence on their viscosity.
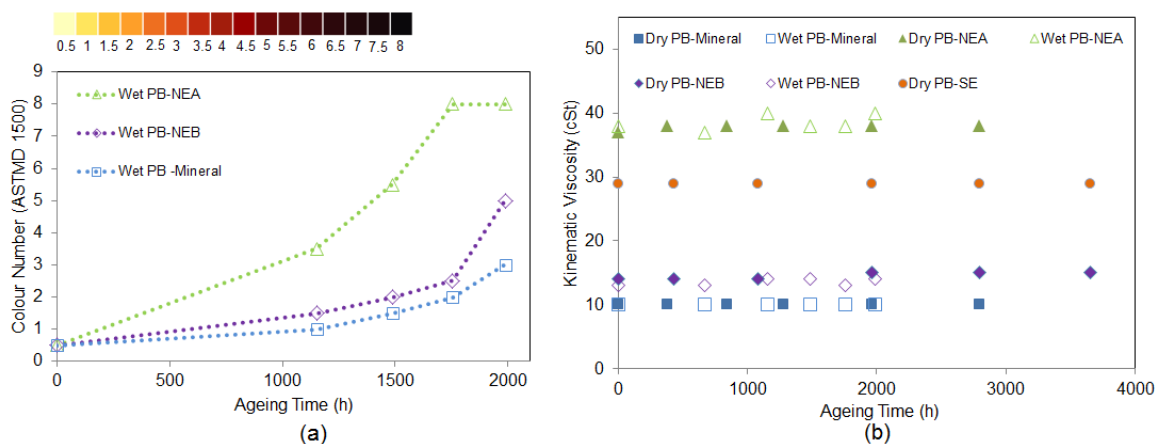
Figure 4.19. (a) Change in colour scale of oil over ageing, (b) Kinematic viscosity of oil over ageing

IEEE Std. C57.152-2013 [103] provides guidelines for assessing the condition of in service mineral oil based on colour. According to that, all the mineral oil samples are categorised as oil in good condition for further use except the 1984 hrs aged mineral oil sample (with wet pressboard). However, if one applies the same interpretation scheme on NEA, oil samples after 1488 hrs, 1752 hrs and 1984 hrs of ageing with wet pressboard insulation can be rated as extremely bad oil whilst the sample at 1152 hrs ageing time can be categorised as severely aged oil. In the case of NEB, samples at 1752 hrs and1984 hrs ageing time (with wet pressboard) can be rated as severely aged and extremely bad oil respectively. It means that sludge should have already formed in NEA and NEB oil samples rated as extremely bad oil and moreover, these oil samples should possess very poor cooling characteristics due to an increase of viscosity. However, it has been observed that no sludge has been formed in aged NEA and NEB oil and they possess cooling characteristics similar to unaged oil (constant viscosity). Moreover, dielectric breakdown strength of 1984 hrs aged oils (mineral, NEA and NEB) has been measured according to the method prescribed in IEC Std. 60156. It indicates that aged NEA possesses the highest breakdown strength with an average value of 68 kV followed by mineral oil (55 kV) and NEB (44 kV). Overall, one can claim that the condition of in service NE oils cannot be evaluated only with their colour change.

Moisture cannot be completely excluded from a transformer as it is a by-product of paper degradation. Therefore, rapid colour change in NE oils could be expected under service conditions compare to mineral oil. Thereby, this research proposes that the colour code defined for mineral oil is not applicable for NE based insulating oils, particularly when an insulation system is moderately wet.

4.10 Experimental Experience on Thin Film Oxidation of NE

Thin films of NE oil naturally occur in an untanked core and coils, hoses, fittings essentially oxidise when such surfaces contact with air [83, 190]. Consequently, a stiff gummy gel is formed. This mechanism has created some problems in our experimental study. It has been observed during the ageing experiment that the top lid and bottom part of the steel containers which contained NE oils and wet pressboard have been completely bonded by a yellowish gummy substance as shown in Figure 4.20. Moreover, in order to obtain an oil sample for analysis, this study has used a valve located at the bottom of the steel chamber. It has been noticed that the valve holes of NE filled containers are completely blocked by a solid substance as shown in Figure 4.20. This study assumes that this problem is created by oxidation of a layer of NE oil that remained in the valve hole (after sampling) due to exposing it to air and intense heat. Therefore, this research proposes to take

practical measures to minimise the time of such surfaces exposure to air and intense heat when it is using NEs.
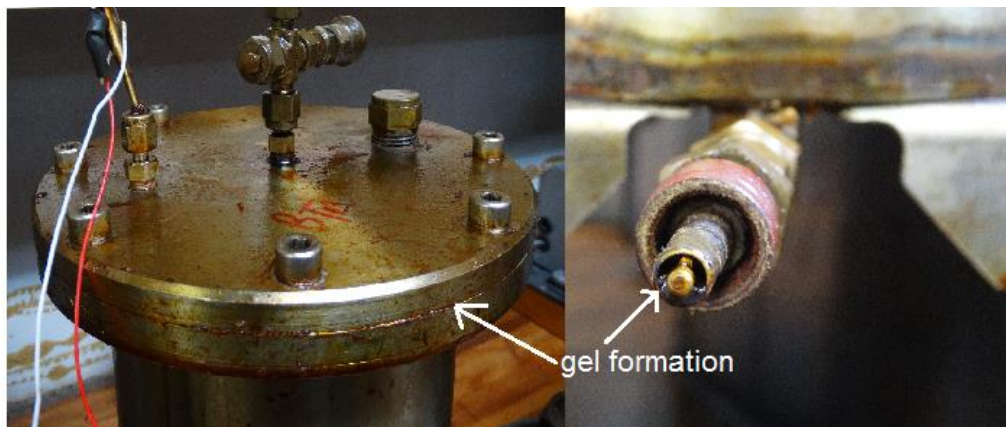
Figure 4.20. Formation of skin of gel due to oxidation of thin film of NE

4.11 Comparison of Dissolved Gases Generation Behaviour of Insulating oils

As already discussed in Chapter 2, there is a greater difference between molecular structures of ester insulating oils and mineral oil. This leads to a quantitatively different dissolved gases generation behaviour for ester insulating oils, but, fortunately, gas composition is the same for all types of oils. Different types of chemical bonds in ester oils such as C=O, C=C and C-H allylic bonds accounts for this quantitative difference. A notable difference is that ester oils yield a large amount of carbon oxides (CO and CO_2) due to breakdown of the carbonyl group (COO) [81, 191]. In the case of NE insulating oils, a radical can easily be formed by eliminating a hydrogen atom in allylic position (next to a C=C bond), because energy required for this mechanism is low such that it is 100, 75 and 50 kcal/mol respectively for a hydrogen atom in saturated, allylic and doubly-allylic methylene group [19]. This could also lead to a different gassing behaviour for NE insulating oils derived from different sources such as sunflower, soy and rapeseed. IEEE Std. C57.155-2014 (draft) has reported that production of methane, ethane and ethylene in NEs is greater due to a low temperature overheating and NE fluids containing linolenic acid generates ethane even under non-fault condition. Ester insulating oils show different gas solubility characteristics compared to mineral oil and gas solubility constants depend on the type of ester too. This makes analysing and interpretation of dissolved gases in ester oils more complex.

This research has made an attempt to predict the gas formation pattern in mineral, NEA, NEB and synthetic ester oils by simulating the same thermal and electric faults in all types of oils. Two different thermal faults have been simulated by subjecting oils to thermal stresses of 120 ℃ and

150 ºC. Low energy electrical discharge faults have been simulated using a standard oil breakdown tester. Moreover, the applicability of dissolved gas analysis (DGA) interpretation schemes including Duval triangle, IEC gas ratio and IEEE key gas method on ester insulating oils is discussed at the end of the section.

4.11.1 Gassing behaviour under low energy electric discharge

A standard transformer oil breakdown tester (100 kV, 2 kVA) was used to create electrical breakdowns in the oil. Firstly 500ml of degassed oil was poured into the test cell of the breakdown tester. Then the top cover was closed and high vacuum grease was applied to all the joints. Gas leaks from the oil were thus avoided. The next, 50, 75 and 100 breakdown tests were individually performed on three different oil samples. The time difference between two consecutive breakdowns was set to 2 minutes. After each breakdown, the oil samples were stirred for 30 s to ensure that the fault gases were homogenously distributed. Since the breakdown current had been limited using an internal circuit, the electrical breakdowns created in the oil could be considered as low energy discharges. These low energy discharge faults were simulated for four different oil types. The dissolved gases in oil after electrical breakdowns were analysed using the method prescribed in ASTM D Std. 3612-02 and the results are shown in Figure 4.21.
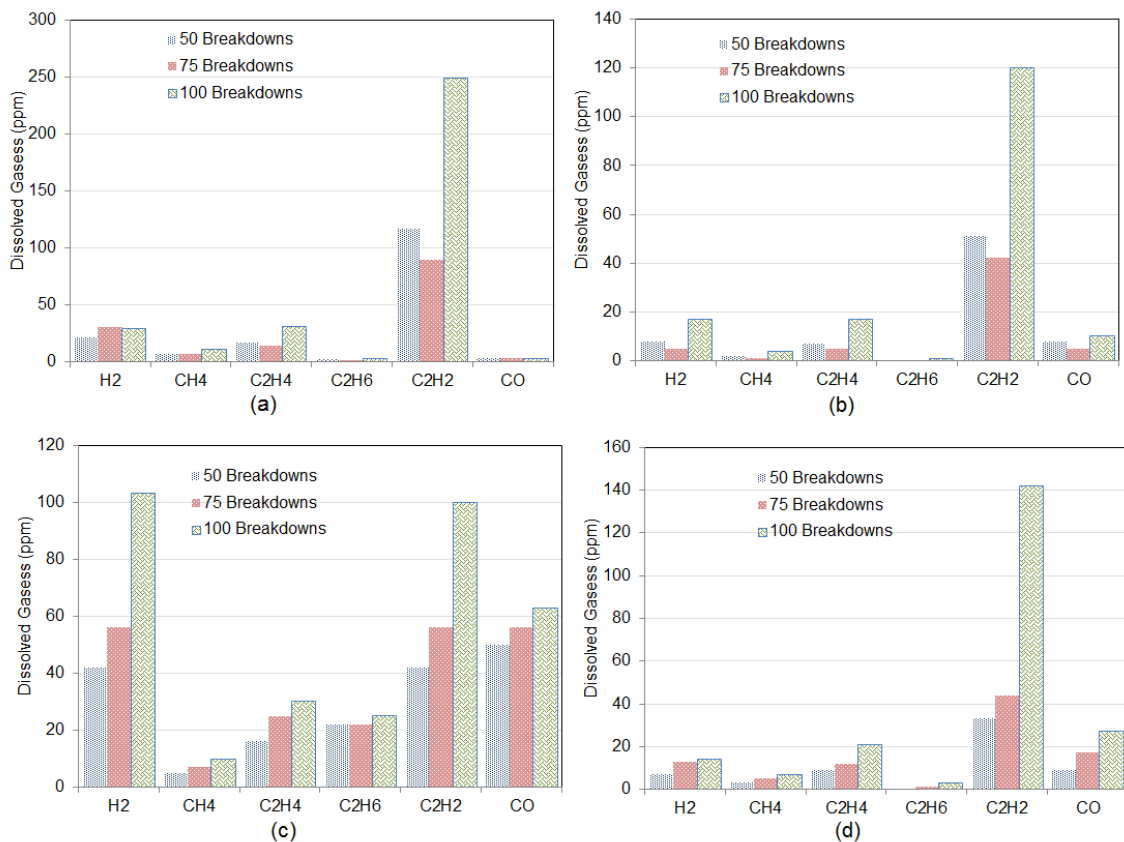
Figure 4.21. DGA results after electrical discharge in oil (a) Mineral oil, (b) NEA, (c) NEB, (d) SE

Figure 4.21 indicates that under low energy electrical arcing conditions, gases produced in all types of oils are mainly acetylene (C_2H_2) but in NEB, additionally a significant quantity of hydrogen is produced. A notable difference in dissolved gas production under low energy discharge is that generation of C_2H_2 in mineral oil is significantly greater compared to ester fluids. Hydrogen, ethylene and methane become the second, third and fourth highest hydrocarbon gases detected in mineral oil. Nearly the same gas generation patterns can be observed in NEA and synthetic ester oils. On the other hand, hydrogen becomes the second highest hydrocarbon gas produced in NEB and one could also assume that hydrogen and acetylene are equally produced in NEB under low energy discharge conditions. Moreover, production of carbon monoxide and ethane in NEB is several orders of magnitude greater than those gases detected in other insulating oils. Overall one can assume that ester oils produce more carbon monoxide due to electric breakdown. The fault gas generation patterns of mineral and ester oils which have been observed under low energy discharge condition show good agreement with the results in [153, 157] indicating the applicability of these results for diagnosis purposes.

4.11.2 Gassing behaviour under thermal fault at 150 ºC

In order to simulate a thermal fault at 150 ºC, 250 ml of degassed oil was poured into a specially designed glass tube (the same glass tube used for ageing dry pressboard insulation). Then air in the headspace was pumped out and the headspace was filled with dry nitrogen. High vacuum grease was applied to all the ground glass joints to ensure a fully sealed environment. Thus, one could assume that there is no gas leak in the system. Then the oil filled glass bottle was placed in the aluminium heater block and the temperature of the heater block was set to 150 ºC (± 2 ºC). Ageing was performed over 72 hrs at this temperature and DGA was performed on two aged oil samples and the average is reported in Figure 4.22. This thermal fault was simulated on all types of oils considered in the previous case. This experimental setup is very simple compared to the method described in [155, 192]. However, in this method there is a possibility to lose of portion of dissolved gases in oil during the sampling.

Figure 4.22 (a) indicates that carbon monoxide is the key combustible gas produced in synthetic ester insulating oil under thermal overheating at 150 ºC followed by ethylene, methane and ethane respectively and they exist in lesser quantities as compared to carbon monoxide. There is no production of hydrogen in synthetic ester oil under this ageing condition. One could assume that mineral oil mainly produces carbon monoxide, ethane and methane under low temperature overheating at 150 ºC with the maximum concentration of carbon monoxide followed by ethane and methane. In the case of NEs, ethane remains as the main combustible gas under simulated thermal

fault and in addition, a substantial concentration of carbon monoxide has also been detected. If one compares the concentration of ethane in NEB to that detected in the other three oils, it clearly shows that production of ethane in NEB is nearly 6, 2 and 30 times greater than that of dissolved in mineral, NEA and synthetic ester oils respectively. Such behaviour for soybean oil based insulating liquids has also been reported in IEEE Std. C57.155-2014 (draft) [191].
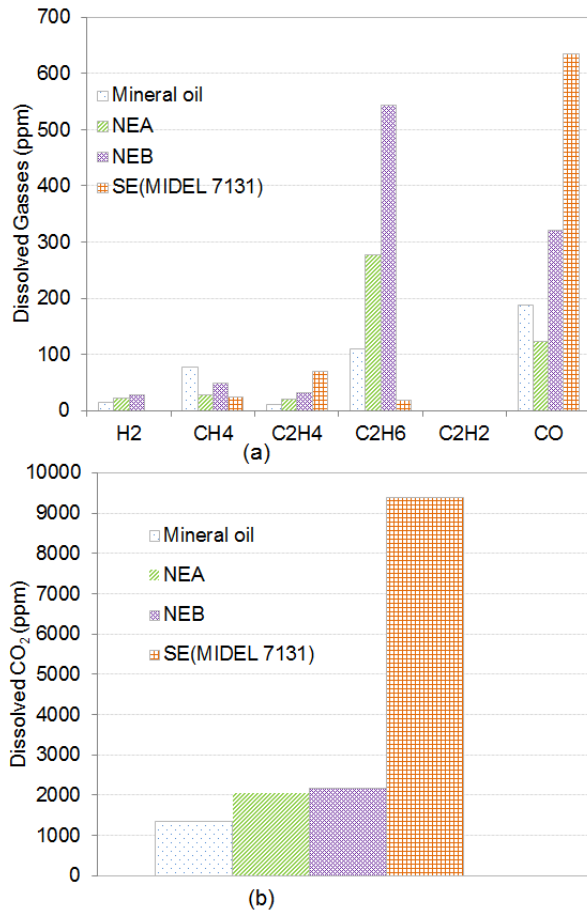
Figure 4.22. Dissolved gas in oil after ageing over 72 hrs @ 150 °C (a) Combustible gases, (b) CO_2

As shown in Figure 4.22 (b) one could express that carbon dioxide is produced abundantly in synthetic ester oil under overheating condition at 150 °C. Moreover, the carbon dioxide concentration in synthetic ester oil is almost 6 times greater than that of mineral oil under similar condition. This behaviour indicates that the rate of carbon dioxide produced from synthetic ester oil could exceed that produced from paper degradation leading to a misinterpretation of DGA results as overheating of cellulose insulation [191]. One can also claim that both types of NEs also produce a larger amount of carbon dioxide than mineral oil due to overheating at 150 °C. On the other hand, carbon dioxide concentration detected in both types of NEs is 4.5 times less than that detected in SE oil.

4.11.3 Thermal fault at 120ºC with pressboard insulation

DGA was performed on mineral, NEA, NEB and SE oil samples aged with dry pressboard insulation over 1960 hrs and 2800 hrs. Figure 4.23 shows that a very low quantity of fault hydrocarbon gases is produced in synthetic ester due to thermal ageing at 120 ºC. Moreover, the production of hydrogen in synthetic ester due to overheating at 120 ºC is greater than other hydrocarbon gases. One could clearly conclude that the hydrocarbon gas generation pattern in synthetic ester oil under an overheating condition at 120 ºC and 150 ºC is dissimilar to some extent because no hydrogen has been detected in synthetic ester oil after overheating at 150ºC.

In the case of NEB, the production of ethane is abundantly high being the predominant hydrocarbon gas for thermal fault at 120ºC followed by methane. A nearly similar gassing pattern has been observed for mineral oil and NEA. Moreover, it can clearly be seen in Figure 4.22 and Figure 4.23 that the order of magnitude of hydrocarbon gases generation in mineral oil, NEA and NEB is nearly similar for both simulated faults at 120 ºC and 150 ºC. It indicates that both faults are in a similar category. It is worthwhile to mention that no acetylene is produced in ester insulating oils due to low temperature overheating (at 120 ºC and 150 ºC). It indicates that acetylene could also be utilised as the key gas for identifying the electric arcing faults in ester insulating oils.
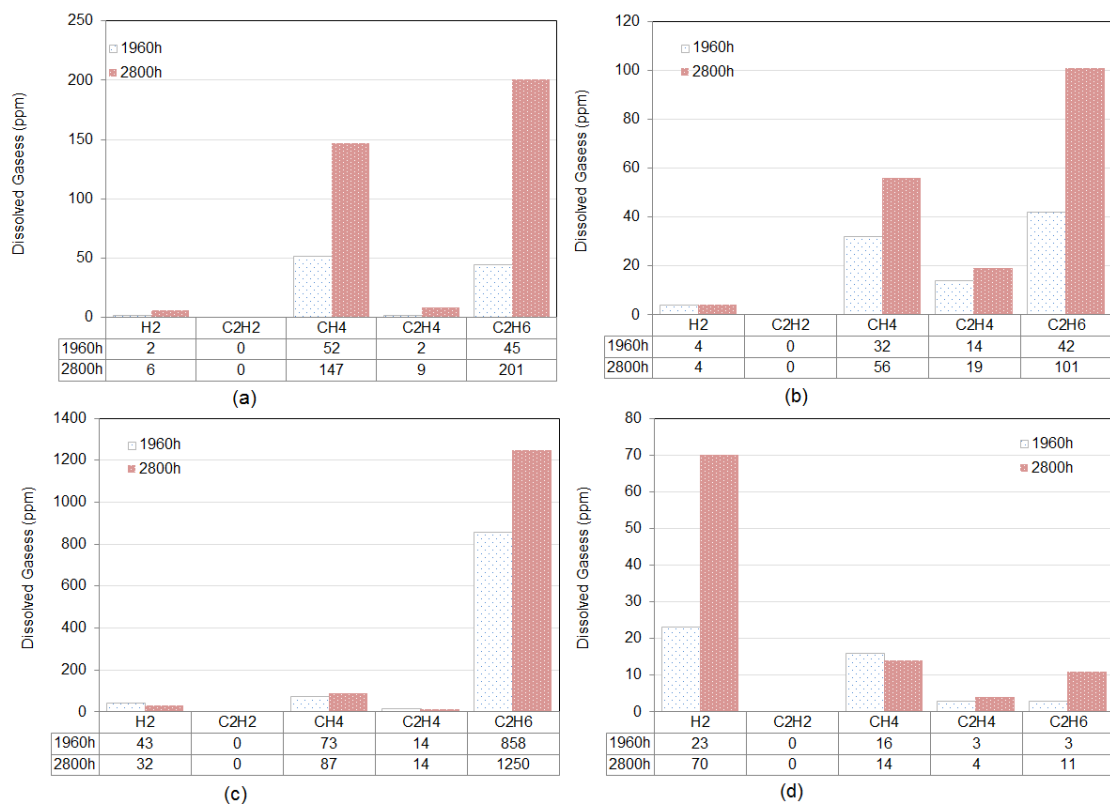
Figure 4.23. Dissolved combustible gases in oil after ageing for 1960 h and 2800 h with PB and copper at 120 ºC (a) Mineral oil (b) NEA, (c) NEB, (d) Synthetic ester
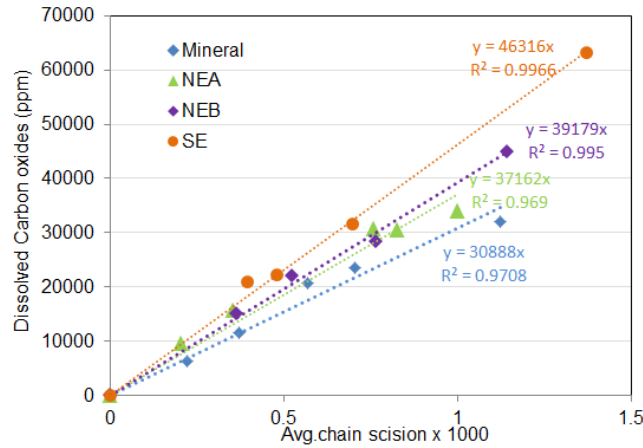
Figure 4.24. Relationship between dissolved carbon oxides and PB degradation (dry PB)

At high temperature, cellulose molecules are decomposed and carbon oxides (CO_2 and CO) produced. In general, a high level of dissolved carbon oxides in oil indicates the thermal degradation of cellulose insulation in the system [176]. Hence, it is possible to assess the level of solid insulation degradation using the amount of CO_2 and CO concentration in oil. In order to understand the correlation between dissolved carbon oxides and the degree of ageing of pressboard insulation, DGA results for CO2 + CO are plotted against the average number of chain scissions of dry pressboard insulation. It can clearly be seen in Figure 4.24 that the relationship between dissolved carbon oxides concentration and the average number of chain scissions of pressboard insulation aged in corresponding oil can be represented using a linear equation with good accuracy. Moreover, the model parameters indicate that dissolved carbon oxides concentration in ester oils is relatively higher than that of in mineral oil for the same degree of pressboard ageing. In the case of synthetic ester, this effect is of paramount significance. It has been reported in [156] that the gas solubility constant of carbon dioxide in NE (FR3) and synthetic ester oils at 20 ºC is 1.5 and 2 times higher than that of mineral oil respectively. In addition, esters themselves produce a larger quantity of carbon oxides due to the breakdown of the carbonyl groups in their molecular structure. This research hypothesises that these two factors result in a higher concentration of carbon oxides in ester oils compared to that of in mineral oil at a similar degree of paper insulation ageing.

4.11.4 Interpretation of DGA Results

The ultimate objective of DGA is to identify the incipient faults in oil–paper insulation systems. This research investigates the application of three widely utilised DGA interpretation techniques namely Duval triangle, IEC gas ratio and IEEE key gas for identifying the incipient faults in an oil-paper insulation system which contains either mineral, NEA, NEB or synthetic ester oil. For this

purpose DGA results of ester and mineral oil samples which have been subjected to the same thermal and electrical faults are interpreted using the above mentioned methods.

In addition to the data presented in Figure 4.21, DGA data of oil samples which have been subjected to 36 electric breakdowns are also considered. In the case of thermal faults at 120 ℃, DGA results of 11 oil samples with different ageing condition (based on ageing time) are utilised to investigate the possibility of identifying low temperature faults in mineral, NEA and NEB oils. In the case of synthetic ester, only 5 samples are diagnosed for thermal fault at 120 ℃.
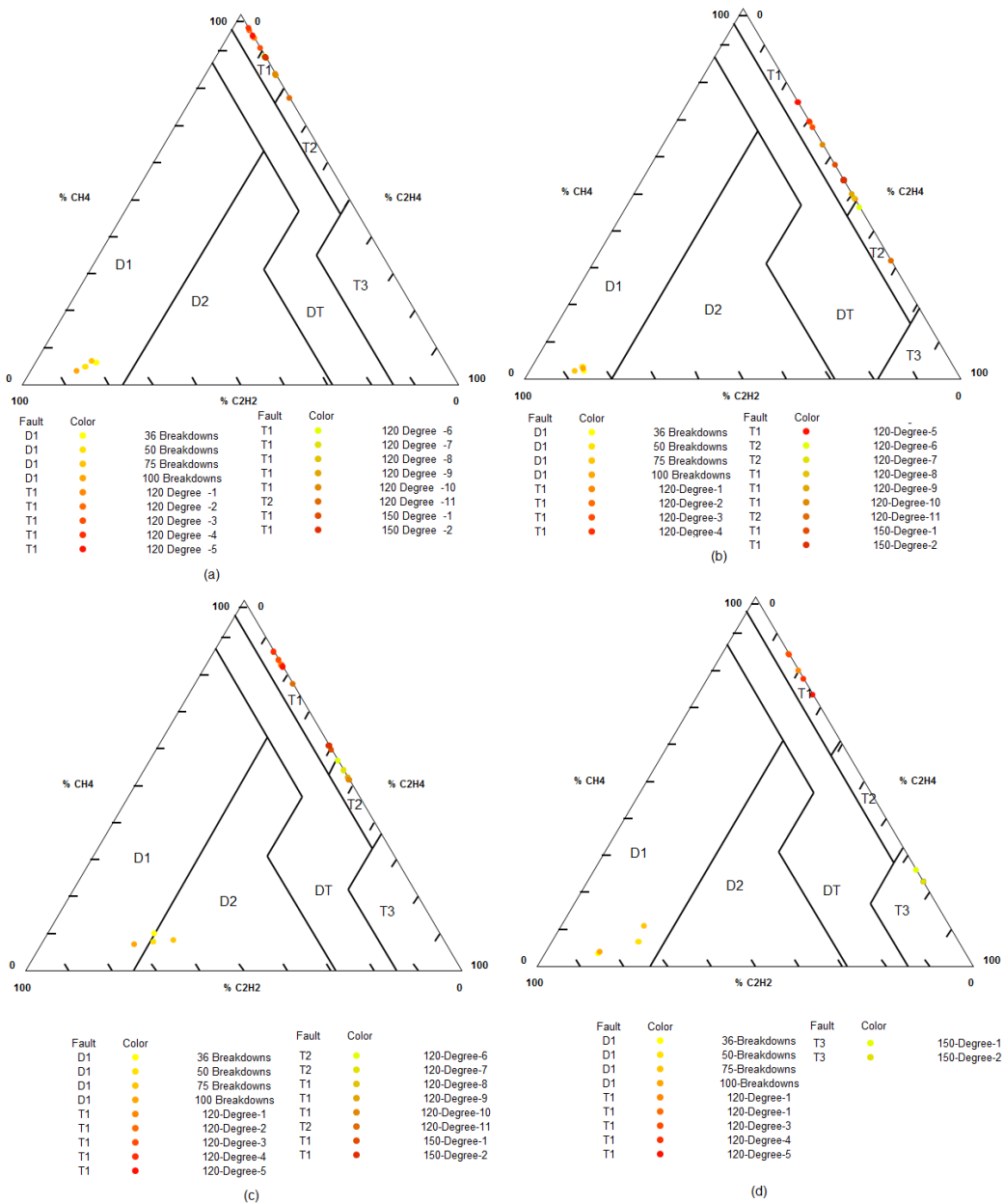
Figure 4.25. Duval triangle diagnostic results (a) Mineral (b) NEA, (c) NEB, (d) Synthetic ester

It is worth mentioning that this study uses the Duval triangle 3 defined for Biotemp, FR3 and MIDEL7131 for diagnosing the DGA results of NEA, NEB and synthetic ester respectively. Figure

4.25 (a) to (d) shows that this method has accurately identified the simulated faults in all types of oils as T1 (thermal fault <300 °C) and D1 (low energy discharge) for most of the cases. However, some of the DGA results of mineral, NEA and NEB oil samples aged at 120 °C have been misinterpreted as fault T2 (300 °C <Thermal Fault<700 °C). In addition, DGA data of synthetic ester oil sample aged at 150 ᵒC was also wrongly diagnosed as T3 fault (Thermal Fault>700 °C) by Duval triangle method. In addition to Duval triangle method, this research uses IEC gas ratio and IEEE key gas methods for interpreting DGA data. Table 4.6 summarises the diagnostic results for gases produced in all types of oil under simulated faults by using Duval triangle, IEC gas ratio and IEEE key gas methods.

Table 4.6. Correctly identified faults for DGA results

Oil type	Fault condition	Duval	IEC 60599 [161]	IEEE key gas
Mineral	Low energy discharge	4 of 3	4 of 4	NA (not applicable)
	120 °C thermal faults	10 of 11	11 of 11	NA
	150 °C thermal faults	2 of 2	2 of 2	NA
NEA	Low energy discharge	4 of 3	3 of 4	NA
	120 °C thermal faults	8 of 11	10 of 11	NA
	150 °C thermal faults	2 of 2	2 of 2	NA
NEB	Low energy discharge	4 of 3	1 of 4	NA
	120 °C thermal faults	9 of 11	11 of 11	NA
	150 °C thermal faults	2 of 2	2 of 2	NA
SE	Low energy discharge	3 of 4	3 of 4	NA
	120 °C thermal faults	5 of 5	3 of 5	5 of 5 overheating cellulose
	150 °C thermal faults	0 of 2	0 of 2	0of 2

Based on the fault diagnosis results shown in Table 4.6, one could conclude that extended Duval triangle and IEC gas ratio methods interpret the DGA results of all types of oils considered in this study with reasonable accuracy. On the other hand, IEEE key gas method possesses the lowest accuracy in diagnosing faults on all types of insulating oil systems with DGA data. IEEE key gas method diagnoses the DGA results of synthetic ester oil aged at 120 °C as overheating of cellulose insulation. This is caused by the production of a large concentration of carbon monoxide due to overheating of synthetic ester oil. In addition, this research has recognised that ethane is the key

fault gas dissolved in NE insulating oil for low temperature overheating faults. Since ethane is mainly produced by a reaction between linolenic acid (present only in NEs) and oxygen, this research proposes ethane as an indicator for NE insulating oil oxidation and to trigger an early warning before oil quality is affected.

4.12 Summary

Overall experimental results presented in this chapter have confirmed that NE insulating oils possess resistance to the ageing of pressboard insulation. This behaviour is mainly caused by high moisture solubility and hydrolysis reaction of NE insulating oils. Experimental results presented in this chapter indicate that the 2-FAL may be less stable in NEA oil. Thus, it is necessary to further investigate whether 2-FAL can be used as a paper insulation ageing indicator for NE based insulation systems. This study has pointed out that acidity and colour of NE ester oils could increase rapidly due to the pronounced hydrolytic degradation in a moisture rich environment. This type of behaviour can be expected after retrofilling of an in-service transformer with NE oil. In such a condition acidity and colour could not reflect the real condition of NE oil. This study has revealed that the acids produced by hydrolysis of NE are not detrimental to paper insulation and not corrosive. However, it is necessary to further investigate the effect of high acidity of aged NE oils on copper and steel, particularly its corrosion effect at high temperature.

The DGA results presented in this chapter have indicated that similar fault gases are produced in both mineral and ester insulating oils. However, there is a significant quantitative difference between fault gases generated in ester and mineral oils. Moreover, gases generated in different esters due to thermal and electrical faults are also not similar in quantity. The results presented in this chapter indicate that dissolved CO_2 in ester oils is greater than mineral oil for similar degree of paper insulation ageing. Moreover, it has been confirmed that synthetic ester oil produces more CO_2 than both NEs and mineral oil under low temperature overheating condition. In case of low temperature overheating condition, NEs produce more C_2H_6 than mineral and synthetic ester. This behaviour is significant for soy oil based NEs. In spite of different gassing behaviour of mineral and ester insulating oils, this research has identified that extended Duval triangle method and IEC gas ratio methods seem to be applicable for diagnosing low temperature overheating and electrical discharge faults in ester insulating oils.

This chapter mainly discussed the changing of chemical and physical properties of insulating oil over thermal ageing. However, the impact of these factors on dielectric response behaviour of insulating oils needs to be investigated. The next chapter presents the main work done in this research to address this issue.

Chapter 5

Modelling and Analysing the Dielectric Response Behaviour of Insulating oil

5.1 Introduction

Dielectric polarisation based measurements have been used as one of the techniques to characterise the quality of insulating oil [193, 194]. Understanding the variation in dielectric response of insulating oil is important to accurately interpret the condition of a transformer's composite insulation system. It has been discussed in Chapter 4 that physicochemical properties of insulating oils markedly change due to ageing under thermo-electrical stresses. In addition, temperature of the oil in an operating transformer is a continuously varying parameter due to dynamic loading conditions experienced by the transformer. Thus, it is important to characterise the influences of ageing and temperature on dielectric response behaviour of different types of insulating oils. In this chapter, the behaviour of two different types of insulating oils including one type of mineral oil and a NE based oil during frequency and time domain dielectric response measurements are analysed for different ageing and temperature conditions.

In the case of dielectric response measurements of insulating oils, parasitic phenomena including electrode polarisation (EP), interfacial polarisation and electro hydrodynamic motion (EHD) arise due to the diverse oil properties and problems inherent in the measuring system. Furthermore, they may impede the determination of intrinsic dielectric parameters of the oil under test. Thus, mathematical and equivalent circuit models analogous to the real physical systems are presented in this chapter to model time and frequency domain dielectric response data of oils respectively. They provide a better understanding of various physical phenomena which have been observed during dielectric response measurements of oil. This chapter is mainly based on two publications of the author [195, 196].

5.2 Measurement Setup

Frequency Domain Spectroscopy (FDS) and polarisation current measurements on oil samples were performed using a three electrode test cell shown in Figure 5.1(a). The test cell has been made of stainless steel in accordance with IEC and Cigre standards [197]. Geometric capacitance of the test

cell is 60 pF and the gap between the measuring electrodes is 2 mm. The oil volume required for a measurement is 50 ml. Here, FDS measurement was executed first, which was followed by the polarisation current measurement. During measurements, the test cell was placed in a temperature controlled oven with a temperature hysteresis of ±2 °C. A commercially available Insulation Diagnostics Analyser (IDA 200) was used to obtain FDS [198]. During the measurement, three leads of the IDA 200 were connected to the electrodes of the test cell placed on an insulation plate as demonstrated in Figure 5.1 (b). In the case of polarisation current measurement, equipment developed at the University of Queensland was used [199]. A highly sensitive 6571A Keithley electrometer is used in the PDC equipment to measure the polarisation current in the nA range.
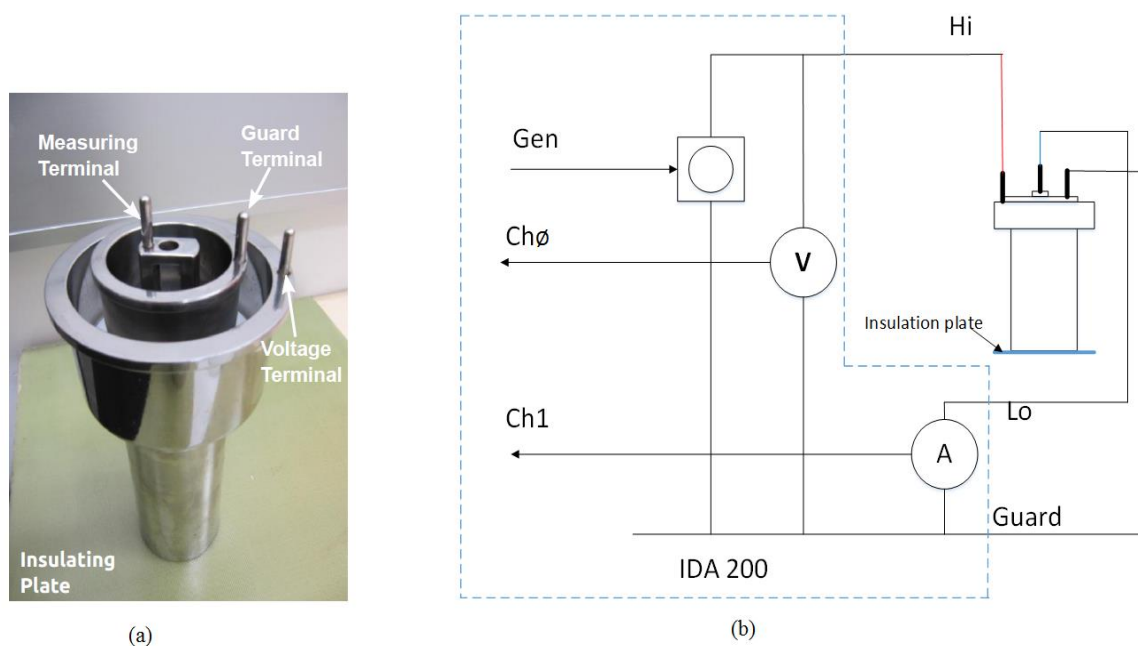
Figure 5.1 (a) Test cell for oil measurements, (b) Schematic circuit diagram for FDS measurement

5.3 Selection of Measurement Voltage

Dielectric response measurement under high field stress may introduce several charge generation and transportation mechanisms which could cause nonlinear behaviour of oil conductivity i.e. voltage dependence conductivity [200, 201]. Therefore, the applied voltage should be low enough to avoid charge carrier injection and field enhancement dissociation (<0.1 kV/mm). Moreover, in order to avoid electrohydrodynamic motion and electroconvection effects, the measuring voltage should be less than 300 V. However, the voltage should be high enough to elude electrochemical polarisation (>1 V) [201]. In addition, when a high field stress is applied for a longer time compared to ion transit time (time taken by an ion to cross the electrode gap), swept out of ionic particles from the bulk may result in lower conductivity. Thereby, this research has used a moderate voltage for dielectric response measurement of oil samples to minimise nonlinear effects. FDS measurements

were performed with a frequency varying sinusoidal signal of 50 Vrms and polarisation current was measured under a DC step voltage of 50 V or 100 V.

5.4 Properties of Oil Samples

This chapter compares the dielectric response behaviour of NEA and shell Diala mineral oil under different ageing conditions. Properties of oil samples including moisture content, acidity, viscosity and ageing conditions are listed in Table 5.1. Relative humidity (RH) presented here has been calculated by considering the moisture saturation levels of mineral and NEA oils at 25 ℃ as 50 ppm and 1100 ppm respectively.

Table 5.1 Properties of oil samples tested in this study

Oil type	Sample Index	Ageing condition @120 ℃	Acidity mgKOH/g	Viscosity @40 ℃ mm²/s	Moisture (ppm)	RH(%)
Mineral	M0	Unaged oil	0	10	1	2
Mineral	M1	Oil only for 384 h	0.01	10	36	72
Mineral	M2	Oil only for 1280 h	0.0	10	36	72
Mineral	M3	Oil, copper, dry PB for 384 h	0.01	10	4	8
Mineral	M4	Oil, copper, dry PB for 1280h	0.01	10	2	4
Mineral	M5	Oil, copper, dry PB for 2800 h	0.01	10	8	16
Mineral	M6	Oil, copper, core steel, PB (2.2%) for 1152 h	0.02	10	20	40
Mineral	M7	Oil, copper, core steel, PB (2.2%) for 1752 h	0.06	10	30	60
Mineral	M8	Oil, copper, core steel, PB (2.2%) for 1984h	0.14	10	32	64
NEA	NA0	Unaged oil	0.03	37	35	3
NEA	NA1	Oil only for 384 h	0.04	37	86	7
NEA	NA2	Oil only for 1280 h	0.07	37	47	4
NEA	NA3	Oil, copper, dry PB for 384h	0.06	38	48	4
NEA	NA4	Oil, copper, dry PB for 1280h	0.26	38	93	7
NEA	NA5	Oil, copper, dry PB for 2800 h	0.59	38	62	6
NEA	NA6	Oil, copper, core steel, PB (2.4%) for 1152 h	2.04	38	239	22
NEA	NA7	Oil, copper, core steel, PB (2.4%) for 1752 h	4.55	38	246	22
NEA	NA8	Oil, copper, core steel, PB (2.4%) for 1984h	6.19	40	184	17

5.5 Investigating the Nonlinear Behaviour under Moderate Voltage

This section presents the influence of measurement voltage on dielectric response of insulating oil at 55 ºC. Figure 5.2 (a) and (b) depict the frequency domain dielectric response as DDF vs. frequency for mineral oil sample M1 and NEA oil sample NA1 respectively for two different measurement voltages, 5 V and 50 V.
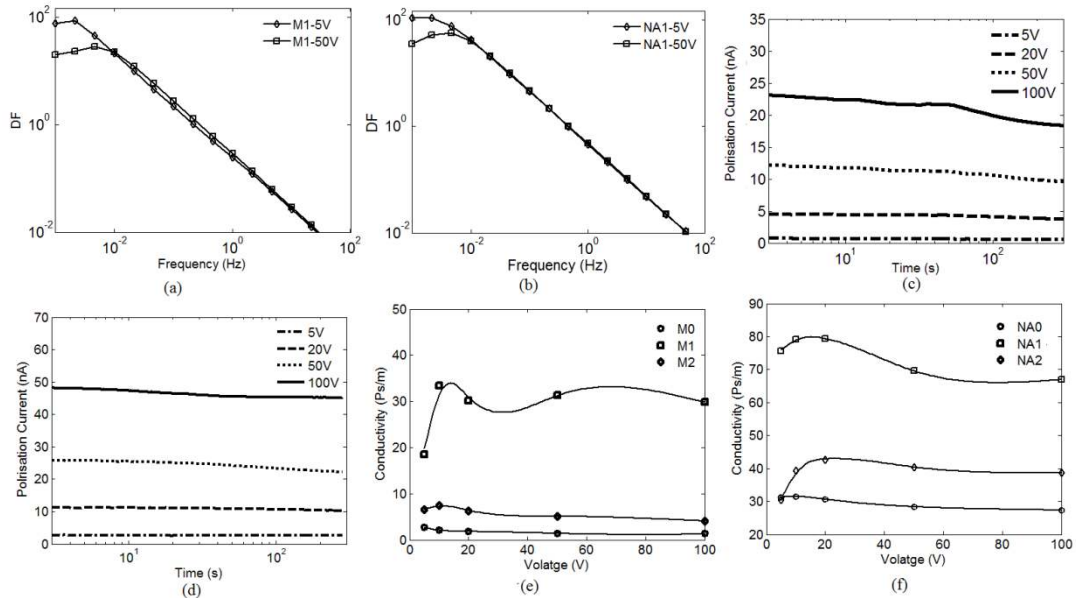
Figure 5.2 (a) FDS -M1, (b) FDS-NA1, (c) Polarisation current -M1, (d) Polarisation current-NA1, (e) Voltage dependence DC conductivity of (M0,M1 & M2), (f) Voltage dependence DC conductivity of (NA0,NA1 & NA2)

Figure 5.2 (a) and (b) indicate that there is no influence of voltage on measured DDF of both types of oils at high frequencies when the measurement voltage is between 5 V and 50 V. On the other hand, DDF of both types of oil shows a clear tendency to decrease with the voltage at a frequency of below 10 mHz. Garton [202] has observed a similar behaviour at power frequency under a higher field stress across a thin oil gap. He has explained this behaviour such that amplitude of motion of ions in the liquids is limited by the width of the electrode gap at a certain electric field and thereby, a further increase of measurement voltage causes to decrease the DDF. Saad et al. [203] have also given a somewhat similar interpretation for this behaviour. When under a low electric field, a similar effect could occur at low frequencies. However, this research does not solely attribute the reduction of DDF at low frequencies to so-called Garton effect and it is characterised as a combination of space charge and Garton effects. Space charge effect is introduced by the accumulation of charges at the electrode liquid interface at low frequencies.

Figure 5.2 (c) and (d) show measured polarisation current response of oil samples M1 and NA1 under different voltage levels between 5 V and 100 V. Measurements have been performed from the

lowest voltage to the highest voltage. It can be seen in Figure 5.2 (c) and (d) that polarisation current does not linearly change with measurement voltage and this characteristic can be clearly identified in DC conductivity vs. voltage graphs in Figure 5.2 (e) and (f). DC conductivity of an oil sample is derived from measured polarisation current using eq (5.1). The average of measured polarisation current in the time range 50-100s is used for calculating the oil conductivity. It shows that conductivity of oil samples M1, M2, NA1 and NA2 firstly increases with voltage and then shows a decreasing trend whilst that of oil samples M0 and NA0 has a decreasing trend with voltage. Once voltage stress is applied across a liquid layer, segregating the ions of the opposite sign will lower the probability of ion recombination [202, 204] and thereby, ion concentration in the liquid phase is increased and gives rise to conductivity. On the other hand, a further increase of applied voltage causes swept out ions from the bulk and decreases the ion concentration in the liquid phase causing a reduction of oil conductivity. These two phenomena account for the variation of measured oil conductivity with voltage as shown in Figure 5.2(e) and (f). Overall, the change of measured conductivity of both types of oil in the voltage range 50-100 V is significantly lower than that in the voltage range 5-50 V. It means that measuring the dielectric response of an oil sample with a voltage signal in the range of 50-100 V is more appropriate.

$$\sigma_{oil} = \frac{Avg.\, I_{pol(50\, s\, to\, 100\, s)} \times \varepsilon_0}{C_0 U} \tag{5.1}$$

Here I_{pol}, ε_0, C_0 and U represent the polarisation current, dielectric permittivity of free space, geometrical capacitance of the test cell and measurement voltage respectively.

5.6 Temperature Dependence of Dielectric Response

This section presents the influence of temperature on dielectric response behaviour of insulating oil. Figure 5.3 (a) and (b) depict the frequency domain dielectric response as complex capacitance vs. frequency for oil samples M8 and NA8 respectively. The measurements on both samples were performed at three different temperature points 35 ℃, 55 ℃ and 75 ℃. Corresponding polarisation current responses of those oil samples are shown in Figure 5.3 (c) and (d). It can be seen in Figure 5.3 (a) and (b) that imaginary capacitance $C''(\omega)$ which represents the conduction and dielectric polarisation losses significantly increases with the temperature. Moreover, an increase of temperature intensifies the low frequency dispersive behaviour of real capacitance $C'(\omega)$. These two phenomena cause to shift the whole response towards high frequency. Figure 5.3 (a) and (b) clearly depict that measured imaginary capacitance of both types of oil increases toward low frequency with -1 gradient. This statement is true at all temperatures. Thereby, one can suggest that the dielectric response of both types of oil is solely characterised by their conductivities and an increase

of conductivity of insulating oil with temperature gives rise to both polarisation current and imaginary capacitance as shown in Figure 5.3. The conductivity of insulating oil is determined by the mobility and density of ions which are provided by dissociation of electrolytic impurities present in the oil. If one assumes that both positive and negative ions in a particular oil possess the same mobility (μ), the electrical conductivity can be written as [194, 205]:

$$\sigma_{oil} = \mu(q_+ + q_-) \tag{5.2}$$

Where, q_+ and q_- denote the positive and negative ions density in oil. Thus, it is clear that conductivity of insulating oil can increase either due to increase of ion mobility or density.
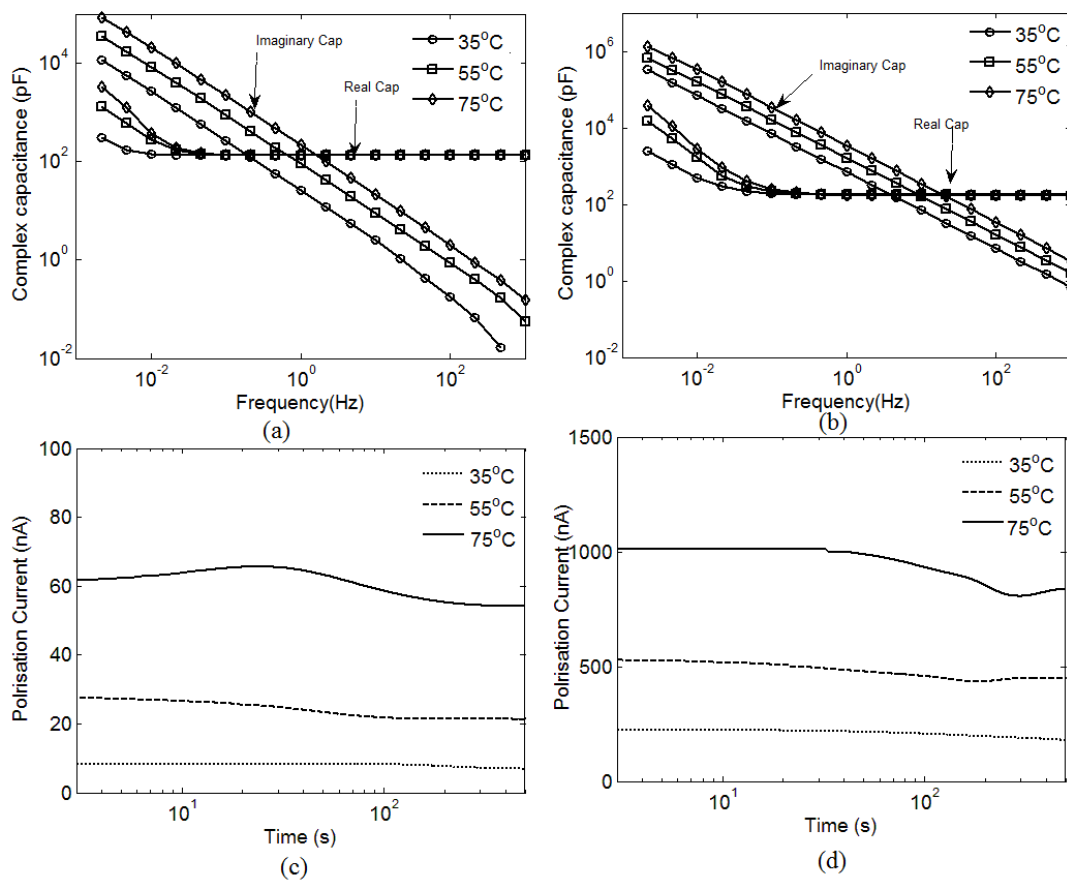
Figure 5.3 Temperature dependence of dielectric response of oil (a) FDS- M8, (b) FDS- NA8, (c) Polarisation current-M8, (d) Polarisation current-NA8

Stokes law indicates that ion mobility in a medium like oil is inversely proportional to the effective viscosity of the medium as given in eq (5.3).

$$\mu = \frac{1}{6\pi\eta r} \tag{5.3}$$

Where η is the viscosity, r is the radius of the ion. Thereby, an increase of oil conductivity with temperature can be assigned to two superimposed effects; increase in fluidity (inverse viscosity) and increase in dissociation of electrolytic impurities to ions with increasing temperature [194, 205].

Temperature dependence of conductivity of insulating oil can be characterised using a so-called Arrhenius type relationship as given in eq (5.4) [205].

$$\sigma_{oil} = \sigma_0 \exp(-E_a / KT) \tag{5.4}$$

Where, E_a, denotes the activation energy for ion motion in oil media and K represents the Boltzmann constant, T is absolute temperature. The conductivity of insulating oil (σ_{oil}) can be calculated using eq (5.5) and measured imaginary capacitance. Thus, the gradient of oil conductivity vs. reciprocal of temperature (1/T) plot gives the activation energy as shown in Figure 5.4(a) and (b). It has been found that activation energy of mineral oil lies between 0.36 eV and 0.47 eV and that of NEA is in the range 0.37 eV to 0.44 eV confirming that conductivity of both types of oil show almost similar temperature dependence characteristics. Moreover, the activation energy values found for mineral oil in this study show good agreement with the value provided in [141].

$$\sigma_{oil} = \frac{C''(\omega) \times \varepsilon_0 \omega}{C_0} \tag{5.5}$$
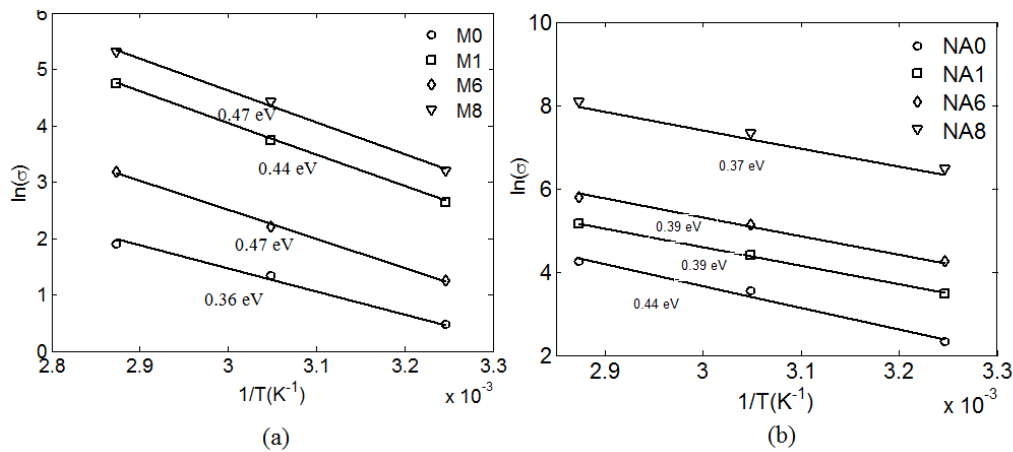
Figure 5.4 Temperature dependence DC conductivity & activation energy (a) Mineral oil, (b) NE

5.7 Influence of Ageing Condition on FDS

Figure 5.5 compares the influence of different ageing conditions on frequency domain dielectric response of both mineral and NE insulating oils. Figure 5.5 (a) and (c) represent the dielectric response as real capacitance vs. frequency for insulating oil aged with dry and wet pressboard insulation respectively. The change in imaginary capacitance of these samples at the same frequency is presented in Figure 5.5(b) and (d). It can be seen in Figure 5.5 that ageing gives rise to

oil conductivity and interfacial effect in a way similar to temperature does. This behaviour is caused by formation of easily dissociable molecules of organic acids and peroxides over thermal ageing in the presence of some dissolved oxygen in oil [15, 202]. Data provided in Table 5.1 confirms that in all cases oil samples are not saturated with moisture. Therefore, this study does not attribute change of oil conductivity over ageing to the moisture content in oil [188].
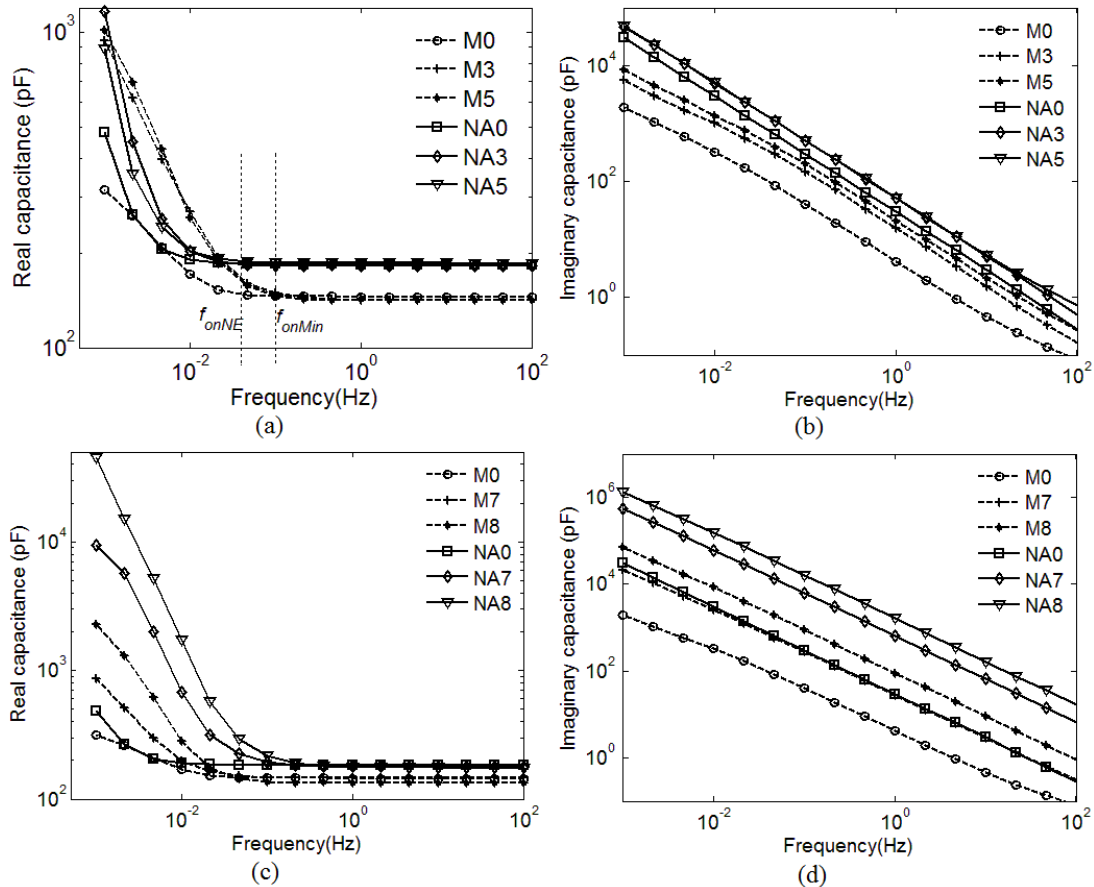
Figure 5.5 Impact of ageing on FDS of insulating oil (a)-(b) FDS of oil aged with dry PB, (c)-(d) FDS of oil aged with wet PB (Broken line for mineral oil, thick line for NE)

In general, conductivity of NEs is greater than typical mineral oil and it is confirmed by the results shown in Figure 5.5 (b) such that even dielectric loss of 2800 hrs aged mineral oil sample (M5) is less than that of unaged NE (NA0). Higher dielectric constant (permittivity) of NE oils causes this behaviour because polar liquids enhance the dissociation of ionic impurities leading to a higher charge density in the system. Oil samples aged with wet pressboard (Figure 5.5(d)) possess very high dielectric loss compared to that of aged with dry pressboard (Figure 5.5(b)) confirming the formation of more dissociable ionic impurities in the presence of moisture in both mineral and NE–paper insulation systems.

The measured real capacitance of both types of insulating oils at high frequencies does not show a measurable change over ageing and remains at a constant value. On the other hand, regardless of the type of oil, the interfacial effect increases the real capacitance by several orders of magnitude at low frequencies and this effect becomes pronounced with ageing.

One can clearly identify in Figure 5.5 (a) that the frequency (f_{on}), at which real capacitance starts to increase is higher for mineral oil compared to that of NE. This could be due to the fact that time taken to travel between electrodes by an ion in mineral oil is less than that in NE, since the NE has a higher viscosity than mineral oil [195]. On the other hand, low frequency dispersion of NE oil samples NA7 and NA8 starts at a higher frequency than mineral oil (M7 and M8). It indicates the presence of different types of high mobility ions in samples NA7 and NA8. These two samples possess very high acidity values (4.05 mg KOH/g and 6.2 mg KOH/g). Thereby, one could clearly mention that very small H^+ ions provided by dissociation of carboxyl acid are the high mobility ions in those samples. This is because the mobility of an ion is inversely proportional to its radius as explained in eq (5.3).
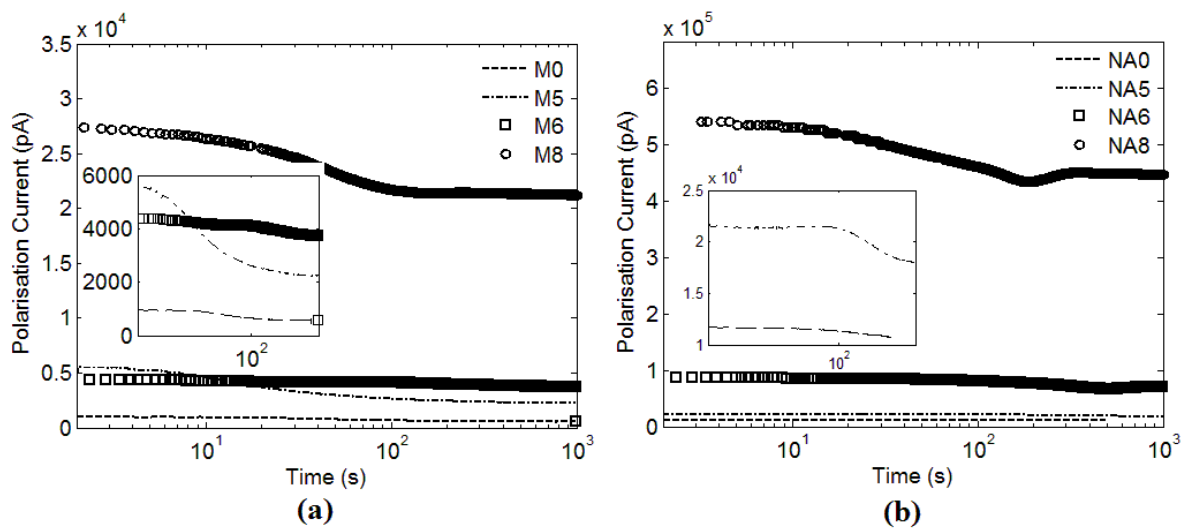
Figure 5.6 Impact of ageing on PDC (a) Mineral oil (b) NE

Figure 5.6 (a) and (b) show the polarisation current responses of mineral and NE oil samples at different ageing conditions respectively. The polarisation current of both types of oils increases over ageing, thus pointing to the feasibility of using polarisation current response to monitor the ageing conditions of insulating oils. Here, samples M8 and NA8 possess the highest polarisation current reflecting that polarisation current measurement also provides similar information as FDS measurements.

5.8 Modelling of Frequency Domain Dielectric Response of Oil

5.8.1 Characterising of low frequency behaviour

In order to characterise the low frequency behaviour, dielectric response of oil samples at three different ageing conditions have been measured in the frequency range 10^{-4}-10^3 Hz for both mineral and NE oils. Figure 5.7 (a) and (b) illustrate the dielectric responses of mineral oil as complex capacitance vs. frequency and AC conductivity vs. frequency respectively. The responses corresponding to NE oil samples are shown in Figure 5.7 (c) and (d).
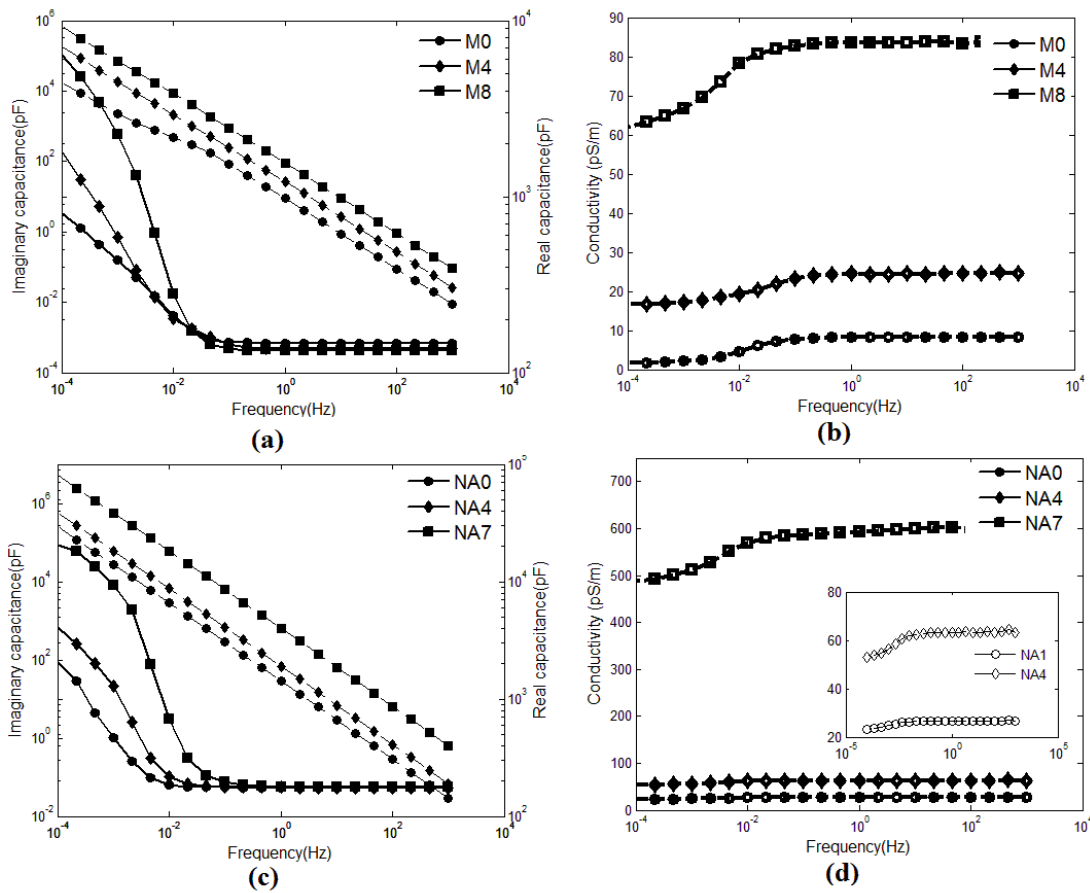
Figure 5.7. Dielectric spectra of insulating oil at 55ºC for three different ageing condition (a) FDS of mineral oil, (b) conductivity of mineral oil, (c) FDS of NE, (d) conductivity of NE

A massive increase can be seen in measured real capacitance of insulating oil at low frequency and the rate of increase is shown to be dependent on the conductivity of corresponding oil sample. Figure 5.7 (a) and (c) show that this effect is more substantial in NE compared to mineral oil such that the rise of real capacitance of the unaged NE oil sample (NA0) is higher than that of 1280hrs aged mineral oil sample (M4).

The low frequency trend of real capacitance of samples M8, NA4 and NA7 has a steep gradient between -1 and -2 at the beginning followed by a gradient of -1 to 0 during the lowest frequency decade. It indicates that this is a somewhat different behaviour compared to the so called Maxwell-Wagner effect. In addition to the rise of real capacitance, there is a substantial decrease in measured conductivity at low frequencies as shown in Figure 5.7 (b) and (d). The observed behaviour is caused by interfacial phenomenon which occurs at the oil and electrode interface namely electrode polarisation.

Generally in ionic liquids, charges arriving at the metallic electrode under electric field stress accumulate in a thin layer immediately next to the electrode surface and form a space charge region as shown in Figure 5.8 [206-210]. This appears as a large impedance connected in series with the bulk material impedance in the electrical circuit. This leads to a massive increase in measured real capacitance at low frequencies. In such a system, the apparent conductivity of the liquid also decreases by several orders of magnitude. This phenomenon is called electrode polarisation and it depends on several external parameters such as conductivity of liquid, temperature, electrode properties including material, structure and roughness. Thereby, we suggest taking special care when low frequency dielectric response data is used to assess the condition of insulating oil as suggested by [209].
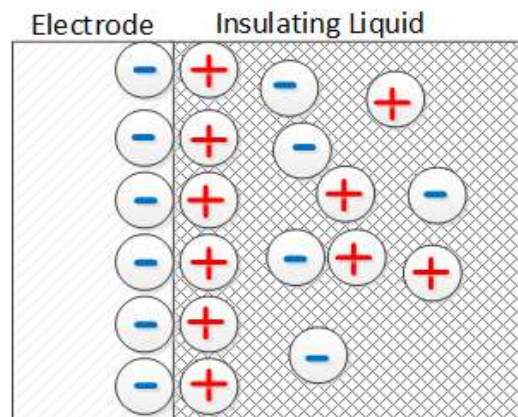
Figure 5.8. Electrical double layer forms at electrode liquid interface

5.8.2 Equivalent circuit for explaining low frequency behaviour

In conventional approaches, electrode polarisation is analysed using an equivalent circuit with a constant phase angle element (universal capacitor) in series with the bulk impedance as shown in Figure 5.9 (a). The frequency domain characteristic of a universal capacitor model is given in eq (5.6). In addition to that, a parallel R-C element connected in series with the intrinsic bulk impedance is also used to characterise the electrode polarisation phenomenon [207, 211].

$$C_n(\omega) = B(j\omega)^{n-1} \Rightarrow 0 \leq n \leq 1 \qquad (5.6)$$

Frequency responses shown in Figure 5.9(a) and (b) respectively for universal capacitor and R-C element based circuits indicate that these equivalent circuits not only represent the upward dispersion in real capacitance but also contribute to large dispersion in imaginary capacitance. Moreover, it can clearly be seen in Figure 5.9 (b) that parallel R-C element circuit can only represent a rise in real capacitance with a constant gradient of -2 in log scale. Therefore, only with a conventional approach, it is difficult to explain observed dielectric response behaviour of insulating oil where the decrease in oil conductivity is very small while capacitance has increased by a couple of decades with different gradients between -2 and 0 at low frequencies.
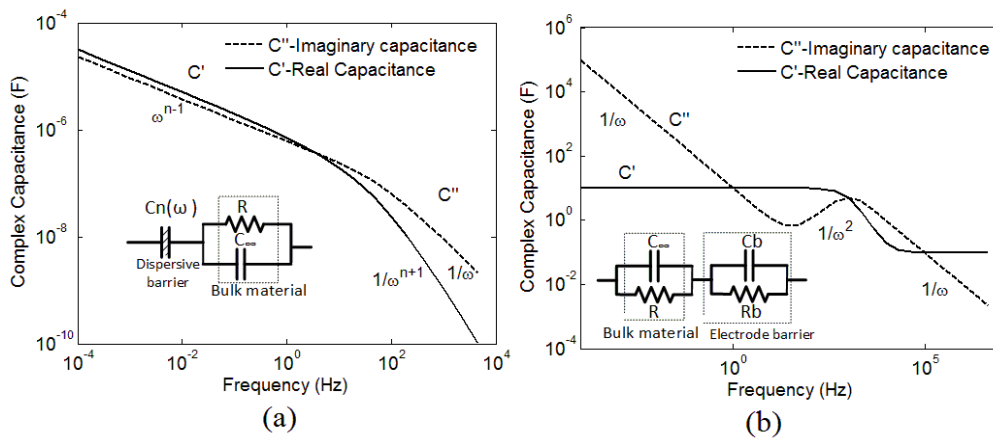
Figure 5.9. Conventional equivalent circuit for representing electrode polarisation

Figure 5.10 (a) demonstrates the complex admittance diagram of the M0 sample derived from its FDS results. The low frequency region of this diagram is similar to the complex admittance diagram of a R-C circuit, which has a universal capacitor, non-dispersive constant capacitive element and a conductive element connected in parallel [110]. Eq (5.7) can be used to calculate the complex admittance when the complex capacitance is known from FDS. Further, in Figure 5.7 one could observe that conductivity has a single point of deflection and then reaches a constant value. Based on this observation, it is assumed that two types of charge are active in these insulating liquids within the considered frequency range. Therefore, to characterise the observed low frequency dispersion a phenomenological equivalent circuit has been proposed as shown in Figure 5.10 (b). Here, C_∞ represents the high frequency capacitance of oil. G_1 and G_2 denote the conductance given by ionic species I_1 and I_2 respectively.

$$Y(\omega) = \left[\underbrace{Y'(\omega) + iY''(\omega)}_{\text{Complex\_Admitance}} \right] = i\omega \left[\underbrace{C'(\omega) - iC''(\omega)}_{\text{Complex\_Capacitance}} \right] \qquad (5.7)$$

It is assumed that I_2 tends to be completely blocked at the electrode surface at low frequencies, whereas I_1 instantaneously discharges without accumulating near the electrodes. This hypothesis is plausible in reality due to the diversity of ion mobility in oil [206] and a multi-step chemical reaction at the electrode liquid interface. That is, neutralisation of ions at the electrode can occur as single or multi step chemical reactions. In the low frequency region, where an electrode blocking state is significant, conductance G_1 of the oil is solely due to the I_1. As the response of the universal capacitor is diminishing at high frequencies, the same circuit presented in Figure 5.10 (b) can be used to model the high frequency behaviour of oil. At high frequencies both types of ions contribute to the conduction process in oil. Frequency domain response of the proposed equivalent circuit can be expressed as in eq (5.8).
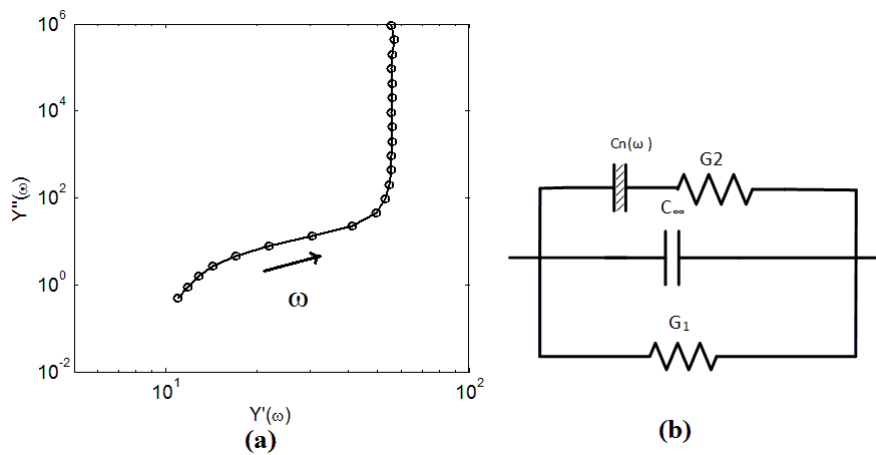
Figure 5.10. (a) The complex admittance diagram of sample M1, (b) Proposed equivalent circuit

$$C(\omega) = \frac{G_1}{j\omega} + \left(\frac{1}{B}\left((j\omega)^{1-n} \right) + j\omega / G_2 \right)^{-1} + C_\infty \tag{5.8}$$

Figure 5.11 (a) and (c) compare the measured frequency domain spectra of real capacitance with the modelled spectra using the proposed equivalent circuit for both mineral and NE oils respectively. As demonstrated by the solid line in Figure 5.11 (a) and (c), FDS of the proposed equivalent circuit yields a satisfying fitting curve of measured real capacitance throughout the observed frequency range. One could observe that below the frequency at which the real capacitance started to rise, the model response slightly deviates from the corresponding measured response. This may be due to the forming of more than one space charge layer at the electrode interface. Diversity of ionic mobility in a liquid could lead to form several space charge layers. Therefore, to increase the accuracy of the model two or more universal capacitors connected in series will be required. However, the measured frequency responses do not provide enough information to confirm such behaviour as the conductivity shows only a single point of deflection in the measured frequency range.

Table 5.2 provides estimated values of pre-exponential factor (B) and exponential factor (n) of the universal capacitor element for representing FDS of mineral and NE oil samples with three different ageing conditions. Parameters are selected using the nonlinear least squares technique in MATLAB environment with $R^2 > 0.93$. The initial values for G_1 and G_2 were obtained by using eq (5.9) with imaginary components of their spectrums at 0.1 mHz and 100 Hz respectively.

$$G = C''(\omega) \times \omega \qquad (5.9)$$
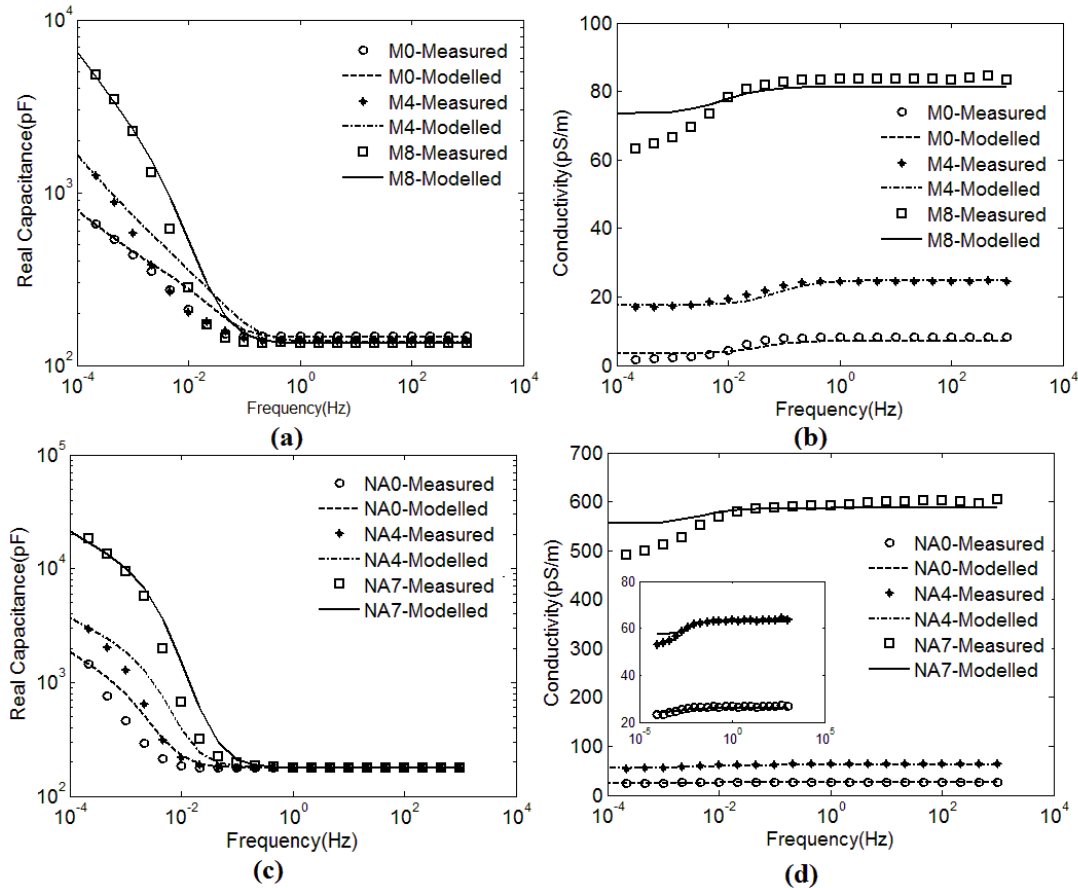
Figure 5.11. Measured and modelled FDS response (a)-(b) Mineral oil, (c)-(d) NE

Figure 5.11 (b) and (d) compare the measured ac conductivity with the calculated value of them using parameters B, n, G_1, G_2 and C_∞ as given in Table 5.2. The modelled data match very well with the measured conductivity in the whole frequency window for oil samples M0, M4 and NA0. On the other hand, reduction of modelled conductivity at low frequencies of oil samples; M8, NA4 and NA7 is lower than the reduction of the measured conductivity. One could claim that charge carrier loss can occur at low frequencies as a consequence of a long measuring time [120]. For example, oxidation results in decreasing charge carriers in the system. This phenomenon leads to decreased conductivity but loss of charges does not contribute to EP. One can also assume that H^+ ions play a role as the main charge carrier in oil sample M8, NA4 and NA7 because acidity values of those

samples are quite high compared to unaged oil. Thus, so-called cathode reaction could remove H^+ ions from the system and gives a similar effect as oxidation.

Table 5.2 Parameters of Equivalent Circuit for representing frequency domain behaviour of oil

Sample ID	G_1 (pS)	G_2 (pS)	C_∞ (pF)	B (pF)	n
M0	24	29	137	71	0.67
M4	112	48	137	111	0.61
M8	500	50	50	262	0.56
NA0	152	10	178	263	0.65
NA4	338	33	178	500	0.73
NA7	3732	200	178	2724	0.7

5.9 Correlation between LFD and Conductivity

This section discusses the correlation between low frequency dispersion (LFD) of real capacitance and AC conductivity of insulating oil. FDS measurement of oil samples aged with and without dry pressboard are considered for this analysis assuming that moisture effects on their ageing characteristic is similar. The change of real capacitance (ΔC) is calculated using eq (5.10).

$$\Delta C = C'_{1mHz} - C'_{100Hz} \tag{5.10}$$

Where, C'_{1mHz} and C'_{100Hz} are real capacitance at 1mHz and 100Hz respectively. Conductivity of a corresponding oil sample at 100 Hz is used for analysis and it is derived from measured imaginary capacitance at 100 Hz and using eq (5.5). This study proposes an empirical formula in the form of eq (5.11) to describe the correlation between the low frequency dispersion (ΔC) and the AC conductivity of insulating oil.

$$\Delta C = \lambda (\sigma_{oil})^b \tag{5.11}$$

Where, λ is a pre-exponential factor and b is a constant. Both parameters depend on temperature, electrode material and type of insulating liquid. Parameters of eq (5.11) have been obtained with a nonlinear least square method using the MATLAB tool with $R^2 > 0.95$. Figure 5.12 (a) and (b) compare the measured and calculated ΔC values for mineral and NE respectively.

As shown in Figure 5.12, the derived model confirms that LFD effect (ΔC) at 55 ℃ is greater than that at 75 ℃ for a similar conductivity value of oil. This phenomenon is due to the fact that an

increase in temperature decreases the effect of electrode polarisation [208] by reducing the ionic hopping time τ_e at the electrode interface as given in eq (5.12).

$$\tau_e = \tau_0 \exp\left(\frac{E_a}{KT}\right) \tag{5.12}$$

Where τ_0 is a constant and E_a is activation energy corresponds to charge hopping at the electrode interface. Therefore, one could expect low dispersion in real capacitance at high temperature. The modelled parameters for eq (5.11) are presented in Table 5.3. These parameters show dependence on both temperature and type of oil. Different liquids show diverse adsorption behaviour at the liquid electrode interface [212]. Adsorption of oil molecules to the electrode blocks the sites for the desired electron transfer across the interface. This may be the reason for having a different EP effect between NE and mineral oil at a similar conductivity.
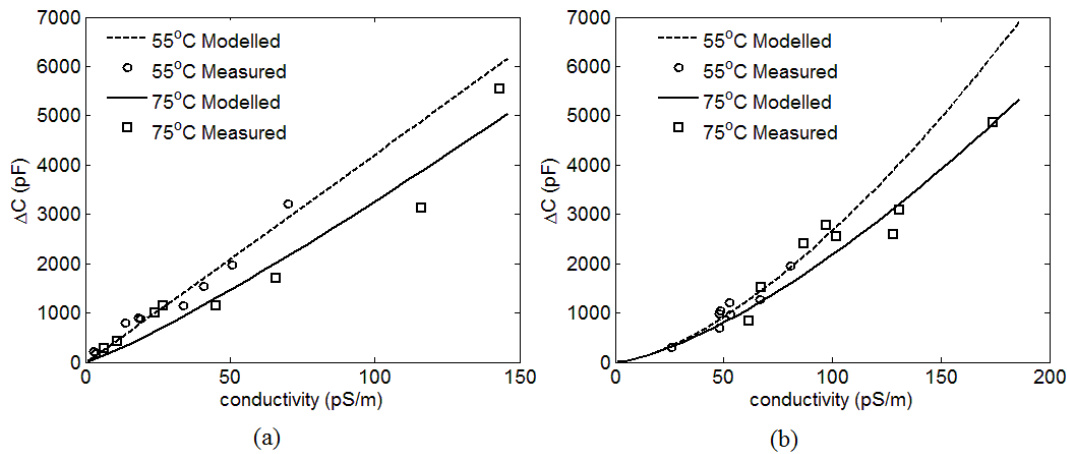
Figure 5.12. (a) LFD effect vs. conductivity for mineral oil, (b) LFD effect vs. conductivity for NE

Table 5.3 Parameters of proposed model for correlating conductivity and LFD of real capacitance

Oil type	Temperature	Λ	b
Mineral	55ºC	40	1.01
	75 ºC	15.74	1.16
NEA	55 ºC	2.28	1.53
	75 ºC	2.88	1.44

5.10 Modelling Time Domain Dielectric Response Behaviour

5.10.1 Characterising behaviour of polarisation current

In order to characterise the charge transport phenomena in different types of insulating oil under a DC electric field, polarisation current responses of mineral and NE oil samples at different ageing

conditions have been measured over 10000 s. The results are shown in Figure 5.13 (a) and (b) for mineral and NE oils respectively.
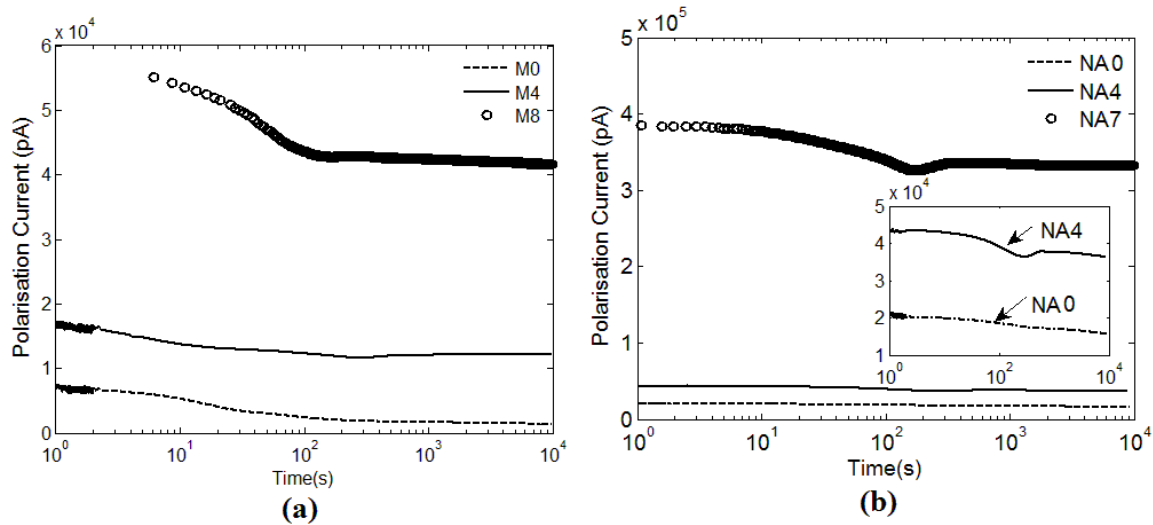
Figure 5.13. Measured polarisation current over 10000 s, (a) Mineral oil (b) NE

It is clear that the polarisation current of oil is highly time dependent; even in unaged oil this effect is significant. This is partly caused by swept out ions in the bulk region and an accumulation of them near the electrodes [200, 201, 213]. Ions that reach the electrode may either discharge or persist as charge particles. It depends on the chemical nature of the ions as well as the physical nature of the electrodes. The accumulation of charge leads to a reduction of conductivity in two ways; first by decreasing the charge carriers in bulk and secondly by dropping effective voltage across the oil gap [214].

In general, interpretation of basic features of the polarisation current curve is difficult due to overlapping of several charging mechanisms having different time constants. However, in the presented results, there are two regions, such that rapid decay of polarisation current during the first 100-200 s and very slow decay components during the rest of the period. In between these two regions there is a plateau in the current waveform. Indeed, this phenomenon is noticeable in aged NE oil. This may be due to a second type of ion, which is still not blocked at the electrode and trapped in the space charge region. A very high electric field in the space charge region causes the acceleration of these trapped charges and enhances the conductivity for a short period of time.

5.10.2 Modelling electrode polarisation and conduction phenomena of insulating liquids under DC field stress

As explained in [213], the apparent conductance of insulating oil (G_t) at the start of the measurement is given by eq (5.13).

$$G_t = G_0 + G_f \tag{5.13}$$

Where, G_0 is the conductance due to the total dissociated charge accumulated at the electrode and G_f is the conductance of the system at steady state. Accumulation of charge near the electrode forms an electrical double layer with capacitance of C, which is in series with the bulk conductance. When the electrode cross sectional area is unity and two electrodes are separated by a distance a, loss of conductance due to charge accumulation can be expressed as [213]:

$$G(t) = \frac{G_0(G_0 - bCU_0)(G_t - bCU_0)e^{-\beta t} - G_f(G_0 - bCU_0)bCe^{-2\beta t}}{\left(G_0 - bCU_0 e^{-\beta t}\right)^2} \tag{5.14}$$

Where, U_0 is the voltage applied across the sample and β is $(G_0/C)-bU_0$. In this study, we consider that U_0 is much greater than the maximum polarisation voltage (G_0/bC) which is equal to the voltage across the electric double layer. Therefore;

$$\frac{bCU_0}{G_0} \gg 1 \tag{5.15}$$

Then eq (5.14) can be approximated as:

$$G(t) = G_0 e^{-bU_0 t} + G_f$$
$$\sigma_{oil}(t) = \sigma_0 e^{-mU_0 t/a^2} + \sigma_f \tag{5.16}$$

When one considers that two types of ions with different mobilities (μ_1, μ_2) such as positive and negative ions are blocked at electrodes, eq (5.16) can be generalised to represent the change of conductivity over time as:

$$\frac{\sigma_{oil}(t) - \sigma_f}{\sigma_0} = \frac{\mu_1}{\mu_1 + \mu_2} e^{-\mu_1 U_0 t/a^2} + \frac{\mu_2}{\mu_1 + \mu_2} e^{-\mu_2 U_0 t/a^2} \tag{5.17}$$

Therefore, polarisation current measured in such a situation can be mathematically represented by

$$I(t) = \alpha_1 * \exp^{(-\tau_1 * t)} + \alpha_2 * \exp^{(-\tau_1 * t)} + I_s \tag{5.18}$$

Where α_1 and α_2 are arbitrary constants decided by the mobilities of ions corresponding to exponential decay currents. I_s is the steady state conduction current component. τ_1 and τ_2 equal to $(\mu_1 U_0 /a^2)$ and $(\mu_2 U_0 /a^2)$ respectively.

As shown in Figure 5.14 (a) to (d), a time domain function with two exponential decay terms can accurately represent the measured polarisation current waveform of both mineral and NE insulating

oils. It confirms that two types of ions with different drift mobilities are blocked at the electrode. Polarisation current of sample M8 possesses only one exponential decay component because the current during the first 5 s has not been recorded in the measured response.
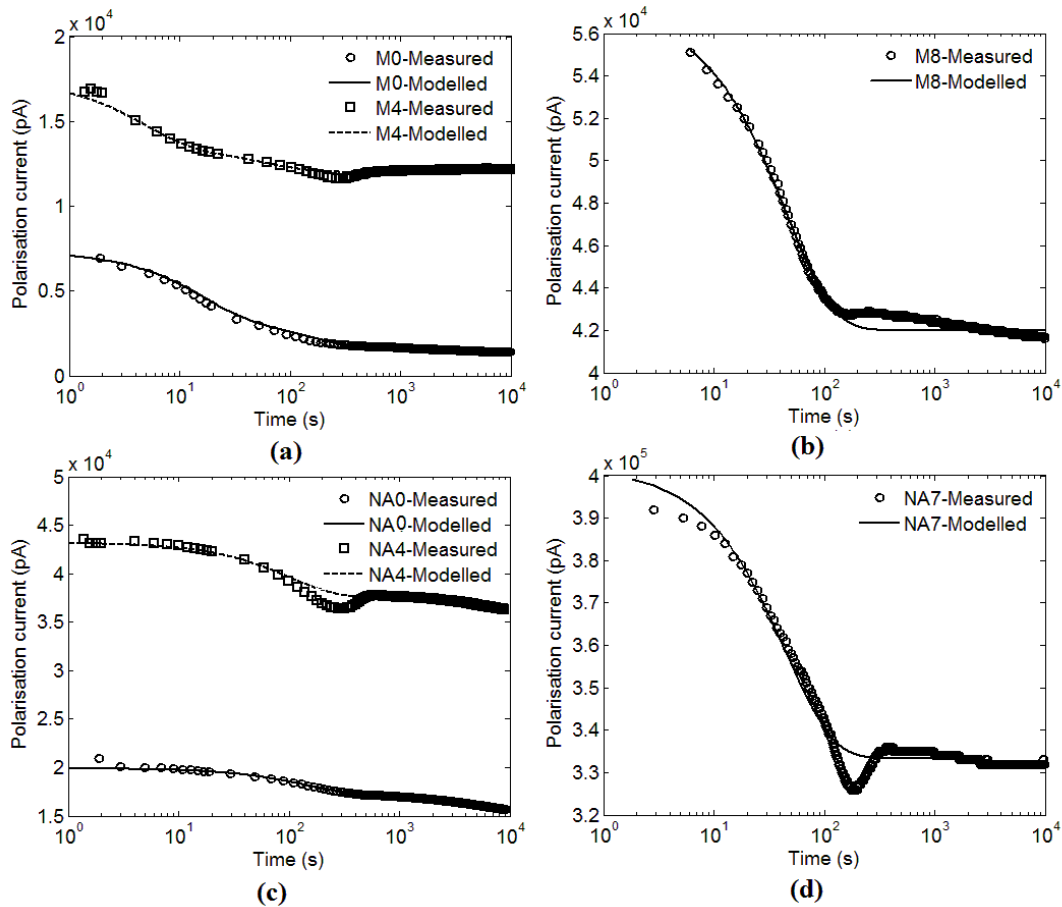
Figure 5.14. Simulated and experimental polarisation current (a)-(b) Mineral oil, (c)-(d) NE

Parameters given in Table 5.4 have been selected using the nonlinear least squares technique in the MATLAB environment with (R^2>0.96). Model parameters show that polarisation current has exponential decay terms with low and fairly large time constants. According to [213], there are mainly two types of ions in insulating liquids, i.e. ions with an equivalent number of oppositely charged ions and partially dissociated molecular size ions. The free ions are quickly removed from the system and that gives a sharp drop in current in a short period, whereas the partially dissociated ions provide a slow decay current. One could claim that this phenomenon causes the observed exponential decay characteristic of polarisation current during a measured time period. In the case of NE, $1/\tau_2$ possess very high values. Therefore, one could also assume that an exponential decay component with a larger time constant represents the loss of ions from NE oil due to a longer measuring time and only one type of ions are blocked at the electrode.

Calculated ion mobility values for mineral oil and NE indicate that they follow the viscosity of the corresponding oil such that ion mobility in mineral oil is higher than that of in NE. However, mobility of type 1 ion in NA7 sample (μ_1) has a value in the same order of magnitude as μ_2 of M8 mineral oil sample. One can assume that very small protonic ions H^+ coming from dissociation of acid causes this behaviour because NE oil sample NA7 has a very high acidity value of 4.55 mg KOH/g. The calculated ionic mobility in mineral oil agrees with the typical range provided in [215] that is 10^{-9} m^2/Vs. It means the modelling technique presented in this research for characterising the polarisation current of insulating oil is accurate.

Table 5.4 Calculated model parameters and ion mobilities for experimental results

Sample ID	α_1 (nA)	α_2 (nA)	I_s (nA)	τ_1 (s^{-1})	μ_1 (m^2/Vs)	τ_2 (s^{-1})	μ_2 (m^2/Vs)
M1	3.36	1.96	1.4	0.062	2.4×10^{-9}	0.014	5.2×10^{-10}
M4	3.9	1.52	12.1	0.22	8.4×10^{-9}	0.017	6.4×10^{-10}
M8	0	15.1	42	-	-	0.022	8.4×10^{-10}
NA1	2.7	2.7	14.5	0.007	2.8×10^{-10}	0.0001	4×10^{-12}
NA4	5.6	1.6	36.2	0.01	4×10^{-10}	0.002	5.6×10^{-11}
NA7	70	8	320	0.022	8.8×10^{-10}	0.0001	4×10^{-12}

Intermediate plateau, which is a result of temporary acceleration of charge in the space charge region, cannot be explained with this model. In fact, it is an intermittent phenomenon which cannot be included in a charge carrier based model. Since the insulation system of a transformer has a layered structure, charge blocking at the liquid and solid insulation interface could create an almost similar effect as we observed here.

5.11 EHD Effect in Highly Conductive Contaminated Oil

Polarisation current measurement of some of the oil samples showed transient behaviour at the beginning as shown in Figure 5.15 (a) and (b). To provide a better understanding of this behaviour, polarisation current responses of mineral oil samples taken from two different transformers owned by one of the Australian utilities have been measured. These samples are named as MF1 and MF2.

In order to make this transient behaviour pronounced, a measurement voltage of 100V is used for polarisation current measurement of samples MF1 and MF2.
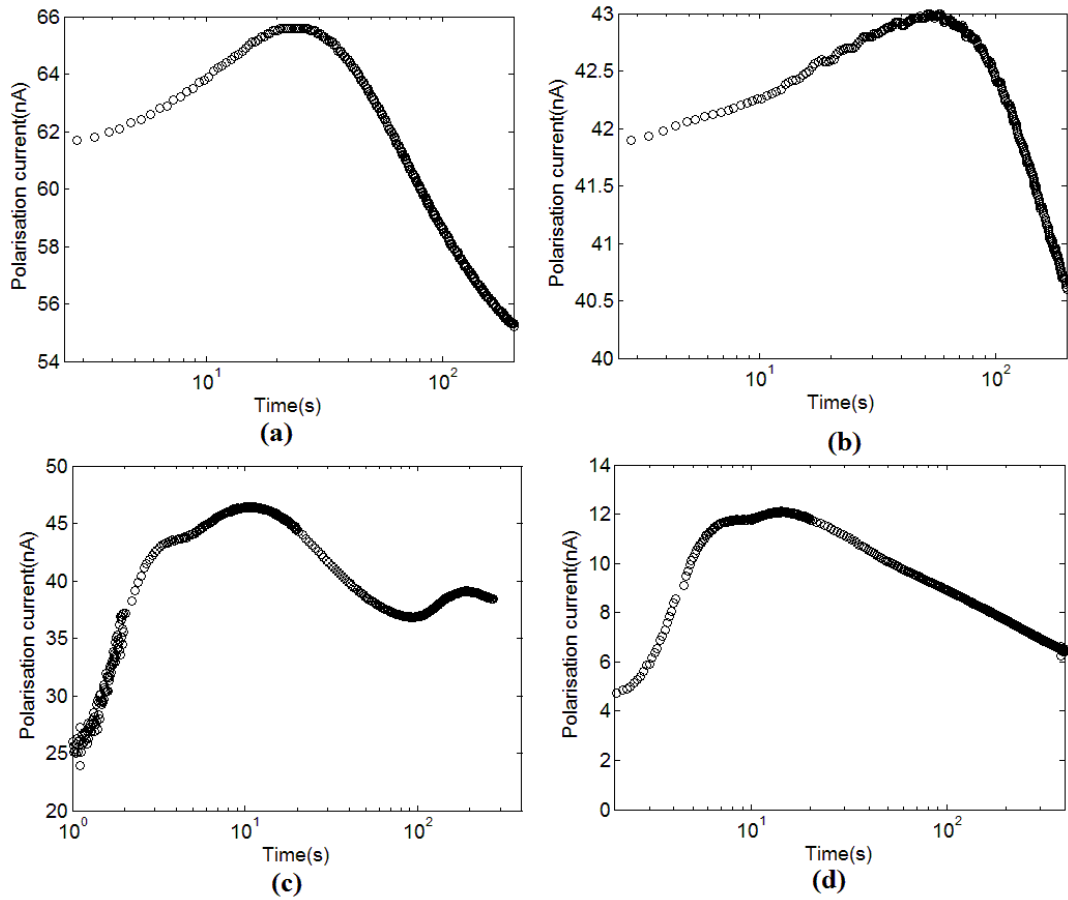
Figure 5.15. Example for EHD motion phenomenon (a) Polarisation current of M8 at 75ºC, (b) Polarisation current of NA6 at 35ºC (c)) Polarisation current of MF1 at 35ºC, (d)) Polarisation current of MF2 at 35ºC

It can be seen in Figure 5.15 (a) and (b) polarisation currents of samples M8 and NA6 increase to a maximum and then exponentially decrease. This behaviour is more substantial in oil samples MF1 and MF2 such that even after 300s, the current is still higher than the initial value. This behaviour is known as electrohydrodynamic (EHD) motion. Particularly, when a metallic electrode is used, a unipolar charge layer spontaneously appears next to the electrode [194, 203, 216]. This is caused by electron tunnelling transfer between the metal and molecular states in the liquid [217]. When the system is excited with low or moderate voltage, the hetero-charges layer either compresses or discharges, while the homo-charges layer displaces towards the counter electrode. This phenomenon induces EHD motion in liquid. It enhances the mobility of charge carriers. Therefore, one can explain that observed transient behaviour of polarisation current is due to EHD motion.

Figure 5.15 shows that there are three distinct regions in measured polarisation current. In the first region, current is continuously increasing due to fluid flow and then in the second region current is

approximately constant due to the constant velocity of the transport charge. In the last region, current is decreasing. The polarisation current starts to decline just after the first charge carrier reaches the electrode. It is called transit time of ions in oil [216]. EHD effect leads to an erroneous and misleading interpretation of the quality of insulating oil. For example, there is a large error in calculated DC conductivity when the measurement is severely affected by EHD motion as shown in Figure 5.15 (c) and (d). Further, the effect of EHD motion on FDS measurement at very low frequencies cannot be ignored. Therefore, it is better to select a very low voltage for the dielectric response measurement of contaminated oil samples taken from field transformers.

5.12 Summary

This chapter compares the dielectric response behaviour of one type of commercially available NE insulating oil to a mineral oil under similar conditions. It shows that conductivity of both oils have almost similar temperature dependence characteristics and ageing results in increasing their conductivities. Moreover, this chapter provides a broader understanding of parasitic phenomena appearing in the dielectric spectra of insulating oil. In order to explain low frequency dispersive behaviour in the FDS of insulating oils, this chapter has proposed an equivalent circuit model. The polarisation current behaviour of insulating oils has been mathematically represented using an exponential model. Both models have been derived based on charge transport phenomenon at the oil-electrode interface. The proposed models have verified that there are two different types of ions present in both mineral and NE oils. Moreover, the exponential model is used to model the polarisation current, which allows the mobility of ions existent in the oil to be calculated.

In this chapter it has been identified that dielectric responses of insulating oils are mainly characterised by their conductivities. The influence of polarisation on dielectric response of oils is mainly introduced by the parasitic phenomena like electrode polarisation. However, in the case of solid insulation materials, their dielectric responses are characterised by a collection of different relaxation conduction processes. In such conditions, dielectric response modelling techniques are typically used to interpret the dielectric response data. Appropriate modelling techniques to represent the frequency and time domain dielectric response data of oil impregnated pressboard insulation are selected in the next chapter.

Chapter 6

Modelling the Dielectric Response of Oil Impregnated Pressboard Insulation

6.1 Introduction

Frequency domain spectroscopy (FDS) and polarisation and depolarisation current (PDC) are collectively known as current based dielectric response measurements. It is generally accepted that the dielectric response of solid phase materials is primarily determined by their morphology and chemical structure. Moreover, dielectric response behaviour of the majority of solid materials is extremely sensitive to the presence of water as an impurity. Thereby, dielectric response method has been widely utilised in the transformer industry as a non-invasive method for determining ageing condition and moisture in solid based insulation. In addition, analysing the microscopic morphology of biological systems with dielectric response method has been widely discussed in the literature.

The dielectric spectrum of a material under investigation is characterised by both conduction and polarisation phenomena. The effect of conduction is dominant in the low frequency region and in long-time polarisation current. Mostly, polarisation of solid materials is a collection of different relaxation mechanisms such as dipole polarisation, Maxwell-Wagner polarisation and quasi-DC conduction (q-dc). Overlapping of different polarisation and conduction processes, results in difficulty in interpretation of raw dielectric response data. In such situations, to discriminate and quantitatively analyse the contribution of conduction and different polarisation phenomena to dielectric response, several mathematical models namely Debye, Cole-Cole, Havariliak–Negami, Jonscher's Universal law and Dissado and Hill's (DH) cluster theory are generally used. However, the majority of these models are suitable only for analytical representation of experimental spectra.

This chapter briefly reviews the different types of dielectric response modelling techniques and their suitability for representing dielectric spectra of oil impregnated pressboard insulation. An equivalent circuit is proposed based on DH cluster framework theory to model the frequency domain dielectric response data of oil impregnated pressboard insulation. In order to derive this circuit, the physics of microscopic level charge transport and polarisation processes that can arise in

oil impregnated pressboard insulation are considered. Moreover, the applicability of the proposed circuit is validated in this chapter. In the case of time domain data modelling, the suitability of extended Debye model and Williams-Watts exponential decay function for interpreting depolarisation current response data is discussed. The content of this chapter is mainly based on two publications of the author [218, 219].

6.2 Modelling the Frequency Domain Dielectric Response Data

6.2.1 Loss peak behaviour

Loss peak is a common phenomenon that appears in frequency domain dielectric spectra of both solid and liquid materials. Debye deduced the first physical interpretation in 1945 for explaining this phenomenon in such a way that relaxation of assembly of non-interacting ideal dipoles in gases and liquid media results in loss peak behaviour in dielectric loss part $\varepsilon''(\omega)$ [220, 221]. A change of complex susceptibility $\chi\,(\omega)$ of a system due to a Debye type relaxation can be characterised using eq (6.1). It can be seen in Figure 6.1 that the Debye model can only be utilised to represent unique symmetrical loss peak behaviour.

$$\chi(\omega) = \frac{1}{1 + \dfrac{i\omega}{\omega_p}} \qquad (6.1)$$

Where, ω_p denotes the angular frequency at which maximum loss occur.
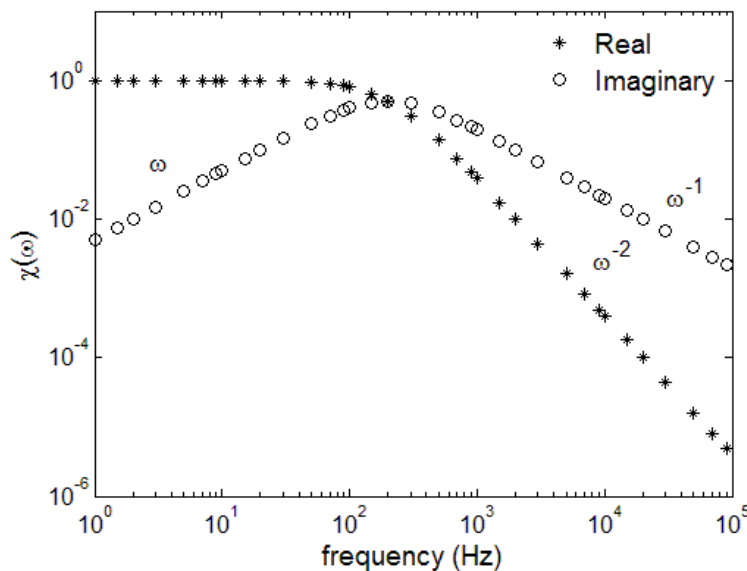
Figure 6.1. Frequency dependency of Debye response

It has been reported in the literature that ideal Debye behaviour can hardly be found in almost all solid and liquid matters because assembly of non-interacting dipoles is idealistic in nature [220-

222]. Therefore, the concept of distribution of relaxation time (DRT) was introduced in order to represent non-Debye behaviour. In this case, contributions from an ensemble of non-interacting dipoles to total relaxation occur in parallel leading to a continuous distribution of dipole relaxation time. However, this is also a physically impractical concept because of the inevitability of intermolecular interactions, particularly in solid phase materials [223]. In the case of pressboard insulation, molecular level dipoles such as hydroxyl and alcohol groups are strongly bonded to each other by intra and intermolecular hydrogen bonds. Thereby, straight forward application of both Debye and DTR concepts for interpretation of polarisation phenomena in oil impregnated pressboard insulation is not plausible.

A broad class of materials including polymer composite, porous materials, colloids and aqueous solutions possess symmetrical broader loss peak behaviour which can be characterised by Cole-Cole (CC) relaxation function given in eq (6.2) [224]. The exponent α ($0 < \alpha \leq 1$) of the CC function determines the degree of broadening of loss peak. Asymptotic behaviour of CC function follows relationships of $\chi'(\omega) \propto \chi''(\omega) \propto \omega^{\alpha-1}$ and $\chi''(\omega) \propto \omega^{1-\alpha}$ in high and low frequency parts of symmetrical loss peak as shown in Figure 6.2(a). Haveriliak-Negami (HN) relaxation function given in eq (6.3) has a kind of universality being applicable for representing both symmetrical and asymmetrical loss peak behaviours appearing in dielectric response of a wide range of materials. Asymptotical behaviour of HN function in the low frequency side of loss peak is similar to CC model whilst susceptibility in the high frequency side obeys the relationship of $\chi'(\omega) \propto \chi''(\omega) \propto \omega^{-\beta(1-\alpha)}$. The exponent β is a parameter in the range 0-1.

$$\chi(\omega) = \frac{1}{1+\left(\dfrac{i\omega}{\omega_p}\right)^{1-\alpha}}$$ (6.2)

$$\chi(\omega) = \frac{1}{\left[1+\left(\dfrac{i\omega}{\omega_p}\right)^{1-\alpha}\right]^{\beta}}$$ (6.3)

Udo et al [225] and Alexander et al [224] have provided a physical interpretation of CC behaviour in a framework of complex system theory. They propose that CC behaviour can be expected when relaxation times corresponding to the motion of electric dipoles interacting with their surrounding matrices possess fractal nature. Moreover, the broadening parameter α indicates the rate of interactions of dipole relaxation units with their surroundings. Nivikov et al [226] have deduced a physical interpretation for CC relaxation considering the morphological properties of

inhomogeneous media. They have proposed that a series of successive relaxation events of different relaxation times in an inhomogeneous medium due to a presence of self-similar fractal ensemble of polarisable entities produces either CC or Haveriliak-Negami type loss peak behaviour. In this regime, it has been assumed that a sequence of relaxation processes starts from the lowest level of self-similarity.
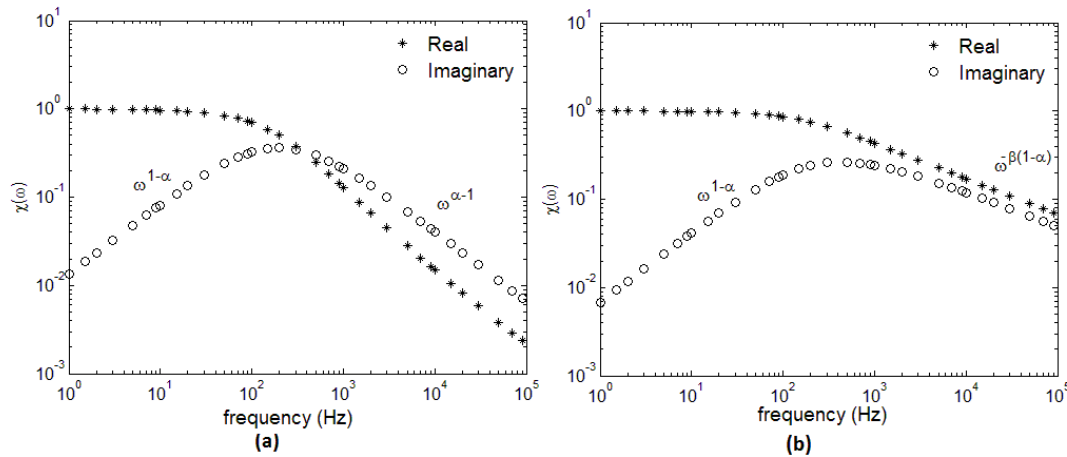
Figure 6.2. Frequency dependency of (a) Cole-Cole response, (b) Havariliak-Negami susceptibility function

This research proposes that matrices of oil filled cavities in pressboard insulation could possess self-similar fractal hierarchical structure on average as shown in Figure 6.3. Moreover, charges blocking at the wall of oil cavities at different size scale of fractal hierarchy under an electric field can be assigned to a sequence of interacting relaxation processes with different relaxation times. Moreover, the relaxation times could also have a hierarchical fractal nature similar to geometry and relaxation starts from the smallest set of cavities. According to Nivikov et al [226], this type of hierarchical relaxation process should lead to a CC or HN relaxation behaviour. However, more details about the microscopic geometry of pressboard insulation are required to confirm whether this type of relaxation exists in the frequency band of our interest (10^{-4}-10^3 Hz) [227].

Chandima et al [127, 138] have observed that there is a loss peak in FDS of oil impregnated pressboard insulation in the frequency range 10^{-4}-10^3 Hz. Moreover, HN relaxation function has been successfully utilised to analyse this behaviour. However, they have not deduced a clear physical interpretation to correlate HN type relaxation and physical properties of oil impregnated pressboard. This research hypothesis that proposed an oil cavity based relaxation process would account for observed loss peak behaviour.
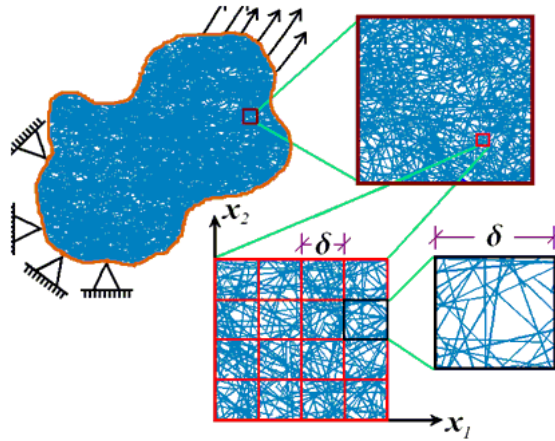
Figure 6.3 Possible self-similar structural organisation in a large network of random fibre [228]

6.2.2 Universal relaxation law

Jonscher has proposed that there are fundamentally two broad classes of dielectric response behaviours, namely loss peak and low frequency dispersion (LFD) which are associated with relaxation of dipolar and charge carrier systems respectively [220]. LFD is a phenomenon which gives steep rise to both real and imaginary susceptibility in the low frequency region as shown in Figure 6.4 (b). Jonscher has first identified a remarkable similarity in both loss peak and LFD behaviours of diverse materials and an electro-chemical process in that they follow fractional power of frequency dependence [113].
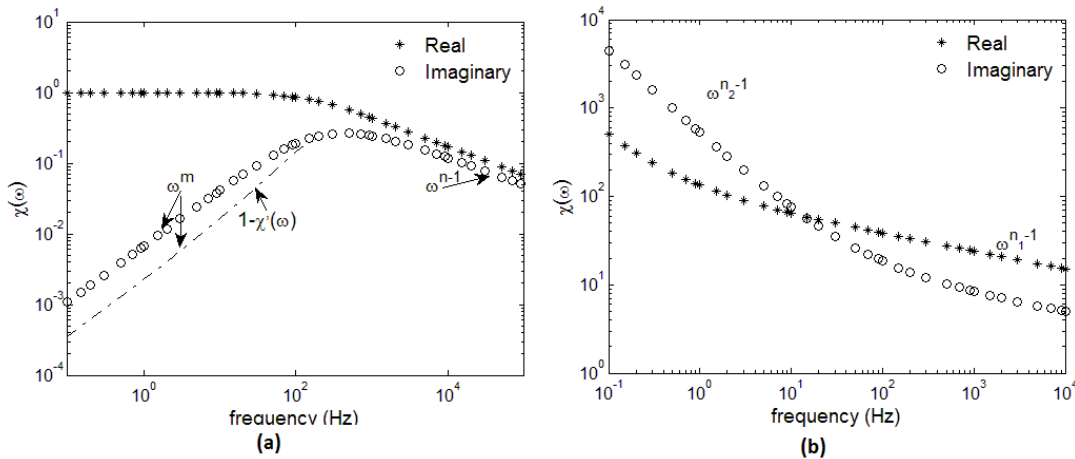
Figure 6.4. Universal behaviour of frequency dependence of dielectric response (a) Loss peak, (b) LFD effect

As appears in Figure 6.4 (a) real and imaginary susceptibilities corresponding to loss peak relaxation obey the fractional power law relationships given in eqns (6.4) and (6.5) at above and below the loss peak frequency ω_p [113] respectively.

$$\chi'(\omega) \propto \chi''(\omega) \propto \omega^{n-1} \qquad (6.4)$$

$$\left[\chi(0) - \chi'(\omega)\right] \propto \chi''(\omega) \propto \omega^m \tag{6.5}$$

Where n and m are parameters which characterise the shape of loss peak and both are in the range 0-1. Thereby, all types of loss peak responses including Debye, CC and HN can be analysed using eqns (6.4) and (6.5) due to their universality [221].

LFD behaviour is always accompanied by two dispersive regions as shown in Figure 6.4 (b) in such a way that susceptibility obeys the relationship given in eq (6.6) at above and below the characteristic frequency ω_c. The values of n_1 and n_2 are in the range 0-1 and they always possess the relationship $n_1 > n_2$. Jonscher assumes that the whole LFD behaviour is a result of two concurrent polarisation processes. Thereby, LFD effect can be mathematically represented by an addition of two different fractional power laws. The exponent of fractional power laws possesses values of n_1-1 and n_2-1.

$$\begin{aligned} \chi'(\omega) \propto \chi''(\omega) \propto \omega^{n_1 - 1} &\Rightarrow \omega \geq \omega_c \\ \chi'(\omega) \propto \chi''(\omega) \propto \omega^{n_2 - 1} &\Rightarrow \omega < \omega_c \end{aligned} \tag{6.6}$$

Susceptibility models explained in eqns (6.4) to (6.6) have a similar form of frequency dependence and thereby, Jonscher has named this characteristic as a "universal" form of dielectric response. Jonscher has claimed that if loss-to-stored energy for a microscopic polarisation in a system is independent of frequency, the dielectric response of the system obeys universal law. It means that values of indexes n, m, n_1, n_2 are determined by the constant ratio of loss-to-stored energy.

Jonscher has deduced a generalised physical interpretation for loss peak behaviour based on the theory of DH many-body interactions. He has hypothesised that two different types of sequential configurational tunnelling transitions namely flip and flip-flop lead to a loss peak behaviour in a system with an ensemble of dipole entities [222]. It means numbers of interacting particles undergo small displacements in which collective effects equals to a single large transition. One can claim that this general interpretation is also valid for oil cavity based loss peak relaxation in pressboard insulation.

Jonscher has suggested that dielectric materials with large densities of low-mobility charge carriers, hopping carrier systems and fast ion conductors show strong LFD effect. This is caused by the giant polarizabilities produced by transport of hopping electrons or ions in random paths over a longer distance [110, 220, 229]. Application of this interpretation for oil impregnated pressboard insulation is plausible because charge transport over a long distance in pressboard insulation at low frequencies mainly occurs via random percolation paths of water molecules. Due to existence of

dead ends of charge percolation paths, giant polarizability could be expected in pressboard insulation at low frequencies. It means oil impregnated pressboard insulation shows strong LFD and an increase of moisture could intensify this effect. However, the use of Jonscher's universal relaxation law in modelling dielectric response data is hampered by two factors. No single function has been defined to characterise LFD and loss peak behaviour in corresponding frequency bands. In addition, there is no clear physical explanation for nature of relaxation corresponding to LFD phenomenon at above and below characteristic frequency ω_c.

Dissado has derived physical interpretation for universal type dielectric response of biological systems based on their structural organisation. He has identified that [227], most of the biological systems are composed of self-similar hierarchal structures on average such that small structural units with their own dielectric responses are embedded in larger units which are themselves embedded in even larger units [227]. The dielectric susceptibility of such material can be characterised by a series of fractional power law similar to eq (6.4). The exponent factor n of such systems is mainly determined by the fractal dimension (d_f) of the self-similar unit. Figure 6.5 (a) shows a self-similar hierarchical structure with fractal dimension d_f equal to 1.77 (Personal communication with L. Dissado). In this way, dielectric response of different sizes of geometry domains has different power law regions in the whole response and they are separated by a plateau. Thus, the overall response can be divided into so-called γ, β and α type relaxation processes which individually obey the universal power law proposed by Jonscher.

(a)   (b)
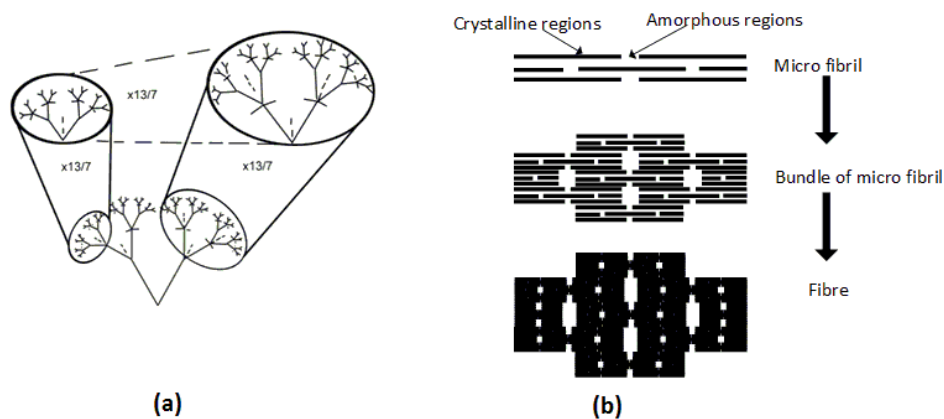
Figure 6.5 (a) Example for self-similar hierarchy, (b) Possible self-similar hierarchy in PB [230]

As shown in Figure 6.5 (b), bundling of microfibrils by layer to layer van der Waals and side to side hydrogen bonds produces macro fibril. Cellulose fibres are produced in a similar way by bundling of macro fibrils. It is illustrated in Figure 6.5 (b) that amorphous regions in pressboard insulation possess self-similar hierarchical fractal geometry similar to the biological systems. In addition,

dipolar molecules such as water and acids produced by ageing reside mainly in amorphous regions due to their high permeability. Thus, one can assume that relaxation of dipolar entities enclosed in amorphous domains with hierarchical fractal geometry could result in a plateau in dielectric response of oil impregnated pressboard insulation. Moreover, the dielectric response obeys the relationship given in eq (6.4) at above the plateau frequency (frequency of loss peak). This interpretation can also be assigned to loss peak observed by Chandima et al [127, 138] in the FDS of oil impregnated pressboard.

6.2.3 DH cluster model

Though, Jonscher's universal law is applicable for representing any form of dielectric response data, it does not enable any physical interpretation for dielectric response data with respect to physicochemical properties of polymeric solids. However, physical interpretation for dielectric response behaviour of a wide range of materials can be derived based on DH cluster theory.

DH cluster theory is a linear dielectric response theory, which describes the two distinct classes of relaxation processes associated with bound charge dipole clusters and potentially mobile charge clusters [118, 231, 232]. The first category describes a cooperative motion (relaxation) of molecular dipoles within a constrained geometrical domain called a cluster followed by the interactive motion between neighbouring clusters. In this regime, displacement of a group of correlated dipoles in a cluster as a cooperated entity is called intra-cluster motion (above the characteristic frequency ω_m). When the frequency of the applied field is less than ω_m, motion of some portion of dipoles sites in a cluster can either correlate with dipole sites of neighbouring clusters or disconnect from them and produce new clusters. This phenomenon is known as inter-cluster motion. This type of intra and inter-cluster dipole relaxation leads to a loss peak in frequency domain. The complex susceptibility of such a relaxation can be described in terms of the Gaussian hyper-geometric function, as in eqns (6.7)- (6.9) [232, 233].

$$\chi^*(\omega) = \chi_0 \frac{\Gamma(1-m)}{m} F(\omega / \omega_p) \tag{6.7}$$

$$\begin{aligned} F(\omega / \omega_m) = F_0^{-1} \left(\omega_m / (\omega_m + i\omega) \right)^{1-n} \times \\ {}_2F_1 \left(1-n, 1-m; 2-n; \omega_m / (\omega_m + i\omega) \right) \end{aligned} \tag{6.8}$$

$$F_0 = \Gamma(2-n)\Gamma(m) / \Gamma(1+m-n) \tag{6.9}$$

Here, $\Gamma(x)$ symbolises the gamma function and ${}_2F_1$ denotes the Gaussian hyper-Geometric function. The amplitude factor χ_0 represents the strength of dipole concentration in a microscopic cluster.

Figure 6.6 shows the changing of complex susceptibility for DH loss peak function. Moreover, it is illustrated in Figure 6.6 that the maximum of loss peak and the rise of real susceptibility linearly increases with dipole strength of the local cluster (χ_0). Parameters m and n remain in a range of 0 to 1 and decide the shape of the loss peak below and above the characteristic frequency respectively. The asymptotical behaviour of equation (6.7) possesses the fractional power law frequency dependence as:

$$\chi'(\omega) \propto \chi''(\omega) \propto \omega^{n-1} \qquad for \quad \omega > \omega_m \qquad (6.10)$$

$$\chi'(0) - \chi'(\omega) \propto \chi''(\omega) \propto \omega^{m} \; for \quad \omega < \omega_m \qquad (6.11)$$

DH loss peak function (6.7) covers a wide range of relaxation phenomena formerly explained with so-called Debye, CC, Davidson-Cole and HN relaxation functions. Moreover, its asymptotical behaviour obeys Jonscher's universal law.
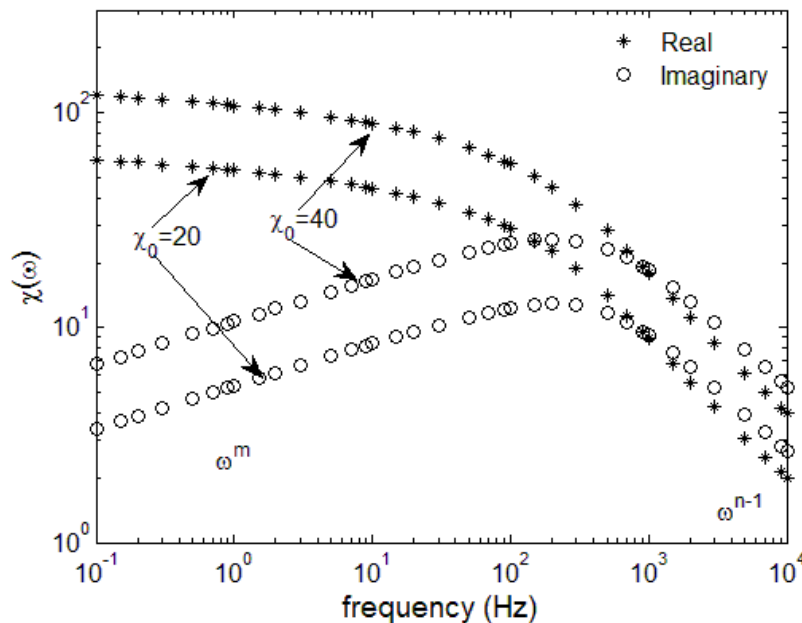
Figure 6.6. Susceptibility vs. frequency for DH loss peak function

The dielectric susceptibilities of a wide range of materials, which are heterogeneous on a microscopic scale in nature such as rock, ceramic, humid cellulose and humid sand largely disperse at low frequencies [115, 118, 229]. This phenomenon is called Quasi-DC (q-dc) conduction by Dissado and Hill. They have proposed that q-dc effect can be expected in a system, when it comprises a matrix of clusters containing ions or ionisable entities. Moreover, effective charge transport between clusters through structured paths is a necessary condition of q-dc effect. In such systems, a transported charge and its counter charge behave as an effective dipole. It provides a

large dipole moment leading to a sharp increase in both real and imaginary susceptibilities at low frequencies. When a system holds q-dc behaviour, frequency dependent susceptibility can be described by eqns (6.12)- (6.14) [234].

$$\chi^*(\omega) = \chi_0 F(\omega / \omega_c) \tag{6.12}$$

$$F(\omega / \omega_c) = F'^{-1}_0 \left(\omega_c / (\omega_c + i\omega)\right)^{1-n2} \times {}_2F_1\left(1-n_2, 1+p; 2-n_2; \omega_c / (\omega c + i\omega)\right) \tag{6.13}$$

$$F'_0 = \Gamma(2-n_2)\Gamma(1-p)\left(\frac{p+n2-1}{p\Gamma(2-n_2-p)}\right) \tag{6.14}$$

Herein, ω_c is the characteristic frequency. Charge carriers in clusters are bound together and give weak dispersion at above the characteristic frequency (ω_c). Charge carriers become free to move along the structured path to a finite distance below the characteristic frequency. It leads to a large dispersion in susceptibility. The power law exponent $n2$ ($0.5 < n_2 < 1$) reflects the binding motion of charges within a cluster when the frequency of applied field is greater than ω_c, At the time equal to (ω_c^{-1}), charge carriers start to move independently from their counter charges along a structured path. This relaxation process is characterised by the exponent factor p, which typically is in the range between 0.5 and unity. Here, charge transport within a cluster is known as intra-cluster transport and that between clusters is denoted as inter-cluster motion. The q-dc relaxation function possesses asymptotical behaviour above and below the characteristic frequency as:

$$\chi'(\omega) \propto \chi''(\omega) \propto \omega^{n2-1} \quad for \quad \omega > \omega_c \tag{6.15}$$

$$\chi'(\omega) \propto \chi''(\omega) \propto \omega^{-p} \quad for \quad \omega < \omega_c \tag{6.16}$$

Though, asymptotical behaviour of DH q-dc effect and Jonscher's universal law of LFD behaviour is similar; there is a fundamental difference between their concepts. Dissado and Hill have considered that intra and inter cluster charge transitions as two sequential processes whilst Jonscher has treated them as parallel processes.

6.2.4 Cluster structure in oil impregnated pressboard insulation

In this research DH cluster theory is used for modelling the frequency domain dielectric response of oil impregnated pressboard. Thus, it is required to identify the possible charge cluster structure in the system. In order that microscopic morphology and hygroscopic behaviour of pressboard insulation are considered.

Pressboards are semi-crystalline materials with highly ordered crystalline and disordered amorphous regions as shown in Figure 6.5 (b). The array of hydroxyl (HO⁻) groups in cellulose polymers are considered as potential moisture absorbent sites. The majority of absorbed water resides in amorphous regions in pressboard such as spherulite and lamellar surfaces [115]. It may be partly due to the fact that microscopic pores in paper structures are mainly associated with amorphous regions. In addition, greater permeability of amorphous regions allows more penetration of water and low molecular acids too.
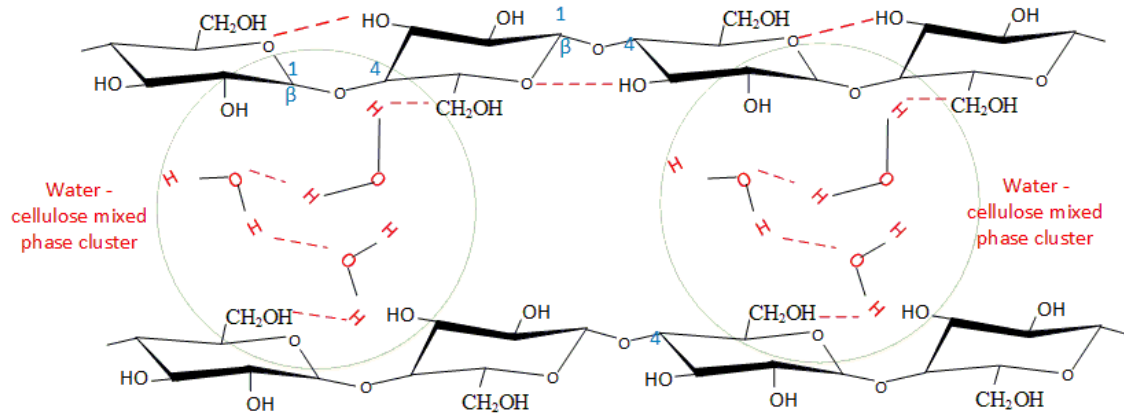
Figure 6.7. Cluster of water cellulose mixed phase in PB insulation

It is accepted that the absorbed moisture in cellulose materials is in the form of clusters [186]. Water clusters are bonded to nearby hydroxyl groups in cellulose through hydrogen bonds. Therefore, it can be considered that amorphous regions in cellulose pressboard insulation are clusters of hydrogen bonding polar molecular groups. Here we present it as a cluster of water-cellulose mixed phase. Since the carbon-6 hydroxyl (6-OH) is the most exposed hydroxyl group in the cellulose polymer, the possible way of forming a cluster of hydrogen-bonds can be represented as Figure 6.7. When the amorphous regions absorb water, the inter-molecular hydrogen bonds in cellulose polymer chains are broken; consequently distances between polymer chains are increased. This causes to decrease the crystallinity of cellulose pressboard insulation by surrounding crystalline areas becoming more amorphous. Subsequently, this phenomenon increases the size of the water-cellulose mixed phase clusters. Eventually, this type of cluster organisation leads to a loss peak at high frequencies due to cooperating microscopic motion of cluster dipoles. It is termed as flip and flip-flop transitions in the concept of the many-body interaction theory [222]. Herein, flip and flip-flop transitions determine the high and low-frequency side of the loss peak.

As a result of water clusters formed at the interface between amorphous and crystalline regions, existence of q-dc behaviour in dielectric response of pressboard material is obvious. In this case,

proton hopping between and within the water oriented charge clusters is the primary mechanism which determines the q-dc behaviour. When hopping distance is less than the cluster correlation length, charge displacement occurs within a cluster following an ion hop (intra cluster motion). This results in changing the centre of motion of all ions within the cluster and produces a cluster dipole which thereby becomes a polarised cooperate entity. This mechanism characterises the q-dc behaviour above the characteristic frequency. When the frequency of the applied field is less than ω_c, proton hopping between clusters cannot be avoided. It occurs through a percolation network of water molecules and hydroxyl groups along the cellulose fibre wall. This is termed as inter cluster hopping and this mechanism determines the dominant q-dc behaviour below the characteristic frequency.

On the other hand, cellulose pressboard insulation contains a matrix of three-dimensional microscopic pores (cavities). As a result of the vacuumed impregnation process, microscopic pores in the pressboard are completely filled with oil. These oil filled cavities can be considered as clusters of electrical charges dipole because oil is a source of ionic impurities. They are physically interconnected via narrow three-dimensional oil filled channels. The cross sectional area of the channels decreases with an increase of distance because cellulose fibres in high-density pressboard are packed very tightly. These oil channels are considered as conducting paths and thereby, the whole system is an ensemble of charge clusters interconnected by weakly conducting paths in a three-dimensional grid. The dielectric response measurement of such systems at low frequencies results in a blocking of the transport of charges at the wall of the cavity leading to a loss peak (interfacial polarisation). Further lowering of the frequency allows the separating of charges over longer distance via the oil filled channel or charge hopping along the cellulose fibre wall. Before a charge can escape from a cluster, it walks along the cavity wall finding a path to escape from the cluster. The latter two processes represent the inter and intra cluster charge transport of so-called q-dc effect. The combined charge transport processes related to oil filled cavities could also lead to loss peak and q-dc behaviour in FDS of oil impregnated pressboard insulation.

6.2.5 Equivalent circuit for modelling the FDS of pressboard insulation

The above mentioned cluster based charge transport and polarisation phenomena in oil impregnated pressboard insulation leads us to propose an equivalent circuit, as shown in Figure 6.8, for modelling the frequency domain dielectric response data of oil impregnated pressboard insulation. This circuit is somewhat similar to that of [114] and has the dispersive capacitive elements of DH-q-dc and DH loss peak. In the proposed circuit, these two capacitive elements are in series because DH loss peak and q-dc processes behave sequentially.
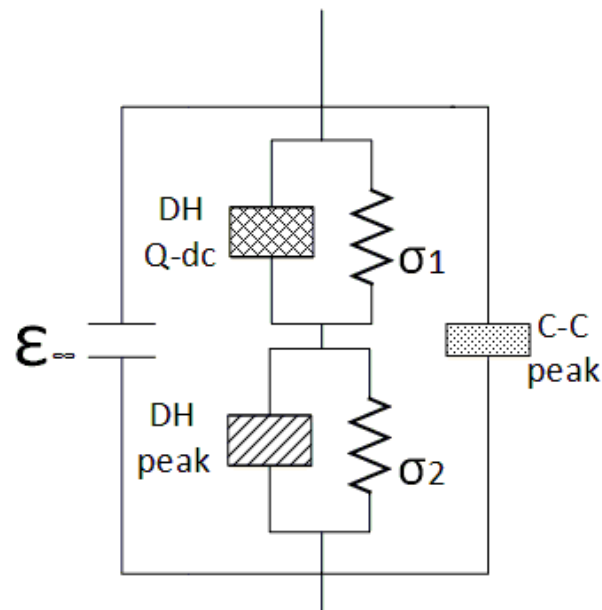
Figure 6.8. Proposed equivalent circuit to represent FDS of oil impregnated PB insulation

However, here we have treated the high frequency permittivity (ε_∞) which represents the strength of dielectric polarisation taking places at high frequencies as an independent element. Thereby, element ε_∞ is in parallel to both loss peak and q-dc elements. In early studies, it has been reported that there is a loss peak at high frequency region due to the segmental vibration of cellulose chains (β relaxation) [235-237]. This loss peak behaviour shows a significant influence on loss part of dielectric response of oil impregnated pressboard insulation in the frequency range 10^1-10^3 Hz, particularly for samples with low moisture content. Nilanga et al [238] have identified that this behaviour can be accurately represented with CC function. Thereby, the C-C peak element in the proposed circuit stands for the β relaxation process. It remains as a parallel element in the equivalent circuit because β relaxation process has a different physical origin compared to DH loss peak and q-dc mechanism.

In this case, σ_2 denotes the short range ions transport mechanism constrained to the small geometrical domains. When the frequency is lowered, charges start to transport over progressively larger distances. However, effective charge transport at low frequencies is very low because the number of effective paths available decreases when the distance becomes longer [118]. In an ideal situation, where a system is below the critical percolation limit, there is no charge transport route across the sample and it yields zero DC conductivity. However, a sample of finite size may have some routes across the sample and show weak DC conductivity. It means that, σ_1 has a finite value since the effective DC conductivity is ($1/(\sigma_1^{-1}+\sigma_2^{-1})$). Moreover, σ_1 is always a much lower value than σ_2.

$$\varepsilon(\omega) = \frac{\left(\varepsilon(\omega)_{loss\_peak} + \dfrac{\sigma_2}{j\omega\varepsilon_0}\right)\left(\varepsilon(\omega)_{q-dc} + \dfrac{\sigma_1}{j\omega\varepsilon_0}\right)}{\varepsilon(\omega)_{loss\_peak} + \varepsilon(\omega)_{q-dc} + \dfrac{\sigma_1}{j\omega\varepsilon_0} + \dfrac{\sigma_2}{j\omega\varepsilon_0}} + \varepsilon(\omega)_{c-c} + \varepsilon_{\infty} \tag{6.17}$$

According to the proposed circuit configuration, the high frequency dispersive behaviour of dielectric response of the pressboard insulation is characterised by the parallel combination of the DH-peak capacitor, σ_2 conductive elements and CC loss peak component. The low frequency behaviour is determined by the parallel arrangement of DH q-dc capacitive element and effective DC conductivity. Eq (6.17) describes the frequency domain response of the proposed equivalent circuit.

6.2.6 Validation of proposed equivalent circuit

In this section, applicability of a proposed equivalent circuit for modelling the FDS data of oil impregnated pressboard insulation is validated. For modelling purposes, the hypergeometric functions correspond to DH loss peak and q-dc capacitive elements are defined in the form of eq (6.18) which converges quicker than the general form. Parameters for the proposed equivalent circuit model have been derived using a MATLAB based optimization routine.

$$F(a,b,c;z) = (1-z)^{-a} F\left(a, c-b, c; \frac{z}{z-1}\right) \tag{6.18}$$
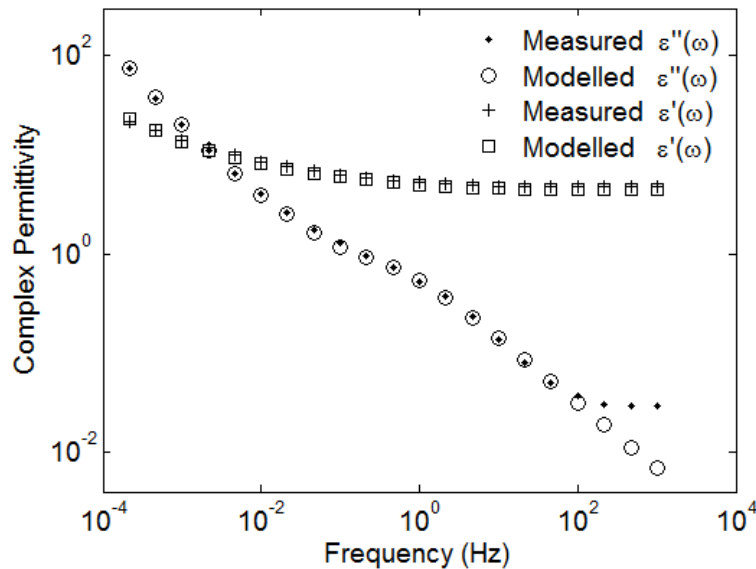
Figure 6.9. Measured and modelled FDS of mineral oil impregnated PB with 1.6% of moisture

It can clearly be seen in Figure 6.9 that measured FDS of mineral oil impregnated pressboard sample with 1.6% of moisture content accurately fits with the modelled response using the proposed equivalent circuit. The corresponding model parameters are shown in Table 6.1. However, the

modelled response slightly deviates from observed loss component of the measured response at the high end of the frequency window. It is due to the fact that this study has not selected the parameters of C-C component, because FDS data does not represent the complete CC relaxation. Thus, one can claim that the proposed equivalent circuit model can be used for explaining dielectric response behaviour of oil impregnated pressboard insulation. However, validity of the proposed model for pressboard insulation impregnated with different types of oils at different degrees of humidity will be investigated in Chapter 7. Moreover, the impact of moisture and diverse oil properties on conduction and polarisation effects in oil impregnated pressboard insulation will also be explained by using equivalent circuit model parameters in the next chapter.

Table 6.1 Equivalent circuit parameters for FDS of mineral oil impregnated PB with 1.6% of moisture

DH loss peak				DH q-dc					σ_1 pS/m	σ_2 pS/m
X_p	ω_p	n_1	m	X_{qdc}	ω_c	n_2	p	ε_∞		
1.05	0.30	0.35	0.1	3.8	0.2	0.90	0.55	5.2	0.08	0.9

6.3 Modelling the Time Domain Dielectric Response

6.3.1 Selecting an appropriate modelling technique

In time domain modelling, the response of the dielectric medium to specified electric excitation is mainly identified using measured depolarisation current (discharge current) [110]. Debye model in the form of eq (6.19) is the most fundamental approach to represent the time domain dielectric response data. However, as mentioned in section 6.2, Debye form of dielectric response function can be hardly found in almost all the solid materials. Curie-von Scweidler model expressed in eq (6.20) shows a satisfactory fitting curve with most of the dielectric response data of a wide range of materials with different exponent values of n for specific time ranges [117]. However, no interpretation has yet been derived for correlating Curie-von Scweidler model parameters to properties of the physical system.

$$f(t) \propto \exp\left(\frac{-t}{\tau}\right)(1/s) \tag{6.19}$$

$$f(t) \propto t^{-n} \ (1/s) \tag{6.20}$$

$$f(t) \propto \frac{1}{(t/\tau)^m + (t/\tau)^n}(1/s) \ where \ 0 < m < 1, 0 < n < 2 \tag{6.21}$$
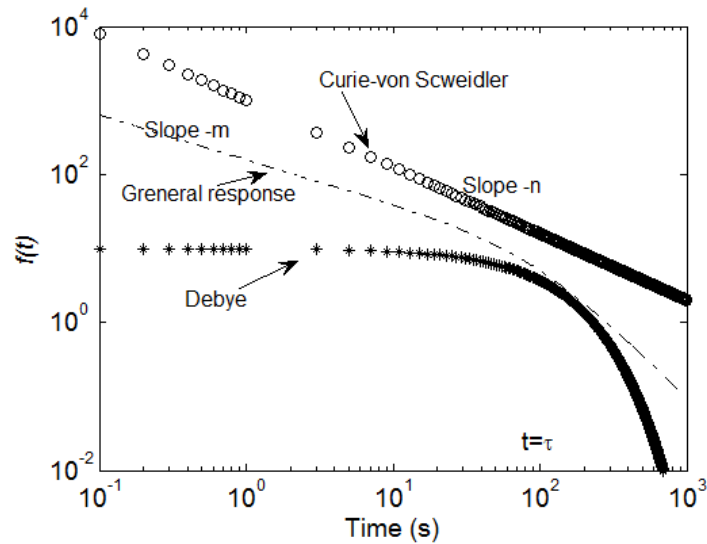
Figure 6.10. Time domain behaviour of different types of dielectric response function

General response model given in eq (6.21) characterises two different process transitions at time $t=\tau$ which gives a logarithm slope of $-m$ and $-n$ below and above τ to discharge current. The asymptotical behaviour of general response indicates universality of time domain response in a way similar to frequency domain loss peak response. Jonscher has identified that exponent n possesses relationship of $1<n<2$ for a dipolar system which possesses loss peak in frequency domain [110]. On the other hand, n possesses a value of less than 1 and obeys relationship $n < m$ for carrier dominant systems which shows LFD behaviour in frequency domain response. Thereby, the general shape of the discharge current should resemble Figure 6.11.
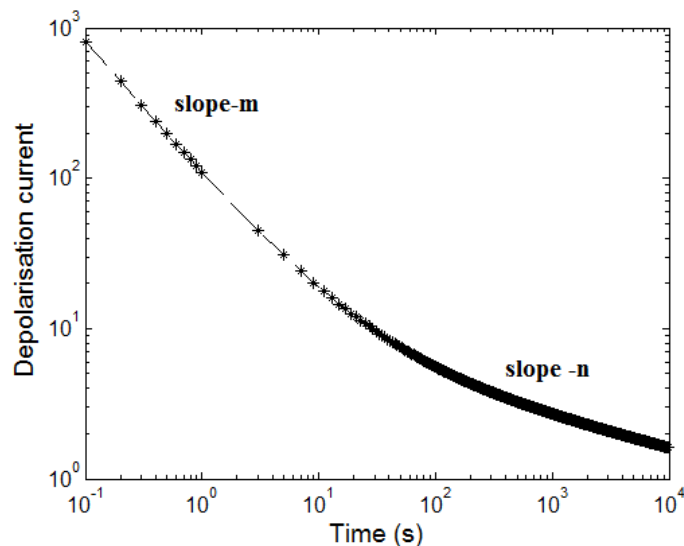
Figure 6.11. General shape of depolarisation current response of carrier dominant system

Oil impregnated pressboard, particularly with high moisture content can be considered as a carrier dominant system. Thus, the measured depolarisation current response should have a general shape

as shown in Figure 6.11. Though, oil impregnated pressboard insulation shows a strong LFD behaviour in frequency domain, the measured depolarisation current response data presented in the literature markedly deviates from the expected shape [130, 134, 219]. Moreover, their trends look like loss peak behaviour which can be explained with a general response model with $1 < n < 2$. This is due to the fact that depolarisation current characterises the true dielectric response function of a material only up to one tenth of charging time [110]. Thereby, the general shape of long time depolarisation current response deviates from the expected shape. In this way, the general response model is not suitable for interpreting the depolarisation current response of oil impregnated pressboard insulation.

Several studies have reported that dielectric response function of oil impregnated paper insulation can be modelled with a series of concurrent Debye relaxation processes with different time constants as given in eq (6.22). This approach is known as extended Debye model [132, 134, 239].

$$f(t) = \sum_{1}^{n} \left(A_i * e^{(-t/\tau_i)} \right) (1/s) \tag{6.22}$$

Here, τ_i is the time constant of ith relaxation and A_i is the corresponding pre-exponential factor. Consequently, PDC response can be modelled with a simple RC equivalent circuit (Figure 3.8), where parallel branches each containing a series connection of a resistor and a capacitor denotes exponential relaxation current components with different relaxation time constants. The parameters τ_i and A_i can be correlated to R and C values of the equivalent circuit using eqns (6.23) and (6.24).

$$\tau_i = R_i C_i \tag{6.23}$$

$$A_i = \frac{(1 - e^{-t_c/\tau_i})}{R_i} \tag{6.24}$$

Saha et al [132] have identified the physical significance of the Debye form of relaxation process in oil impregnated pressboard insulation with respect to the chemical structure of cellulose. According to Saha all polar groups in cellulose polymers can have a different configuration of neighbouring molecules. Thus, the response time of the polar groups after the application of an electric field may differ from one to another leading to a series of Debye relaxation processes [132]. However, non-interacting relaxation of different polar groups can hardly be seen in solid material like pressboard. Thus, this research proposes new philosophy to characterise the extended Debye type relaxation processes in pressboard insulation from the perspective of hierarchical semi crystalline structural organisation of cellulose.

Cellulose has organisational hierarchy under a microscopic view as shown in Figure 6.5 (b), i.e. small elementary fibrils are embedded within larger units called bundles, which are themselves embedded in even larger units called fibres. Ultimately, layers of fibres are embedded in cellulose paper and layers of cellulose paper embedded in pressboard. Therefore, one can assume that the separation of ions resides in amorphous regions due to an external electric field charging the crystalline amorphous interfaces at different levels of the organisational hierarchy. Dipoles induced by charging of crystalline surfaces physically separated by crystalline regions. Thereby, relaxation of such dipoles can be considered as non-interaction type dipole moment. This behaviour results in a series of Debye relaxation processes and their time constants are decided by the size scale of geometrical hierarchy. It suggests that charge separation in a coarse level of geometry such as in fibre and paper layer has large time constants. Moreover, separation of charge over long distance is difficult as the number of charge transport paths decreases with distance. Electrically this behaviour can be modelled by selecting a high resistance value for the R-C branches, which possess high relaxation time constants. Therefore, this research proposes that extended Debye approach is a good way to characterise the depolarisation current behaviour of oil impregnated pressboard insulation.

It has been reported that dielectric response function of a wide range of polymeric and glass substances obey the Williams-Watts polarisation stretch exponential decay function given in eq (6.25). Thereby, it is known as a "universal" model of dielectric response function.

$$f(t) \propto \exp\left[\left(-\frac{t}{\tau}\right)^{\gamma}\right](1/s) \tag{6.25}$$

Where γ is a constant in the range 0-1 and τ is the time constant of the particular relaxation process. Michel et al [240] have assumed that there are wide varieties of polar groups in polymer molecules and their dipole moments remain frozen as the field is removed. Moreover, they have hypothesised that there are mobile defects in the system and a dipole is relaxed once a defect reaches a frozen dipole site. Here, diffusion of defects towards dipole sites is executed as a continuous time random walk. When a system has this type of dipole relaxation behaviour, its dielectric response function obeys Williams-Watts relaxation law.

In the case of oil impregnated pressboard insulation, transport of charge mainly occurs along a percolation network of water molecules in a random manner. In the presence of an electric field, charges can accumulate at the dead ends of percolation paths (mostly crystalline surfaces) and acts as an ensemble of large dipoles [116]. Once the electric field is removed, these temporary dipoles are relaxing and contribute to depolarisation current. The relaxation process also occurs by charge

hopping along random paths in a way similar to defect movement described by Michel [240]. Thus, one can also assume that Williams-Watts function could be suitable for representing depolarisation current response data of oil impregnated pressboard insulation. Thus, this research proposed eq (6.26) to represent the depolarisation current of oil impregnated pressboard insulation. The Debye component in eq (6.26) represents the microscopic interfacial polarisation phenomenon in oil filled cavities. The contribution of Debye component may be significant only for samples with low moisture contents.

$$I_{depol}(t) = A_w \exp\left(-\frac{t}{\tau_w}\right)^{\gamma} + A_{db} \exp\left(-\frac{t}{\tau_{db}}\right) \tag{6.26}$$

Where A_w and A_{db} represent the magnitude factors and τ_w and τ_{db} denote the time constant of Williams-Watts and Debye relaxation processes respectively.

6.3.2 Validation of applicability extended Debye model and William –Watts function.

It can be seen in Figure 6.12 (a) that depolarisation current response of mineral oil impregnated pressboard insulation can be equivalent to five different Debye relaxation processes. The corresponding R and C model parameters can be found in Figure 6.12 (a).
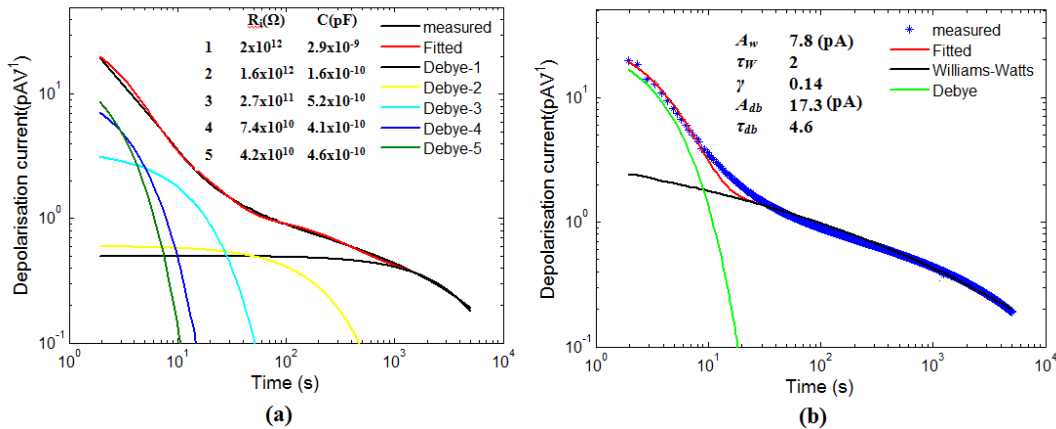
Figure 6.12. Comparison of modelled and measured depolarisation current of mineral oil impregnated PB at 2.4% of moisture (a) Extended Debye method (b) Williams-Watt function

As shown in Figure 6.12(b), one can claim that Williams-Watts function based model defined in eq (6.26) also represents the measured depolarisation current of the sample with reasonable accuracy. It means that both extended Debye and Williams-Watts function based models can be used to interpret the time domain dielectric response data of oil impregnated pressboard insulation. However, applicability of these techniques for different types of oil impregnated pressboard at

different degrees of humidity will be discussed in Chapter 7. Moreover, correlation between model parameters and moisture content of the pressboard insulation will also be identified in Chapter 7.

6.4 Summary

Different types of dielectric response modelling techniques and their appropriateness for analysing the dielectric response data of oil impregnated pressboard insulation have been discussed in this chapter. Based on DH cluster framework theory, a new hierarchical circuit has been proposed to analyse the frequency dependence conduction and polarisation phenomena in oil impregnated pressboard insulation. Moreover, the proposed model has been validated for analysing the FDS of mineral oil impregnated pressboard insulation. The suitability of extended Debye model and Williams-Watts polarisation stretch exponential decay function for representing depolarisation current response of mineral oil impregnated pressboard insulation has also been validated. However, applicability of proposed time and frequency domain modelling techniques on different types of oil impregnated pressboard at different degrees of humidity is investigated in the next chapter.

Chapter 7

Influence of Moisture Ageing and Temperature on Dielectric Response Behaviour of Pressboard Insulation

7.1 Introduction

Experimental results presented in Chapter 4 and previously published works clearly indicate that an increase of moisture content in the oil-paper system in a transformer accelerates the ageing process of paper insulation. Moreover, high moisture in paper insulation significantly reduces the dielectric strength of the insulation system. Moreover, it also causes gas bubbles to evolve in the case of sudden temperature rise due to an emergency overloading condition. Thereby, utilities have an incentive to estimate the amount of moisture in the solid insulation of transformers using a reliable tool with the aim to maximise the lifetime and minimise the risk of catastrophic failure.

The equilibrium chart method is the conventional approach to estimate the moisture content in transformer solid insulation by measuring the water content in oil. However, this method has been proven to be errorroneous because transformers in service experience dynamic temperature variation which makes it virtually impossible to reach moisture equilibrium between oil and paper insulation. On the other hand, dielectric response based measurements namely FDS and PDC have been utilised as reliable tools for estimating the moisture content of solid insulation in mineral oil filled transformers. This is due to the fact that dielectric response of a transformer is not significantly influenced by moisture equilibrium between oil and paper insulation. However, ageing of oil-paper composite insulation and temperature largely influence the dielectric response behaviour of transformer insulation in a way similar to moisture. Therefore, good understanding of effects of ageing and temperature on dielectric response of transformer solid insulation is required to quantify the contribution of moisture. Otherwise, it may cause a large error in estimated moisture content in transformer solid insulation using dielectric response measurements. This issue has been well studied for mineral oil-paper insulation systems over the last two decades but not enough systematic studies have been performed for ester–paper insulation systems. In order to fill this knowledge gap,

this research investigates the dielectric response behaviour of ester impregnated pressboard insulation under varying moisture, ageing and temperature conditions. This chapter mainly focuses on frequency domain dielectric response measurement and PDC measurement will also be presented for some cases.

In this chapter, dielectric response data of pressboard insulation impregnated with Shell Diala mineral oil, NEA, NEB and synthetic ester oils are presented. Dielectric response measurements on all four types of unaged pressboard samples in a range of moisture content from 0.3% to 8.8% have been performed at 35, 55 and 75ºC. This is intended to understand the influence of moisture and temperature on dielectric response behaviour of unaged solid insulation. In order to understand the collective effects of ageing and moisture, dielectric response measurements on pressboard insulation samples aged in NEA and NEB have also been performed. Furthermore, the results are compared with dielectric response data of mineral oil impregnated pressboard insulation with similar ageing conditions. This chapter analyses both time and frequency domain dielectric response data of pressboard insulation using corresponding mathematical and equivalent circuit models proposed in Chapter 6. It enhances the understanding of impact of diverse oil properties and moisture on conduction and polarisation effects in pressboard insulation. At the end of this chapter, applicability of a commercially available FDS based moisture diagnostic tool on new and aged ester based insulation systems is investigated. The content of this chapter is mainly based on [218, 219, 241].

7.2 Experimental Procedure

7.2.1 Preparation of pressboard sample with different moisture level

A set of disc shaped pressboard samples with a diameter of 100 mm was prepared from high density pressboard insulation (1.2 gcm^{-3}) sheets with a textured surface and thickness of 1.5 mm. Then vacuum drying and oil impregnation processes described in section 4.3 were used to prepare dry oil impregnated pressboard insulation samples from mineral oil, NEA, NEB and synthetic ester. However, in this case vacuum drying process was conducted at 95ºC for 48 hrs. In order to prepare samples with different moisture contents, dry oil impregnated pressboard samples were then inserted into five different humidity control chambers. The humidity inside the chambers was controlled at constant levels using saturated salt solutions prepared with Lithium bromide (LiBr), Lithium chloride (LiCl), Magnesium chloride (MgCl$_2$), Magnesium nitrate (Mg(NO$_3$)$_2$) and Sodium Chloride(NaCl). In each container, pressboard samples were arranged in a vertical stack and they were separated by copper bars as shown in Figure 4.1 to allow moisture diffusion through both surfaces. This moisture diffusion process was conducted at 50 ºC for 28 days which is far greater

than the minimum time required for reaching equilibrium homogeneous moisture distribution in pressboard insulation with a thickness of 1.5 mm at any humidity condition. Equilibrium relative humidity for selected aqueous salt solution and expected equilibrium moisture content in pressboard at corresponding relative humidity are listed in Table 7.1. In order to identify the unaged oil impregnated pressboard samples with different moisture level, the following ID format is used in this chapter.
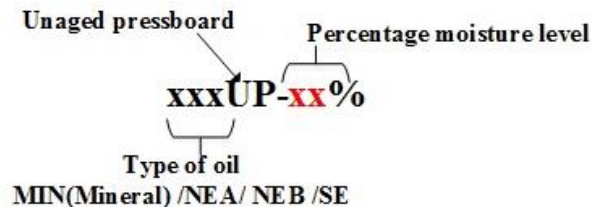
Figure 7.1. Name format for unaged PB samples

Table 7.1. Equilibrium relative humidity of saturated salt solution and expected moisture level in PB insulation

Salt solution	Relative humidity @ 50 ºC (%)[242]	Expected moisture level in pressboard (%) [150]
LiBr	5.5±0.5	1.0-1.5
LiCl	11.3±0.3	2.0-2.5
$MgCl_2$	30.5±0.2	3.7-4.2
$Mg(NO_3)_2$	45.4±0.6	5.0-5.5
NaCl	74.4±0.9	8.0-9.0

7.2.2 Preparation of aged pressboard samples

Another three sets of pressboard samples with initial moisture content of 2.2 %, 2.4 % and 2.0 % were aged in three different hermetically sealed stainless steel chambers which contained mineral oil, NEA and NEB respectively. The ageing process was performed at 120 ºC with a power transformer proportion of copper conducting bars and core steel. The ageing process was stopped at regular intervals of 28, 48, 62, and 84 days and samples were taken out for dielectric response analysis. Before taking a sample out, ageing chambers were kept at room temperature for 7 days and thereby, one can assume that the distribution of ageing by-products between oil and pressboard could have attained the equilibrium condition at the time of sampling. This research investigates the dielectric response of three categories of aged samples from each type of oil impregnated pressboard insulation such as:

- ➢ 28, 48, 62, and 84 days aged pressboard samples taken from chambers at equilibrium condition (after keeping chambers for 7 days at room temperature)

- ➢ Dry aged samples: This set of samples was prepared by subjecting 28, 48 and 84 days aged samples to a vacuum drying process at 95-105 ℃ for 12 hrs. This dry set of aged pressboard samples was analysed to discriminate the sole contribution of ageing on dielectric response behaviour of pressboard insulation.

- ➢ Wet aged samples : In order to prepare wet aged samples, a set of 28 and 48 days aged pressboard samples was placed in a humidity chamber for 60 days at 45 ℃ where relative humidity inside the chamber was controlled with MgCl$_2$ (Magnesium Chloride) salt solution.

In order to identify the aged pressboard samples with different moisture levels and ageing conditions, the following ID format is used in this chapter.
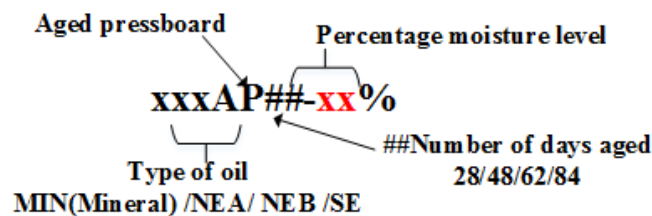
Figure 7.2. Name format for aged PB samples

7.2.3 Calculate the time required for moisture equilibrium in pressboard.

This section presents the finite element based analysis used for calculating the minimum time (t_0) required to reach homogeneous equilibrium moisture distribution in pressboard insulation under constant humidity and temperature environment. Moisture diffusion in pressboard is a conjunction of several mass transfer mechanisms including, capillary flow, Knudsen diffusion and moisture transfer due to heat and pressure gradient and external forces [243]. Moreover, it is influenced by sample thickness, temperature, number of active surfaces, etc. In this study, we consider one dimensional diffusion along thickness with two active surfaces. Therefore, moisture diffusion along the thickness of pressboard sample can be expressed with Fick's second law as in eq (7.1) [244-246].

$$\frac{\partial m(x,t)}{\partial t} = \frac{\partial}{\partial x}\left(D \frac{\partial m(x,t)}{\partial x} \right) \qquad (7.1)$$

Where *m(x, t)* is the moisture concentration and *x* is depth along thickness. *D* is diffusion coefficient which depends on local moisture concentration and temperature (*T*) as given in eq (7.2) [244].

$$D(\mathrm{m},T) = D_0\, e^{km(x,t)+E_a(1/T_0-1/T)} \tag{7.2}$$

Where D_0 (m^{2}s^{-1}) is the diffusion constant at reference temperature T_0 (K). E_a and k are activation energy for the moisture diffusion process and dimensionless constant respectively. Eq (7.1) is a nonlinear second order differential equation, which can be solved by using several numerical methods suggested in literature namely finite difference, finite volume and Crank-Nicolson method. This research has used finite difference methods and considered the values given in [247] for diffusion coefficient, coefficient (k) and activation energy of mineral oil and ester oil impregnated pressboard.
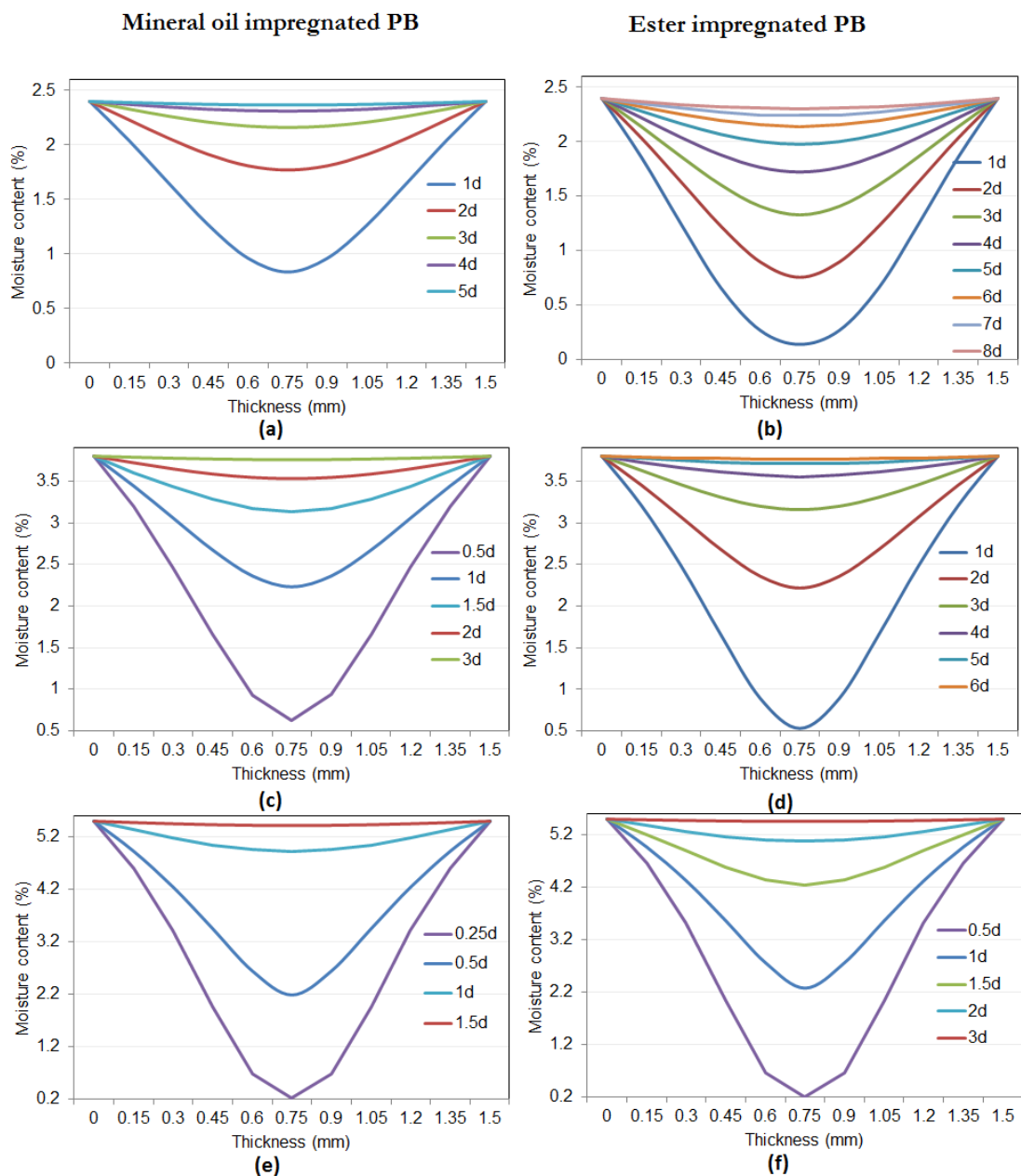
Figure 7.3. Simulated moisture concentration along thickness of PB sample under relative humidity of (a)-(b) 11 % (c)-(d) 31 %, (e)-(f) 47 %

Finite difference solution of eq (7.1) can be written as [248, 249]

$$m(x,t+\Delta t) = m(x,t) + 0(\Delta t,(\Delta x)^2) + D_0 e^{km(x,t)} \times e^{E_a\left(\frac{1}{T_0}-\frac{1}{T}\right)}\Delta t \begin{Bmatrix} k(m(x+\Delta x,t)-m(x,t)^2 / (\Delta x)^2 \\ +(m(x+\Delta x,t)-2m(x,t)+m(x-\Delta x,t)) / (\Delta x)^2 \end{Bmatrix} \quad (7.3)$$

Where $\Delta t/\Delta x^2 \leq 0.5$ and for this study Δt and Δx were selected as 10 ms and 0.15 mm respectively. In order to determine the time varying moisture content of pressboard samples under a constant relative humidity and temperature condition, eq (7.3) is implemented in MATLAB software with the following boundary conditions.

$$m(0,0) = C(l,0) = m_c\%$$
$$m(x,t) = 0 \qquad for\ x \neq 0, l$$

Where l is the thickness of the pressboard sample (1.5 mm) and m_c is the final equilibrium moisture content in a pressboard sample for a corresponding relative humidity. Figure 7.3 shows the simulated results for both mineral and ester impregnated pressboard samples under a relative humidity of 11 % (a-b), 31 % (c-d) and 46 % (e-f). It can clearly be seen in Figure 7.3 that the value of t_0 is inversely proportional to the relative humidity. Moreover, t_0 of ester impregnated pressboard is almost double compared to that of mineral oil impregnated pressboard at similar relative humidity. The calculated values of t_0 for a mineral oil impregnated pressboard sample under a constant relative humidity of 6 %, 11 %, 31 %, 46 %, 75 % at 50 ℃ are approximately 8, 5, 3, 1.5 and 0.5 days respectively. The corresponding values for an ester impregnated pressboard samples are 14, 8, 6, 3, and 1 days respectively. In this study a moisture diffusion process at all relative humidity levels has been performed over 28 days at 50 ℃. Thus, one could assume that there is no influence from inhomogeneous moisture distribution on dielectric response measurement results presented in this chapter.

7.2.4 Measurement setup

The three electrode test cell shown in Figure 7.4 was utilised to measure the dielectric response of oil impregnated pressboard samples. During measurements the test cell was filled with 350 ml of oil and a constant pressure of 2 MPa was applied on the sample using a hydraulically operated piston connected to the upper voltage electrode. In order to obtain FDS of a sample, the test cell was placed in a temperature controlled oven and was connected to a commercially available frequency domain dielectric response analyser (IDA 200/IDAX 350). Measurements were performed in a range of frequencies from 10^{-4}-10^3 Hz at three different temperature points; 35 ℃, 55 ℃ and 75 ℃ under sinusoidal voltage excitation of 10 V$_{rms}$.
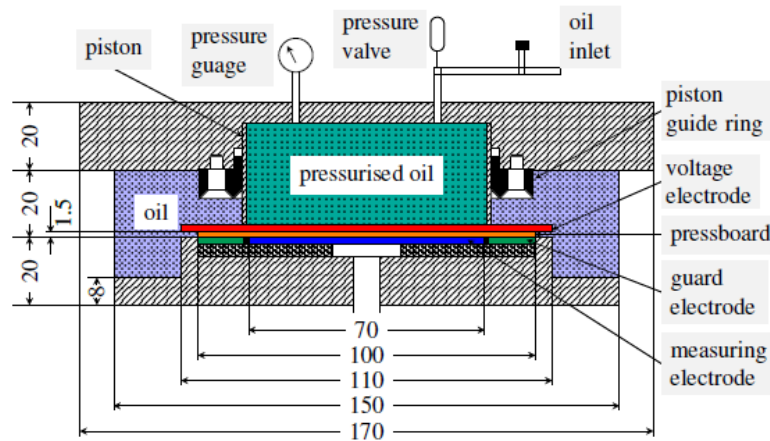
Figure 7.4. The test cell for dielectric response measurement on oil impregnated PB sample [123]

In the case of PDC measurements, equipment developed by the researchers at the University of Queensland was used [119]. Two measurement voltages were used in this research for samples with low and high moisture contents; 500 V and 50 V respectively. Polarisation current was measured over 7500 s while depolarisation current was measured only for 5000 s.

7.3 Dielectric Response of Unaged Oil Impregnated Pressboard Insulation

7.3.1 Investigate the impact of impregnated liquid on FDS

Figure 7.5 (a) and (b) respectively depict the change of real and imaginary permittivity of mineral, NEA, NEB and synthetic ester insulating oils impregnated dry pressboard samples with nearly the same low moisture content (0.6-0.8%) at 55 ℃ over a frequency range of 10^{-4}-10^3 Hz . It clearly shows that the general shape of the dielectric response of all three types of ester impregnated pressboard samples is qualitatively similar to that of the mineral oil impregnated pressboard sample. It implies that impregnation of pressboard with both natural and synthetic esters does not cause an extra relaxation.

Figure 7.5 (a) shows that high frequency constant real permittivity values of ester impregnated pressboard samples which reflect the strength of dipole, electronic and quantum resonance type polarisation processes are greater than that of mineral oil impregnated pressboard samples. This behaviour is caused by the higher dielectric constant value of ester insulating oils. Moreover, an increase in real permittivity of ester impregnated pressboard specimens in the low frequency region is greater than that of mineral oil impregnated pressboard. Imaginary permittivity also follows a similar behaviour and it becomes noticeable when frequency is less than 10Hz for all types of ester impregnated samples. This behaviour reveals that both conduction and polarisation phenomena in

ester insulating oil impregnated pressboard are more prominent than in the mineral oil impregnated pressboard insulation. Moreover, the experimental results presented in [145] have also depicted similar behaviour confirming accuracy of our measurement.
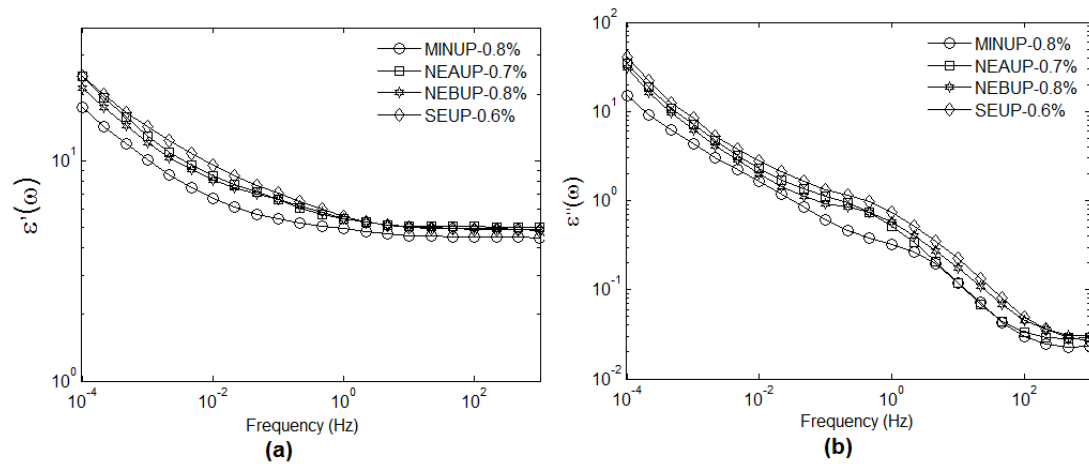
Figure 7.5. FDS of relatively dry unaged PB insulation samples (a) Real permittivity, (b) Imaginary permittivity
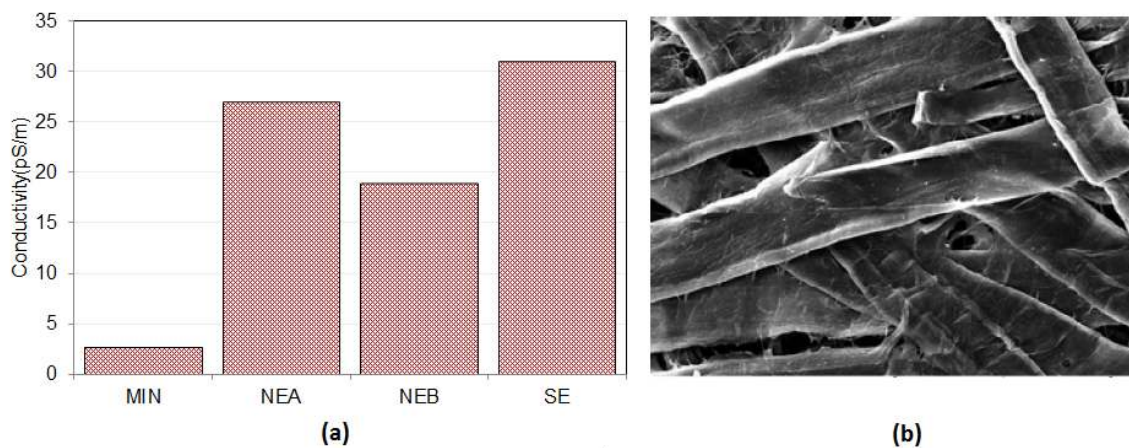
Figure 7.6. (a) Measured conductivity of four different types of oils used in this study at 55 ° C, (b) Scanning electron microscope (SEM) image of unaged PB insulation[250]

It is generally accepted that conductivity of ester insulating oils is larger than mineral oil [27]. Figure 7.6 (a) clearly shows that measured conductivity of new synthetic ester possesses the highest values of 37 pS/m followed by NEA (27 pS/m) and NEB (19 pS/m). New mineral oil has the lowest conductivity and it is almost 10 and 15 times lower than that of NEA and synthetic ester oil respectively at the same temperature. Figure 7.6 (b) shows a SEM image of unaged pressboard insulation. It indicates that there are considerable volumes of free inter and intra fibre spaces in the pressboard structure which can be occupied by oil due to vacuum impregnation. Thus, one can assume that charge density in a high conductive ester oil impregnated pressboard sample is greater than that of a mineral oil impregnated sample. This phenomenon causes larger polarisation and

conduction effects in ester impregnated pressboard insulation than the mineral oil impregnated one. This hypothesis is confirmed by the fact that the real and imaginary permittivities of pressboard insulation at low frequencies follow the order of magnitude of conductivity of impregnated oil.

7.3.2 Effect of moisture on frequency domain dielectric response

Figure 7.7 compares the effect of moisture on frequency domain dielectric response of mineral and NEA oil impregnated pressboard insulation at 55 °C. Figure 7.7 (a) and (c) respectively show the FDS of mineral and NEA impregnated samples with moisture content less than 3 % whereas that of samples with moisture contents greater than 3 % is presented in Figure 7.7 (b) and (d).
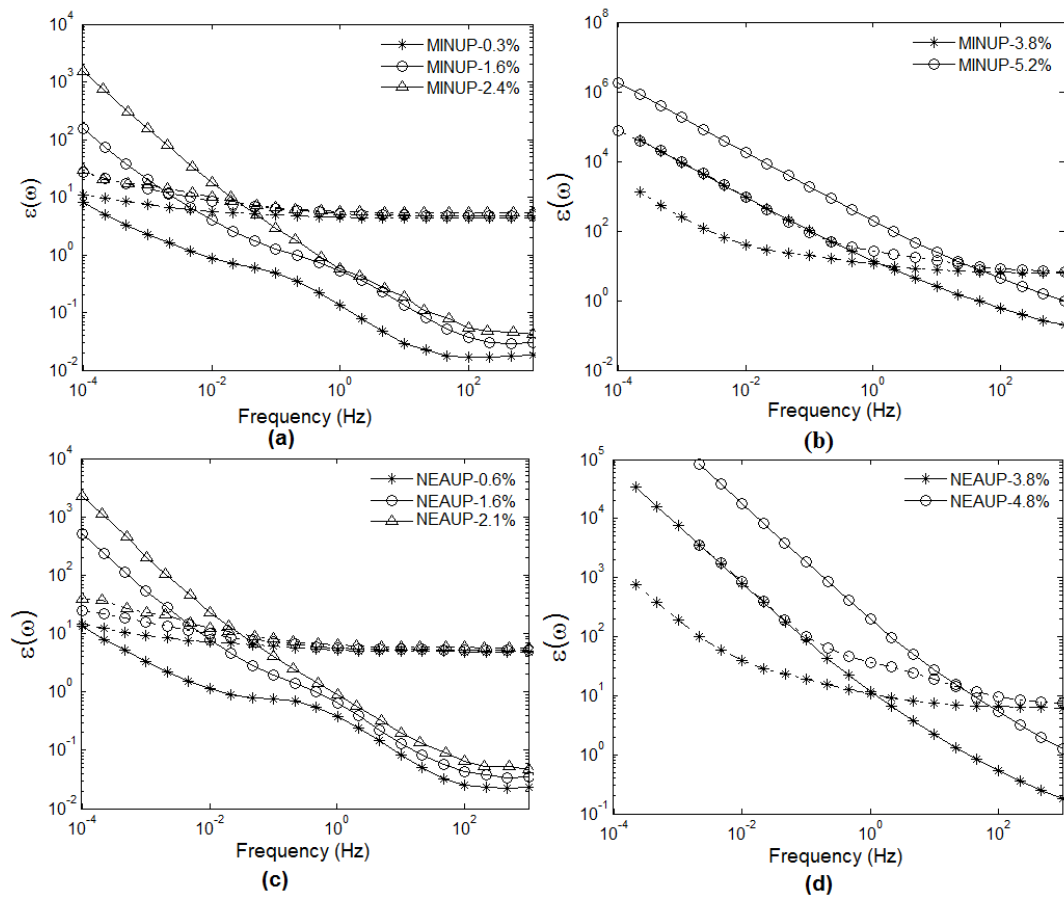
Figure 7.7. FDS response of PB insulation at different moisture level (a) Mineral oil impregnated (0<m<3%), (b) Mineral oil impregnated (m> 3%), (c) NEA impregnated (0.5<m<3%), (d) NEA impregnated (m> 3%) : Thick lines represent the $\varepsilon''(\omega)$ and broken lines represent the $\varepsilon'(\omega)$

It is clearly seen that moisture largely influences the dielectric response by increasing the polarisation and conduction mechanisms of both types of oil impregnated pressboard insulation. Thus, increasing moisture content tends to shift the whole response along the frequency axis toward high frequency together with an upward magnitude shift. However, the general shape of dielectric response of both types of pressboard remains nearly the same with increasing moisture level. FDS

of samples impregnated with NEB and synthetic ester have depicted similar behaviour with increasing moisture level and those results are presented in Figure A.1 (Appendix A).

One can clearly see a local minimum in the dielectric loss part ($\varepsilon''(\omega)$) at the high end of the frequency window, particularly when a sample has a moisture content less than 3 %. Moreover, it shows a tendency to increase with moisture and also shifts along the frequency axis towards high frequency. In particular, minimum in dielectric loss part of samples with moisture content greater than 3 % is not visible in the observed frequency range and it may occur above 1 kHz. This local minimum in the imaginary part of permittivity is caused by β relaxation due to the segmental vibration of cellulose molecular chains [235-237]. When the moisture level in a pressboard sample is high, the pronounced conduction and polarisation effects at low frequencies could mask the effect of β relaxation leading to no local minimum in the observed frequency spectra. Since the $\varepsilon'(\omega)$ remains at a constant value at high frequencies, dielectric dissipation factor (tanδ) also has a local minimum similar to $\varepsilon''(\omega)$ at the same frequency. Some scholars have established empirical relationships between the minimum value of tanδ and moisture content of paper insulation [124]. In the case of oil-paper insulation system of a transformer, properties of paper insulation dominate in the frequency range 10^1-10^3 Hz. Thus, one can claim that an increase in the minimum value of tanδ in FDS of a transformer also indicates the rise of moisture content in paper insulation [139].

Figure 7.7 clearly depicts two other key features in frequency domain dielectric spectra of both types of samples such that a local peak in dielectric loss component in the mid frequency band followed by an upward dispersion in both real and imaginary permittivities towards low frequency. Peak in dielectric loss component is not clearly visible in the FDS of samples with moisture content greater than 3 %. However, dispersion in real permittivity of those samples indicates the presence of pronounced loss peak behaviour.

In the case of pressboard insulation with low moisture contents, weak loss peak phenomenon shown in Figure 7.7 (a) and (c) arises mainly due to accumulation of charge at microscopic interfaces of oil filled cavities. Moreover, a layered structure of pressboard may also cause an interfacial polarisation leading to a peak in dielectric loss component [109]. However, this interfacial polarisation phenomenon could diminish with increasing moisture. On the other hand, intense loss peak is expected as a consequence of β_{wet} relaxation originated by collective motion of water cellulose mixed phase dipole clusters in amorphous regions of pressboard insulation. Moreover, Figure 7.7 (b) and (d) confirm the existence of intense peak due to β_{wet} relaxation in samples with moisture content greater than 3 % via the presence of dispersion in real part of permittivity of corresponding samples at high frequencies .

The upward dispersion of real and imaginary permittivity at low frequencies is named low frequency dispersion (LFD) by Jonscher [251] and quasi-DC (q-dc) conduction by Dissado and Hill [118]. It can be seen in Figure 7.7 (a) and (c) that both mineral and NEA impregnated pressboard samples with moisture content less than 3 % possess week q-dc effect giving relatively low increase to real permittivity at low frequencies. On the other hand, it is clearly seen in Figure 7.7 (b) and (d) that the q-dc process has fully developed in pressboard samples when their moisture content is greater than 3 %. In the case of a sample with nearly 5 % of moisture, both real and imaginary permittivities increase towards low frequency with a slope of nearly -1/decade over 3 frequency decades. This effect largely increases the value for $\varepsilon'(\omega)$ at low frequencies such that $\varepsilon'(\omega)$ of sample MINUP-5.2% and NEAUP-4.8% at 10^{-3}Hz is 10^4 and $8*10^3$ respectively. Figure A.1 (b) and (d) of Appendix A show that both NEB and synthetic ester impregnated pressboard insulation with moisture content of greater than 3 % also possess similar behaviour at low frequencies.

The q-dc effect of oil impregnated pressboard insulation is associated with the charge hopping along the percolation network of water molecules in the system. In the case of a charge percolation system, there are dead ends of percolation paths. In the presence of an electric field, charges can accumulate in these dead ends and act as a set of large dipoles [116]. The dead ends are not permanent and they have limited lifetimes. The lifetime of dead ends decreases with increasing moisture contents and subsequently leads to the increase of the average dipole length. When a system possesses this type of charge transport phenomenon, it can be expected to have a pronounced q-dc effect at lower frequencies such that its effect is extending to high frequency with increasing moisture. It is generally accepted that once moisture content reaches a value of 3%, a monolayer of water is formed in pressboard insulation [252]. Thus, one could assume that longer charge percolating paths exist in the pressboard insulation with moisture content greater than 3%. This could be the reason for the pronounced q-dc effects shown in Figure 7.7 (b) and (d).

$\varepsilon''(\omega)$ represents the collective effect of both conduction and dielectric losses. The contribution of conductivity to dielectric loss part is inversely proportional to frequency. Therefore, one could assume that an increase of dielectric loss part with moisture content, particularly in the low frequency region is also caused by the rise of DC conductivity. It is clear that the increase of moisture content leads to increase the number of charge carrier transport paths, which are extended over the entire sample size and subsequently increases the apparent DC conductivity. Moreover, high dielectric constant of water enhances the dissociation of the ionic impurities residing in the system and water molecules themselves dissociate into hydroxyl (OH^-) and hydronium ions (H_3O^+) [121]. In this way, an increase of moisture content results in increasing charge carrier density in the

system. This mechanism may also give rise to DC conductivity of oil impregnated pressboard insulation [121].

7.3.3 Effect of moisture on time domain dielectric response

Figure 7.8 (a) and (b) depict the normalised PDC response data of mineral and NEA impregnated pressboard insulation at two different moisture levels. It is clear that both polarisation and depolarisation currents increase with moisture content. This behaviour is caused by an increase in both conduction and polarisation phenomena as explained with FDS data. One notable fact that can be seen in Figure 7.8 (a) and (b) is that the measured polarisation current is significantly higher than the depolarisation current for all cases. It means that conduction effect mainly characterises the measured polarisation current responses leading to a nearly time independent polarisation current as shown in Figure 7.8. Pressboard samples impregnated with NEB and synthetic ester have depicted similar behaviour and those results are presented in Figure A.2.
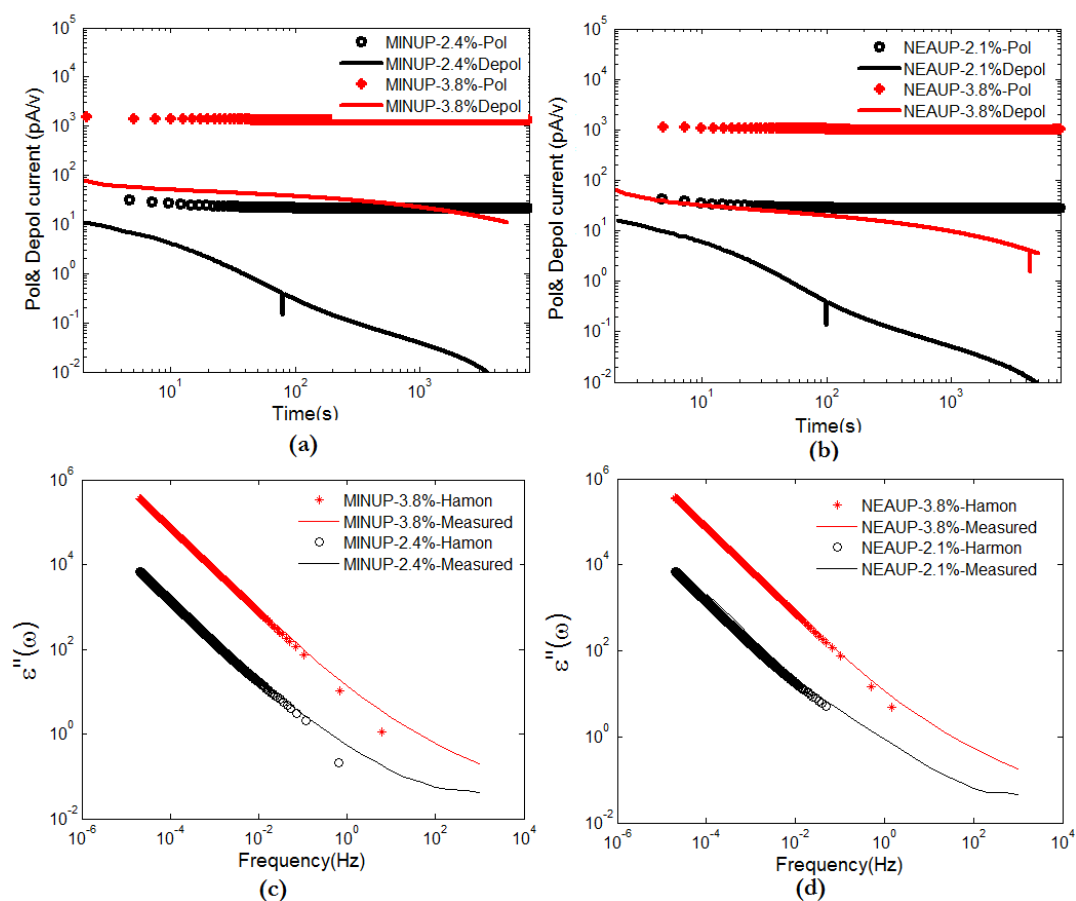
Figure 7.8. PDC response of PB insulation at 55ºC (a) Mineral oil impregnated, (b) NEA impregnated, (c) Harmon approximation for mineral oil impregnated, (d) Harmon approximation for NEA impregnated

Time domain dielectric response data can be mapped into the frequency domain using so-called Harmon approximation [117]. Thus, an imaginary part of dielectric susceptibility $\chi''(\omega)$ can be expressed in terms of measured depolarisation current using eq (7.4).

$$\chi''(\omega) = -\frac{I(t)_{depol}}{\omega C_0 U_0} \ where \ \ \omega t \approx 0.63 \tag{7.4}$$

DC conductivity (σ) can be derived using PDC data and eq (3.18). Thereby, imaginary part of permittivity in the frequency domain can be calculated using eq (7.5).

$$\varepsilon''(\omega) = \chi''(\omega) + \frac{\sigma}{\omega \varepsilon_0} \tag{7.5}$$

Due to practical limitations, polarisation and depolarisation current data has only been recorded for times greater than 1 s. Thus, Hamon approximation can only be used to derive data in low frequencies (< 1 Hz). Figure 7.8 (c) and (d) clearly show that measured frequency domain dielectric loss part show satisfactory fitting curve with modelled data using Hamon approximation in low frequency region. It confirms that both time domain and frequency domain dielectric response data provides the same information with respect to polarisation and conduction phenomena of material under investigation. Thereby, this study mainly uses frequency domain measurement which characterises polarisation phenomena at both high and low frequencies.

7.3.4 Effect of moisture on frequency dependent AC conductivity

Figure 7.9 represents the measured conductivity vs. frequency of oil impregnated pressboard insulation at different moisture levels. We can see that frequency dependency of conductivity is stronger in the sample with low moisture content but becomes much less at high humidity. An almost similar behaviour has been observed in conductivity spectra of NEB and synthetic ester impregnated pressboard insulation (refer Figure A.3, Appendix A).

The main feature that can be identified in conductivity spectra is that conductivity remains constant at low frequencies and then continues to increase with a fractional power law of frequency. This is a typical feature of a system of charge carriers hopping within a disordered distribution of sites such as humid cellulose [116]. This behaviour at low frequencies can be explained by an equation in the form of eq (7.6).

$$\sigma(\omega) = \sigma_{dc}(1 + (\tau_c \omega)^{\beta}) \tag{7.6}$$

Where, σ_{dc} is the frequency independent conductivity at low frequencies. It represents the collective effect of both DC conduction and q-dc effects. The influence of q-dc effect on σ_{dc} is significant when a sample contains a moisture level of greater than 3 %. β has values in the range 0-1. In this case, we assume $1/\tau_c$ (cut-off frequency) is the frequency which the loss peak relaxation process starts to be dominant over the conduction effects and it is supposed to increase with moisture.
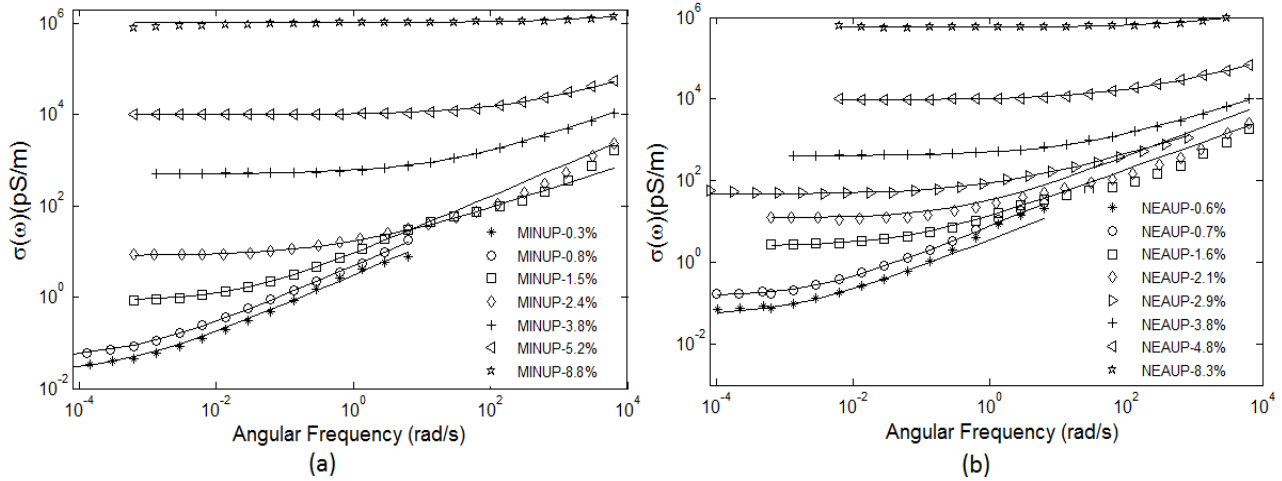
Figure 7.9. Conductivity spectra of PB with different moisture contents at 55°C (a) Mineral oil impregnated, (b) NEA impregnated(thick line present the modelled data)

Parameters; σ_{dc}, β and τ_c for conductivity spectra of all types of oil impregnated pressboard insulation have been selected using the nonlinear least squares technique in MATLAB environment with $R^2>0.95$. Continuous lines in Figure 7.9 show that the proposed model yields a satisfying fitting curve of the measured response. Model parameters have been calculated for conductivity spectra measured at three different temperature points; 35 °C, 55 °C and 75 °C.

Table 7.2. Selected model parameters of conductivity spectra: mineral oil impregnated PB at 55 °C

Sample ID	σ_{dc}(pS/m)	$1/\tau_c$ (rad/s)	β
MINUP-0.3%	2.2×10^{-2}	4.5×10^{-4}	0.61
MINUP-0.8%	4.5×10^{-2}	6.6×10^{-4}	0.63
MINUP-1.6%	8.0×10^{-1}	2.5×10^{-2}	0.6
MINUP-2.4%	8.1	7.6×10^{-1}	0.6
MINUP-3.8%	5.0×10^{2}	2.0×10^{1}	0.5
MINUP-5.2%	9.9×10^{3}	3.3×10^{2}	0.53
MINUP-8.8%	1.04×10^{6}	5.2×10^{4}	0.52

Table 7.3 Selected model parameters of conductivity spectra: NEA impregnated PB at 55 ℃

Sample ID	σ_{dc}(pS/m)	$1/\tau_c$ (rad/s)	β
NEAUP-0.6%	$5.0x10^{-2}$	$1.44x10^{-3}$	0.68
NEAUP-0.7%	$1.47x10^{-1}$	$3.24x10^{-3}$	0.69
NEAUP-1.6%	2.5	$7.7x10^{-2}$	0.6
NEAUP-2.1%	$1.25x10^{1}$	$4.5x10^{-1}$	0.64
NEAUP-2.9%	$4.7 x10^{1}$	1.3	0.5
NEAUP-3.8%	$4.5 x10^{2}$	$17.2x10^{1}$	0.53
NEAUP-4.8%	$9.6x10^{3}$	$1.6x10^{2}$	0.52
NEAUP-8.3%	$5.7x10^{5}$	$5.5x10^{3}$	0.52

One can clearly see in Table 7.2 and Table 7.3 (Tables A.1 and A.2) that σ_{dc} and cut-off frequency possess clear increasing trends with moisture indicating their applicability to assess the moisture in pressboard insulation. Thus, identifying the relationship between these two parameters and moisture content is needed.

7.3.5 Relationship between σ_{dc} and moisture content

It is generally accepted that a monolayer of water molecules is formed in pressboard insulation when its moisture content reaches 3 % [122]. Moreover, extended phase of water which behaves like bulk water is established in pressboard insulation when its moisture content rises above the limit of 6 % [252]. When the moisture content is less than 3%, water molecules in the system are spatially distributed and physically isolated. Thus, this research claims that dependence of σ_{dc} on moisture content changes at these two critical moisture levels and the exponential relationship given in eq (7.7) is proposed to correlate moisture content and σ_{dc}.

$$\sigma_{dc} = \psi e^{\left(\frac{\xi m}{(m+3)^{0.33}(m+6)^{0.33}}\right)} \tag{7.7}$$

Where, ψ is an arbitrary constant which depends on impregnated liquids and ageing condition of pressboard insulation. ζ is exponential factor which depends on the charge transport mechanism of the system. Figure 7.10 presents a comparison between dependence of experimentally obtained frequency independent conductivity (σ_{dc}) on the moisture content with the one modelled using eq (7.7). It is clearly apparent that measured conductivity data shows a good fit with modelled data for corresponding ψ and ζ values given in Table 7.4.
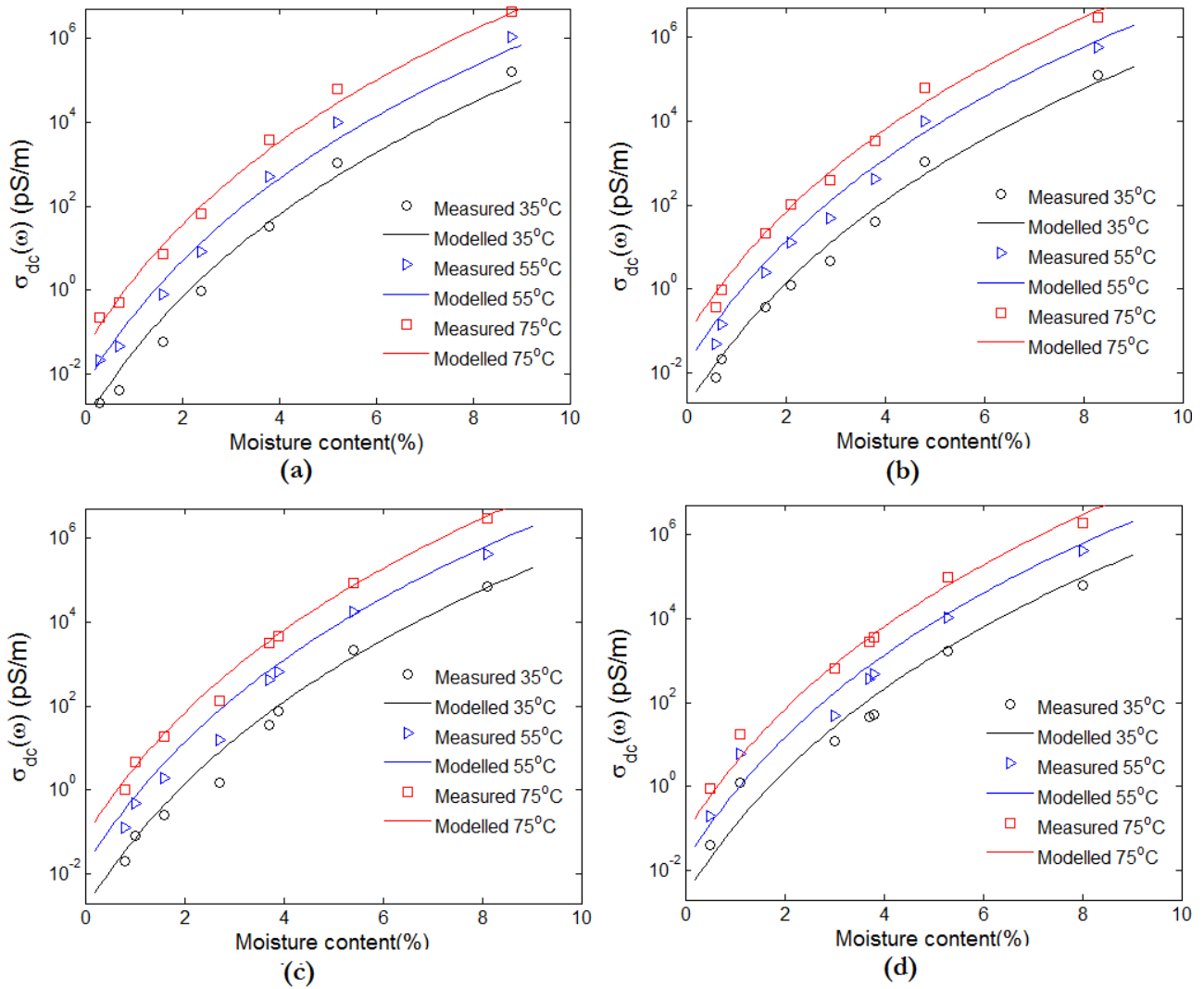
Figure 7.10. Measured and modelled conductivity vs. moisture content of PB (a) Mineral oil impregnated, (b) NEA impregnated, (c) NEB impregnated, (d) synthetic ester impregnated

Table 7.4. Selected parameters for exponential model of conductivity vs. moisture content (m)

Type of oil	35 °C		55 °C		75 °C	
	ψ	ζ	ψ	ζ	ψ	ζ
Mineral	8.0×10^{-4}	11.5	6.0×10^{-3}	11.5	4.0×10^{-2}	11.5
NEA	1.4×10^{-3}	11.5	1.14×10^{-2}	11.5	7.4×10^{-2}	11.5
NEB	1.4×10^{-3}	11.5	1.14×10^{-2}	11.5	7.4×10^{-2}	11.5
Synthetic ester	2.5×10^{-3}	11.5	1.6×10^{-2}	11.5	7.5×10^{-2}	11.5

A noticeable fact is that the same relationship is possessed by both types of NE impregnated pressboard insulation. In addition, the values of ζ listed in Table 7.4 confirm that it is no longer an unknown parameter and remains at a constant value of 11.5. The effect of diverse properties of oils

on low frequency conductivity is reflected by parameter ψ. The value of ψ corresponding to synthetic ester impregnated pressboard insulation is the highest followed by NE and mineral oil impregnated pressboard respectively. It indicates that for a similar moisture content synthetic ester impregnated pressboard has the highest dielectric and conduction loss in low frequency region whereas NE impregnated pressboard possesses moderate behaviour. Moreover, one could also suggest that values of ψ presented in Table 7.4 follow the order of magnitude of conductivity of impregnated oil. One deficiency of this model is that it indicates the impact of diverse oil properties on σ_{dc} is significant even for a sample with very high moisture content. However, this issue will not significantly influence the real time application of this model because the moisture content of solid insulation of transformers is typically in the range of 0.5-4%.

Temperature dependence of pre-exponential factor ψ can be explained with a so-called single Arrhenius type eq (7.8) where T is absolute temperature and T_0 is reference temperature (298 K). $E_{\psi a}$ is activation energy corresponding to low-frequency conductivity. Thereby, the generalised formula as given in eq (7.9) can be utilised to characterise the dependence of conductivity on both moisture (m) and temperature (T).

$$\psi = \psi_0 e^{\frac{-E_{\psi a}}{K}(1/T - 1/T_0)} \tag{7.8}$$

$$\sigma_{dc}(T,m) = \psi_0 e^{\frac{-E_{\psi a}}{K}(1/T - 1/T_0)} e^{\left(\frac{11.5m}{(m+3)^{0.33}(m+6)^{0.33}}\right)} \tag{7.9}$$
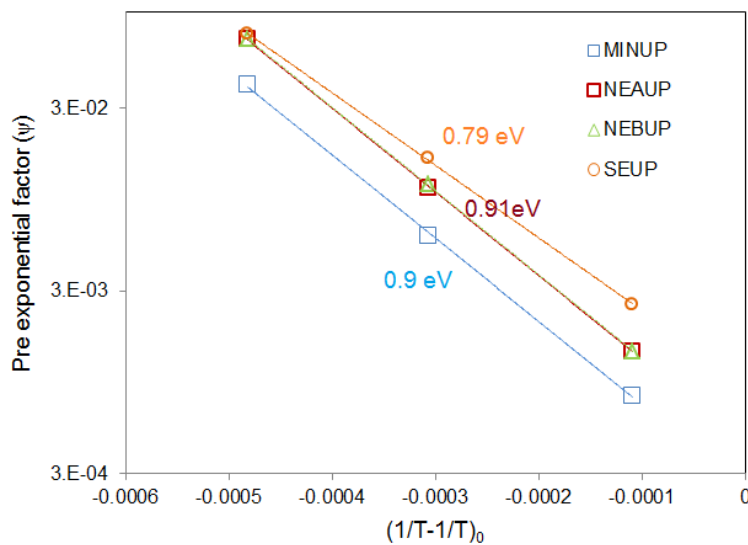
Figure 7.11. Temperature dependence of ψ

The activation energy $E_{\psi a}$ can be calculated by multiplying the gradient of log (ψ) vs. reciprocal of absolute temperature plot and Boltzmann constant. As shown in Figure 7.11, for mineral oil and

NE impregnated pressboard insulation, the activation energies found are 0.90 eV and 0.91 eV respectively and they show a good match with the values given in [124, 253]. On the other hand, synthetic ester impregnated pressboard insulation possesses activation energy of 0.79 eV indicating its less temperature dependence behaviour.

In the case of a transformer insulation system, low frequency conductivity of paper insulation can easily be derived from its FDS data. Thus, eq (7.9) with selected parameters in this research can be utilised to estimate moisture in paper insulation of ester and mineral oil filled transformers.

7.3.6 Relationship between moisture content and cut-off frequency

This research has identified that the relationship between cut off frequency ($1/\tau_c$) and moisture content can also be presented with a similar form of equation which is used to explain dependence of σ_{dc} on moisture content in pressboard insulation.

$$\tau_c^{-1}(T,m) = \psi_c e^{\left(\frac{\zeta_c m}{(m+3)^{0.33}(m+6)^{0.33}}\right)} \qquad (7.10)$$

Where, $1/\tau_c$ is the cut off frequency of AC conductivity response. ψ_c and ζ_c stand for arbitrary constants associated with the relationship of cut off frequency and moisture content.
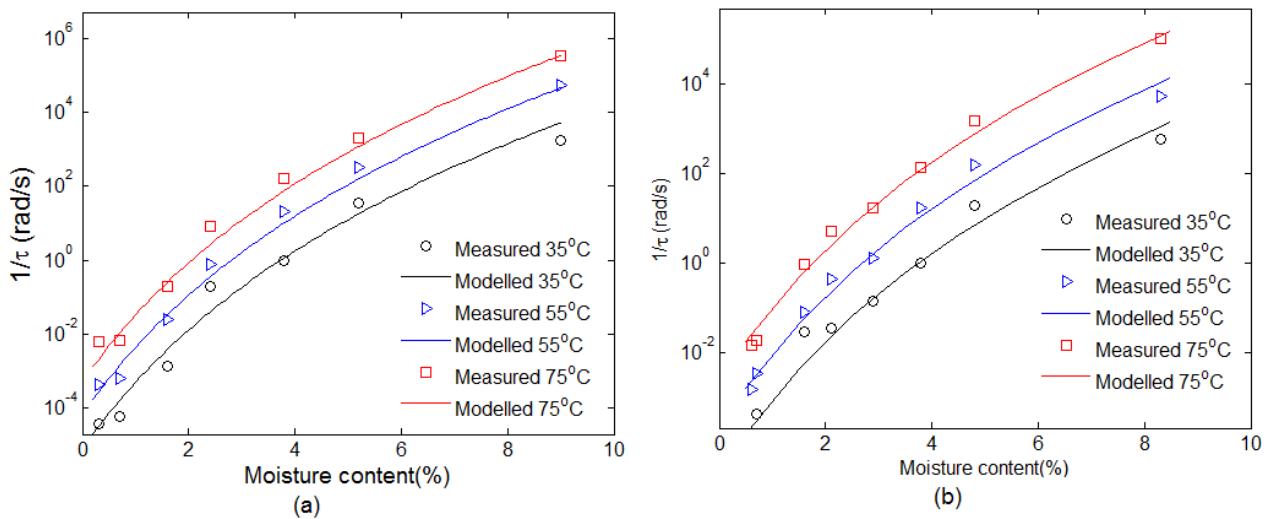
Figure 7.12. Measured and modelled cut off frequency conductivity spectra vs. moisture content of PB (a) Mineral oil impregnated (b) NEA impregnated

Figure 7.12 shows that calculated cut off frequency data from experimental conductivity spectra shows a good fit with that of modelled data using parameter values given in Table 7.5 for mineral oil and NEA impregnated pressboard insulation. Comparison of modelled and experimental data of NEB and synthetic ester impregnated pressboard insulation is presented in Figure A.4 (refer

Appendix A). In this case, exponential factor ζ_c possesses a value of 13.5 for mineral oil impregnated pressboard whereas that of all other types of pressboard is 11.5.

Table 7.5. Selected parameters for exponential model of cut off frequency vs. moisture

Type of oil	35 ºC		55 ºC		75 ºC	
	ψ_c	ζ_c	ψ_c	ζ_c	ψ_c	ζ_c
Mineral	8.0×10^{-6}	13.5	7.0×10^{-5}	13.5	5.2×10^{-4}	13.5
NEA	2.0×10^{-5}	11.5	2.2×10^{-4}	11.5	2.2×10^{-3}	11.5
NEB	2.0×10^{-5}	11.5	2.2×10^{-4}	11.5	2.2×10^{-3}	11.5
Synthetic ester	4.4×10^{-5}	11.5	2.5×10^{-4}	11.5	1.5×10^{-2}	11.5

A similar method which applied for conductivity model was used to calculate the activation energy corresponding to ψ factor of cut off frequency model. As shown in Figure 7.13, for mineral oil and NE impregnated pressboard insulation, the activation energy value found is 1 eV and that of for synthetic ester impregnated pressboard is 0.83 eV.
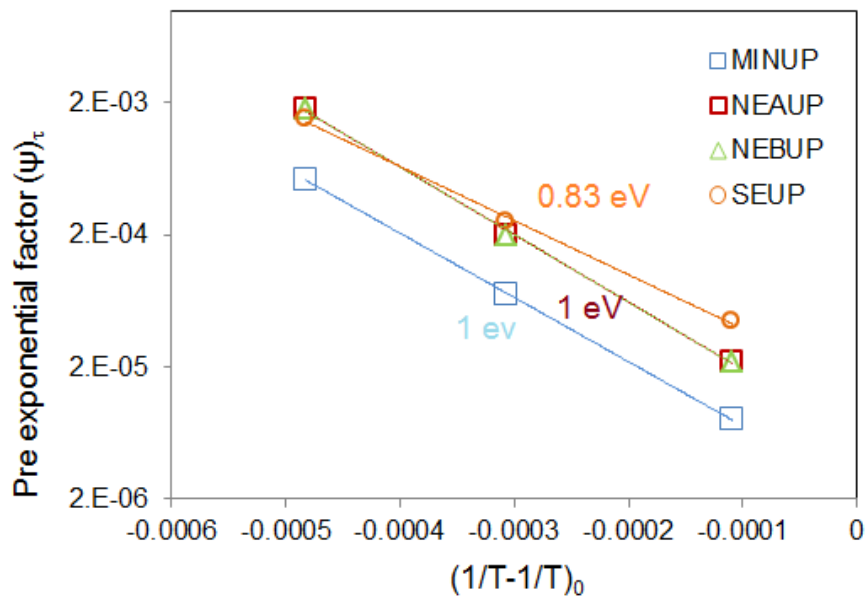
Figure 7.13 Temperature dependence of ψ_c

The discrimination of the dielectric response of paper insulation from the FDS of oil-paper composite insulation of a transformer is difficult. Thus, practical use of established relationships between cut off frequency, moisture content and temperature cannot be confirmed in this research.

7.4 Quantitative Determination of Polarisation and Conduction Phenomena in Oil Impregnated Pressboard Insulation

7.4.1 Through modelling of FDS data

In order to quantify and discriminate the influence of moisture and diverse oil properties on different relaxation and DC conduction processes in oil impregnated pressboard insulation, this research models the observed frequency domain spectra using the hierarchical equivalent circuit proposed in section 6.2.5 (refer Figure 6.8). The equivalent circuit mainly consists of two dispersive capacitive elements connected in series. These capacitive elements stand for DH loss peak and DH q-dc behaviour. Parameters of the proposed equivalent circuit model have been derived using a MATLAB based optimization routine. Calculated circuit parameters for mineral and ester impregnated pressboard insulation at different levels of moisture content are presented in Table 7.6.

Table 7.6. Selected equivalent circuit model parameters for FDS response at 55ºC

Sample ID	DH loss peak				DH q-dc					σ_1	σ_2
	X_p	ω_p	n_1	M	X_{qdc}	ω_c	n_2	p	ε_∞	pS/m	Ps/m
MINUP−0.3%	0.35	0.12	0.35	0.1	1.4	0.08	0.90	0.55	4.3	0.001	0.03
MINUP−0.8%	0.55	0.70	0.35	0.1	1.9	0.15	0.90	0.55	4.5	0.002	0.6
MINUP−1.6%	1.05	0.30	0.35	0.1	3.8	0.2	0.90	0.55	5.2	0.08	0.9
MINUP−2.4%	0.18	1.10	0.60	0.1	5.2	0.32	0.90	0.55	5.3	3.3	1.3
MINUP−3.8%	1.70	2.40	0.60	0.1	146	12.7	0.75	0.90	5.7	80	95
MINUP−5.2%	3.20	21.0	0.60	0.1	223	19.0	0.65	0.90	5.8	1400	1800
NEAUP−0.6%	1.25	0.16	0.30	0.1	3.8	0.02	0.90	0.55	4.8	0.003	0.15
NEAUP−0.7%	1.40	0.20	0.30	0.1	4.0	0.05	0.90	0.55	5.2	0.01	0.75
NEAUP−1.6%	1.05	0.32	0.30	0.1	6.6	0.08	0.90	0.55	5.2	0.4	1.5
NEAUP−2.1%	0.30	0.80	0.60	0.1	10.4	0.16	0.90	0.55	5.3	1.8	4.2
NEAUP−3.8%	1.70	1.60	0.60	0.1	151	0.64	0.75	0.90	5.8	75	90
NEAUP−4.8%	5.40	15.0	0.60	0.1	230	12.7	0.65	0.90	5.8	1200	1900
NEBUP−0.8%	1.40	0.32	0.35	0.1	3.8	0.05	0.90	0.55	4.8	0.01	0.7
NEBUP−1.1%	1.70	0.45	0.35	0.1	5.7	0.13	0.90	0.55	5.2	0.05	2
NEBUP−1.6%	1.00	0.80	0.35	0.1	7.6	0.15	0.90	0.55	5.2	0.22	2.2
NEBUP−2.7%	0.30	0.95	0.60	0.1	10.4	0.19	0.90	0.55	5.3	3	5
NEBUP−3.8%	1.70	1.90	0.60	0.1	151	0.31	0.75	0.90	5.8	85	140
NEBUP−5.4%	5.40	23.8	0.60	0.1	291	19.0	0.65	0.90	5.8	2000	3500
SEUP−0.6%	2.00	0.24	0.35	0.1	5.7	0.03	0.90	0.55	4.8	0.015	0.9
SEUP−1%	3.90	0.95	0.32	0.1	10.4	0.13	0.90	0.55	5.2	0.7	10
SEUP−3%	4.80	1.30	0.40	0.1	63	0.32	0.90	0.60	5.8	8	18
SEUP−3.8%	1.70	1.60	0.60	0.1	156	2.40	0.75	0.90	5.8	80	95
SEUP−5.3%	4.50	16.0	0.60	0.1	264	8.00	0.65	0.90	5.8	1800	2000

X_p and X_{qdc} stand for magnitude of loss peak and q-dc behaviour respectively. Estimation of accurate power law exponents and amplitude factors is extremely dependent on the selection of

appropriate initial values for those parameters. The initial parameter values have been selected to better match with the physical condition of corresponding pressboard specimens.
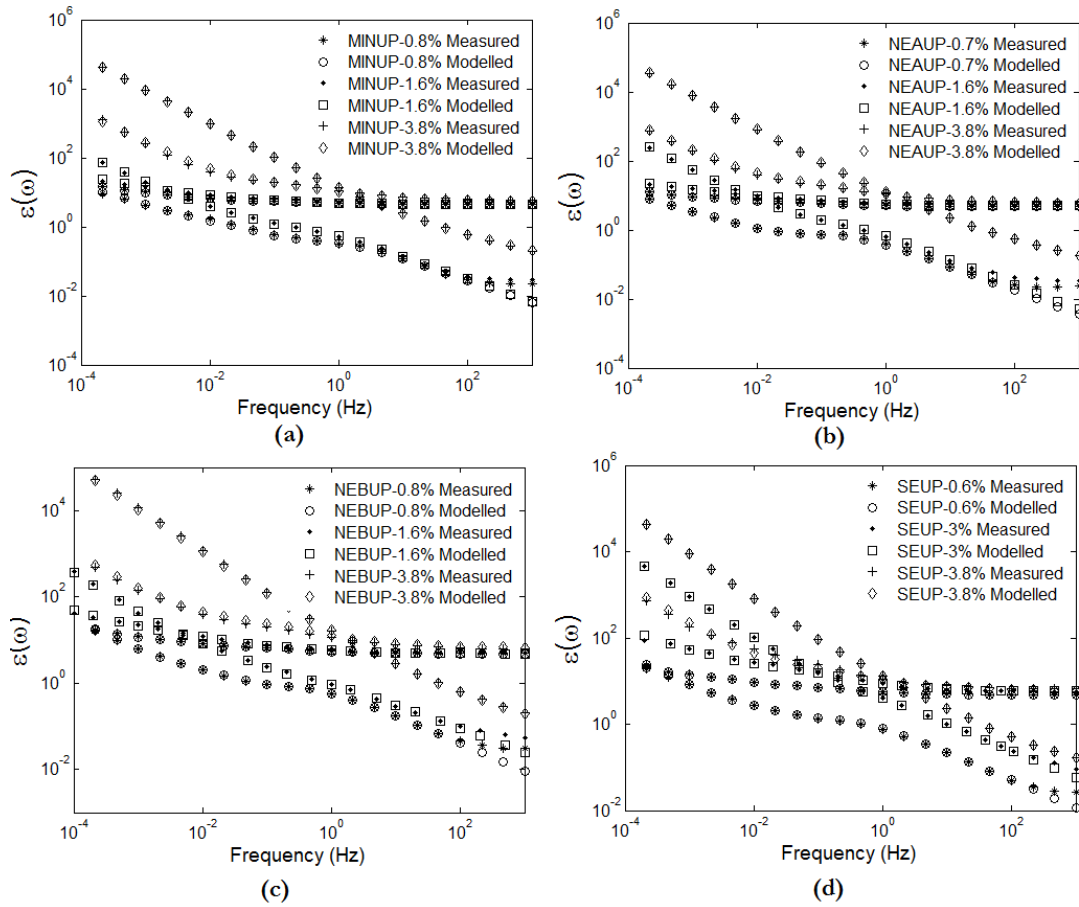
Figure 7.14. Comparison of modelled and measured FDS spectra at 55ºC (a) Mineral oil impregnated, (b) NEA impregnated, (c) NEB impregnated (d), synthetic ester impregnated

Figure 7.14 presents the comparison of experimental and modelled dielectric response data of all four types of pressboard insulation samples for three different moisture levels. It is clear that the FDS of the proposed equivalent circuits yields a satisfying fitting curve of the measured response throughout the observed frequency range. It confirms the validity of proposed cluster based physical interpretation for dielectric response data of all types of oil impregnated pressboard insulation. It means that correlated motion of a group of electric dipoles in a constraint geometrical domain called cluster give loss peak behaviour in high frequency. This is followed by q-dc type relaxation due to effective charge transport between charge clusters through percolation bond created by spatially distributed matrix of water molecules in the system. As explained in section 6.2.5, charge dipole clusters could be either oil or water associated. It discusses the physical significance of model parameters with respect to moisture contents and diverse oil properties in the proceeding section.

Calculated values of ε_∞ show an increasing trend with moisture for all types of oil impregnated pressboard insulation. This behaviour is caused by dipole polarisation of water molecules at high frequencies. ε_∞ of mineral oil impregnated pressboard is varying in the range 4.3-5.8 whilst that of ester impregnated pressboard is changing in the range of 4.8 to 5.8.

As shown in Table 7.6, the estimated value of p possesses a value of 0.55, when a pressboard sample contains a moisture level of less than 3%. This somewhat deviates from the value of p expected for a typical system with hydrogen bonds, which is in the range of 0.8-1 [115, 254]. In oil impregnated pressboard at lower frequencies, charge transport may occur between charge clusters associated with oil cavities through a matrix of narrow oil filled channels giving a value of p approaching unity. In contrast, charge hopping will occur between spatially distributed water molecules in a diffusive manner when a sample contains a low moisture content giving weak q-dc dispersion with p close to 0.5. Therefore, based on the modelling results it is confirmed that the dominant charge transport mechanism between oil based clusters at a low moisture content is that of the diffusive charge hopping between spatially distributed water molecules. Moreover, charge transport mechanism is independent of the diverse properties of impregnated oil.

The parameter X_{qdc} which represents the strength of q-dc relaxation is significantly lower for all samples with a moisture content of less than 3%. Moreover, the value of exponent n_2 always remains at 0.9 indicating weak dispersion in both real and imaginary permittivities above the characteristic frequency. Thus, one can claim that oil dependent charge clusters govern the dielectric response behaviour of pressboard insulation with low moisture content (<3%) giving weak dispersion to dielectric constant regardless of type of impregnated oil.

On the other hand, it is clearly seen in Table 7.6 that exponential factor p takes a value of 0.9 for all cases where pressboard specimens are containing moisture content greater than 3%. Furthermore, X_{qdc} is several orders of magnitude greater than that of pressboard samples with low moisture level (<3%) and value of n_2 reaches 0.6 when moisture content reaches about 5%. All four types of pressboard insulation with a moisture content of greater than 3% follow a similar trend indicating a pronounced q-dc effect. Thus, one could claim that if both real and imaginary permittivities in dielectric response of an oil-paper system increase toward low frequencies with nearly -0.9 gradients, the paper insulation in that system has a moisture content of greater than 3%.

Modelling results indicate that characteristic frequency of q-dc process (ω_c Hz) increases with moisture content. In the case of the q-dc process, ω_c denotes the rate of charge escape from the cluster and charge transfer to nearby clusters through weakly conducting connections (bonds of a

percolation model matrix) [227]. It is accepted that the principal charge transportation mechanism in cellulose is the proton hopping along a percolation network of water molecules and CHOH groups in cellulose polymer. Therefore, it is clear that an increase of moisture content results in a growing number of charge transport routes, which provide support to charge transition between and within the clusters shifting the q-dc response towards high frequencies.

It can clearly be seen in Table 7.6 that when water dependent charge clusters dominate, pressboard possesses stronger and broader loss peak than in the case when oil dependent clusters dominate. It has been noticed that loss peak relaxation process is also shifted towards higher frequencies with an increase of moisture content. Calculated data shown in Table 7.6 provides evidence for this behaviour such that characteristic frequencies of DH loss peak (ω_p Hz) show a tendency to increase with moisture content. This effect is more significant when the pressboard holds moisture content higher than 3%. Increase of moisture results in swelling of the pressboard and decreases the spatial hindrance of microscopic motion of the water–cellulose mixed phase clusters. This may be one possible reason for the shifting of the DH loss peak toward higher frequencies with moisture.

It can be seen in Table 7.6 that X_p, X_{qdc}, σ_1 and σ_2 of pressboard samples NEAUP-0.7%, NEBUP-0.8% and SEUP-0.6% are higher than those of pressboard specimen MINUP-0.8%. However, they have almost similar moisture contents. This implies that the high conductivity and moisture solubility of ester boost the free and bound charge carrier concentration in the system leading to high conductive and polarisation effects. This hypothesis is confirmed by the modelled parameters of samples MINUP-1.6%, NEAUP-1.6% and NEBUP-1.6%. Moreover, the model parameters indicate that the conduction and polarisation effects in sample NEAUP-2.1% are stronger than that of sample MINUP-2.4%. On the other hand, model parameters (X_p, X_{qdc}, σ_1 and σ_2) which reflect the strength of polarisation and conduction phenomena of specimens MINUP-3.8%, NEAUP-3.8%, NEBUP-3.8% and SEUP-3.8% are in similar order of magnitudes. It implies that when water oriented clusters dominate in pressboard, the effect of diverse properties of impregnated oil on dielectric response behaviour is not significant. Moreover, in such a condition the amount of water is the main factor which determines the dielectric response behaviour of pressboard insulation. This hypothesis is confirmed by the facts that parameters X_{qdc}, σ_1 and σ_2 of samples MINUP-5.2%, NEAUP-4.8%, NEBUP-5.4% and SEUP-5.3% nearly follows the order of moisture content in those samples.

This study calculates the effective DC conductivity of pressboard insulation using model parameters σ_1 and σ_2 presented in Table 7.6. Effective DC conductivity is $1/(1/\sigma_2+1/\sigma_2)$, because these two elements are electrically in series [255]. Figure 7.15 manifests that effective DC conductivity

exponentially increases with moisture content. The magnitude of effective DC conductivity is governed by three factors; mobile charge density, charge mobility and the number of effective charge transport paths across the samples. Here we hypothesise that the effect of mobile charge density is dominant when a sample contains low moisture level and thereby, effective DC conductivity of ester impregnated pressboard should be higher than that of mineral oil impregnated pressboard. We propose that the number of charge transport paths across a sample is solely determined by the concentration of water and moreover, charge mobility is inversely proportional to the distance between water molecules [253]. Thus, DC conductivity for all type of oil impregnated pressboard insulation with higher moisture level should be in a similar range. It is clear that the experimental results shown in Figure 7.15 confirm our physical interpretation corresponding to effective DC conductivity.
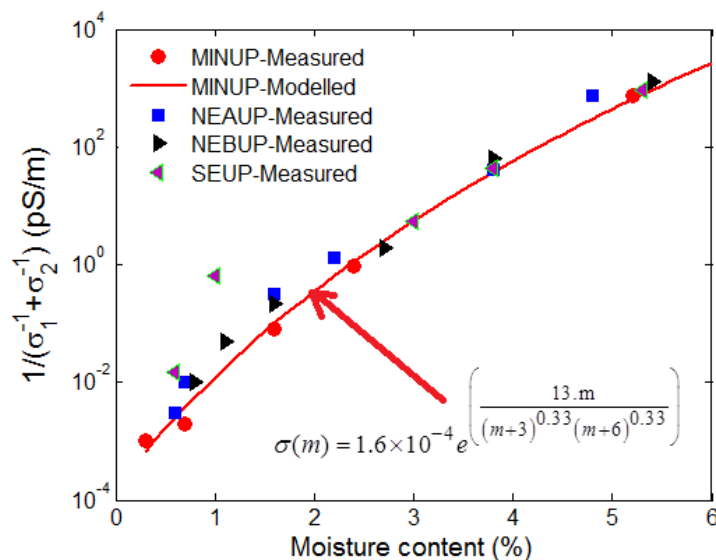
Figure 7.15. Variation of effective DC conductivity with moisture at 55ºC

In estimating moisture content in the solid insulation of a transformer, low frequency behaviour of dielectric response of pressboard insulation is very important. The effect of DC conductivity on dielectric response is dominant at low frequencies because the contribution of DC conductivity to dielectric loss is inversely proportional to frequency. An exponential relationship between effective DC conductivity and moisture content of mineral oil impregnated pressboard has been deduced. Figure 7.15 shows that if one uses the proposed model it overestimates the moisture content in ester impregnated pressboard insulation, particularly when a sample contains low moisture content. However, it clearly shows that the error in the estimated moisture content is in the range between 0% and +0.5% for all cases except SEUP-1%. It means the DC conductivity model given in Figure 7.15 can be applied on ester based insulation systems for assessing the moisture content in paper insulation.

7.4.2 Modelling the depolarisation current response data

Figure 7.16 shows that depolarisation current responses of all types of oil impregnated pressboard insulation with moisture content in the range 2.1- 3 % can be modelled with five different Debye type relaxation processes. In addition, depolarisation current responses of all types of samples with moisture content of 3.8 % have also been modelled with a similar number of Debye functions. A comparison of modelled and measured data of those samples is presented in Figure A.5 (Appendix A). The Debye relaxation with the smallest time constant represents the microscopic interfacial polarisation phenomenon in oil filled cavities. Thus, it is clear that the other four Debye processes represent the relaxation of four different groups of dipoles in pressboard insulation. As explained in section 6.3, one could assume that four different dipole groups are produced by blocking of mobile charges at crystalline interfaces of four different size scale of pressboard structure.
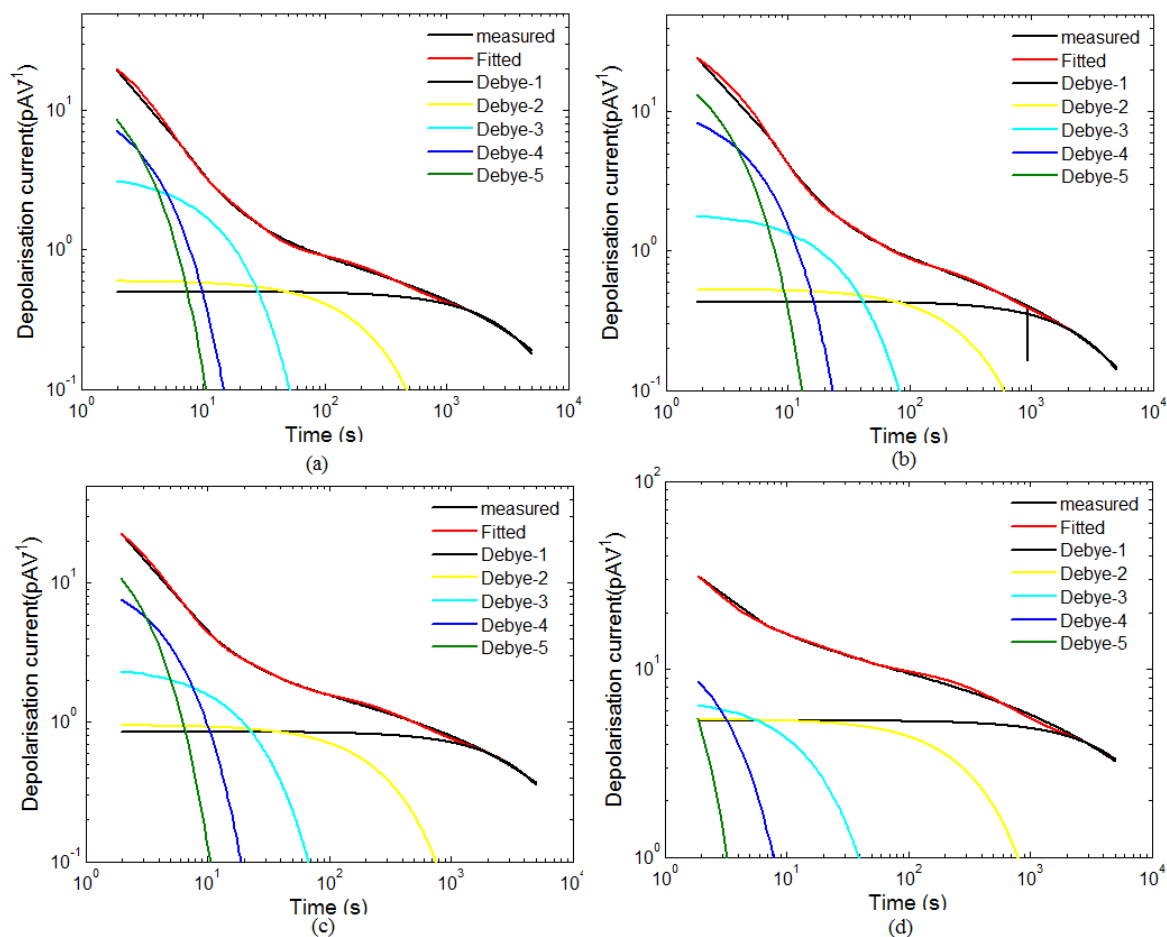
Figure 7.16. Comparison of experimental and the modelled depolarisation current with extended Debye methods (a) MINUP-2.4%, (b) NEAUP-2.1%, (c) NEBUP-2.7%, (d) SEUP-3% at 55ºC

Since depolarisation current response is a collection of Debye processes, its behaviour can be represented using a RC equivalent circuit as shown in Figure 3.8. The physical significance of the

RC equivalent circuit parameters with respect to moisture content of pressboard samples will be discussed in the proceeding section.

It can be seen in Figure 7.17 that irrespective of the type of impregnated oils, the resistance values of all the branches markedly decrease with the increase of moisture while capacitances show the opposite behaviour. It means that an increase of moisture reduces the resistance to charge transport in pressboard insulation and thereby large dipoles are produced by separation of charge over a long distance. Branches 1 and 2 which have the largest and second largest time constants (R*C) represent the long time depolarisation current. Thus, the behaviour of R and C elements of those two branches is very important, because in the case of a transformer long-time depolarisation current is determined by the properties of paper insulation while short term depolarisation current is determined by the interfacial polarisation phenomenon at the oil-paper interface. Change of circuit parameters of branches 1 and 2 shows good consistency with moisture regardless of type of impregnated oil. Therefore, one can clearly claim that decrease of resistance value and increase of capacitance corresponds to long-term depolarisation current of any type of oil filled transformer indicating an increase of moisture in paper insulation and vice-versa. However, more research will be required for discriminating the effect of moisture on R and C elements of aged oil-paper systems.
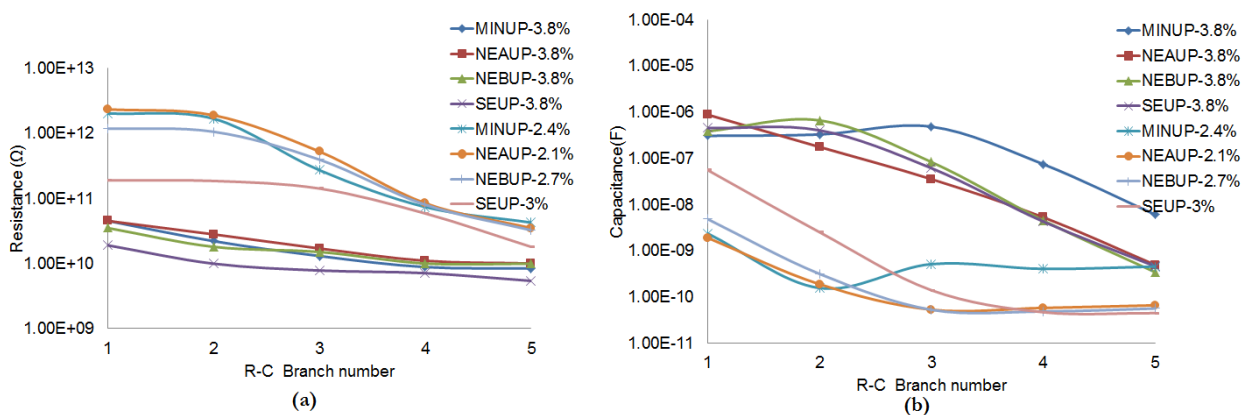
Figure 7.17. Equivalent circuit model parameters (a) Resistance (b) capacitance

This research hypothesises that relaxation of induced temporary dipoles in the solid phase of oil impregnated pressboard insulation may follow Williams-Watts stretched exponential function. Thereby, depolarisation current response can be represented using eq (6.26) where it is addition of a Debye and William-watt function. The Debye component represents the microscopic interfacial polarisation phenomenon in oil filled cavities.

It can be seen in Figure 7.18 that depolarisation current response of all types of oil impregnated pressboard insulation can be accurately modelled using eq (6.26). A comparison of modelled and

measured depolarisation current responses for samples MINUP-3.8%, NEAUP-3.8%, NEBUP-3.8% and SEUP-3.8% is presented in Figure A.6 (Appendix A). Calculated model parameters for all types of pressboard insulation at two different moisture levels have been listed in Table 7.7.
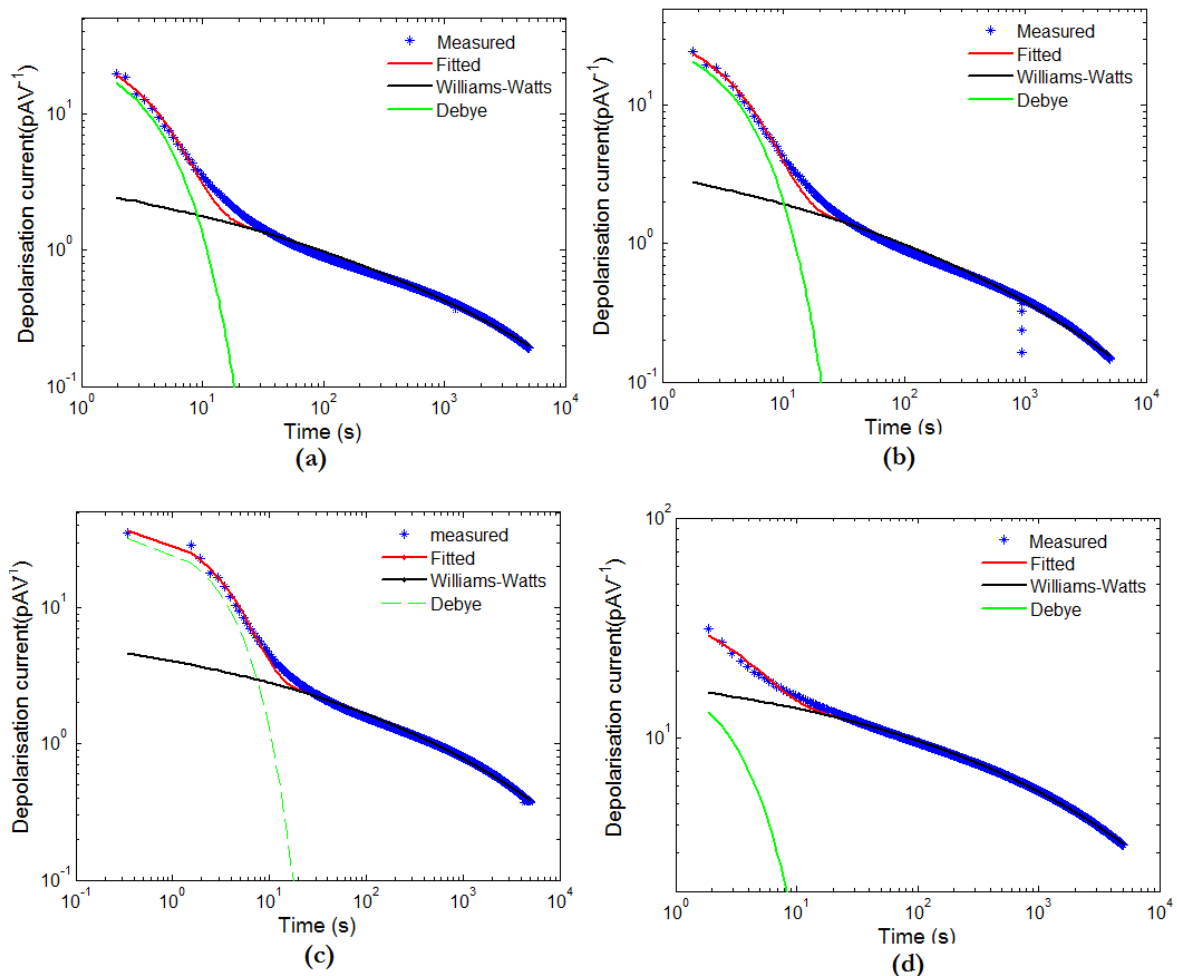
Figure 7.18 Comparison of experimental depolarisation current response with the modelled response using Williams-Watts function (a) MINUP-2.4%, (b) NEAUP-2.1%, (c) NEBUP-2.7%, (d) SEUP-3%

The calculated model parameters indicate that the contribution of a Debye component to the depolarisation current is insignificant when the pressboard insulation has a higher moisture level. These results confirm that dielectric relaxation phenomena in solid phase of oil impregnated pressboard mainly follow the Williams-Watts function. The parameters γ and τ_w of Williams-Watts function significantly change with moisture indicating their applicability in moisture estimation in transformer solid insulation. The variation of γ with moisture shows good consistency and less dependency on diverse oil properties. It means that value of γ nearly follows the magnitude of moisture content in pressboard insulation.

Table 7.7. Modelled parameters to represent depolarisation current with Williams-Watts function

Sample ID	Parameters of Williams-Watt function			Parameters of Debye function	
	$A_w(pA)$	$\tau_w(s)$	γ	$A_{db}(pA)$	$\tau_{db}(s)$
MINUP-2.4%	7.8	0.5	0.14	17.3	4.6
MINUP-3.8%	472	769	0.3	2.5	0.002
NEAUP-2.1%	8.9	0.5	0.15	23.3	4.5
NEAUP-3.8%	318	588	0.3	2.5	0.002
NEBUP-2.7%	8.2	5	0.16	18.3	4.5
NEBUP-3.8%	432	833	0.3	2.5	0.002
SEUP-3%	24.5	142	0.2	22	3.5
SEUP-3.8%	518	416	0.3	5	0.002

7.5 Impact of Ageing on Dielectric Response Behaviour

Figure 7.19 presents the comparison between frequency domain dielectric response of unaged and aged dry pressboard insulation which are impregnated with mineral oil, NEA and NEB. Moisture contents in aged pressboard samples are nearly similar to that of in unaged samples. Thereby, one could attribute any changes in dielectric response pattern in aged pressboard to ageing by-products present in the system. Table 7.8 depicts a comparison of DP values of pressboard insulation at different ageing stages.

Table 7.8. Comparison of DP value of PB aged in different oils

Ageing time (days)	DP value		
	Mineral	NEA	NEB
0	1200	1200	1200
28	495	640	625
48	350	481	432
84	298	458	338

Figure 7.19 shows that FDS responses of all three types of aged samples qualitatively resemble unaged dry pressboard such that it can be identified by two major relaxation processes in the frequency range 10^{-4}-10^3 Hz. They are loss peak due to charges blocking at the microscopic interfaces of oil filled cavities and q-dc effect due to the presence of thermally activated hopping charge carriers in the system [251].
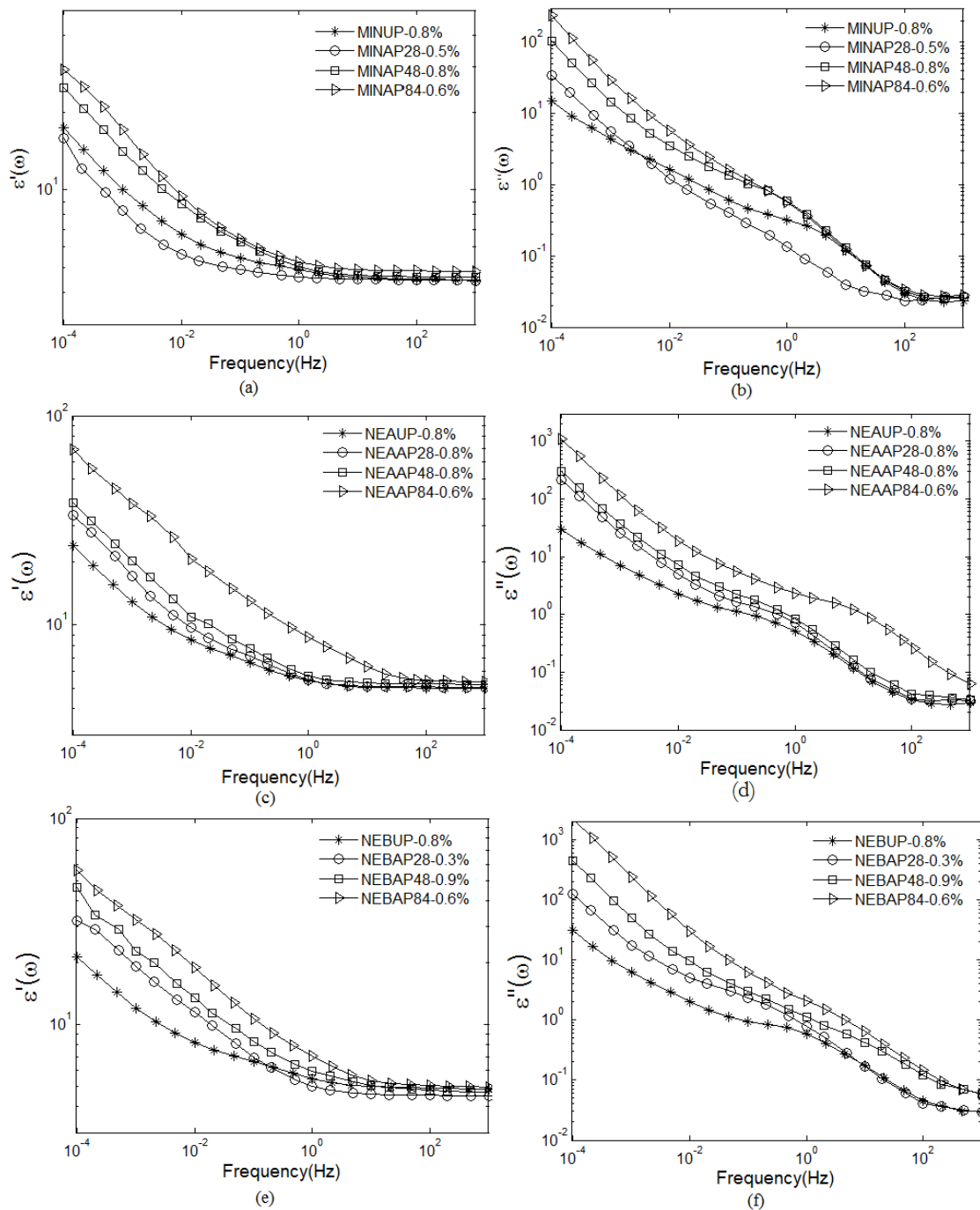
Figure 7.19. Comparison of the impact of ageing on FDS of PB insulation (a)-(b) aged in mineral oil (c)-(d) aged in NEA, (e)-(f) aged in NEB

Figure 7.19 (a) and (b) indicate that the complex permittivity of mineral oil impregnated pressboard shows a clear tendency to increase with ageing particularly at low frequencies, whereas local maxima in loss part of the sample MINAP28-0.5% has diminished. This behaviour is possibly due to evaporating of mineral oil in that specimen during the vacuum drying process, since mineral oil has a relatively low boiling point. However, with further ageing, radicals are formed on the cellulose surface and facilitates to chemically attach low molecular weight oil molecules [177] avoiding them

from evaporating during the process of vacuum drying. Thus, a pronounced loss peak behaviour is visible in FDS of samples MINAP48-0.8% and MINAP84-0.6%.

Figure 7.19 (c)-(f) shows that oil dependent loss peak of both types of NE impregnated samples becomes prominent with ageing. Moreover, the increase of imaginary and real permittivity at low frequencies which represents the strength of q-dc and DC conduction effects in combination is of paramount significance in pressboard insulation aged in NE oils compared to that of pressboard insulation aged in mineral oil. If one compares the dielectric responses of 84 days aged samples, it can be clearly identified that both real and imaginary permittivities of samples aged in NEs are several orders of magnitude greater than those of samples aged in mineral oil at low frequencies. However, they possess almost the same moisture content and a low degree of ageing compared to the sample aged in mineral oil. Thus, one can clearly claim that ageing of oil-pressboard composite insulation intensifies both the conduction and polarisation phenomena in pressboard insulation in a way similar to moisture does and this effect is of paramount significance in NE–pressboard systems.

A myriad of polar and conductive substances, particularly low molecular acids and soots are produced during ageing of oil-pressboard insulation [60, 61]. These by-products mostly reside in pressboard insulation and mainly enhance the q-dc and conduction effects giving a higher imaginary and real permittivity at low frequencies. However, a considerable concentration of ageing by-products is needed for a contribution comparable to that of moisture. Thus, this research does not totally ascribe to the increase of polarisation and conduction phenomena in aged pressboard to ageing by-products.

With ageing, cellulose fibres are significantly destroyed and become much shorter and thinner [250]. This results in formation of large oil filled cavities and conductive oil paths across the sample. Thus, one can assume that penetration of high conductive aged oil into pressboard with ageing also causes to intensify both conduction and polarisation phenomena. It is generally accepted that NE insulating oils are highly oxidation susceptible and oxidation of NE oils produces gummy waxes. These waxes deposit on the wall of cellulose fibres and it enhances the long range charge transport along the surfaces of fibres [114]. This may also be a cause for having higher conduction and polarisation phenomena in pressboard aged in NE than that of aged in mineral oil.

Figure 7.20 (a) shows that there is an exponential relationship between σ_{dc} calculated using eq (7.6) and reciprocal of DP of pressboard insulation aged in both mineral and NE oils. 1/DP represents the degree of ageing because it is proportional to the number of chain scissions. Established

relationships confirm that pressboard insulation aged in NEs possess higher σ_{dc} than that of mineral oil impregnated pressboard insulation at a similar degree of ageing.
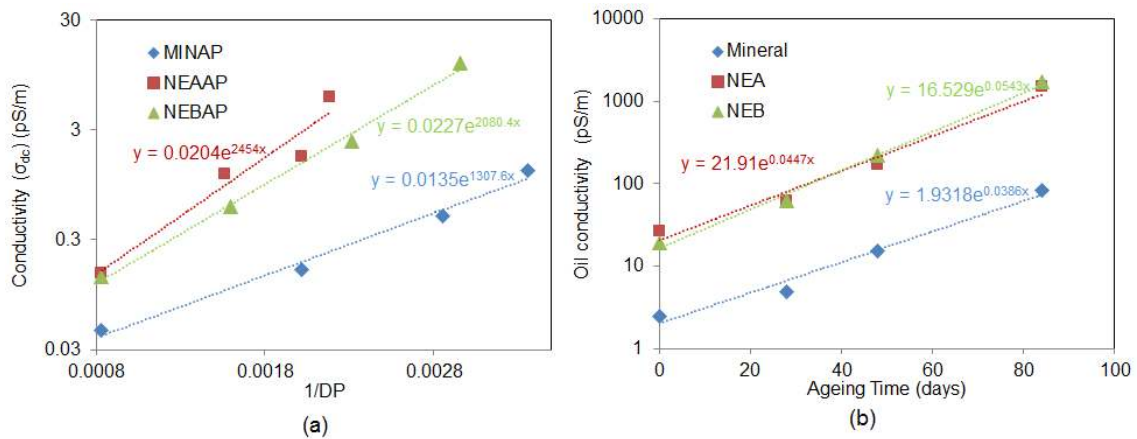
Figure 7.20. (a) Change of σ_{dc} of PB over ageing, (b) Change of oil conductivity over ageing

Figure 7.20 (b) shows that oil conductivities also increase exponentially with ageing time. The increasing trend of conductivities of NEA and NEB oils is almost the same and their conductivities at 1984 hrs of ageing are about 20 times higher than that of mineral oil with a similar ageing time. Thus, one could claim that exponential increase in σ_{dc} of dry aged pressboard insulation is mainly caused by penetration of high conductive oil into a destroyed cellulose structure. This hypothesis is confirmed by the fact that calculated σ_{dc} values presented in Figure 7.20 (a) nearly follow the order of the magnitude of the oil conductivity in the pressboard. Moreover, in this case contribution of low molecular acids to σ_{dc} can be neglected because of the fact that they could have evaporated during the process of vacuum drying.
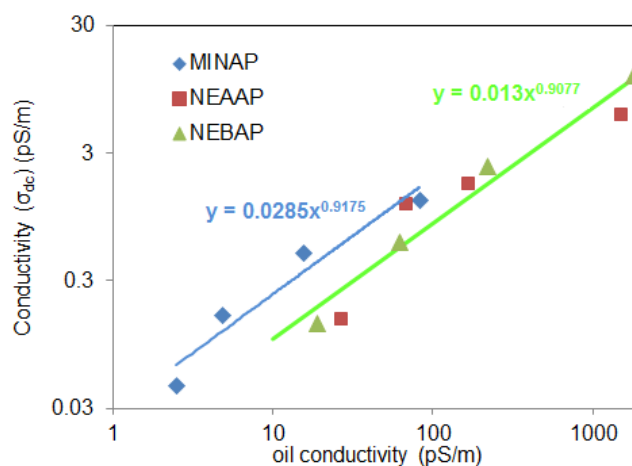
Figure 7.21. Relationship between oil conductivity and σ_{dc} of PB

Figure 7.21 shows that contribution of oil conductivity to σ_{dc} can be explained with a power law equation for both mineral oil and NE impregnated pressboard insulation. Thus, this research

proposes an improved model as eq (7.11) for moisture diagnostic of mineral and NE oil based insulation systems using low frequency conductivity (σ_{dc}). The value of S for mineral and NE impregnated pressboard insulation is 2.85×10^{-2} and 1.3×10^{-2} respectively and ς possesses values of 0.92 and 0.91. S and ς are the parameters of the power law relationship which correlate the σ_{dc} of aged dry pressboard insulation and oil conductivity.

$$\sigma_{dc}(T,m) = \psi_0 e^{\frac{-E_{\psi a}}{K}(1/T_0 - 1/T)} e^{\left(\frac{11.5m}{(m+3)^{0.33}(m+6)^{0.33}}\right)} + S(\sigma_{oil})^\varsigma \qquad (7.11)$$

7.6 Combined Effect of Moisture and Ageing on FDS

Figure 7.22 (a)-(c) compare the influence of moisture on FDS behaviour of the pressboard samples aged in mineral oil, NEA and NEB respectively. It can be clearly identified that influence of moisture on dielectric response of aged pressboard qualitatively resembles that of unaged pressboard insulation. It means no additional relaxation process arises in the system.
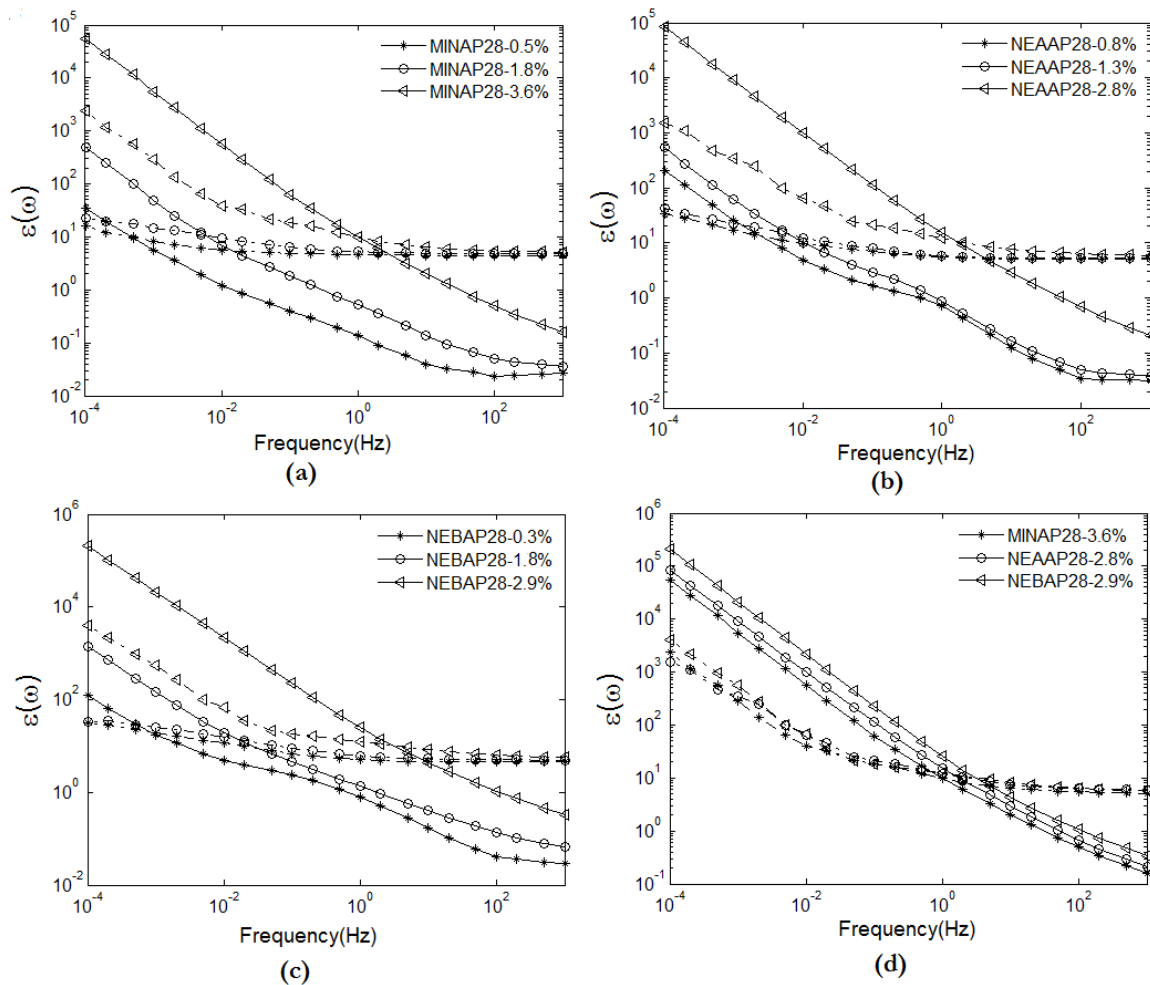
Figure 7.22. Impact of moisture on FDS of aged PB (a) MINAP28 (b) NEAAP28 (c) NEBAP28 (d) 28 days aged PB with relatively high moisture contents

If one compares the results shown in Figure 7.22 (a)-(c) with FDS data of corresponding un-aged pressboard specimens shown in Figure 7.7 and A.1, it clearly indicates that the effect of moisture on FDS of aged PB is greater than that of un-aged pressboard insulation. This effect is of paramount significance for pressboard aged in NEs. It has already been mentioned in section 7.3 that moisture itself enhances both polarisation and conduction effects in pressboard insulation. This study proposes that there is a synergetic effect of moisture and ageing by-products on FDS response of aged pressboard insulation. It means that moisture causes to dissociate low molecular acids and ionic impurities which are mostly available in aged pressboard. This behaviour increases charge density in the system with moisture and intensifies the conduction and polarisation phenomena giving larger value to real and imaginary permittivities at low frequencies for aged pressboard insulation with relatively high moisture contents.

Figure 7.22 (d) compares the dielectric responses of relatively wet pressboard samples aged in mineral, NEA and NEB oils. It indicates that mainly dielectric loss component of pressboard specimen aged NEs is greater than that of the pressboard specimen aged in mineral oil. On the other hand, moisture content of wet mineral oil impregnated pressboard specimen is about 0.7% greater than that of NE impregnated aged pressboard specimens considered here. This case demonstrates that enhancement of conduction phenomenon in NE impregnated pressboard insulation due to dissociation of ageing by-products in water is more prominent than that of pressboard insulation aged in mineral oil. Thus, one can claim that ageing of NE-paper composite material produces more water soluble conductive substances than ageing of mineral oil-paper insulation system leading to higher conduction effect. It means synergism of ageing by-products and moisture is more effective in NE-paper systems.

Table 7.9. Estimated moisture content in moderately wet aged PB using σ_{dc} based model

Sample ID	Estimated moisture content (%)	Error
MINAP28-1.8%	1.8	0.0
MINAP28-3.5%	3.8	0.3
NEAAP28-1.3%	1.3	0.0
NEAAP28-2.8%	3.6	0.7
NEBAP28-1.8%	1.9	0.1
NEBAP28-2.9%	3.8	0.9

This research investigates the effect of this synergism on σ_{dc} based moisture diagnostic model given eq (7.11) when the moderately aged pressboard insulation contains relatively high moisture contents. The results shown in Table 7.9 confirm that though the effect of oil conductivity has been considered in eq (7.11), it overestimates the moisture content of moderately aged pressboard

insulation. This behaviour is of paramount significance for NE impregnated wet aged pressboard such that estimated moisture content of samples NEAAP28-2.8% and NEBAP28-2.8% is 0.7 % and 0.9 % respectively higher than the actual value. On the other hand, one can claim that the proposed improved σ_{dc} base model estimates the moisture content in all types of aged samples with reasonable accuracy when their moisture content is less than 2 %.

7.7 Effect of Temperature on FDS

7.7.1 Unaged pressboard insulation

Figure 7.23 presents the dielectric response as $\varepsilon(\omega)$ vs. frequency for mineral and NEA impregnated pressboard insulation with two different moisture levels at three distinct temperature points of 35, 55, and 75 ºC.
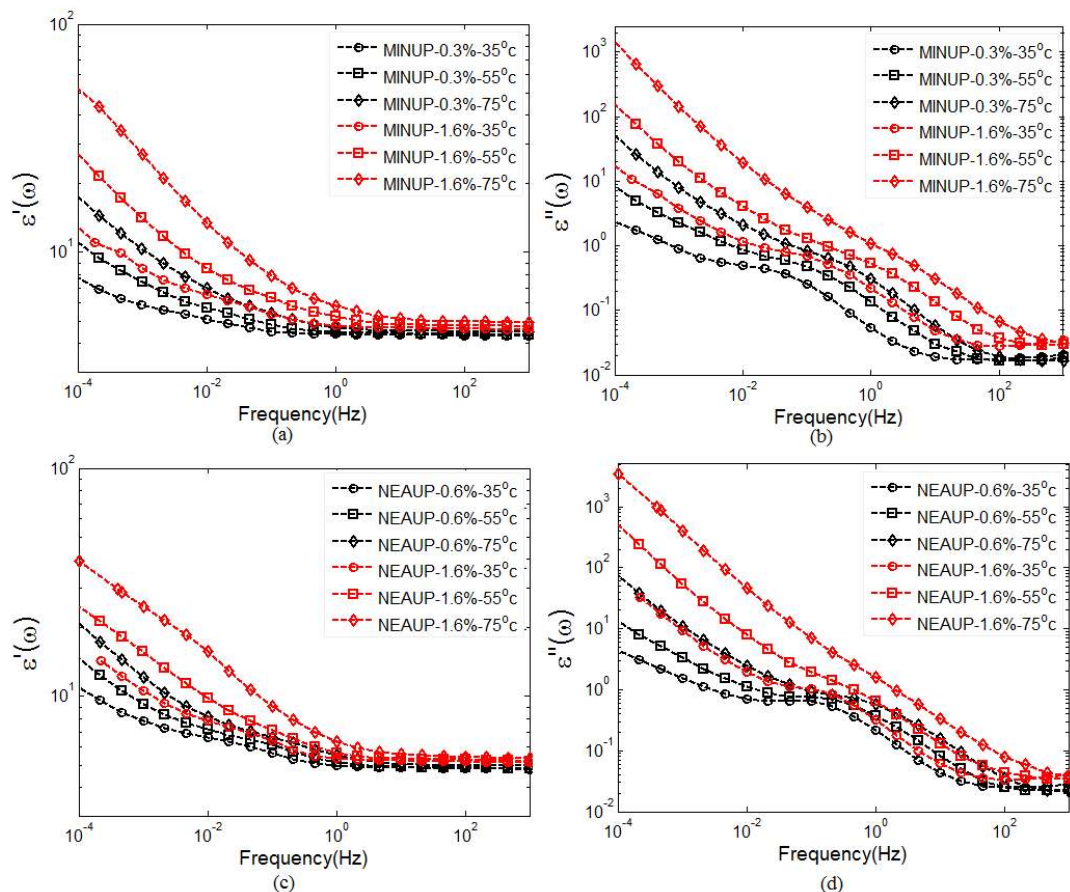
Figure 7.23. Temperature dependence of FDS responses (a) Real permittivity of MINUP, (b) Imaginary permittivity of MINUP, (c) Real permittivity of NEAUP, (d) Imaginary permittivity of NEAUP

Figure 7.23 manifests that temperature largely influences the dielectric response by increasing dielectric polarisation and conduction phenomena in pressboard insulation analogous to how moisture and ageing do. Thus, increasing of the measurement temperature shifts the dielectric

response along the frequency axis toward higher frequency. Pressboard insulation samples impregnated with NEB and synthetic ester also show similar behaviour with increasing temperature (refer Figure A.7 in Appendix A).

The increase of polarisation and conduction effects with temperature is caused by two superimposed effects: increase in hopping charge carrier density and increase in the mobility of charge carriers residing in pressboard insulation [199]. Self-dissociation of water molecules and ionic impurities in oil at high temperature mainly contributes to enhance the charge carrier density in the unaged pressboard insulation. Charge carrier hopping between localised sites which are created by the adjacent water molecules is the main mechanism of long range charge transport in pressboard insulation. The frequency of charge transfer between such sites increases with temperature due to the raising of thermal vibration of mobile charge carriers in the system. Subsequently, this phenomena increases charge carrier mobility in the system leading to higher conduction and polarisation effects.

Though, the amplitude and characteristic frequency of relaxation processes can be expected to be temperature dependent, the spectral shape of the frequency response of a given material does not usually change with temperature as shown in Figure 7.23, unless the material alters its structural organisation significantly [110]. This allows normalising of frequency responses obtained at different temperature points on to a reference temperature to form a master curve. When all relaxation processes in the observed frequency range have the same physical origin, the frequency shift required to form the master curve can be characterised by an equation of Arrhenius type with single activation energy E_a as in eq (3.29). On the other hand, when they have different physical origins, different activation energy values are needed [29]. Thus, it is clear that activation energy is the factor which reflects the temperature dependence of dielectric response.

Figure 7.24 indicates that low and high frequency regions of FDS of samples MINUP-0.3% and MINUP-1.6% should be shifted at two different rates in the lateral direction to obtain the master curve at the reference temperature of 35 ℃. Similar behaviour has been observed for samples MINUP-0.8%, NEAUP-0.6%, NEAUP-0.8%, NEAUP1.6%, NEBUP-0.8%, NEBUP-1.1%, NEBUP-1.6%, SEUP-0.6% and SEUP-1%.

This study calculates the equivalent circuit model parameters for dielectric response of those samples at different temperatures. Then it has been identified that frequency shift of ω_p and σ_2 for the above mentioned pressboard samples to obtain a master curve can be evaluated using eq (3.29) with activation energy values in the range of 0.45-0.55 eV. On the other hand, frequency shift of q-

dc relaxation and σ_1 need higher activation energy. This confirms that when the moisture content is low, clusters associated with oil filled cavities could govern the DH loss peak relaxation and short range ion transport mechanisms in oil impregnated pressboard as explained in section 7.4. Thus, one can claim that DH loss peak relaxation and σ_2 may have low activation energy as these are consequences of ion transport in the liquid phase. This is suggested based on the calculated activation energy of nearly 0.5 eV, which is close to the activation energy of oil conductivity in Chapter 5 [124]. On the other hand, q-dc relaxation and σ_1 may have higher activation energy as they are consequences of charge transport along convoluted paths in the solid phase. Moreover, in all other cases frequency shift required to form the master curve can be characterised by single activation energy.
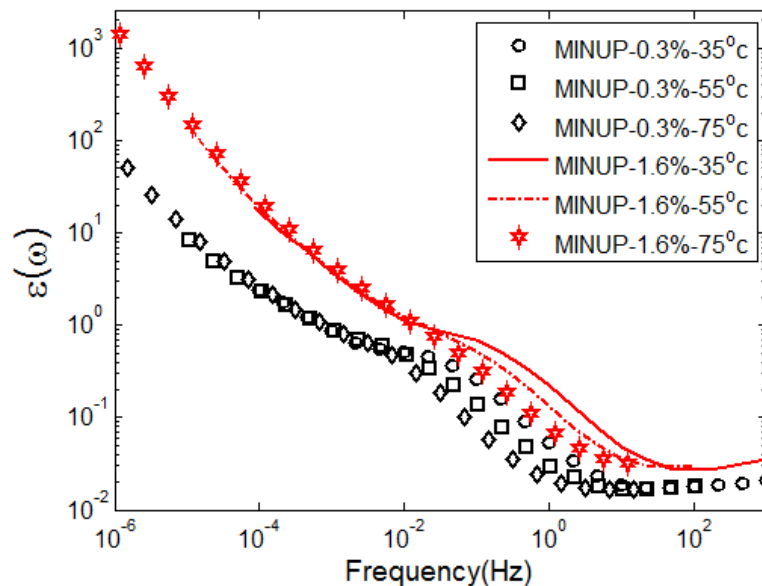
Figure 7.24. Master curve $\varepsilon''(\omega)$ with single frequency shift

Figure 7.25 compares activation energy for frequency domain dielectric response of different types of oil impregnated pressboard insulation considered in this research at various degrees of humidity. In the case of specimens MINUP-0.6%, MINUP-0.8%, etc. activation energy corresponding to low frequency region of FDS is considered. In all types of oil impregnated samples, the initial increase of moisture causes activation energy to first increase and then decrease to about 0.7 eV when the moisture content is high as 8 %. Thus, one can hypothesise that when moisture content of pressboard insulation is very high; the charge transport in the system is close to the nature of bulk water because conductivity of water corresponds to an activation energy of 0.44 eV. In the case of mineral oil impregnated pressboard, activation energy changes in the range 1-1.1 eV for samples

containing a moisture level of less than 4%. These results show good agreement with data presented in [124] confirming accuracy of our experimental results.
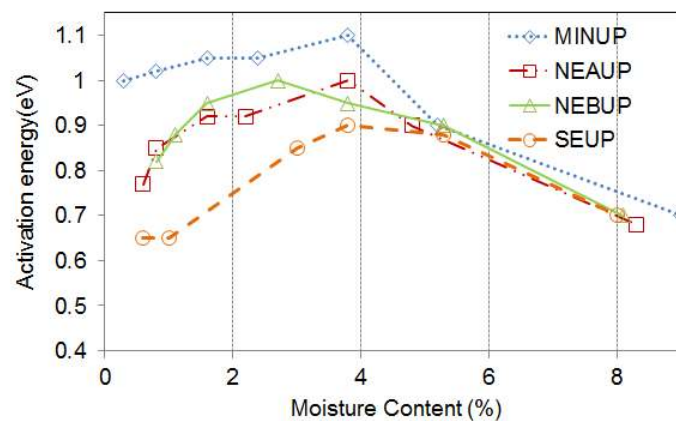
Figure 7.25. Change of activation energy with moisture

The noticeable fact that can be seen in Figure 7.25 that activation energy values of natural and synthetic ester impregnated pressboard insulation are lower than that of mineral oil impregnated pressboard when they have a moisture content of less than 4 %. In unaged pressboard specimens, water is the key factor, which governs both the polarisation and conduction effects. It is generally accepted that when pressboard has low moisture content, water molecules are strongly bound to the OH groups of cellulose chains. As mineral oil possesses hydrophobic characteristics, it does not change the physical state of water in the system. On the other hand, ester molecules easily form hydrogen bonds with free water, causing a significant concentration of moisture in the oil medium. Therefore, one could hypothesise that due to strong electrostatic attraction of OH groups in cellulose polymer, proton mobility along the cellulose fibre surface via strongly bonded water molecules is lower than that via water molecules in ester oil medium. This may lead to low activation energy of ester impregnated pressboard insulation when a sample contains low moisture. Since synthetic esters are more hygroscopic than NEs, this effect is more significant for synthetic ester impregnated pressboard. For example activation energy of low frequency response of sample SEUP-0.6% and SEUP- 1% is 0.65 eV. Moreover, this value is closer to the activation energy of liquid water.

At high moisture content (M >4%) all the samples have the same activation energy. It indicates that in this condition the activation energy is governed solely by the connections of the water system in solid medium.

7.7.2 Aged pressboard insulation

This research has identified that dielectric responses of aged mineral oil, NEA and NEB impregnated pressboard specimens require two lateral shifts in order to obtain a master curve when their moisture content is below 2%. Moreover, activation energy corresponding to characteristic frequency of oil dependent loss peak is in the range 0.35-0.6 eV for all cases. In the case of FDS response of a transformer insulation system, dielectric response behaviour of pressboard insulation at high frequencies is less significant. Thereby, this research analyses the temperature dependence of FDS for aged pressboard insulation using activation energy corresponding to the low frequency region.

Figure 7.26 (a) compares the temperature dependence of dielectric response of dry aged pressboard insulation over thermal ageing. In order to identify the influence of moisture on temperature dependence behaviour of aged pressboard insulation, activation energies of 28 days aged pressboard samples at three different moisture levels have been calculated and presented in Figure 7.26 (b). Figure 7.26 (a) manifests that initial ageing gives rise to activation energy leading to a stronger temperature dependence behaviour and further ageing results in lowering that effect. This behaviour is of paramount significance for pressboard aged in NEA in such a way that activation energy of 84 days aged samples is 0.5eV. The reduction of activation energy can be correlated to the ageing process such that intra and inter-fibre contacts are broken allowing aged conductive oil penetration between the fibres [255]. Thereby, ions transport in aged pressboard insulation could be governed by their movement in the oil reducing the activation energy towards that of oil conductivity.
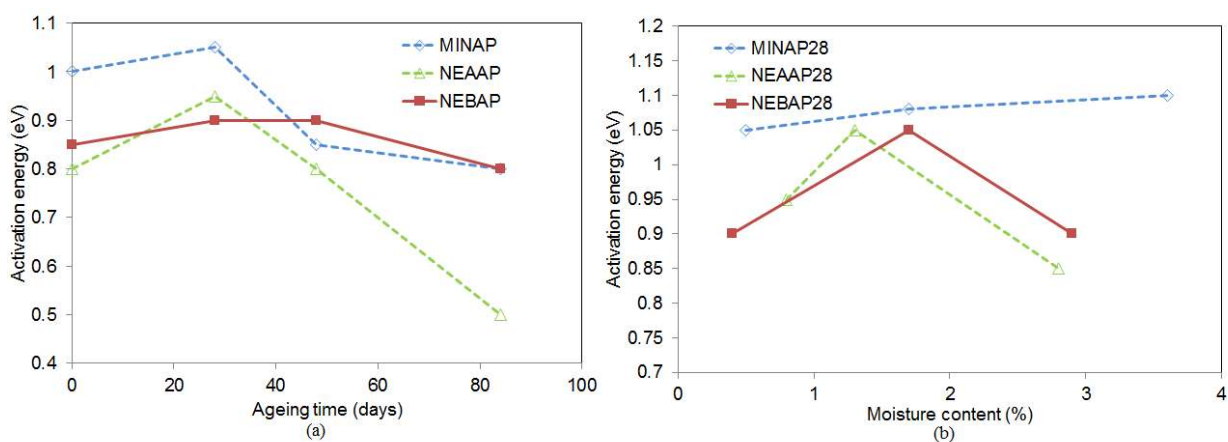
Figure 7.26. (a) Change of activation energy over thermal ageing, (b) Effect of moisture on activation energy of aged PB

As shown in Figure 7.26 (b) one can assume that the influence of moisture on the temperature dependence characteristic of moderately aged mineral oil impregnated pressboard resembles that of unaged pressboard insulation. Moreover, a higher activation energy value indicates that the temperature dependence of aged mineral oil impregnated pressboard insulation is stronger than that of both NEA and NEB impregnated pressboard insulation at a similar degree of ageing and moisture level.

7.8 Applicability of Commercially Available FDS Based Moisture Diagnosing Tools on Ester Oil Based Insulation Systems

7.8.1 Overview to method of moisture analysis

The prime concern of FDS measurement is to determine the moisture content in the solid insulation of transformers without obtaining a paper sample which is known as a destructive method. In a particular transformer, comparison of FDS responses acquired at regular intervals provides a better understanding on change of moisture content in the solid insulation. However, most of the commercialised tools propose a different approach to determine moisture content in a transformer solid insulation using FDS measurement. In this regime, the measured frequency domain response of a transformer is compared with a modelled response which is obtained using FDS responses of paper based insulation with known physical conditions such as moisture and degree of ageing.

This section discusses the applicability of a commercialised FDS based moisture diagnosing tool namely MDOS which has been established for mineral oil-paper insulation systems on ester-paper insulation systems. In order to determine moisture content in solid insulation, MDOS software requires measurement temperature and geometrical parameters of the insulation system (X and Y). This software characterises the effect of temperature on FDS behaviour of paper and oil insulation with two different activation energy values of 0.9 eV and 0.4 eV respectively. Experimental data reported in Chapter 5 indicates that activation energy of 0.4 eV is reasonable to represent the temperature dependence of FDS of all types of insulating oil. However, based on results of [124] and our experiments, we have utilised an activation energy of 1 eV for paper based insulation.

Due to a limited number of ester filled transformers in the Australian power system and the difficulty of accessing those units, field measurements in this research were hampered. Therefore, a set of data was obtained using FDS response data of aged and unaged pressboard insulation with a moisture content of less than 4% and so-called X-Y model [141]. In this study, we have selected values of 30 % and 20 % for parameters X and Y respectively. Then simulated data has been analysed using MDOS tool by setting all parameters including oil conductivity, permittivity, X and

Y to simulated values, for example, *X* is 30 % and *Y* is 20 %. Moreover, permittivity of esters set to 3.2 and a value of 2.2 is used as permittivity of mineral oil.

7.8.2 Unaged oil-paper system

Figure 7.27 presents a comparison of moisture diagnostic results for unaged oil-paper systems using the MDOS tool and Karl Fischer titration (KFT). This research performs KFT on two pressboard samples from each batch and average moisture content is reported. Thereby, one can assume that KFT method determines the exact moisture content of a pressboard sample.
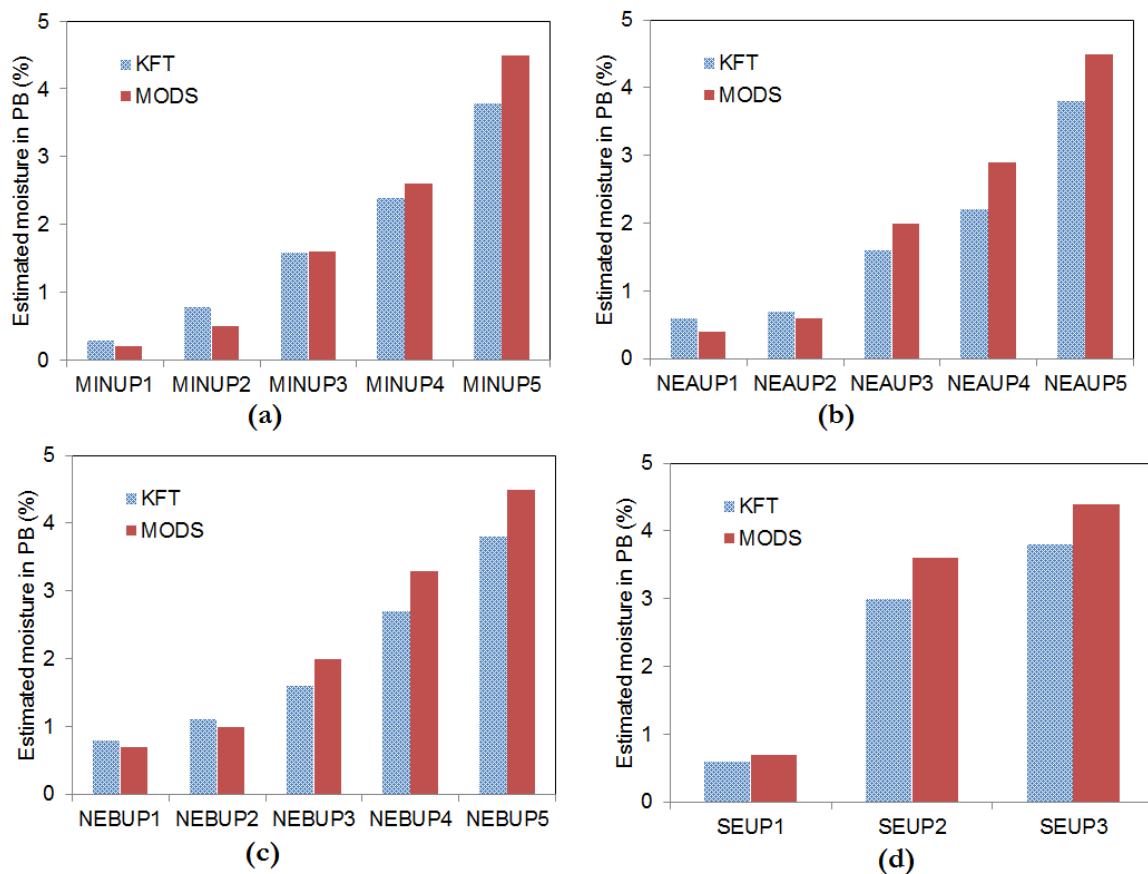
Figure 7.27.Comparison of the estimated moisture content in unaged PB insulation with KFT method and MDOS tools (a) Mineral oil impregnated (b) NEA impregnated (c) NEB impregnated (d) Synthetic ester impregnated

It can be seen in Figure 7.27 that the MDOS tool estimates the moisture content in mineral oil impregnated pressboard insulation with reasonable accuracy except sample MINUP-3.8%. Moreover, despite higher conduction and polarisation effects, the MDOS tool estimates the moisture content in relatively dry ester impregnated pressboard insulation with good accuracy. On the other hand, moisture contents in moderately wet ester impregnated samples are overestimated by the MDOS software. The maximum difference of estimated moisture contents is +0.7 %, +0.6 % and +0.6 % for samples NEAUP-2.2%, NEBUP-2.7% and SEUP-3% respectively. Moreover, the

estimated moisture content in all the samples with 3.8% of moisture is 0.6-0.7 % higher than the actual value indicating low accuracy of the MDOS tool when diagnosing wet insulation systems irrespective of the type of oil in the system.

7.8.3 Aged oil-paper systems

In the case of aged pressboard insulation, more than one sample with different moisture content and similar ageing condition has been considered for some cases. Thus, x, y and z are used in sample names to denote samples with different moisture level and similar ageing condition. Figure 7.28 indicates that estimated moisture content of 28 days and 48 days aged mineral oil impregnated pressboard insulation using MDOS software are quite similar to actual moisture contents except that of MINAP28-x (3.6 %). On the other hand, the estimated moisture content in 84 days aged mineral oil impregnated samples are significantly larger than the actual values (0.5 %, 0.6 %) in spite of the fact that there is no large difference in degree of ageing of 48 days and 84 days aged samples. However, there is a large increment in oil conductivity during 48 to 84 days (refer Figure 7.20). It implies that though MDOS has been implemented for mineral oil–paper insulation systems, special care must be taken in analysing the moisture content in solid insulation of a mineral oil filled transformer with the MDOS tool when the oil conductivity is high.

	MINAP 28-x	MINAP 28-y	MINAP 28-z	MINAP 48-x	MINAP 48-y	MINAP 84-x	MINAP 84-y	NEAAP 28-x	NEAAP 28-y	NEAAP 28-z	NEAAP 48-x	NEAAP 48-y	NEAAP 84-x	NEBAP 28-x	NEBAP 28-y	NEBAP 28-z	NEBAP 48-x	NEBAP 48-y	NEBAP 84-x	NEBAP 84-y
KFT	0.5	1.8	3.6	0.8	2.5	0.5	1.3	0.8	1.3	2.8	0.8	1	0.6	0.4	1.8	2.9	0.9	2	0.6	1.7
MODS	0.6	1.9	4.6	0.9	2.6	0.9	1.9	1.4	2.1	4.5	1.7	2.1	2.6	1.1	2.6	4.5	2	3.1	2.9	3.3
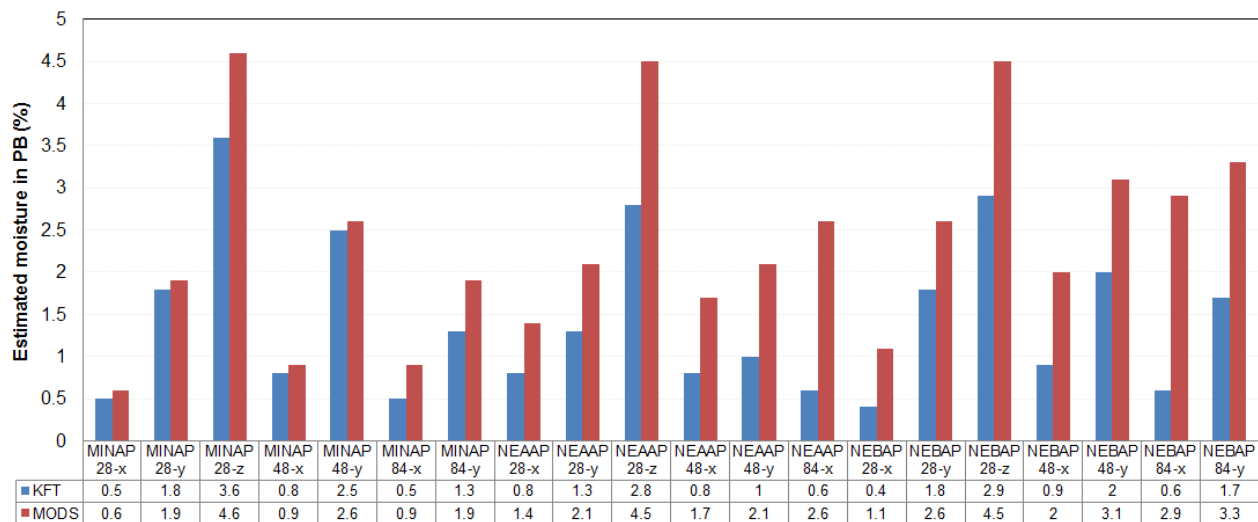
Figure 7.28. Comparison of estimated moisture content in aged PB with KFT method and MDOS tools

It can clearly be seen in Figure 7.28 that MDOS software overestimates the moisture content in aged NE–paper insulation systems. Moreover, the error has an increasing trend with ageing time and it is in the range +0.4 % to +2.2 %. A noticeable fact that can be seen in Figure 7.28 is that the error in estimated moisture content of sample NEAAP84 is significantly greater than that of samples NEAAP48-x and NEAAP48-y in spite of the fact that those samples have almost similar

degrees of ageing as given in Table 7.8. Comparison of diagnostic results corresponding to 84 days and 48 days aged NEB impregnated pressboard insulation also shows somewhat similar behaviour. In both cases conductivities of NE oils have largely increased during this period. It means increase of oil conductivity could be one of main reasons for the increasing trends of error in estimated moisture content using MDOS over ageing time. This is because, high conductive oil penetrates into partially destroyed cellulose structure of aged pressboard and it increases the conductive loss of the pressboard in a way similar to the effect of moisture. Overall, one can claim that FDS based moisture diagnosing tools established for mineral oil-paper insulation systems are not directly applicable for aged NE–paper insulation systems. Thus, this research proposes to consider the findings and interpretation provided in this chapter when extending FDS based moisture diagnosing tool for ester-paper insulation systems.

7.9 Summary

This chapter compares the dielectric response behaviours of high density pressboard insulation impregnated with mineral and ester insulating oils at different degrees of humidity, ageing and temperatures. In order to determine moisture content in unaged mineral oil, NE and synthetic ester impregnated pressboard insulation, this chapter proposed two universal type of models based on low frequency conductivity (σ_{dc}) and characteristic frequency ($1/\tau_c$) of conductivity response.

In this chapter, the contribution of DC conductivity and different relaxation processes to FDS response of oil impregnated pressboard insulation has been discriminated using an equivalent circuit model defined based on DH cluster theory. Moreover, selected model parameters indicate that high conductivities of ester oils significantly influence both conduction and polarisation effects of pressboard insulation with a moisture content of less than 3%. However, the effect of diverse oil properties diminishes when the moisture level of pressboard insulation is higher than 3% where water oriented charge clusters are formed in pressboard. This chapter has identified that an increase of oil conductivity causes pronounced conduction and polarisation effects in aged pressboard insulation. Thus, an improved σ_{dc} based moisture diagnostic model has been produced by incorporating the effect of oil conductivity. The improved model can be used to accurately estimate the moisture content in an aged pressboard with moisture content of <2%. σ_{dc} based model defined for unaged pressboard insulation characterises the sole effect of moisture on dielectric response and improved model quantify the effect of both moisture and aged oil in pressboard insulation. However, single effect of pressboard ageing by-products on FDS has not been quantified in this thesis.

Experimental results presented in this chapter have revealed that FDS of ester impregnated pressboard insulation possesses low temperature dependent behaviour than that of mineral oil impregnated pressboard insulation. This behaviour is caused by the hygroscopic nature of ester oils. The temperature dependence of FDS has been quantified by calculating activation energy required for constructing a master curve at reference temperature of 35ºC. It is clearly found that activation energy of ester impregnated pressboard insulation is lower than that of mineral oil impregnated pressboard.

At the end of this chapter, it has been verified that FDS based moisture diagnosing tools established for mineral oil-paper systems can be applied on unaged relatively dry ester-paper insulation system. However, their application on aged NE-paper insulation systems will result in misleading interpretation.

Chapter 8

Conclusions and Recommendation for Future Research

8.1 General

In this thesis, a broader understanding of insulation materials used in oil filled transformers including their chemical compositions and degradation mechanisms in a typical transformer operating environment is provided. This thesis has mainly focused on understanding the ageing behaviour of ester-paper composite materials compared to that of mineral oil-paper systems. An extensive literature survey conducted in this research has revealed that cellulose and mineral oil are still the preferred choice for transformer insulation but there is a rising demand for natural and synthetic ester insulating oils, which have a higher fire point and excellent biodegradable characteristics as a substitute for mineral oil. However, the present understanding on ageing behaviour of ester-paper composite insulation systems and knowledge on application of existing condition monitoring tools for ester based insulation are inadequate for cost effective field application. To reduce this knowledge gap, this research has carried out a series of controlled laboratory experiments to understand the behaviour of ester-paper composite insulation in typical transformer operating conditions. Moreover, experimental results have been analysed through the comparisons made based on the limiting values provided in related IEEE and BS standards and properties of mineral oil.

The accelerated ageing experiments conducted in this research have confirmed the longer life expectancy of cellulose insulation materials in NE insulating oils. Moreover, it has been recognised that variation of physical and chemical properties of natural and synthetic ester oils such as DDF, colour and acidity over ageing is completely different to mineral oil. It means that set limits of corresponding parameters defined for mineral oil cannot be used to assess the condition of ester oils. Thus, further research will be required to accurately determine the degree of insulation quality of aged ester oils by measuring their chemical, physical and electric properties.

This research has experimentally verified that dielectric response of mineral and NE insulating oils is mainly governed by their conductivities. Moreover, the conductivities of mineral and NE insulating oils are primarily characterised by two types of ions in the system which have two different ionic mobilities. In addition, it has been observed that temperature dependence of conductivity of both mineral and NE insulating oils (i.e. activation energy) is almost similar and it is in the range 0.37-0.44 eV and 0.36-0.46 eV respectively. This research has recognised that dielectric response measurements of insulating oils are typically subjected to parasitic phenomena such as electrode polarisation and electrode hydrodynamic motion which impede the determination of intrinsic dielectric parameters of oil under test.

FDS and PDC measurements performed on well-defined high density pressboard insulation samples (i.e. moisture and temperature controlled) have revealed that dielectric response behaviour of ester impregnated pressboard insulation qualitatively resembles that of mineral oil impregnated pressboard insulation. It means no additional relaxation process arises in pressboard insulation due to impregnation with ester oil. However, diverse oil properties, particularly high conductivities of ester oils show a significant influence on dielectric response behaviour of pressboard insulation by increasing both conduction and polarisation phenomena.

The work presented in this thesis has mainly concentrated on FDS measurements. This thesis has analysed frequency domain dielectric response data of different types of oil impregnated pressboard insulation under varying moisture, temperature and ageing conditions. Moreover, physical interpretations are provided by considering the diverse properties of oil in the pressboard insulation. The physical interpretations provided in this thesis will be extremely useful to those who are interested in the use of FDS measurements to determine moisture in new and aged ester–paper insulation systems in transformers. Furthermore, this study has used Hamon approximation to calculate the low frequency dielectric response data from measured PDC response and compared with measured data. Both the calculated and measured response agreed very well. It means that measurements have been performed in the linear region.

This research has confirmed that three relaxation processes together with DC conductivity characterise the frequency domain dielectric response of pressboard insulation in the frequency range 10^{-4}–10^3 Hz. The three relaxation processes include β relaxation due to segmental vibration of molecular side groups of cellulose; β_{wet} relaxation caused by cellulose water mixed phase cluster vibration or due to microscopic interfacial polarisation at the interface of oil filled cavities and q-dc relaxation process at low frequencies. When a pressboard insulation sample contains a moisture level of less than 3 %, it possesses weak q-dc behaviour.

The experimental results presented in this thesis have confirmed that moisture, ageing and temperature largely influence the FDS of pressboard insulation by increasing both polarisation and conduction effects. The effects of these factors on FDS of mineral, NE and synthetic ester oil impregnated pressboard insulation are quantitatively different. For example a pressboard insulation sample aged in NE possesses higher conduction and polarisation effects than samples aged in mineral oil under the same conditions.

8.2 Main Findings and Contribution

> **Life advantage of cellulose insulation in natural ester**

Accelerated ageing experiments performed with wet pressboard insulation in mineral oil, NEA and NEB indicates that the reaction rate corresponding to ageing of pressboard insulation in mineral oil is 1.75 and 1.55 times higher than that of in NEA and NEB respectively. This research confirms that this advantage of NE is mainly caused by high moisture solubility and hydrolytic degradation of NE oils. Moreover, it has been identified that long chain fatty acids produced by hydrolytic degradation of NE are not detrimental to pressboard insulation. Moreover, they show a protective behaviour to cellulose insulation via trans-esterification. Measured FTIR spectra on pressboard samples aged in NE has confirmed the esterification of fatty acids with cellulose.

> **Assessing the quality of NE insulating oils with their physical and chemical properties**

This research pointed out that acidity and colour of NE oils increase rapidly due to pronounced hydrolytic degradation in a moisture rich environment. For an in-service transformer, moisture in its paper insulation can increase to about 2 % after 10-15 years of operation. In such a situation rapid increase in acidity and colour change of NE insulating oil will be expected. Moreover, retrofilling of an in-service transformer with NE oil could also create a similar environment. Thus, in this type of condition acidity and colour change with existing set limits in the standards cannot be utilised to determine the suitability of in-service aged NE insulating oil for further use. On the other hand, experimental results presented in this thesis have confirmed that DDF, viscosity and dielectric breakdown voltage collectively can indicate the overall condition of NE insulation oils which have been subjected to hydrolytic degradation. Moreover, it is proposed to increase the set limiting values given for acidity of serviced aged NE oils.

> **Assessing degree of ageing of pressboard insulation with FTIR technique**

Experimental results presented in this thesis have shown that absorbance intensity of FTIR spectra of pressboard insulation in the frequency band 1500-500 cm^{-1} gradually decreases over thermal ageing regardless of the type of impregnated liquids. This spectral band primarily represents the vibration of molecular bonds in the cellulose polymer chain. Therefore, reduction of absorbance

intensity peaks in this spectral band can be assigned to the reduction of particular bonds in the cellulose polymer due to a decrease in degree of polymerisation of pressboard insulation over ageing. This changing pattern of FTIR spectra of pressboard insulation with reduction of DP provides an indication about novel ways of monitoring solid insulation in an oil filled transformer using a FTIR sensor.

➢ **DGA analysis of natural and synthetic ester**

This research identified that similar fault gases are produced in mineral, NEs and synthetic ester insulating oils. However, there are significant quantitative differences between fault gases generated in ester and mineral oils due to the difference in their molecular structures. In spite of different gassing behaviour of mineral and ester insulating oils, this research has confirmed that extended Duval triangle and IEC gas ratio methods can be applicable for diagnosing low temperature overheating and electrical discharge faults in ester insulating oil. In addition, this research has recognised that ethane is the key fault gas dissolved in NE insulating oil for low temperature overheating faults. Since ethane is mainly produced by a reaction between linolenic acid (present only in NEs) and oxygen, this research proposes ethane as an indicator for NE insulating oil oxidation and as an early warning trigger before oil quality is affected.

➢ **Avoid cold trap in ageing experiment**

This research has observed that dry pressboard insulation aged in mineral oil shows similar resistance to ageing as in natural and synthetic ester insulating oils in spite of the fact that ester insulating oils are far more hygroscopic than mineral oil. This research has understood that this behaviour is caused by a cold trap naturally occurring at the top of the ageing tubes. Therefore, this thesis proposes to consider this effect in designing future laboratory experiments.

➢ **Modelling the electrode polarisation phenomena and calculate ionic mobility in oil**

This thesis proposes two new models for characterising the frequency and time domain dielectric response data of insulating oils based on the charge transport phenomenon at the electrode interface. The equivalent circuit proposed in this thesis clearly explains the low frequency dispersive behaviour of FDS of insulating oil as a consequence of partly blocked electrode. Moreover, such behaviour cannot be described with existing models which used to explain electrode polarisation phenomena. The exponential model deduced in this research to represent the polarisation current response of insulating oils allows to discriminate the types of ions in the system and calculates the mobility of corresponding ions. It has been identified that both mineral and NE oils mainly have two different types of ions with different ionic mobilities.

➢ **Modelling the dielectric response behaviour of pressboard insulation**

This thesis has proposed a new equivalent circuit based on DH cluster framework theory to explain the frequency domain dielectric response behaviour of pressboard insulation. It allows us to discriminate the contribution of different relaxation processes and DC conductivity to dielectric response. Moreover, the equivalent circuit parameters clearly explain the effects of moisture and diverse oil properties on conduction and polarisation phenomena of pressboard insulation. Overall, the proposed circuit improves the understanding of the physics of microscopic level charge transport and polarisation processes that arise in the system. Through analysing the FDS data with the proposed equivalent circuit, it has been realised that oil oriented charge clusters govern the dielectric response behaviour of pressboard insulation when the moisture content is less than 3%. On the other hand, water based charge clusters determine the dielectric response behaviour of pressboard insulation with moisture content of greater than 3 %. It means the effect of diverse oil properties on dielectric response is masked by the dominant effect of moisture at such a high moisture level.

➢ **Guide to moisture analysis in ester based system using FDS**

In order to determine moisture content in unaged mineral oil, NE and synthetic ester impregnated pressboard insulation, this thesis has proposed a universal type of model based on low frequency conductivity (σ_{dc}) and characteristic frequency ($1/\tau_c$) of conductivity response. Moreover, σ_{dc} based model has been improved by considering the contribution of oil conductivity to low frequency conductivity. It has been verified that improved σ_{dc} based models can be used for moisture diagnosing in moderately aged mineral oil-paper and NE-paper insulation systems with reasonable accuracy when the paper insulation contains a moisture content of less than 2%. However, the synergetic effect of moisture and ageing by-products on conduction and polarisation phenomena in aged pressboard causes a large error in estimated moisture content using the improved σ_{dc} based model when the pressboard insulation contains higher moisture. This research proposes that dissociable ageing by-products in aged oil in the pressboard play a major role for this synergetic effect. Thereby, it is worth determining the relationship between ψ factor (corresponds to σ_{dc} model) and oil conductivity in future experiments. Subsequently, σ_{dc} based model with modified ψ factor can be utilised as an alternative method to accurately determine the moisture in aged oil–paper systems.

Experimental results presented in this thesis have shown that FDS of ester impregnated pressboard insulation has a different temperature dependence behaviour compared to that of mineral oil impregnated pressboard insulation due to the hygroscopic nature of ester oils. That is activation

energy of ester impregnated pressboard insulation is lower than that of mineral oil impregnated pressboard. Importantly this fact should be considered when the available FDS based moisture analysis software is extended to ester oil-paper insulation systems.

In this thesis, it has been verified that the FDS based moisture diagnosing tool established for mineral oil-paper system namely MDOS can be used with unaged relatively dry ester-paper insulation system. However, application of MDOS on aged NE-paper insulation system will result in misleading interpretation due to a large positive error in estimated moisture content.

8.3 Future research

This research proposes a number of recommendations for future research as below:

➢ **2-FAL as an ageing indicator in natural ester based insulating systems**

This research proposes that oxidation inhibitors and higher acidity levels of aged NE insulating oils have a significant influence on the thermal stability of 2-FAL and partition of 2-FAL between paper and oil insulation. Thus, it is recommended to study thermal stability and partition behaviour of 2-FAL in NE insulating oils.

➢ **Methanol as an ageing indicator in ester based insulating system**

Rupturing of 1, 4-β glycosidic bonds in cellulose molecules results in formation of methanol (CH_3OH). Recent studies have identified the existence of strong correlation between degree of ageing of cellulose insulation paper and the production of CH_3OH. In the case of mineral oil-paper system in a transformer, some portion of methanol produced by the degradation of paper based insulation dissolves in oil. Moreover, thermal stability of dissolved CH_3OH in mineral oil has been experimentally confirmed in transformer operating environment. Therefore, this research suggests to identify the relationship between dissolved CH_3OH in ester insulating oils and paper insulation ageing condition (based on tensile strength) through controlled ageing experiment.

➢ **Study the influence of acid generation in NEs on paper ageing**

This research hypothesises that high molecular weight acids produced by hydrolytic degrdation of NE insulating oils delay the ageing process of paper insulation. To confirm this hypothesis, this thesis proposes to study the ageing behaviour of cellulose insulation in aged NE oil with a high acidity value.

➢ **Understanding insulating quality of NE based insulating oils**

This research has observed that colour, acidity and DDF of NE insulating oils rapidly change due to thermal ageing in a moisture rich environment. Moreover, it has been noticed that ageing rate of pressboard insulation in NE insulating oils with dark colour and very high acidity value is much

lower than that of in mineral oil with a lower acidity value. Thus, this thesis proposes further research to identify suitable limiting values for acidity and colour number of service aged NE oils.

➢ **Understand the effect of oil conductivity on dielectric response**

This thesis has identified that an increase of oil conductivity over ageing is the main factor which causes to increase the dielectric polarisation and conduction phenomena in pressboard insulation. Thus, this thesis proposes to measure FDS of four sets of aged pressboard specimens impregnated with insulating oil with four different conductivities under varying humidity conditions. Then it is suggested to find the correlation with oil conductivity and ψ factor of σ_{dc} based moisture diagnosing model. Subsequently, this model will be a good alternative method to determine moisture in solid insulation of new and aged transformer insulation systems.

➢ **Mixing effect**

This research proposes to investigate the effect of mixing of NE insulating oils with mineral and synthetic ester oils on ageing behaviour of paper insulation. Moreover, it is needed to investigate the effect of mixing on oil related condition monitoring tools.

References

1. T. O. Rouse, "Mineral insulating oil in transformers," IEEE Electrical Insulation Magazine, Vol. 14, Issue 3, pp. 6-16, 1998.

2. A. P. Kumar and R. P. Singh, "Biocomposites of cellulose reinforced starch: Improvement of properties by photo-induced crosslinking", Journal of Bioresource Technology, Vol. 99, pp. 8803-8809, 2008.

3. L. C. H. Y. Bertrand, Valagro, "Vegetable oils as substitute for mineral insulating oils in medium-voltage equipments", presented at the Cigre, Paris, 2004

4. J. Jalbert, E. Rodriguez-Celis, S. Duchesne, B. Morin, M. Ryadi, and R. Gilbert, "Kinetics of the production of chain-end groups and methanol from the depolymerization of cellulose during the ageing of paper/oil systems. Part 3: extension of the study under temperature conditions over 120 °C," Journal of Cellulose, Vol. 22, pp. 829-848, 2015

5. A. M. Emsley and G. C. Stevens, "Kinetics and mechanisms of the low-temperature degradation of cellulose", Journal of Cellulose, Vol. 1, pp. 26-56, 1994.

6. J. Unsworth and F. Mitchell, "Degradation of electrical insulating paper monitored with high performance liquid chromatography", IEEE Transactions on Electrical Insulation, Vol. 25, pp. 737-746, 1990.

7. A. M. Emsley, X. Xiao, R. J. Heywood, and M. Ali, "Degradation of cellulosic insulation in power transformers. Part 2: formation of furan products in insulating oil", in IEE Proceedings of Science, Measurement and Technology, Vol. 147, pp. 110-114, 2000.

8. S. Levchik, J. Scheirs, G. Camino, W. Tumiatti, and M. Avidano, "Depolymerization processes in the thermal degradation of cellulosic paper insulation in electrical transformers", Journal of Polymer Degradation and Stability, Vol. 61, pp. 507-511, 1998.

9. Cigre working group. D. (TF13), "Furanic Compounds for Diagnosis", in Cigre brochure 496, 2012.

10. A. M. Emsley, X. Xiao, R. J. Heywood, and M. Ali, "Degradation of cellulosic insulation in power transformers. Part 3: effects of oxygen and water on ageing in oil", IEE Proceedings Science, Measurement and Technology, Vol. 147, pp. 115-119, 2000.

11. C. P. McShane, K. J. Rapp, J. L. Corkran, G. A. Gauger, and J. Luksich, "Aging of Kraft paper in natural ester dielectric fluid", in Proceedings of IEEE 14th International Conference on Dielectric Liquids, pp. 173-177, 12-12 July 2002.

12. R. S. G. J. Pukel, F. Baumann,H. M. Muhr, R. Eberhardt, B. Wieser, D. Chu, "Power Transformers with environmentally friendly and low flammability ester liquids", presented at the Cigre Paris, 2012.

13. X. Junru, L. Jian, and Z. Zhaotao, "Influence of water content on the aging performance of natural ester-paper insulation," in International Conference on High Voltage Engineering and Application, pp. 663-666, 17-20 Sept. 2012, Shanghai China.

14. D. P. Stockton, J. R. Bland, T. McClanahan, J. Wilson, D. L. Harris, and P. McShane, "Natural Ester Transformer Fluids: Safety, Reliability; Environmental Performance," in IEEE Technical Conference on Petroleum and Chemical Industry, pp. 1-7, 17-19 Sept. 2007, Calgary, Alta.

15. I. Fofana, A. Bouaicha, M. Farzaneh, and J. Sabau, "Ageing Behaviour of Mineral Oil and Ester Liquids: a Comparative Study," in Annual report of IEEE conference on Electrical Insulation and Dielectric Phenomena, pp. 87-90, 26-29 Oct. 2008, Quebec, QC

16. I. Fofana, A. Bouaicha, M. Farzaneh, J. Sabau, D. Bussieres, and E. B. Robertson, "Decay products in the liquid insulation of power transformers", in IET Electric Power Applications, Vol. 4, pp. 177-184, 2010.

17. M. J. Heathcote, "Basic Materials", in J and P Transformer Book - A Practical Technology of the Power Transformer (13th Edition),: Elsevier, 2007.

18. N. J. Fox and G. W. Stachowiak, "Vegetable oil-based lubricants—A review of oxidation" in Tribology International, Vol. 40, pp. 1035-1046, 2007

19. F. D. Gunstone, "The chemistry of oil and fat". Oxford: Blackwell, 2004.

20. I. A. Metwally, "Failures, Monitoring and New Trends of Power Transformers", IEEE Potentials Magazine Vol. 30, Issue 3, pp. 36-43, 2011.

21. V. Sokolov, Z. Berler, and V. Rashkes, "Effective methods of assessment of insulation system conditions in power transformers: a view based on practical experience", in Proceeding of Electrical Insulation and Electrical Manufacturing & Coil Winding Conference, pp. 659-667, 1999, Cincinnati, OH.

22. L. Yu, L. Jian, and Z. Zhaotao, "Gases dissolved in natural ester fluids under thermal faults in transformers," in IEEE Conference Record of the International Symposium on Electrical Insulation, pp. 223-226, 10-13 June 2012, San Juan, PR

23. Y. Lijun, L. Ruijin, S. Caixin, and S. Huigang, "Study on the Influence of Natural Ester on Thermal Ageing Characteristics of Oil-paper in Power Transformer", in International Conference on High Voltage Engineering and Application, pp. 437-440, 9-12 Nov. 2008, Chongqing .

24. R. L. Liao, SW; Sun, CX; Yang, LJ; Sun, HG, "A comparative study of thermal aging of transformer insulation paper impregnated in natural ester and in mineral oil," Euro. Trans. Electr. Power, Vol. 20, pp. 518-533, 2010.

25. D. Martin, C. Ekanayake T. Saha, Hui Ma, N. Lelekakis, K. Williams, "State of the Art Review On Managing Vegetable Oil Filled Transformers", presented in the Cigre Study Committee B3 & Study Committee D1 colloquium, September 2013, Brisbane , Australia.

26. T. V. Oommen and T. A. Prevost, "Cellulose insulation in oil-filled power transformers: part II maintaining insulation integrity and life", IEEE Electrical Insulation Magazine, Vol. 22, Issue 1, pp. 5-14, 2006.

27. M. Koch and T. Prevost, "Analysis of dielectric response measurements for condition assessment of oil-paper transformer insulation", IEEE Transactions on Dielectrics and Electrical Insulation, Vol. 19, pp. 1908-1915, 2012.

28. Cigre working group. D1.01.09, "Dielectric Response Methods for Diagnostics of Power Transformers", Cigre Brochure 216, 2004.

29. Cigre working group. D. T. 14, "Dielectric Response Diagnoses For Transformer Windings", Cigre brochure 414, 2010.

30. M. Koch, S. Raetzke, and M. Krueger, "Moisture diagnostics of power transformers by a fast and reliable dielectric response method", in Conference Record of the IEEE International Symposium on Electrical Insulation, pp. 1-5, 6-9 June 2010, San Diego, CA

31. H. R. Sheppard, "A Century of Progress in Electrical Insulation 1886-1986", IEEE Electrical Insulation Magazine, Vol. 2, Issue 5, pp. 20-30, 1986.

32. M. Schaible, "Electrical Insulating Papers - an Overview", IEEE Electrical Insulation Magazine, Vol. 3, Issue 1, pp. 8-12, 1987.

33. L. Ruijin, H. Jian, G. Chen, M. Zhiqin, and Y. Lijun, "A comparative study of physicochemical, dielectric and thermal properties of pressboard insulation impregnated with natural ester and mineral oil" in IEEE Transactions on Dielectrics and Electrical Insulation , Vol. 18, pp. 1626-1637, 2011.

34. R. M. Morais, W. A. Mannheimer, M. Carballeira, and J. C. Noualhaguet, "Furfural analysis for assessing degradation of thermally upgraded papers in transformer insulation", IEEE Transactions on Dielectrics and Electrical Insulation, Vol. 6, pp. 159-163, 1999.

35. E. T. Norris, "High-voltage power-transformer insulation", in Proceedings of the Institution of Electrical Engineers, Vol. 110, pp. 428-440, 1963.

36.   A. M. Emsley and G. C. Stevens, "Review of chemical indicators of degradation of cellulosic electrical paper insulation in oil-filled transformers", in IEEE Proceeding of Science, Measurement and Technology, Vol. 141, pp. 324-334, 1994.

37.   T. A. Prevost and T. V. Oommen, "Cellulose insulation in oil-filled power transformers: Part I - history and development", IEEE Electrical Insulation Magazine, IEEE, Vol. 22, Issu 1, pp. 28-35, 2006.

38.   K. Yew, "Factors Affecting the Assessment of Insulation Condition of Power Transformer by Frequency Domain Spectroscopy Measurements ", PhD Thesis, School of Information Technol and Elec Engineering, The University of Queensland Australia, 2009.

39.   ASTM Std. D4063-2009, "Specification for Pressboard for Electrical Insulating Purposes"

40.   IEC Std. 60641-3-1-2008, "Specification for Pressboard and press paper for electrical insulation purposes".

41.   Weidmann Compendium, "Moisture in cellulose insulation," 2001.

42.   M. Koch, S. Tenbohlen, and T. Stirl, "Diagnostic Application of Moisture Equilibrium for Power Transformers", IEEE Transactions on Power Delivery, Vol. 25, pp. 2574-2581, 2010

43.   J. Dai and Z. D. Wang, "A Comparison of the Impregnation of Cellulose Insulation by Ester and Mineral oil", IEEE Transactions on Dielectrics and Electrical Insulation, Vol. 15, pp. 374-381, 2008.

44.   T. Suzuki and M. Takagi, "Oil Impregnation in Transformer Boards (2) Theoretical Analysis of Changes in Impregnation Depth", IEEE Transactions on Electrical Insulation, Vol. EI-19, pp. 344-349, 1984.

45.   T. Suzuki and M. Takagi, "Oil Impregnation in Transformer Boards (1) Measurement of Impregnation Depth and Internal Pressure", IEEE Transactions on Electrical Insulation, Vol. EI-19, pp. 340-343, 1984.

46.   W. Shugg, "Chapter 11:Dielectric Papers and Boards in Handbook of electrical and electronic insulating materials,", pp. 319-332, 1995.

47.   D. H. Shroff and A. W. Stannett, "A review of paper aging in power transformers" , IEE conference Proceeding on Generation, Transmission and Distribution, Vol. 132, pp. 312-319, 1985.

48.   T. Jeffries, "Biodegradation of lignin-carbohydrate complexes", Journal of Biodegradation, Vol. 1, pp. 163-176, 1990.

49.   A. Emsley, R. Heywood, M. Ali, and C. Eley, "On the kinetics of degradation of cellulose", Journal of Cellulose, Vol. 4, pp. 1-5, 1997.

50. A. M. Emsley, "The kinetics and mechanisms of degradation of cellulosic insulation in power transformers", Journal of Polymer Degradation and Stability, Vol. 44, pp. 343-349, 1994.

51. R. O. Smail, Jr., "Industrial laminates: manufacture, materials, and applications," in Proceedings of the Electrical Electronics Insulation and Electrical Manufacturing & Coil Winding conference pp. 539-543, 18-21 Sep 1995, Rosemont, IL.

52. K. Chen, D.-K. Liu, X. Wang, and T.-J. Xia, "Study on manufacture of electric insulating paper and press board from non-wood fibres pulp," in Proceedings of the 3rd International Conference on Properties and Applications of Dielectric Materials, Vol.1, pp. 462-465, 8-12 Jul 1991, Tokyo.

53. N. Lelekakis, J. Wijaya, D. Martin, T. Saha, D. Susa, and C. Krause, "Aging rate of grade 3 presspaper insulation used in power transformers", in IEEE Transactions on Dielectrics and Electrical Insulation, Vol. 21, pp. 2355-2362, 2014

54. T. A. Prevost, "Thermally upgraded insulation in transformers," in Proceedings of the Electrical Insulation Conference and Electrical Manufacturing Expo, pp. 120-125, 26-26 Oct. 2005, Indianapolis, IN .

55. D. J. T. Hill, T. T. Le, M. Darveniza, and T. Saha, "A study of degradation of cellulosic insulation materials in a power transformer. Part 2: tensile strength of cellulose insulation paper", Journal of Polymer Degradation and Stability, Vol. 49, pp. 429-435, 1995.

56. A. de Pablo, "Furfural and ageing: how are they related," in IEE Colloquium on Insulating Liquids pp. 5/1-5/4, 1999.

57. A. Denat, B. Gosse, and J. P. Gosse, "Ion injections in hydrocarbons," Journal of Electrostatics, Vol. 7, pp. 205-225, 1979.

58. F. Shafizadeh and Y. L. Fu, "Pyrolysis of cellulose", Journal of Carbohydrate Research, Vol. 29, pp. 113-122, 1973.

59. K. Kato, "Pyrolysis of Cellulose Part III Comparative Study of the Volatile Compunds From Pyrolysate of Cellulose", in Journal of Agricultural and Biological Chemistry, Vol.31, pp. 657-663, 1967.

60. L. E. Lundgaard, W. Hansen, and S. Ingebrigtsen, "Ageing of Mineral Oil Impregnated Cellulose by Acid Catalysis", in IEEE Transactions on Dielectrics and Electrical Insulation, Vol. 15, pp. 540-546, 2008.

61. L. E. Lundgaard, W. Hansen, S. Ingebrigtsen, D. Linhjell, and M. Dahlund, "Aging of Kraft paper by acid catalyzed hydrolysis," in IEEE International Conference on Dielectric Liquids, pp. 381-384, 26 June-1 July 2005.

62. L. E. Lundgaard, W. Hansen, D. Linhjell, and T. J. Painter, "Aging of oil-impregnated paper in power transformers", IEEE Transactions on Power Delivery, Vol. 19, pp. 230-239, 2004.

63. J. Łojewska, P. Miśkowiec, T. Łojewski, and L. M. Proniewicz, "Cellulose oxidative and hydrolytic degradation: In situ FTIR approach" , Journal of Polymer Degradation and Stability, Vol. 88, pp. 512-520, 2005.

64. B. A. Eichenberger, "Three-stage hydrolysis of cellulose", Master Thesis, University of Southern California, Ann Arbor, 1974.

65. A. M. Emsley "Influence of cellulose degradation on insulation life in power transformers", in Proceedings of the International Conference on Cellulose and Cellulose Derivatives: Physico-Chemical Aspects and Industrial Applications pp. 115-124, 1993.

66. S. Margutti, G. Conio, P. Calvini, and E. Pedemonte, "Hydrolytic and Oxidative Degradation of Paper," in Journal of Restaurator Vol. 22, ed, 2001, p. 67.

67. IEEE Std. C57.91-2011 (Revision of IEEE Std C57.91-1995),"IEEE Guide for Loading Mineral-Oil-Immersed Transformers and Step-Voltage Regulators - Redline" .

68. H. M. Wilhelm, L. Tulio, R. Jasinski, and G. Almeida, "Aging markers for in-service natural ester-based insulating fluids", IEEE Transactions on Dielectrics and Electrical Insulation, Vol. 18, pp. 714-719, 2011.

69. I. L. Hosier, A. Guushaa, E. W. Westenbrink, C. Rogers, A. S. Vaughan, and S. G. Swingler, "Aging of biodegradable oils and assessment of their suitability for high voltage applications", in IEEE Transactions on Dielectrics and Electrical Insulation, Vol. 18, pp. 728-738, 2011.

70. A. Darwin, C. Perrier, and P. Foliot, "The use of natural ester fluids in transformers," in Proceedings of MATPOST conference, Paper, 2007, pp. 15-16, 2007, Lyon (France).

71. Cigre working group. A2.35, "Experinece in Service with New Insulating Liquids", Cigre Brochure 436, 2010.

72. T. V. Oommen, C. C. Claiborne, and J. T. Mullen, "Biodegradable electrical insulation fluids", in Proceedings of the Electrical Insulation and Electrical Manufacturing & Coil Winding Conference, pp. 465-468, 22-25 Sep 1997, Rosemont, IL.

73. ABB Brochure, "BIOTEMP® dielectric insulating fluid," March 2011.

74. L. Rongsheng, C. Tornkvist, V. Chandramouli, O. Girlanda, and L. A. A. Pettersson, "Ester fluids as alternative for mineral oil: The difference in streamer velocity and LI breakdown voltage", in IEEE conference on Electrical Insulation and Dielectric Phenomena, pp. 543-548, 18-21 Oct. 2009, Virginia Beach, VA.

75. S. P. Moore, W. Wangard, K. J. Rapp, D. L. Woods, and R. M. Del Vecchio, "Cold Start of a 240-MVA Generator Step-Up Transformer Filled With Natural Ester Fluid", in IEEE Transactions on Power Delivery, Vol. 30, pp. 256-263, 2015.

76. T. M. P. T. Rob Milledge, , "Introduction to BIOTEMP The superior, biodegradable, high fire point, dielectric insulating fluid", in ABB seminar presentation, July 2011, Australia.

77. P.K.B. Hodges, "Mineral base oils and oxidation stabilitty", in Hydraulic Fluids, Elsevier, 1996.

78. M. R. Meshkatodd, "Aging Study and Lifetime Estimation of Transformer Mineral Oil", in American Journal of Engineering and Applied Sciences, Vol. 1, pp. 384-388, 2008.

79. A. Ciuriuc, M. S. Vihacencu, L. M. Dumitran, and P. V. Notingher, "Comparative study on power transformers vegetable and mineral oil ageing", in International Conference on Applied and Theoretical Electricity, pp. 1-6, 25-27 Oct. 2012, Craiova.

80. L. Kaanagbara, H. I. Inyang, J. Wu, and H. Hilger, "Aromatic and aliphatic hydrocarbon balance in electric transformer oils", Journal of Fuel, Vol. 89, pp. 3114-3118, 2010.

81. T. V. Oommen, "Vegetable oils for liquid-filled transformers"., IEEE Electrical Insulation Magazine, Vol. 18, Issue 1 pp. 6-11, 2002.

82. F. H. Smith "Vegetable oil refining", Journal of the American Oil Chemists' Society, Vol. 33, pp. 473-476, 1956.

83. IEEE Std. C57.147-2008, "IEEE Guide for Acceptance and Maintenance of Natural Ester Fluids in Transformers".

84. S. Tenbohlen and M. Koch, "Aging Performance and Moisture Solubility of Vegetable Oils for Power Transformers", IEEE Transactions on Power Delivery, Vol. 25, pp. 825-830, 2010.

85. G. J. Pukel, R. Schwarz, F. Baumann, H. M. Muhr, R. Eberhardt, B. Wieser, D. Chu, "Power Transformer with environmentally friendly and low flammability ester liquids," presented at the Cigre, Paris, 2012.

86. D. Rooney and L. R. Weatherley, "The effect of reaction conditions upon lipase catalysed hydrolysis of high oleate sunflower oil in a stirred liquid–liquid reactor", in Journal of Process Biochemistry, Vol. 36, pp. 947-953, 2001.

87. C. P. McShane, "Relative properties of the new combustion resistant vegetable oil based dielectric coolants," in the Records of Industry Applications Society 47th Annual conference on Petroleum and Chemical Industry, pp. 265-272, 2000, San Antonio, TX.

88. IEC Std. 61099-2010, "Insulating liquids - Specifications for unused synthetic organic esters for electrical purposes".

89.   IEC Std. 61203- "Synthetic organic esters for electrical purposes - Guide for maintenance of transformer esters in equipment".

90.   V. N. Bakunin and O. P. Parenago, "Mechanism of thermo-oxidative degradation of polyol ester lubricants", Journal of Synthetic Lubrication, Vol. 9, pp. 127-143, 1992.

91.   D. J. T. Hill, T. T. Le, M. Darveniza, and T. Saha, "A study of the degradation of cellulosic insulation materials in a power transformer. Part III: Degradation products of cellulose insulation paper" in Journal of Polymer Degradation and Stability, Vol. 51, pp. 211-218, 1996.

92.   J. Jalbert, R. Gilbert, P. Tétreault, B. Morin, and D. Lessard-Déziel, "Identification of a chemical indicator of the rupture of 1,4-β-glycosidic bonds of cellulose in an oil-impregnated insulating paper system", in Journal of Cellulose, Vol. 14, pp. 295-309, 2007.

93.   M. C. Lessard, L. Van Nifterik, M. Masse, J. F. Penneau, and R. Grob, "Thermal aging study of insulating papers used in power transformers," in IEEE Annual Report of the Conference on Electrical Insulation and Dielectric Phenomena, Vol.2, pp. 854-859, 20-23 Oct 1996, Millbrae, CA

94.   J.C Duart, l. C. Bates R. Asano JR, l. Cheim, E. W. Key , D. B. Cherry, C. C. Claiborne, "Thermal Aging Study of Cellulosic Materials in Natural Ester Liquid for Hybrid Insulation Systems", presented at the Cigre, Paris, 2012.

95.   M. L. Coulibaly, C. Perrier, M. Marugan, and A. Beroual, "Aging behavior of cellulosic materials in presence of mineral oil and ester liquids under various conditions", IEEE Transactions on Dielectrics and Electrical Insulation, Vol. 20, pp. 1971-1976, 2013.

96.   Y. Lijun, L. Ruijin, S. Caixin, Y. Jianguo, and Z. Mengzhao, "Influence of vegetable oil on the thermal aging rate of kraft paper and its mechanism," in International Conference on High Voltage Engineering and Application pp. 381-384, 11-14 Oct. 2010, New Orleans, LA.

97.   Y. Lijun, L. Ruijin, C. Sun, and Z. Mengzhao, "Influence of vegetable oil on the thermal aging of transformer paper and its mechanism", in IEEE Transactions on Dielectrics and Electrical Insulation, Vol. 18, pp. 692-700, 2011.

98.   S. Singha, R. Asano, G. Frimpong, C. C. Claiborne, and D. Cherry, "Comparative aging characteristics between a high oleic natural ester dielectric liquid and mineral oil", in IEEE Transactions on Dielectrics and Electrical Insulation, Vol. 21, pp. 149-158, 2014.

99.   B. Chatterjee, C. Biswendu, C. Sivaji, D. Debangshu, and M. Sugata, "Recent Trends in the Condition Monitoring of Transformers Theory, Implementation and Analysis", Springer-Verlag London 2013

100. M. Koch, M. Krueger, and M. Puetter, "Advanced insulation diagnostic by dielectric spectroscopy," in Asia Pacific Technical conference, 2009, Sydney, Australia.

101. J. H. Yew, M. K. Pradhan, and T. K. Saha, "Effects of moisture and temperature on the frequency domain spectroscopy analysis of power transformer insulation", in IEEE Power and Energy Society General Meeting - Conversion and Delivery of Electrical Energy in the 21st Century, pp. 1-8, 20-24 July 2008, Pittsburgh, PA ..

102. IEC Std. 60156-1995, "Insulating liquids –Determination of the breakdown voltage at power frequency".

103. IEEE Std. C57.152-2013,"IEEE Guide for Diagnostic Field Testing of Fluid-Filled Power Transformers, Regulators, and Reactors"

104. EEE Std. 62-1995,"IEEE Guide for Diagnostic Field Testing of Electric Power Apparatus - Part 1: Oil Filled Power Transformers, Regulators, and Reactors".

105. British Std. EN 61203:1995, "Synthetic organic esters for electrical purposes. Guide for maintenance of transformer esters in equipment".

106. D. Martin, W. Guo, N. Lelekakis, and N. Heyward, "Using a remote system to study the thermal properties of a vegetable oil filled power transformer: How does operation differ from mineral oil", in IEEE PES Innovative Smart Grid Technologies Asia coference , pp. 1-5, 13-16 Nov. 2011, Perth, WA .

107. J. Duart and L. C. Bates, "Aging of high temperature insulation systems with alternative fluids," in the Confrence Records of the IEEE International Symposium on Electrical Insulation , pp. 1-5, 6-9 June 2010, San Diego, CA.

108. Y. Feldman, A. Puzenko, and Y. Ryabov, "Dielectric Relaxation Phenomena In Complex Materials." vol. 133, New York: John Wiley & Sons Inc, pp. 1-125, 2006.

109. W. S. Zaengl, "Dielectric spectroscopy in time and frequency domain for HV power equipment. I. Theoretical considerations" , in IEEE Electrical Insulation Magazine, Vol. 19, issue 5, pp. 5-19, 2003.

110. A. K. Jonscher, Dielectric Relaxation in solid. London: Chelsea Dielectric press, 1996.

111. T. Prodromakis and C. Papavassiliou, "Engineering the Maxwell–Wagner polarization effect", in Journal of Applied Surface Science, vol. 255, pp. 6989-6994, 2009.

112. A. K. Jonscher and L. Levesque, "Volume low-frequency dispersion in a semi-insulating system", IEEE Transactions on Electrical Insulation, Vol. 23, pp. 209-213, 1988.

113. A. K. Jonscher, "The 'universal' dielectric response. I", in IEEE Electrical Insulation Magazine, vol. 6, pp. 16-22, 1990.

114. A. A. Abdelmalik, S. J. Dodd, L. A. Dissado, N. M. Chalashkanov, and J. C. Fothergill, "Charge transport in thermally aged paper impregnated with natural ester oil", in IEEE Transactions on Dielectrics and Electrical Insulation, Vol. 21, pp. 2318-2328, 2014.

115. L. A. Dissado and R. M. Hill, "Anomalous low-frequency dispersion. Near direct current conductivity in disordered low-dimensional materials", in Journal of the Chemical Society, Faraday Transactions 2: Molecular and Chemical Physics, Vol. 80, pp. 291-319, 1984.

116. J. H. Christie, S. H. Krenek, and I. M. Woodhead, "The electrical properties of hygroscopic solids", in Journal of Biosystems Engineering, Vol. 102, pp. 143-152, 2009.

117. A. Helgeson, "Analysis of Dielectric Response Measurement Methods and Dielectric Properties of Resin-Rich Insulation During Processing", PhD Thesis Electric Power Engineering, Kungl Tekniska Hogskolan, Stockholm, 2000.

118. L. Dissado, "Dielectric Response in Springer Handbook of Electronic and Photonic Materials, Springer Unite Staes, pp. 187-212, 2007.

119. T. K. Saha and P. Purkait, "Investigation of polarization and depolarization current measurements for the assessment of oil-paper insulation of aged transformers", in IEEE Transactions on Dielectrics and Electrical Insulation, Vol. 11, pp. 144-154, 2004.

120. J. H. Christie, S. R. Sylvander, I. M. Woodhead, and K. Irie, "The dielectric properties of humid cellulose", in Journal of Non-Crystalline Solids, Vol. 341, pp. 115-123, 2004

121. M. Nilsson, G. Alderborn, and M. Strømme, "Water-induced charge transport in tablets of microcrystalline cellulose of varying density: dielectric spectroscopy and transient current measurements", in Journal of Chemical Physics, Vol. 295, pp. 159-165, 2003.

122. M. Nilsson and M. Strømme, "Electrodynamic Investigations of Conduction Processes in Humid Microcrystalline Cellulose Tablets", in Journal of Physical Chemistry B, Vol. 109, pp. 5450-5455, 2005.

123. R. B. Jadav, C. Ekanayake, and T. K. Saha, "Understanding the impact of moisture and ageing of transformer insulation on frequency domain spectroscopy", IEEE Transactions on Dielectrics and Electrical Insulation, Vol. 21, pp. 369-379, 2014.

124. D. Linhjell, L. Lundgaard, and U. Gafvert, "Dielectric response of mineral oil impregnated cellulose and the impact of aging", in IEEE Transactions on Dielectrics and Electrical Insulation, Vol. 14, pp. 156-169, 2007.

125. T. K. Saha and P. Purkait, "Understanding the impacts of moisture and thermal ageing on transformer's insulation by dielectric response and molecular weight measurements", in IEEE Transactions on Dielectrics and Electrical Insulation, Vol. 15, pp. 568-582, 2008.

126. Y. Ryabov, A. Gutina, V. Arkhipov, and Y. Feldman, "Dielectric Relaxation of Water Absorbed in Porous Glass", in Journal of Physical Chemistry B, Vol. 105, pp. 1845-1850, 2001.

127. C. Ekanayake, "Diagnosis of Moisture in Transfomer Insulation- Application of frequency domain spectroscopy", PhD Thesis, Department of Material and manufacturing Technology, Chalmers, 2006.

128. S. A. Bhumiwat, "Advanced Applications of Polarisation / Depolarisation Current Analysis on Power Transformers," in confrence Records of IEEE International Symposium on Electrical Insulation, pp. 474-477, 9-12 June 2008, Vancouver, BC

129. S. Sarkar, T. Sharma, A. Baral, B. Chatterjee, D. Dey, and S. Chakravorti, "An expert system approach for transformer insulation diagnosis combining conventional diagnostic tests and PDC, RVM data", in IEEE Transactions on Dielectrics and Electrical Insulation, Vol. 21, pp. 882-891, 2014.

130. V. Der Houhanessian and W. S. Zaengl, "Application of relaxation current measurements to on-site diagnosis of power transformers" , in IEEE Annual Report of the confrence on Electrical Insulation and Dielectric Phenomena, Vol.1, pp. 45-51, 19-22, Oct 1997, Minneapolis, MN.

131. A. Baral and S. Chakravorti, "Assessment of non-uniform aging of solid dielectric using system poles of a modified debye model for oil-paper insulation of transformers", in IEEE Transactions on Dielectrics and Electrical Insulation, Vol. 20, pp. 1922-1933, 2013.

132. T. K. Saha, P. Purkait, and F. Muller, "Deriving an equivalent circuit of transformers insulation for understanding the dielectric response measurements", IEEE Transactions on Power Delivery, Vol. 20, pp. 149-157, 2005.

133. I. Fofana, H. Hemmatjou, and F. Meghnefi, "Effect of thermal transient on the polarization and depolarization current measurements", in IEEE Transactions on Dielectrics and Electrical Insulation, Vol. 18, pp. 513-520, 2011.

134. T. K. Saha and P. Purkait, "Impact of the condition of oil on the polarisation based diagnostics for assessing the condition of transformers insulation," in IEEE Power Engineering Society General Meeting, Vol.2, 1881-1886, 12-16 June 2005.

135. T. Leibfried and A. J. Kachler, "Insulation diagnostics on power transformers using the polarisation and depolarisation current (PDC) analysis", in Conference Record of the IEEE International Symposium on Electrical Insulation pp. 170-173, 7-10 Apr 2002, Boston, MA.

136. U. Gafvert, L. Adeen, M. Tapper, P. Ghasemi, and B. Jonsson, "Dielectric spectroscopy in time and frequency domain applied to diagnostics of power transformers", in Proceedings of

the 6th International Conference on Properties and Applications of Dielectric Materials,Vol.2 , pp. 825-830 , 2000, Xi'an.

137. V. Der Houhanessian and W. S. Zaengl, "Time domain measurements of dielectric response in oil-paper insulation systems", in Conference Record of the IEEE International Symposium on Electrical Insulation, Vol.1, pp. 47-52, 16-19 Jun 1996, Montreal, Que.

138. C. Ekanayake, S. M. Gubanski, A. Graczkowski, and K. Walczak, "Frequency response of oil impregnated pressboard and paper samples for estimating moisture in transformer insulation", in IEEE Transactions on Power Delivery, Vol. 21, pp. 1309-1317, 2006.

139. M. Koch and M. Kruger, "A fast and reliable dielectric diagnostic method to determine moisture in power transformers", in International Conference on Condition Monitoring and Diagnosis, pp. 467-470, 7-11 Sept. 2008, Mie.

140. J. H. Yew, T. K. Saha, and A. J. Thomas, "Impact of temperature on the frequency domain dielectric spectroscopy for the diagnosis of power transformer insulation", in IEEE Power Engineering Society General Meeting, pp, 1-7, 2006, Montreal, Que.

141. "User Manual for Insulation Diagnostic System IDAX 350", 2012.

142. M. Ohlen and P. Werelius, "Dielectric Frequency Response and temperature dependence of power factor", in Conference Record of the IEEE International Symposium on Electrical Insulation, pp. 1-7, 6-9 June 2010, San Diego, CA.

143. W. Guo and T. K. Saha, "Study on Moisture in Oil-Paper Insulation by Frequency Domain Spectroscopy", in Asia-Pacific,Power and Energy Engineering Conference, pp. 1-4, 25-28 March 2011, Wuhan.

144. S.M. Gubanski (chair) , G. Csépes, V. Der, Houhanessian, J. Filippini, P. Guuinic, U. Gäfvert, V., Karius, J. Lapworth, G. Urbani, P. Werelius, W.Zaengl, "Dielectric response methods for diagnostics of power transformers", IEEE Electrical Insulation Magazine, Vol. 19, Issue 3, pp. 12-18, 2003.

145. J. Hao, R. Liao, Z. Ma, and L. Yang, "Influence of natural ester on frequency dielectric response of impregnated insulation pressboard" , in IET Science, Measurement & Technology, Vol. 6, pp. 403-411, 2012.

146. T. K. Saha, M. Darveniza, D. J. T. Hill, and T. T. Le, "Electrical and chemical diagnostics of transformers insulation. B. Accelerated aged insulation samples", in IEEE Transactions on Power Delivery, Vol. 12, pp. 1555-1561, 1997.

147. T. K. Saha, M. Darveniza, D. J. T. Hill, and T. T. Le, "Electrical and chemical diagnostics of transformers insulation. A. Aged transformer samples", in IEEE Transactions on Power Delivery, Vol. 12, pp. 1547-1554, 1997.

148.   IEC Std. 60814-1997, "IEC standrad for Determination of water by automatic coulometric Karl Fischer titration".

149.   T. K. Saha, "Review of modern diagnostic techniques for assessing insulation condition in aged transformers", IEEE Transactions on Dielectrics and Electrical Insulation, Vol. 10, pp. 903-917, 2003.

150.   Y. Du, M. Zahn, B. C. Lesieutre, A. V. Mamishev, and S. R. Lindgren, "Moisture equilibrium in transformer paper-oil systems", IEEE Electrical Insulation Magazine, Vol. 15, issue 1pp. 11-20, 1999.

151.   T. V. Oommen, "Moisture Equilibrium Charts for Transformer Insulation Drying Practice", in IEEE Transactions on Power Apparatus and Systems, Vol. PAS-103, pp. 3062-3067, 1984.

152.   Z. Zhaotao, L. Jian, S. Grzybowski, and Z. Ping, "Moisture equilibrium in vegetable oil and paper insulation system", in IEEE Annual Report Conference on Electrical Insulation and Dielectric Phenomena, pp. 428-431, 16-19 Oct. 2011, Cancun.

153.   C. Perrier, M. Marugan, and A. Beroual, "DGA comparison between ester and mineral oils," IEEE Transactions on Dielectrics and Electrical Insulation, Vol. 19, pp. 1609-1614, 2012.

154.   IEEE Std. C57.104-1991,"IEEE Guide for the Interpretation of Gases Generated in Oil-Immersed Transformers".

155.   M. Jovalekic, D. Vukovic, and S. Tenbohlen, "Dissolved gas analysis of alternative dielectric fluids under thermal and electrical stress", in IEEE International Conference on Dielectric Liquids, pp. 1-4, 26-30 June 2011, Trondheim.

156.   Cigre working group D1.32, "DGA in Non-Mineral Oils and Load Tap Changersand Improved DGA Diagnosis Criteria", Cigre Brochure 443, 2010.

157.   I U. K. Imad, W. Zhongdong, I. Cotton, and S. Northcote, "Dissolved gas analysis of alternative fluids for power transformers", IEEE Electrical Insulation Magazine, Vol. 23, issue 5, pp. 5-14, 2007.

158.   C. Perrier, M. Marugan, M. Saravolac, and A. Beroual, "DGA comparison between ester and mineral oils", in IEEE International Conference on Dielectric Liquids, pp. 1-4, 26-30 June 2011, Trondheim.

159.   K. Kjnar, "Transformer Lecture, "The Transformer and its Maintenance", Available: www.klassenhydrolics.com.March 2005.

160.   S. Singh and M. N. Bandyopadhyay, "Dissolved gas analysis technique for incipient fault diagnosis in power transformers: A bibliographic survey", IEEE Electrical Insulation Magazine, Vol. 26, Issue 6, pp. 41-46, 2010.

161. IEC Std. 60599-2007, "IEC standard for Mineral oil impregnated electric equipment in servece -Guide to the interpretation of dissolved and free gases analysis".

162. M. Duval, "The duval triangle for load tap changers, non-mineral oils and low temperature faults in transformers", in IEEE Electrical Insulation Magazine, Vol. 24, issue 6, pp. 22-29, 2008

163. A. Akbari, A. Setayeshmehr, H. Borsi, E. Gockenbach,I. Fofana, "Intelligent agent-based system using dissolved gas analysis to detect incipient faults in power transformers. IEEE Electrical Insulation Magazine, p. 27-40, Vol 26. Issue 6, 2010.

164. M. Duval,L. Lamarre, "The duval pentagon-a new complementary tool for the interpretation of dissolved gas analysis in transformers", IEEE Electrical Insulation Magazine, Vol.**30**, Isuue 6: pp. 9-12, 2014.

165. M.U. Farooque, Jamia Millia Islamia, S.A. Wani, and S.A. Khan. "Artificial neural network (ANN) based implementation of Duval pentagon" in International Conference on Condition Assessment Techniques in Electrical Systems, pp 46-50, 10-12 Dec. 2015 Bangalore, India,

166. J. Scheirs, G. Camino, M. Avidano, and W. Tumiatti, "Origin of furanic compounds in thermal degradation of cellulosic insulating paper", in Journal of Applied Polymer Science, Vol. 69, pp. 2541-2547, 1998.

167. A. J. Kachler and I. Hohlein, "Aging of cellulose at transformer service temperatures. Part 1: Influence of type of oil and air on the degree of polymerization of pressboard, dissolved gases, and furanic compounds in oil", IEEE Electrical Insulation Magazine, Vol. 21, Issue 2, pp. 15-21, 2005.

168. L. Cheim, D. Platts, T. Prevost, and X. Shuzhen, "Furan analysis for liquid power transformers", IEEE Electrical Insulation Magazine, Vol. 28, Issue 2 pp. 8-21, 2012.

169. D. Feng, "Life Expectancy Investigation Of Transmission Power Transformers", PhD Thesis, School of Electrical and Electronic Engineering, University of Manchester, 2013

170. R. Blue, D. Uttamchandani, and O. Farish, "Infrared detection of transformer insulation degradation due to accelerated thermal aging", in IEEE Transactions on Dielectrics and Electrical Insulation, Vol. 5, pp. 165-168, 1998.

171. De Pablo and B. Pahlavanpour, "Furanic compounds analysis: a tool for predictive maintenance of oil filled electrical equipment", Electra Cigre Group 15.01.03 1997.

172. X. Chendong, "Monitoring paper insulation aging by measuringfurfural content of oil", in 7th International Symposium on High Voltage Engineering, pp 139-142, Aug. 26–30, 1991.

173. S. Okabe, S. Kaneko, M. Kohtoh, and T. Amimoto, "Analysis results for insulating oil components in field transformers", IEEE Transactions on Dielectrics and Electrical Insulation, Vol. 17, pp. 302-311, 2010.

174. A. Abu-Siada and S. Islam, "A new approach to identify power transformer criticality and asset management decision based on dissolved gas-in-oil analysis", IEEE Transactions on Dielectrics and Electrical Insulation, Vol. 19, pp. 1007-1012, 2012.

175. IEEE Std C57.106-2006 (Revision of IEEE Std C57.106-2002)"IEEE Guide for Acceptance and Maintenance of Insulating Oil in Equipment"..

176. J. Jung-Il, A. Jung-Sik, and H. Chan-Su, "Accelerated aging effects of mineral and vegetable transformer oils on medium voltage power transformers", in IEEE Transactions on Dielectrics and Electrical Insulation, Vol. 19, pp. 156-161, 2012.

177. Kapila Bandara, Chandima Ekanayake, Tapan K. Saha, Pratheep Kumar, "Understanding the Ageing Aspects of Natural Ester Based Insulation," (Accpted 27th August 2015) IEEE Transactions on Dielectrics and Electrical Insulation, 2015..

178. Kapila Bandara, Chandima Ekanayake, Tapan K. Saha,, "Comparative study to understand behaviour of natural ester as transformer insulating liquid", in IEEE 11th conference on the Properties and Applications of Dielectric Materials, pp. 975-978 2015, Sydney, Australia.

179. Kapila Bandara, Chandima Ekanayake, Tapan K. Saha,, "Comparative study to understand behaviour of natural ester as transformer insulating liquid", presented in IEEE 10th International Conference on Industrial and Information Systems, pp 117-121 , 2015, Peradeniya Sr Lanka.

180. Kapila Bandara, Chandima Ekanayake, Tapan Saha, Hui Ma "Performance of Natural Ester as a Transformer Oil in Moisture-Rich Environments", J. Energies, Vol.9, Issue 4, DOI: 10.3390/en9040258, 2016

181. Cargill Broacher for FR3 Fluid, "Loading guide A and B factors for Envirotemp FR3 fluid and thermally upgraded Kraft insulation", April 2013.

182. W. Abtew and A. Melesse, " Chapter 5:Vapor Pressure Calculation Methods in Evaporation and Evapotranspiration, Springer Netherlands, pp. 53-62, 2013.

183. M. H. G. Ese, K. B. Liland, C. Lesaint, and M. Kes, "Esterification of low molecular weight acids in cellulose", in IEEE Transactions on Dielectrics and Electrical Insulation, Vol. 21, pp. 662-665, 2014.

184. T. Kondo, "The assignment of IR absorption bands due to free hydroxyl groups in cellulose", in Journal of Cellulose, Vol. 4, pp. 281-292, 1997.

185. B. Hinterstoisser, M. Åkerholm, and L. Salmén, "Effect of fiber orientation in dynamic FTIR study on native cellulose", in Journal of Carbohydrate Research, Vol. 334, pp. 27-37, 2001.

186. A.-M. Olsson and L. Salmén, "The association of water to cellulose and hemicellulose in paper examined by FTIR spectroscopy", in Journal of Carbohydrate Research, Vol. 339, pp. 813-818, 2004.

187. H. Yang, R. Yan, H. Chen, D. H. Lee, and C. Zheng, "Characteristics of hemicellulose, cellulose and lignin pyrolysis", in Journal of Fuel, Vol. 86, pp. 1781-1788, 2007.

188. C. T. Duy, A. Denat, O. Lesaint, N. Bonifaci, and Y. Bertrand, "Moisture and temperature effects on conduction and losses in modified rape-seed insulating oil", in IEEE Annual Report of the Conference on Electrical Insulation and Dielectric Phenomena , pp. 647-650, 14-17 Oct. 2007, Vancouver, BC.

189. W K Subczynski, J. S. Hyde, "Diffusion of oxygen in water and hydrocarbons using an electron spin resonance spin-label technique", in Journal of Biophysical Vol. 45, pp. 743-748, 1984

190. J. Viertel, K. Ohlsson, and S. Singha, "Thermal aging and degradation of thin films of natural ester dielectric liquids", in IEEE International Conference on Dielectric Liquids, pp. 1-4, 26-30 June 2011, Trondheim

191. IEEE PC57.155/D5, "IEEE Draft Guide for Interpretation of Gases Generated in Natural Ester and Synthetic Ester Immersed Transformers", pp. 1-63, 2014.

192. K. S. Kassi, I. Fofana ; F. Meghnefi ; Z. Yeo, Impact of local overheating on conventional and hybrid insulations for power transformers. IEEE Transactions on Dielectrics and Electrical Insulation, Vol.22 Issue 5, pp. 2543-2553, 2015.

193. A. A. S. Akmal, H. Borsi, E. Gockenbach, V. Wasserberg, and H. Mohseni, "Dielectric behavior of insulating liquids at very low frequency", IEEE Transactions on Dielectrics and Electrical Insulation, Vol. 13, pp. 532-538, 2006.

194. R. Bartnikas, Engineering Dielectric, Electrical Insulating Liquids vol. III: ASTM Publication 1994.

195. Kapila. Bandara, C. Ekanayake, and T. K. Saha, "Comparative study for understanding the behaviour of natural ester with mineral oil as a transformer insulating liquid", in IEEE Conference on Electrical Insulation and Dielectric Phenomena , pp. 792-795, 2014, Desmoines, IA.

196. Kapila Bandara, C. Ekanayake, and T. Saha, "Modelling the dielectric response measurements of transformer oil", IEEE Transactions on Dielectrics and Electrical Insulation, Vol. 22, pp. 1283-1291, 2015.

197. IEC Std.-60247 for Insulating liquids "Measurement of relative permittivity,dielectric dissipation factor (tanδ) and DC resistivity",2004.

198. C. Ekanayake, T. K. Saha, H. Ma, and D. Allan, "Application of polarization based measurement techniques for diagnosis of field transformers," in IEEE Power and Energy Society General Meeting, pp. 1-8, 25-29 July 2010, Minneapolis, MN.

199. T. K. Saha and P. Purkait, "Investigations of Temperature Effects on the Dielectric Response Measurements of Transformer Oil-Paper Insulation System", in IEEE Transactions on Power Delivery, Vol. 23, pp. 252-260, 2008.

200. M. Hilaire, C. Marteau, and R. Tobazéon, "Apparatus developed for measurement of the resistivity of highly insulating liquids", in IEEE Transactions on Electrical Insulation, Vol. 23, pp. 779-789, 1988.

201. R. Tobazéon, J. C. Filippini, and C. Marteau, "On the measurement of the conductivity of highly insulating liquids", in IEEE Transactions on Dielectrics and Electrical Insulation, Vol. 1, pp. 1000-1004, 1994.

202. C. G. Garton, "Dielectric loss in thin films of insulating liquids", in Part I: General, Journal of the Institution of Electrical Engineers, Vol. 88, pp. 245-248, 1941.

203. A. Saad and R. Tobazeon, "The Electrical Behavior of an Insulating Liquid Layer between Polymer Sheets Under AC Voltage", in IEEE Transactions on Electrical Insulation, Vol. EI-20, pp. 359-364, 1985.

204. R. W. Rennell and J. C. Anderson, "Dielectric and conductivity measurements on thin liquid films of n-heptanol", Journal of Radio and Electronic Engineer, Vol. 45, pp. 401-408, 1975.

205. T. W. Dakin, "Conduction and polarization mechanisms and trends in dielectric", in IEEE Electrical Insulation Magazine, Vol. 22, issue 5, pp. 11-28, 2006.

206. S. Emmert, M. Wolf, R. Gulich, S. Krohns, S. Kastner, P. Lunkenheimer, and A. Loidl, "Electrode polarization effects in broadband dielectric spectroscopy" , in The European Physical Journal B, Vol. 83, pp. 157-165, 2011.

207. F. Bordi, C. Cametti, and T. Gili, "Reduction of the contribution of electrode polarization effects in the radiowave dielectric measurements of highly conductive biological cell suspensions", in Journal of Bioelectrochemistry, Vol. 54, pp. 53-61, 2001.

208.   A. Serghei, M. Tress, J. R. Sangoro, and F. Kremer, "Electrode polarization and charge transport at solid interfaces", in Journal of Physical Review B, Vol. 80, p. 184301, 11/05/ 2009.

209.   A. A. Shayegani, H. Borsi, E. Gockenbach, and H. Mohseni, "Application of low frequency dielectric spectroscopy to estimate condition of mineral oil", in IEEE International Conference on Dielectric Liquids, pp. 285-288, 26 June-1 July 2005.

210.   Z. Yuan, H. Miao, G. Chen, G. Wilson, and P. Jarman, "Frequency-dependence of conductivity of new mineral oil studied by dielectric spectroscopy," in International Conference on High Voltage Engineering and Application, pp. 634-637, 17-20 Sept. 2012, Shanghai.

211.   P. B. Ishai, M. S. Talary, A. Caduff, E. Levy, and Y. Feldman, "Electrode polarization in dielectric measurements: a review", in Journal of Measurement Science and Technology, Vol. 24, p. 102001, 2013.

212.   H. Shiroishi, "Adsorption and Electrode Processes in Molecular Catalysts for Energy Conversion. vol. 111, Springer Berlin Heidelberg, 2009, pp. 329-365.

213.   A. Gemant, "Ionic Mobilities in Insulating Liquids", in Journal of Physical Review, Vol. 58, pp. 904-908, 1940.

214.   H. Sato, Y. Nonaka, and T. Takada, "Electric field distribution in transformer oil containing an additive using the Kerr-effect technique under various DC stress conditions", in Conference Record 10th International Conference on Conduction and Breakdown in Dielectric Liquids, pp. 474-478, 10-14 Sep 1990, Grenoble.

215.   Cigre working gruoup. A2.D1.41, "HVDC transformer Insulation, oil conductivity", Cigre Brochure 646 2016.

216.   S. Theoleyre and R. Tobazeon, "The role of the diffuse layer in the transient conduction of insulating polar liquids", in the Journal of Physical Chemistry, Vol. 89, pp. 20-21, 1985.

217.   T. J. Lewis, "The basic processes of conduction in dielectric liquids", in IEEE 11th International Conference on Conduction and Breakdown in Dielectric Liquids, pp. 32-41, 19-23 Jul 1993, Baden-Dattwil.

218.   Kapila Bandara, C. Ekanayake, Tapan K. Saha, "Analysis of Frequency Domain Dielectric Response of Pressboard Insulation Impregnated with Different Insulating Liquids (Accpted 22nd Feb. 2016)," IEEE Transactions on Dielectrics and Electrical Insulation, 2016.

219.   Kapila Bandara, C. Ekanayake, Tapan K. Saha, "Analysis of Frequency Domain Dielectric Response of Pressboard Insulation Impregnated with Different Insulating Liquids (Accpted 22nd Feb. 2016)," IEEE Transactions on Dielectrics and Electrical Insulation, 2016.

220. A. K. Jonscher, "Dielectric relaxation in solids", in Journal of Physics D: Applied Physics, Vol. 32, p. R57, 1999.

221. D. K. Das-Gupta and P. C. N. Scarpa, "Modeling of dielectric relaxation spectra of polymers in the condensed phase", in IEEE Electrical Insulation Magazine, Vol. 15, Issue2, pp. 23-32, 1999.

222. A. K. Jonscher, "A new understanding of the dielectric relaxation of solids", in Journal of Materials Science, Vol. 16, pp. 2037-2060, 1981.

223. R. M. Hill and L. A. Dissado, "Debye and non-Debye relaxation", in Journal of Physics C: Solid State Physics, Vol. 18, p. 3829, 1985.

224. A. Puzenko, P. B. Ishai, and Y. Feldman, "Cole-cole broadening in dielectric relaxation and strange kinetics" , in Physical Review Letters, Vol. 105, p. 037601, 2010.

225. U. Kaatze, E. Levy, Y. Feldman, P. Ishai, and A. Puzenko, "Dielectric spectra broadening as the signature of dipole-matrix interaction. I. Water in nonionic solutions", in Journal of Chemical Physics, Vol. 136, pp. 114502-114502-5, 2012.

226. V. V. Novikov and V. P. Privalko, "Temporal fractal model for the anomalous dielectric relaxation of inhomogeneous media with chaotic structure", in Journal of Physical Review E - Statistical, Nonlinear, and Soft Matter Physics, Vol. 64, pp. 315041-3150411, 2001.

227. L. A. Dissado, "A fractal interpretation of the dielectric response of animal tissues", in Journal of Physics in Medicine and Biology, Vol. 35, p. 1487, 1990.

228. H. H.-M. Catalin R. Picu , Ali Shahsavari. Project report Mechanics of Fiber Networks, Computational nano Mechanics, Scientific Computation Research Center ,Rensselaer Polytechnic Institute New York (http://www.scorec.rpi.edu/nanomechanics/mechanics_of_fiber_networks.htm.

229. A. K. Jonscher, "Low-Frequency Dispersion In Carrier-Dominated Dielectrics", in Philosophical Magazine B: Physics of Condensed Matter; Statistical Mechanics, Electronic, Optical and Magnetic Properties, Vol. 38, pp. 587-601, 1978.

230. D. V. D. Reyden, "Recent scientific research in paper conservation" ,Journal of the American Institute for Conservation, Vol. 31, No. 1, pp. 117-138, 1992.

231. N. M. Chalashkanov, S. J. Dodd, L. A. Dissado, and J. C. Fothergill, "Re-examination of the dielectric spectra of epoxy resins: bulk charge transport and interfacial polarization peaks", in IEEE Transactions on Dielectrics and Electrical Insulation, Vol. 21, pp. 1330-1341, 2014.

232. L. A. Dissado and R. M. Hill, "The fractal nature of the cluster model dielectric response functions", in Journal of Applied Physics, Vol. 66, pp. 2511-2524, 1989.

233. L. A. Dissado, "Dielectric Relaxation and the Structure of Condensed Matter", in Physica Scripta, Vol. 1982, p. 110, 1982.

234. R. Hill and C. Pickup, "Barrier effects in dispersive media", in Journal of Materials Science, Vol. 20, pp. 4431-4444, 1985.

235. J. Einfeldt, D. Meißner, and A. Kwasniewski, "Contributions to the molecular origin of the dielectric relaxation processes in polysaccharides – the high temperature range", in Journal of Non-Crystalline Solids, Vol. 320, pp. 40-55, 2003.

236. J. Einfeldt and A. Kwasniewski, "Characterization of different types of cellulose by dielectric spectroscopy", in Journal of Cellulose, Vol. 9, pp. 225-238, 2002/09/01 2002.

237. J. Einfeldt, D. Meißner, and A. Kwasniewski, "Polymerdynamics of cellulose and other polysaccharides in solid state-secondary dielectric relaxation processes", inProgress in Polymer Science, Vol. 26, pp. 1419-1472, 2001.

238. C. Ekanayake. Nilanga Abeywickrama, Yuriy V. Serdyuk and Stanislaw M. Gubanski, "Effects of the Insulation Quality on the Frequency Response of Power Transformers," Journal of EET, vol. Vol. 1, No 4, pp. 534-542, 2006.

239. M. Hui, T. K. Saha, and C. Ekanayake, "Interpretation of dielectric response measurements of transformer insulation under temperature variations and transient effects", in IEEE Power and Energy Society General Meeting, pp. 1-8, 22-26 July 2012, San Diego, CA.

240. M. F. Shlesinger and E. W. Montroll, "On the Williams--Watts Function of Dielectric Relaxation", Proceedings of the National Academy of Sciences of the United States of America, Vol. 81, pp. 1280-1283, 1984.

241. Kapila Bandara, Chandima Ekanayake, Tapan K. Saha,, "Influence of Moisture and Ageing on Dielectric Response of Ester and Mineral Oil Impregnated Pressboard Insulation," in IEEE Asia-Pacific Power and Enegy Engineering, pp 1-5, 2015, Brisbane Australia.

242. ASTM Std. E104-2012, "Standard Practice for Maintaining Constant Relative Humidity by Means of Aqueous Solutions".

243. D. F. Garcia, R. Villarroel, B. Garcia, and J. C. Burgos, "A review of moisture diffusion coefficients in transformer solid insulation - Part 2: Experimental validation of the coefficients", in IEEE Electrical Insulation Magazine, Vol. 29, Issue 2, pp. 40-49, 2013.

244. S. D. Foss and L. Savio, "Mathematical and experimental analysis of the field drying of power transformer insulation", in IEEE Transactions on Power Delivery, Vol. 8, pp. 1820-1828, 1993.

245. C. Yi, M. Hui, T. Saha, and C. Ekanayake, "Understanding Moisture Dynamics and Its Effect on the Dielectric Response of Transformer Insulation", IEEE Transactions on Power Delivery, Vol. 30, pp. 2195-2204, 2015.

246. L. J. Zhou, G. N. Wu, and J. Liu, "Modeling of transient moisture equilibrium in oil-paper insulation", IEEE Transactions on Dielectrics and Electrical Insulation, vol. 15, pp. 872-878, 2008.

247. Z. Zhaotao, L. Jian, L. Ruijin, and S. Grzybowski, "Moisture diffusion invegetable oil-paper insulation", in IEEE International Conference on Dielectric Liquids, pp. 1-4, 26-30 June 2011, Trondheim.

248. J. Crank, The mathematics of diffusion vol. viii. Oxford, [Eng]: Clarendon Press,, 1975.

249. B. V. Hahn, Dan, "Essential Matlab for Engineers and Scientists", vol. 5, Jordan Hill, GBR: Academic Press, 2013.

250. W. Shi-Qiang, Z. Guan-Jun, W. Jian-Lin, Y. Shuang-suo, D. Ming, and H. Xin-Bo, "Investigation on dielectric response characteristics of thermally aged insulating pressboard in vacuum and oil-impregnated ambient", in IEEE Transactions on Dielectrics and Electrical Insulation, Vol. 17, pp. 1853-1862, 2010.

251. A. K. Jonscher, "Low-frequency dispersion in volume and interfacial situations", in Journal of Materials Science, Vol. 26, pp. 1618-1626, 1991.

252. F. Khan and N. Pilpel, "An investigation of moisture sorption in microcrystalline cellulose using sorption isotherms and dielectric response", in Journal of Powder Technology, Vol. 50, pp. 237-241, 1987.

253. P. Zukowski, T. N. Koltunowicz, K. Kierczynski, J. Subocz, M. Szrot, and M. Gutten, "Assessment of water content in an impregnated pressboard based on DC conductivity measurements theoretical assumptions", in IEEE Transactions on Dielectrics and Electrical Insulation, Vol. 21, pp. 1268-1275, 2014.

254. P. M. Suherman and G. Smith, "A percolation cluster model of the temperature dependent dielectric properties of hydrated proteins", in Journal of Physics D: Applied Physics, Vol. 36, p. 336, 2003.

255. A. A. Abdelmalik, S. J. Dodd , L. A. Dissado, N. M. Chalashkanov, "Charge Transport in Paper Impregnated with Natural Ester Oil", IEEE transactions on Dielectrics and Electrical Insulation, Vol 21, pp. 2318 - 2328, 2014.

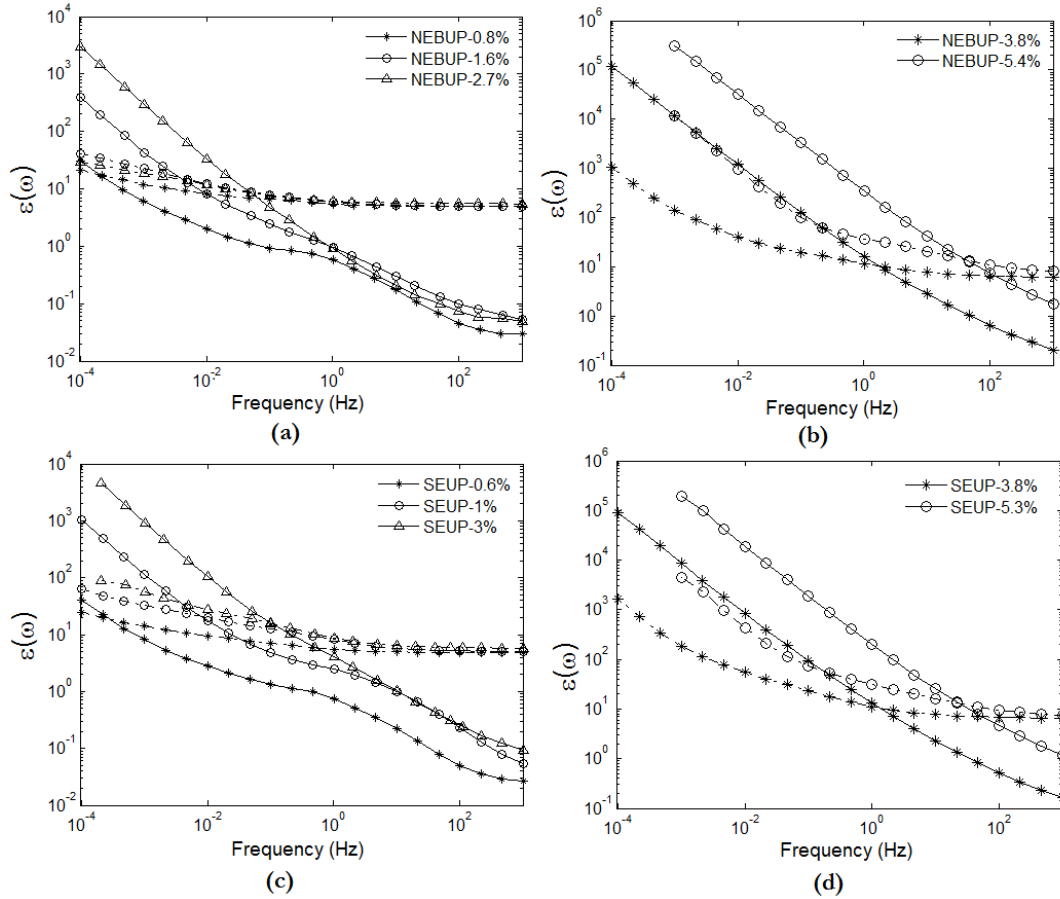# **Appendix A**: Dielectric Response of oil impregnated Pressboard

Figure A.1. FDS of (a)-(b) Mineral oil impregnated (c)-(d) Synthetic ester impregnated: dotted lines real permittivity solid lines imaginary permittivity
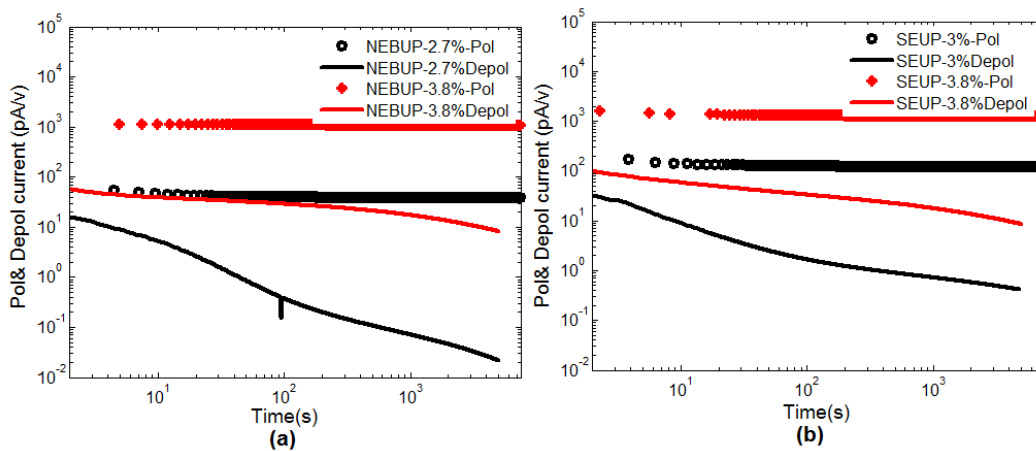

Figure A.2. PDC response of NEB and synthetic ester impregnated pressboard at two different moisture level at 55°C
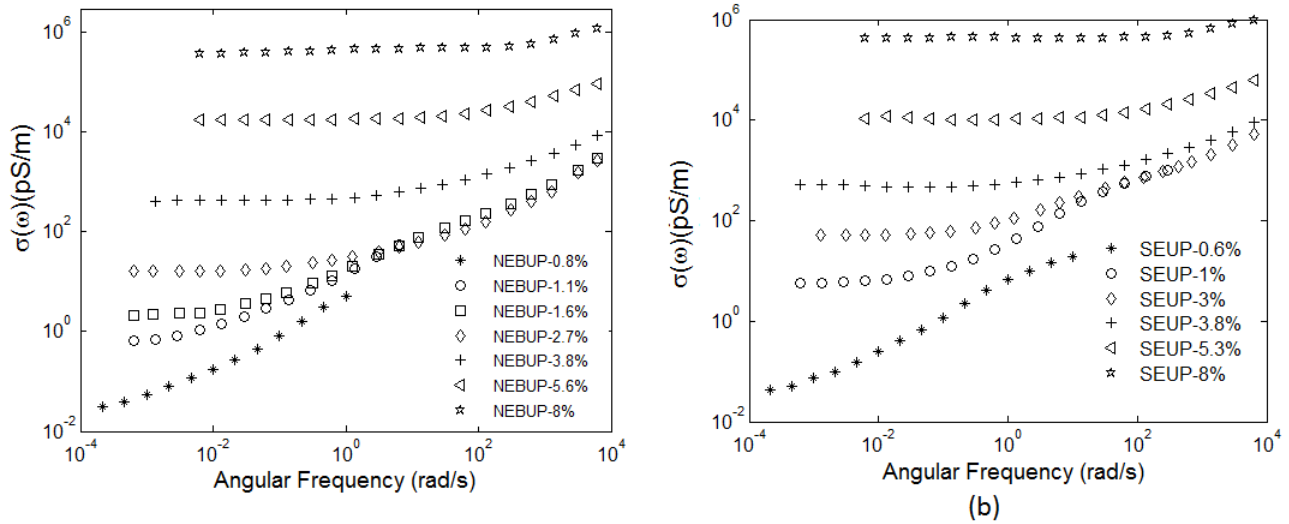
Figure A.3. Frequency dependence conductivity at 55ºC (a) NEB impregnated pressboard (b) synthetic ester impregnated pressboard

Table A.1. Selected parameters for conductivity based model: NEB impregnated at 55 ºC

Sample ID	σ_{dc}(pS/m)	$1/\tau_c$ (rad/s)	β
NEBUP-0.8%	1.3×10^{-1}	2.1×10^{-3}	0.7
NEBUP-1.1%	4.7×10^{-1}	3.8×10^{-3}	0.6
NEBUP-1.6%	1.88	3.7×10^{-2}	0.64
NEBUP-2.7%	1.6×10^{1}	1.3	0.5
NEBUP-3.6%	4.2×10^{2}	2.5×10^{1}	0.53
NEBUP-3.8%	6.4×10^{2}	3.3×10^{1}	0.51
NEBUP-5.4%	17.3×10^{3}	3.6×10^{2}	0.53
NEBUP-8%	4.2×10^{5}	4.0×10^{3}	0.7

Table A.2. Selected parameters for conductivity based model: synthetic ester impregnated at 55 ºC

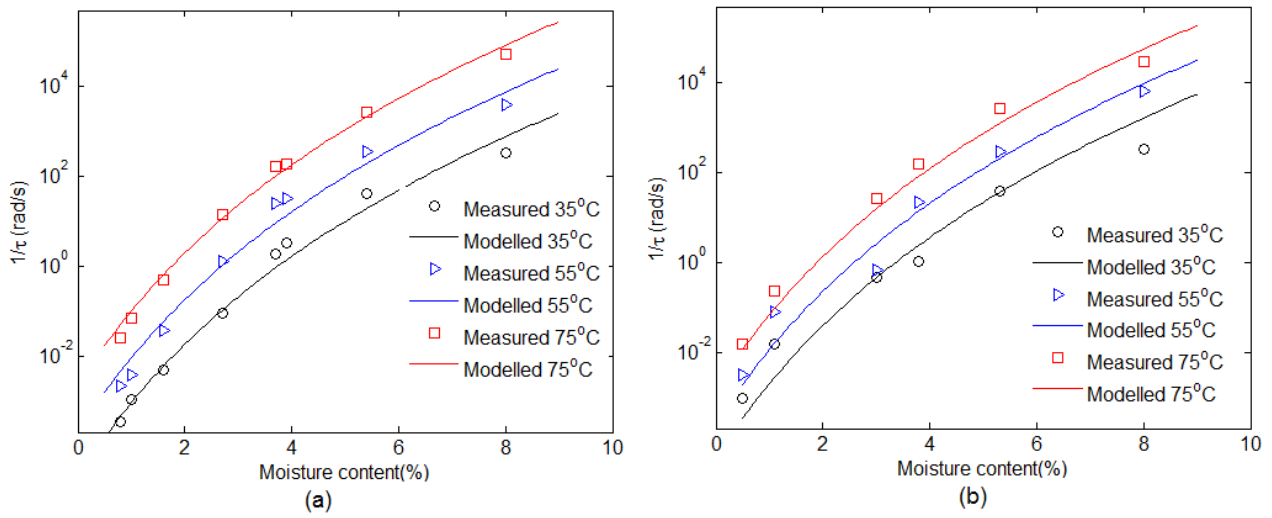| Sample ID	σ_{dc}(pS/m)	$1/\tau_c$ (rad/s)	β
SEUP-0.6%	2×10^{-1}	3.1×10^{-3}	0.7
SEUP-1%	6.0	7.7×10^{-2}	0.6
SEUP-3%	4.7×10^{1}	6.8×10^{-1}	0.64
SEUP-3.8%	4.7×10^{2}	2.2×10^{1}	0.5
SEUP-5.3%	10.3×10^{3}	3.0×10^{2}	0.53
SEUP-8%	4.15×10^{5}	6.6×10^{3}	0.51

Figure A.4. Measured and modelled cut off frequency Vs moisture content of oil impregnated pressboard (a) NEB (b) synthetic ester
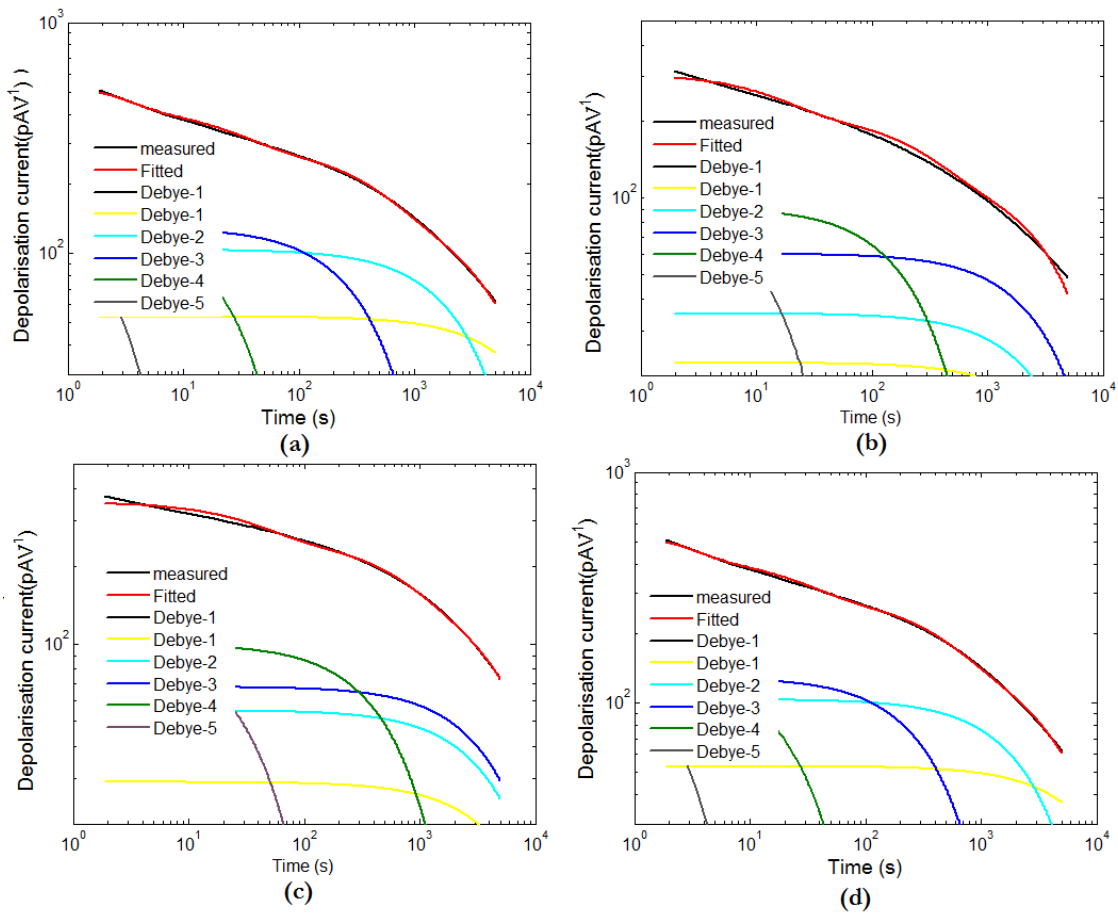

Figure A.5. Comparison of experimental and modelled depolarisation current with extended Debye model (a) MINUP-3.8% (b) NEAUP3.8 % (c) NEBUP-3.8% (d) SEUP-3.8%
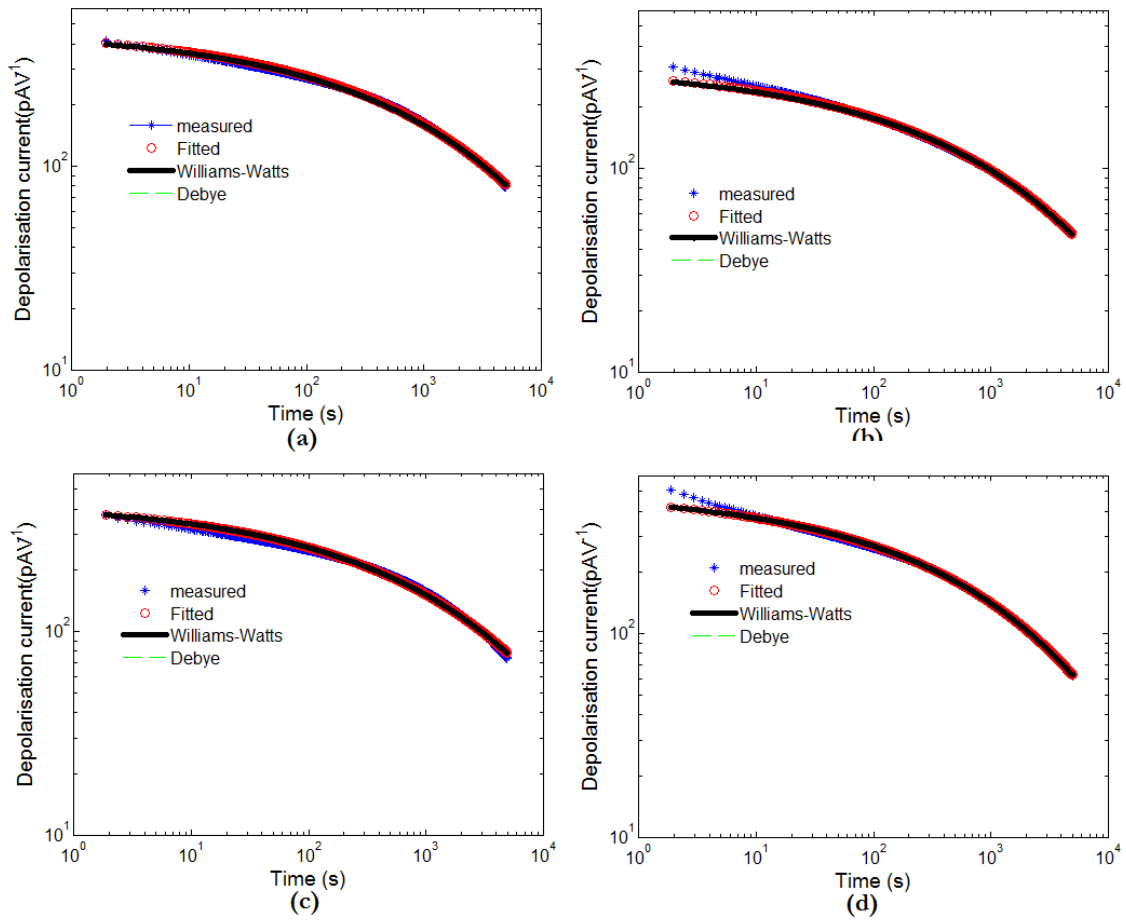
Figure A.6. Comparison of experimental and modelled depolarisation current with Williams-Watt function based model (a) MINUP-3.8%, (b) NEAUP-3.8%, (c) NEBUP-3.8%, (d) SEUP-3.8%
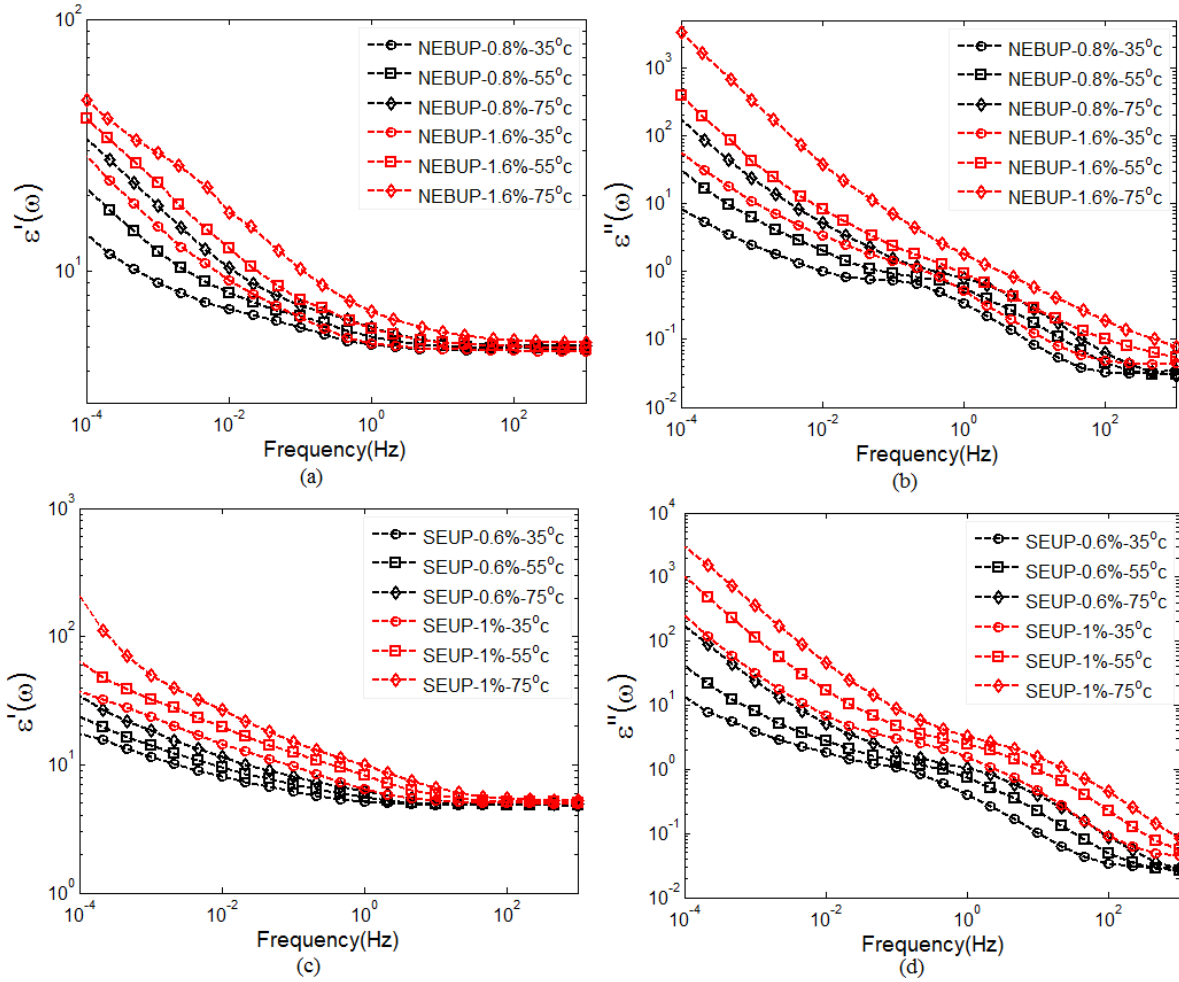
Figure A.7. FDS responses at three different temperatures (a)-(b) NEBUP (c)-(d) SEUP